Molecular Interaction of Flagellar Export Chaperone FliS and its Interacting Partner HP1076 in *Helicobacter pylori*

LAM, Wai Ling

A Thesis Submitted in Partial Fulfillment of

the Requirements for the Degree of

Doctor of Philosophy

in

Biochemistry

The Chinese University of Hong Kong
September 2010

ProQuest LLC
789 East Eisenhower Parkway
P.O. Box 1346
Ann Arbor, MI 48106-1346

Thesis/ Assessment Committee

Professor Shaw Pang-Chui (Chair)

Professor Au Wing-Ngor (Thesis Supervisor)

Professor Ng Tzi-Bun (Committee Member)

Acknowledgements

I would like to express my gratitude towards my supervisor Prof. Au Wing-Ngor, Shannon for her guidance, valuable advice and endless support throughout my five-year study. And I would like to thank our collaborator, Dr. Ling Kin-Wah for his support on the bacterial culture of *H. pylori* and generous gift of *H. pylori* MtZ-R clinical isolates. Also I would like to thank everyone who technically support this research project, Dr. Woo Eui-Jeon for the help in data collection and phase determination of HP1076; Dr. Kotaka Masayo for the help in data collection of binary complex; Dr. Leung Yun-Chung for his help in ITC assays; Miss Tam Wai-Kwan for her assistance on molecular cloning and transformation of *H. pylori*; Miss Helen Tsai for her help in mass spectrometry.

I would also like to give special thanks to all the members in Prof. Au's group, especially Dr. Xu Zheng, Miss. Chau So-Fun, Cherry, Miss Cheung Sao-Fong Crystal, Miss Ho Hei Ming, Frances, Miss. Lam Suk-Mi, Levina, Mr. Lam Kwok-Ho and Miss Hon Ching-Yi, Jenny for their experimental support and encouragement.

Last but not least, I would like to give the deepest thanks to my family for their endless support and love, who give me enough strength to go through all difficulties.

Thank you all!

Abstract

Helicobacter pylori is a pathogenic bacterium and adheres to the gastric mucosal cells. Chronic infection would lead to gastritis or peptic ulceration and is one of the leading causes of gastric cancer. Formation of functional flagella is essential for infection, that it aids in motility of bacteria and colonization on gastric epithelial cells. The process is complex and involves more than 50 proteins in assembly of structural proteins, regulatory proteins, an export apparatus, a motor and a sensory system. Cytosolic chaperones are required to bind to exported proteins in order to facilitate the export or prevent the aggregation of proteins in cytosol. Divergence is found in flagellar system *H. pylori* that may account for survival inside gastric environment.

FliS is an export chaperone that binds to flagellin molecules in cytosol in order to prevent pre-mature polymerization. Disruption of FliS would result in formation of shorter flagella and impaired adhesion ability to epithelial cells. Previous yeast two-hybrid study has identified various FliS associated proteins in *H. pylori*, but with no known implications. Here, we have demonstrated the interaction of FliS and a hypothetical protein HP1076 by biochemical and biophysical methods. Moreover, HP1076 possesses anti-aggregation ability on insoluble FliS-mutants and chaperone activity. Thus, HP1076 is proposed to be a co-chaperone that promotes the folding

and chaperone activity of FliS. FliS is demonstrated to have a broad range of substrate specificity that binds to flagellin and flagellar related proteins which may play a key role in flagellar export system different from other flagellated bacteria.

The crystal structures of FliS, HP1076 fragment and FliS/HP1076 complex are determined at 2.7Å, 1.8Å and 2.7Å resolution respectively to provide better understanding of their molecular interactions. FliS consists of four helices and HP1076 consists of helical rich bundle structure with three helices and three β strands that share similar fold to that of a flagellin homologue, hook-associated protein and FliS, suggesting HP1076 is involved in flagellar system. The FliS/HP1076 complex reveals an extensive electrostatic and hydrophobic binding interface which is distinct from the flagellin binding pocket on FliS. HP1076 stabilizes two alpha helices of FliS and therefore the overall bundle structure. Our findings provide new insights into the flagellar export chaperones and other secretion chaperones in Type III secretion system.

A HP1076 null mutant has been constructed to provide a better understanding of the biological significance of HP1076 in *H. pylori*. The ΔHP1076 mutant displays impaired motility and resistance to the antibiotic drug metronidazole. Using a proteomic study, an overall of 40 differentially expressing proteins involved in metabolism and pH homeostasis for bacterial survival, adhesion for colonization,

virulence factor to gastric epithelial cells and antigenic proteins have been identified. The virulence factor, Cag pathogenicity island protein (Cag 26) and urease UreA and UreB are confirmed to have enhanced and reduced expression in null mutants. These findings may provide new insight into the infection of *H. pylori*.

摘要

幽門螺旋桿菌是一種黏附到胃黏膜細胞的致病細菌，感染細菌會導致慢性胃炎或消化性潰瘍，它更是胃癌主要死因之一。鞭毛的形成對於細菌的移動力及胃黏膜上的生存機會有舉足輕重的影響。超過五十多個蛋白於鞭毛形成過程中擔當不同角色，包括調控、組裝、輸出系統結構、馬達及感應系統。輸出系統中的分子伴侶(chaperones)與導出的蛋白質有交互作用，以促進蛋白質的傳導或防止蛋白質在細胞質內自我聚集(aggregation)。

FliS 是輸出系統中的分子伴侶，負責防止鞭毛蛋白(flagellin)自我聚集。有研究發現 FliS 變異株的鞭毛比較短小及黏附能力減弱。酵母菌雙雜交系統推測出與 FliS 有關的蛋白，但未有任何已知的影響。本文證實 FliS 與一功能未明的蛋白質(HP1076)有交互作用。此外，HP1076 對不溶性 FliS 有抗聚集能力，可能擔當 FliS 的分子伴侶(co-chaperone)。另外，FliS 對鞭毛蛋白與鞭毛相關蛋白(flagellar related proteins)同樣具有交互作用, FliS 的作用可能有別於其他鞭毛的細菌，於鞭毛輸出系統中具關鍵作用。

FliS，HP1076 及 FliS/HP1076 複合體的晶體結構分別得到解析度 2.7Å, 1.8Å 和 2.7Å，有助了解它們相互作用。FliS 是由四個螺旋結構組成。而 HP1076 則由三個螺旋及三條β 摺疊組成，與鞭毛相關蛋: flagellin homologue, hook-associated protein, FliS 的結構相似，顯示 HP1076 於鞭毛系統有相應作用。HP1076 透過 electrostatic 和 hydrogen interactions 穩定 FliS 的α 螺旋結構。這樣的相互作用為

第三型輸出系統分子伴侶帶來新的見解。

本文發現 HP1076 變異株的移動力減弱及對抗生素甲硝唑（Metronidazole）產生抗藥性。利用蛋白質組研究發現 40 個蛋白質有不同的差異表達，包括負責代謝和穩定 pH 以維持細菌生存，黏附作用，毒性因子及細胞抗原。其中兩個毒性因子 Cag 26 及尿素酶 (Urease UreA, UreB) 的表達均分別證實有增強或減弱。這些結果顯示 HP1076 在幽門桿菌的感染中擔當一定的角色。

Table of Contents

Abbreviations used in this study

%	Percentage
°C	Degree Celsius
10 X	Ten times
3D	Three dimensional
Å	Angstrom
A	Ampere
aa	Amino acid
APS	Ammonium persulfate
ATP	Adenosine triphosphate
Bis-tris	Bis[2-Hydroxyethyl]imino-tris[hydroxymethyl]methane)
bp	Base pair
BSA	Bovine serum albumin
$CaCl_2 \cdot 2H_2O$	Calcium chloride
CHAPS	3-[(3-Cholamidopropyl)-Dimethylammonio]-1-Propane Sulfonate
C-terminal	Carboxyl-terminal
DALI	Distance matrix alignment
DNA	Deoxyribonucleic acid
ddH_2O	Double distilled water/ deionized water
dNTP	Deoxynucleic triphospahte
DTT	Dithiothreitol
EDTA	Ethylenediaminetetraacetic acid
Fig.	Figure
g	Gram(s)
GST	Glutathione-S-transferase
HEPES	4-(2-Hydroxyethyl)piperazine-1-ethanesulfonic acid
hr	Hour(s)
IPTG	Isopropyl-beta-D-thiogalactopyranoside
k	Kilo, 10^3
K	Kelvin
kb	Kilo-base
kb/min	Kilo base pairs per minute
KCl	Potassium chloride
kDa	Killo-Dalton
KH_2PO4	Potassium phosphate, monobasic

KOAc	Potassium acetate
l	Liter
M	Mili, 10^{-3}
M	Molar
MES	2-(N-morpholino) ethanesulfonic acid
$MgCl_2$	Magnesium chloride
min	Minute(s)
mm	Milimeter
$MnCl_2 \cdot 4H_2O$	Manganese chloride
n	Nano, 10^{-9}
$Na_2HPO_4 \cdot 7H_2O$	Sodium phosphate, dibasic
NaOH	Sodium hydroxide
NCBI	National Center for Biotechnology Information
Ni	Nickel
nm	Nano-meter
OD_{600}	Optical density at 600 nm
PAGE	Polyacryamide gel electrophoresis
PCR	Polymerase chain reaction
PEG	Polyethylene glycol
PMSF	Phenylmethyl-sulfonyl fluoride
$RbCl_2$	Rubidium chloride
rmsd	Root mean square deviation
rpm	Revolutions per minute
SDS	Sodium dodecyl sulfate
sec	Second(s)
TEMED	N,N,N',N'-Tetranethyl-ethylene diamine
Tris	Tris[hydroxymethyl]aminomethane
U	Unit
UV	Ultra-violet
V	Voltage
v/v	Volume per volume
w/v	Weight per volume
WT	Wild-type
μ	Micro, 10^{-6}

Abbreviations and symbols of amino acids

Amino Acid	Three-letter Abbreviation	One-letter Abbreviation
Alanine	Ala	A
Arginine	Arg	R
Asparagines	Asn	N
Aspartate	Asp	D
Cysteine	Cys	C
Glutamine	Gln	Q
Glutamate	Glu	E
Glycine	Gly	G
Histidine	His	H
Isoleucine	Ile	I
Leucine	Leu	L
Lysine	Lys	K
Methionine	Met	M
Phenylalanine	Phe	F
Proline	Pro	P
Serine	Ser	S
Threonine	Thr	T
Tryptophan	Trp	W
Tyrosine	Tyr	Y
Valine	Val	V

List of Figures

List of Table

Chapter 1 Introduction

1.1 *Helicobacter pylori*

Helicobacter pylori is a gram-negative, flagellated and spiral-shaped bacterium firstly isolated from the biopsy samples of patients with chronic gastritis, duodenal ulcer or gastric ulcer by Barry J. Marshall and Robin Warren in 1982 (Marshall and Warren, 1984). It was a breakthrough on the pathogenesis of gastric diseases as most of people at that time did not believe that the extremely acidic environment could accommodate pathogenic bacterium. The Nobel Prize in Physiology or Medicine in 2005 was awarded to the two scientists for their discovery of *H. pylori* and its role in gastritis and peptic ulcer diseases. The complete genome of *H. pylori* strain 26695 was sequenced in 1997 (Tomb *et al.*, 1997), which allowed extensive studies on pathogenesis and infection of bacteria to host, so as to provide insight into the therapeutic development.

1.2 Relationship of *H. pylori* and gastric diseases

H. pylori is mostly acquired during childhood through fetal-oral route or contaminated water (Peter and Beglinger, 2007). It colonizes in the stomach of almost 50% of human population in the world and persists in gastric mucosal cells in human for the whole life if not being treated (Portal-Celhay and Perez-Perez, 2006)

as no symptoms are developed in early infection. When the symptoms appear, the disease usually comes to the severe stage. Chronic infection can cause chronic gastritis, carcinoma, peptic ulcer diseases or duodenal ulcer (Fox *et al.*, 1990; Suerbaum *et al.*, 1993). Gastric cancer is the fourth most common cancer and the second leading cause of cancer-related death worldwide especially in developing countries (Crew and Neugut, 2006). Almost half of the cases are related to *H. pylori*. Infected patients with *H. pylori* would have six folds increase in developing gastric cancer (Wong *et al.*, 1999; *Helicobacter* and Cancer Collaborative Group, 2001). Thus, *H. pylori* is closely related to gastric cancer and classified as Group I carcinogen by International Agency for Research on Cancer, IARC.

Whether an infected people would eventually develop gastric cancer, which depends on numerous factors including virulence of bacterial strain with CagA-positive (Blaser *et al.*, 1995; Gwack *et al.*, 2006; Plummer *et al.*, 2007) or VacA-positive (Figura *et al.*, 1989), host genetic diversity with interleukin-1 polymorphism or proinflammatory cytokine gene polymorphisms (El-Omar *et al.*, 2000; Machado *et al.*, 2001; El-Omar *et al.*, 2003), environmental and lifestyle factors with preserved salty food (Tsugane *et al.*, 1994; World Health Organization, 2003) or smoking habit (International Agency for Research on Cancer, 2004; Ando *et al.*, 2006).

1.3 Mode of infection

As illustrated in Fig.1.1A, the bacterium targets the protective mucous layer of the epithelial cells in stomach and swims through the thick mucus layer by the motion of the flagella which is also known as a colonization factor important for pathogenesis (O' Toole *et al.*, 2000). It finally anchors to the epithelial cells with adhesin proteins (Labigne and de Reuse, 1996). The bacterium produces a large amount of urease enzymes to hydrolyze urea into ammonium and carbon dioxide, thus neutralizing the acidic environment for survival (Mobley *et al.*, 1988, Marais *et al.*, 1999) (Fig.1.1B). Hydrolysis of urea also helps to provide proton motive force for bacterium to swim across the mucus layer (Nakamura *et al.*, 1998). Elevating the pH by ammonia would reduce the viscosity of the mucous layer from a thick gel-like structure into a more solution form, providing flexibility for the bacterium to swim freely (Celli *et al.*, 2009). The bacterium also secrets VacA toxin which forms pores on the cell membrane promoting the access of urea for hydrolysis (Iwamoto *et al.*, 1999). The bacteria then migrate, proliferate and form the infectious focus attaching on and causing damage to the epithelial cells (Fig.1.1C). Ammonia produced during hydrolysis by urease would also damage the architecture of gastric epithelial cells.

H. pylori initiates cellular degradation of gastric epithelial cells by secreting effector proteins. Injected cytotoxin CagA induces secretion of interleukin IL-8

(Censini *et al.*, 1996) and recruitment of neutrophil to the site of infection. It alters tyrosine phosphorylation and dephosphorylation of cellular proteins and itself is also tyrosine phosphorylated which interferes the signaling transduction pathway of epithelial cells resulting in enhanced cell proliferation, damage of DNA by production of reactive oxygen species and apoptosis (Asahi *et al.*, 2000; Stabile and Smith, 2005; Minohara *et al.*, 2007; Zhong *et al.*, 2007). On the other hand, VacA suppresses the immune response making favor for the persistence of bacteria (Molinari *et al.*, 1998). All these damages would favor the progression of infected cells into carcinogenesis (Jaiswal *et al.*, 2001; Peter and Beglinger, 2007) (Fig.1.1D).

Studies using *H. pylori*-infected animal models in piglet (Eaton *et al.*, 1992), mice (Ottemann and Lowernthal, 2003) and gerbil (Kavermann *et al.*, 2003) showed that the infection rate of immotile strains was lower, and highly motile strains were usually isolated from the animals. Thus, the motility of the flagella is an essential component for colonization and infection.

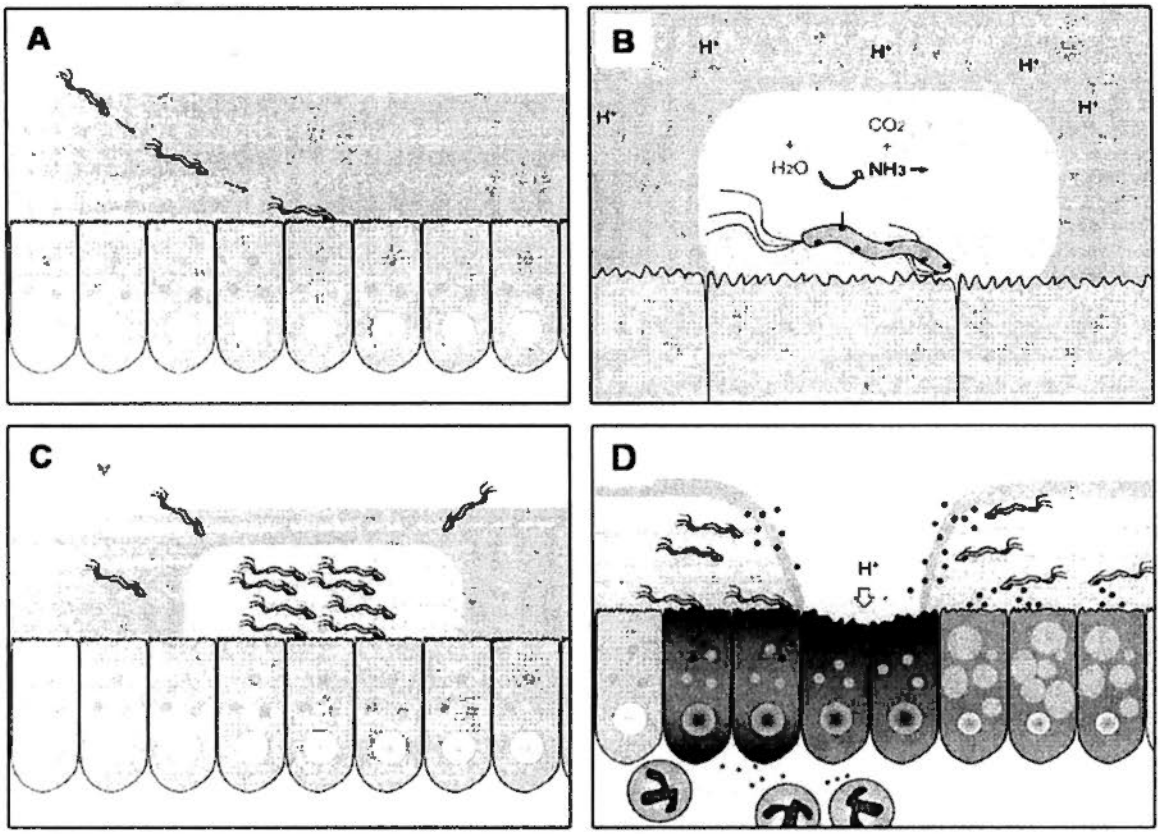

Fig.1.1 Mode of infection of *H. pylori* in gastric epithelial cells
H. pylori targets gastric epithelial cell (A), and neutralizes gastric acid by urease enzymes (B). The bacterium forms infectious body (C) and causes damage (D). (Adapted from http://ca.wikipedia.org/wiki/Helicobacter_pylori)

1.4 Flagellar assembly pathway

Assembly of a functional flagellum is a complex and ordered mechanism which includes more than 50 proteins including structural proteins, regulatory proteins, an export apparatus, a motor and a sensory system to process and respond to the environmental signals (Aldridge and Hughes, 2002; Macnab, 2003).

1.4.1 Assembly of core structure

For the genomic sequence analysis, the core structure of the flagella in *H. pylori* is suggested to be similar to the well-known flagella models in *E. coli* or *Salmonella* (Fig.1.2). The whole structure spans from the cytoplasmic membrane through peptidoglycan layer to the extracellular space of the outer membrane. Flagellum consists of three parts including basal body, hook and filament (Minamino and Namba, 2004). The basal body is formed by a MS-ring inserted into inner membrane and a C-ring complex attached to the cytoplasmic side of MS-ring. The C-ring is a motor-switch that provides motion force to flagella. A type III export apparatus is assembled attaching to the basal body. Then, the rod proteins are inserted into the outer membrane. The hook is formed on the structure of rod to connect the basal body and the filament. The outermost part is the filament which is formed by the polymerization of flagellin molecules, FliC. However, in *H. pylori*, the flagellin molecules contain major flagellin FlaA and minor flagellin FlaB (Kostrzynska *et al.*, 1991). The composition of the flagellin FlaA and FlaB molecules may be varied for adaption to the environmental changes (Johensans *et al.*, 1995). Filament cap protein, FliD forms cap complex at the distal end of filament to assist the incorporation of flagellin molecules and prevent the leakage of the flagellin molecules. The FliD complex induces conformation changes of exported flagellin molecules and it moves

outwards to allow the incorporation of flagellin to growing flagella (Ikeda *et al.*, 1987; Yonekura *et al.*, 2000).

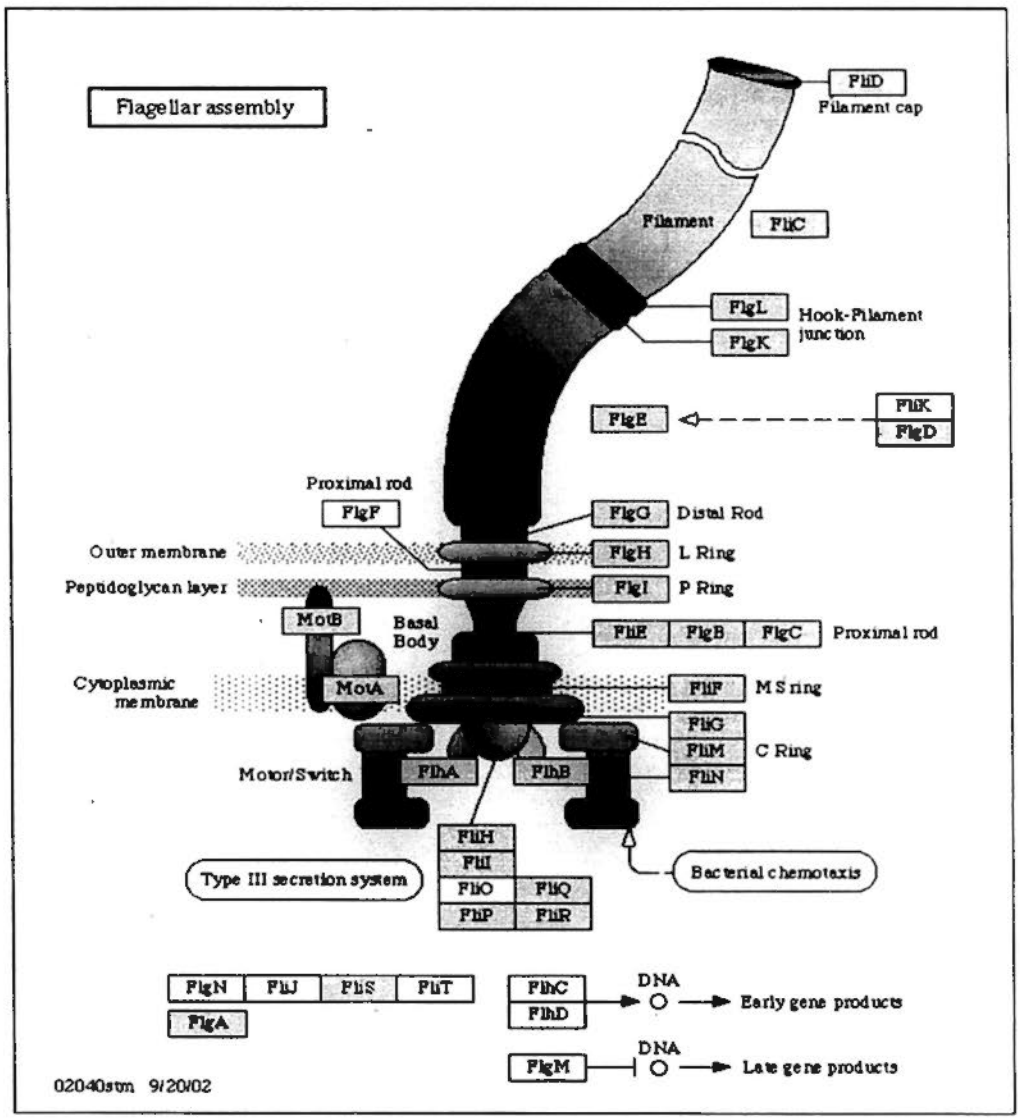

Fig.1.2 Model of flagella assembly in *E. coli*
The figure shows the distribution of proteins involved in different steps of assembly. (Adapted from http://www.genome.ad.jp/kegg/pathway/eco/eco02040.html)

1.4.2 Protein export by Type III export apparatus

Based on the similarity of the flagellar core structure in *H. pylori* and *Salmonella*, the flagellar export mechanism resembles to the type III secretion system for exporting virulence factor (Bennett and Hughes, 2000) in some ways though the molecular basis of export system in *H. pylori* has not been fully elucidated. The general export apparatus is composed of flagellum-specific ATPase (FliI), flagellar assembly protein H (FliH) and flagellar biosynthesis proteins (FlhA, FlhB, FliO, FliQ, FliP and FliR) (Minamino and Macnab, 1999).

Extensive studies have been performed to elucidate the export system in *Salmonella*. The structural proteins synthesized inside the cytosol must be secreted sequentially for incorporation into a flagellar structure and this is assisted by export chaperones. Chaperones are small cytosolic proteins with molecular weight around 20 kDa, acidic pI and full of helical structures. They often possess a characteristic amphipathic helix at the C-terminal but do not share similarity in primary protein sequences (Wattiau *et al.*, 1996; Bennett and Hughes, 2000). In *Salmonella*, chaperones FlgN, FliT and FliS target hook-associated proteins (HAPs) FlgK and FlgL, filament cap protein, FliD (Fraser *et al.*, 1999; Bennett *et al.*, 2001) and flagellin FliC (Auvray *et al.*, 2001) respectively. The chaperones bind to the C-terminal regions of structural proteins to mask the regions mediating the

interaction with their subunits (Parsot *et al.*, 2003). The chaperones facilitate the export of structural proteins by preventing them from pre-mature aggregation in cytosol or by directing them to the export apparatus with interaction to the membrane-associated ATPase, FliI (Thomas *et al.*, 2004; Imada *et al.*, 2010). A regulator FliH binds to FliI to inhibit the ATP hydrolysis activity until the substrates are delivered for export (Auvray *et al.*, 2002). The inhibitory effect of FliH might be relieved by induced conformation change of FliI upon binding with chaperone-substrate complexes (Thomas *et al.*, 2004; Imada *et al.*, 2010) or by a general chaperone FliJ that binds to FliI to activate the ATPase activity (Evans *et al.*, 2006). ATP hydrolysis provides energy for translocation of export substrates by unfolding the chaperones. The unloaded chaperones, FliT and FlgN but not FliS are then recycled by binding to FliJ which is presumably bound to the FliH proteins and cytoplasmic domains of the export apparatus proteins, FlhA and FlhB, at the docking site for export chaperone (Fraser *et al.*, 2003; Minamino *et al.*, 2000b). FliJ is also a general chaperone protein that binds to filament-type and rod/hook-type substrates and is essential for their export (Minamino *et al.*, 2000a, b). It also prevents the aggregation of over-produced export substrates, FliE and FlgG in cytosol (Minamino *et al.*, 2000b). FliJ works in different ways to facilitate the export of the structural proteins in flagellar assembly.

1.4.3 Sheath formation in flagella

The flagella in *H. pylori* is covered by sheath layer extended from the outer membrane and is composed of double layer of lipopolysaccharides (LPS) and proteins which help to protect flagellin molecules from disintegration in highly acidic environment (Geis *et al.*, 1993), which is also reported in related bacterium *Campylobacter jejuni* (Logan *et al.*, 1983).

1.5 Regulation of flagellar assembly

All the genes in flagellar system in *H. pylori* are important for infection as mutagenesis of any one single gene would reduce the infection of stomach (Kim *et al.*, 1999; Foynes *et al.*, 2000) or change morphology of flagella. Thus, the formation of functional flagellar is tightly regulated and ordered.

1.5.1 Transcriptional regulation

Flagellar proteins in *H. pylori* are classified into 4 classes, 1, 2, 3 and intermediate classes encoding regulatory and chemotatic proteins, middle flagellar structure genes of rod-hook, flagellin and sheath proteins, late flagellar structure gene of major flagellin and intermediate genes with structural and regulatory roles respectively (Fig.1.3; Niehus *et al.*, 2004). Transcription of each class is regulated by one specific sigma factor or in a combination of σ^{80}, σ^{54} (RpoN), σ^{28} and regulators.

RpoN is regulated by activator FlgR and FlgS, and also by a newly identified chaperone HP0958 (Brahmachary *et al.*, 2004; Pereira *et al.*, 2005). Biosynthesis of one class of genes has to be completed prior to transcriptional activation of next class of genes. In *Salmonella*, completion of hook-basal body structure would activate the translocation of specific anti-sigma factor FlgM from the cytosol to outside through the entire flagellar structure in order to relieve the inhibitory effect on σ^{28}, that the class 3 genes can then be transcribed (Karlinsey *et al.*, 2000a; Chadsey and Hughes, 2001). The basal proteins, FlhA and FlhF, work as master regulators on controlling the transcription of class 2 and 3 genes. Interestingly, the expression level of some hypothetical proteins such as HP1076, HP1233 and HP1154 with unknown biological roles, were found to be altered in the deletion mutant of sigma factors (Niehus *et al.*, 2004). This finding may account for the uniqueness of the flagellar system in *H. pylori*.

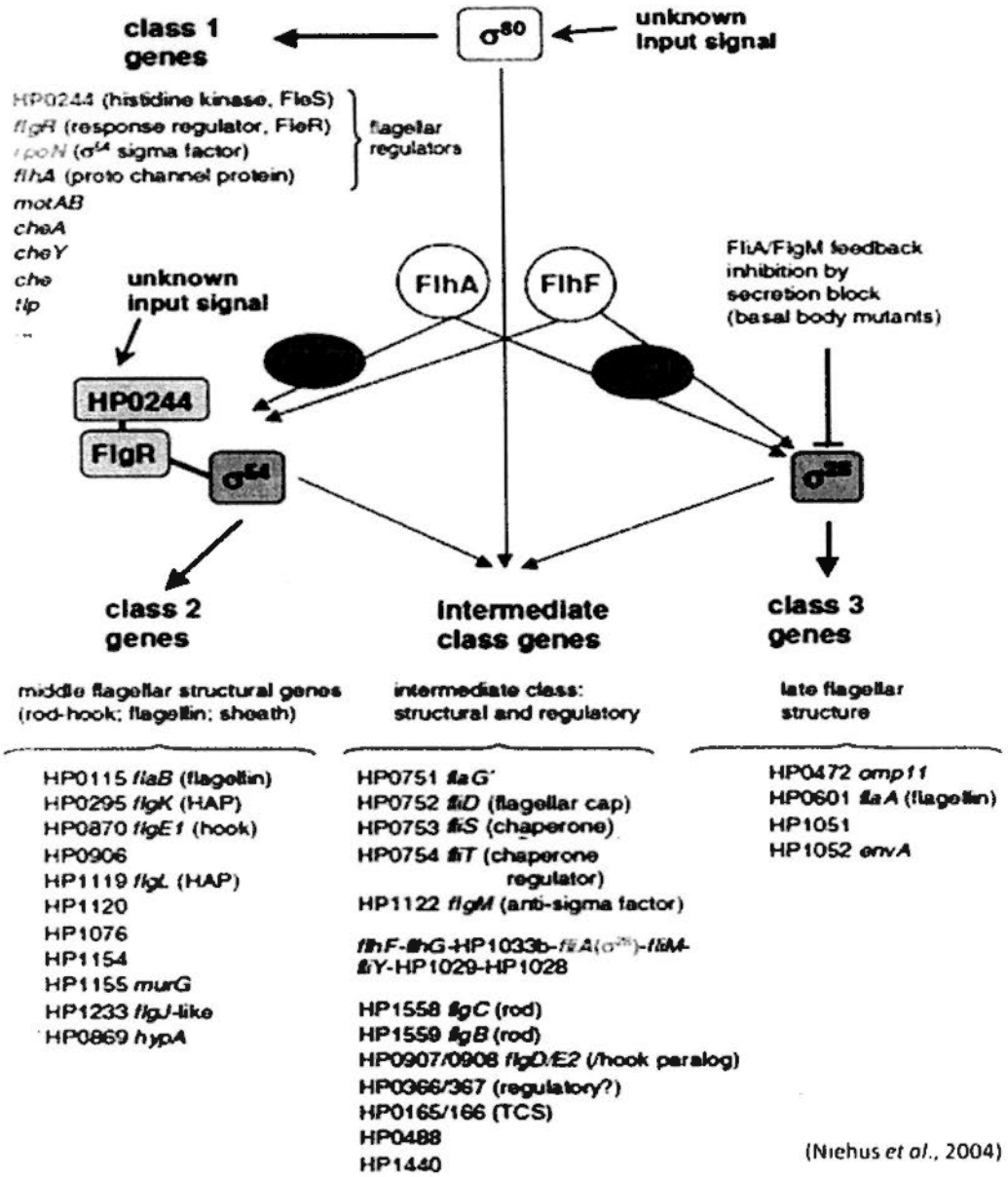

Fig.1.3 Transcriptional regulation of the flagellar assembly pathway of *H. pylori* Different classes of genes are regulated by sigma factors (σ^{80}, σ^{54} and σ^{28}) and other regulators, FlgM, FlgR and HP0244. The genes without any annotation are without any known functions.

1.5.2 Regulatory roles of Type III chaperones

The chaperone proteins FlgN, FliS and FliT not only bind to structural protein substrates, but also have regulatory roles on flagellar assembly. In *Salmonella*, FlgN regulates the translation of FlgM through a negative loop regulation in response to

the stage of flagellar assembly, while its binding with hook-associated proteins would inhibit the regulation on FlgM translation (Karlinsey *et al.*, 2000b; Aldridge *et al.*, 2003). FliT and FliS are the negative factors for the export of FlgM in *Salmonella* (Yokoseki *et al.*, 1996; Kutsukake *et al.*, 1999). FliT is also shown to interact and inhibit the binding of RNA polymerase to the promoter of class 2 genes and therefore hamper the transcription initiation (Yamamoto and Kutsukake, 2006).

1.6 Divergence of flagellar system in *H. pylori*

About 24 genes constructing the core flagellar structure display sequence similarity among 41 flagellated bacteria species including *H. pylori*, *Campylobacter jejuni*, *Aquifex aeolicus*, *Thermotoga maritime*, *E. coli* and *Salmonella* (Liu and Ochman, 2007). However, there is diversity in the organization of flagellar genes and structural assembly of the flagellar proteins (Penn and Luke, 1992). More studies show that there is divergence of flagellar system in epsilon proteobacteria including *H. pylori* and *C. jejuni* (Niehus *et al.*, 2004; Andersen-Nissen *et al.*, 2005; Galkin *et al.*, 2008).

First, additional homologous flagellar genes are present in *H. pylori* genome including flagellin protein A (HP0601), flagellin B (HP0115) and flagellin B homologue (HP0295) and flagella hook protein FlgE (HP0870 and HP0908) (Tomb

et al., 1997; Marais *et al.*, 1999).

Second, flagellar genes in *H. pylori* are distributed among the whole genome and flagellar genes are organized in cluster and operon in *Salmonella* and *E. coli*. Fig.1.4 illustrates the genomic organization of the hook associated protein FlgK. In *Salmonella* and *E. coli*, FlgK is located with flagellar genes encoding homologue FlgL, flagellar basal body P-ring protein FlgI and flagellar rod assembly protein FlgJ; while *H. pylori* FlgK is located with genes of diverse functional roles but not involved in flagellar assembly pathway including hypothetical proteins (HP1117 and HP1120), gamma-glutamyltranspeptidase (HP1118) and cytosine specific DNA methyltransferase (HP1121).

Third, regulation of the flagellar assembly reveals that *H. pylori* utilizes a four-tiered regulatory hierarchy by various sigma factors and novel genes, while two alternative sigma factors are used to coordinate flagellar gene regulation in enterobacteriaceae (Aldridge and Hughes, 2002; Niehus *et al.*, 2002; 2004). The flagellar master regulator in enterobacteriaceae is not found in the *H. pylori* genome, and *H. pylori* utilizes putative basal body protein FlhA and FlhF as the master regulator. Novel genes (HP1076, HP1233 and HP1154) with uncharacterized function are identified in class 2 and are mainly regulated by RpoN. Inactivation of these novel genes results in altered flagellar morphology (Niehus *et al.*, 2004).

HP1233 and HP1154 show low sequence identity of 13% and 5% to *Salmonella* flagellar muramidase FlgJ protein and UDP-glucuronyl transferase respectively, while HP1076 shows no sequence homology.

Fourth, the electron microscopy imaging of the filament of *Salmonella* and *C. jejuni* (Galkin *et al.*, 2008) reveals that glycosylation of the flagellin molecules is required for the formation of filament to provide normal motility. Different symmetry of filament and less protofilament is found in epsilon proteobacteria when compared with that of *Salmonella*. Moreover, the flagellin from epsilon proteobacteria *H. pylori* and *C. jejuni* evade from the activation of the vertebrate Toll-like receptor 5 (TLR5). Studies of the TLR5 recognition sites on flagellin (Smith *et al.*, 2003; Andersen-Nissen *et al.*, 2005) reveal proper folding and specific amino acid change in the recognition site of the D0 region required for polymerization and motility that accounts for the evasion. This escape from the TLR5 recognition is critical for colonization to mucosal surfaces and survival for the epsilon proteobacteria in infected hosts.

At last, *Salmonella* acquires different specific type III chaperons, FliS, FlgN and FliT, which are in helical structure that bind and mask the domains of exported flagellar substrates to prevent the self-assembly inside cytosol before incorporation into growing flagellum, while only one chaperone FliS is identified in *H. pylori*

responsible for export of flagellin molecules and no homologue of FliT and FlgN proteins are found in *H. pylori* genome. Moreover, the general chaperone FliJ is not identified in *H. pylori* that the *H. pylori* homologue (HP0256) only plays a role in motility and expression of membrane and adhesion proteins involved in pathogenesis (Douillard *et al.*, 2010). Thus, other *H. pylori* flagellar proteins may function similarly as chaperone FliT and FlgN, or FliS is a general chaperone for different export substrates. All theses remained unclear as the molecular basis of the flagellar export has not been determined.

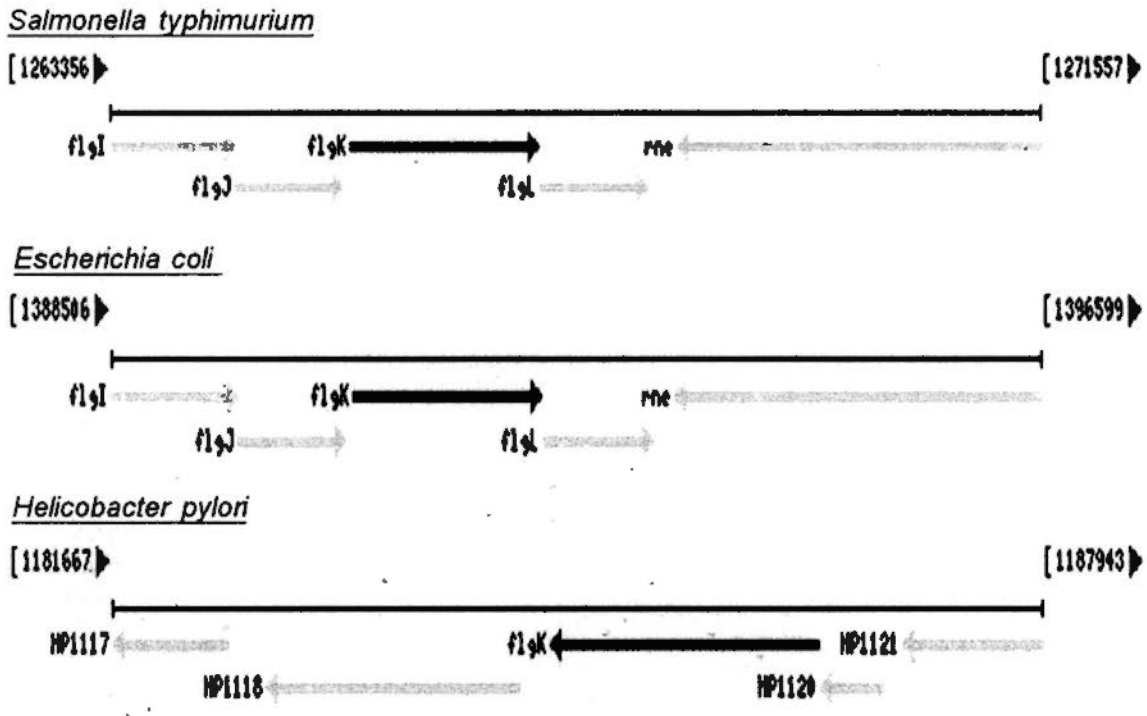

Fig.1.4 Genomic organization of FlgK gene in *Salmonella, E. coli* and *H. pylori* The red arrows indicate the gene FlgK, with genes located upstream and downstream of FlgK. The search was performed with genome database in NCBI.

1.7 Flagellar chaperone FliS

Deletion mutant of *fliS* gene in *Salmonella* (Yokoseki *et al.*, 1995) has been shown to have shorter filament and impaired flagellar export, and similar effect on flagellation is also observed in ΔFliS mutants in *E. coli* (Kawagishi *et al.*, 1992) and *Bacillus subtilis* (Chen and Helmann, 1994). FliS is found to be the early gene product in the flagellar assembly pathway. Studies in *Salmonella* show that FliS functions as a specific export chaperone to prevent pre-mature polymerization of flagellin molecules FliC in cytosol mediated by the C-terminal disordered region (last 40 amino acid residues) of FliC (Auvray *et al.*, 2001; Ozin *et al.*, 2003). The binding of FliS induces a conformational change on the C-terminal region of FliC from a disordered form into an α-helix structure that FliC is stabilized. The FliS-FliC interaction is very strong with an association constant of 1.9×10^7 M^{-1} (Muskotál *et al.*, 2006). The interaction is further supported when the first crystal structure of FliS and C-terminal fragment of flagellin (464-518 residues) from thermophilic gram negative bacterium *Aquifex aeolicus* was solved (Evdokimov *et al.*, 2003). FliS adopts a four-helical up-and-down bundle structure noted as α1-4 and the N-terminal 2-15 amino acid residues form a cap localized inside a cavity of the bundle of FliS (Fig.1.5A). Upon the binding with FliC, the N-terminal cap of FliS is displaced outwards and interacts with the helical region of FliC (510-518 residues) and the

cavity is now occupied by the helical region from 499-510 residues (Fig.1.5B). The interaction between FliS and FliC is through extensive hydrophobic interactions and a few side-chain mediated hydrogen bonding and salt bridges formation. Specifically, these involve residues Tyr8, Ile22, Leu66, Leu70, Asn81, Leu82, Tyr86, Ala116 and Trp117 on FliS and $_{503}$LAQANA$_{508}$ on FliC. From Fig.1.6A, Tyr8 from the FliS N-terminal cap forms hydrogen bond with Leu66 and Tyr86. These interactions are replaced with Gln505 on FliC upon FliS-FliC interaction suggesting that Gln505 can compensate the bond formation and retain the protein folding of the helices of FliS (Fig.1.6B). But it is not clear if FliS functions as the same way in other bacteria.

In *H. pylori*, deletion *fliS* mutant results in non-motile and non-flagellated phenotype which is because of the reduced expression levels of flagellin A and B subunits and flagellar hook subunit FlgE (Allan *et al.*, 2000). Moreover, the adherence ability to the gastric mucosal cells is also reduced that affects the infection (Zhang *et al.*, 2002). *fliS* is further supported to be essential in the gastric colonization in gerbil model (Kavermann *et al.*, 2003). FliS is classified in the intermediate class with regulatory roles on flagellar assembly (Niehus *et al.*, 2004) suggesting that it plays a role in the flagellar system. However, the mechanism of involvement of FliS in *H. pylori* flagellar export system remains to be elucidated.

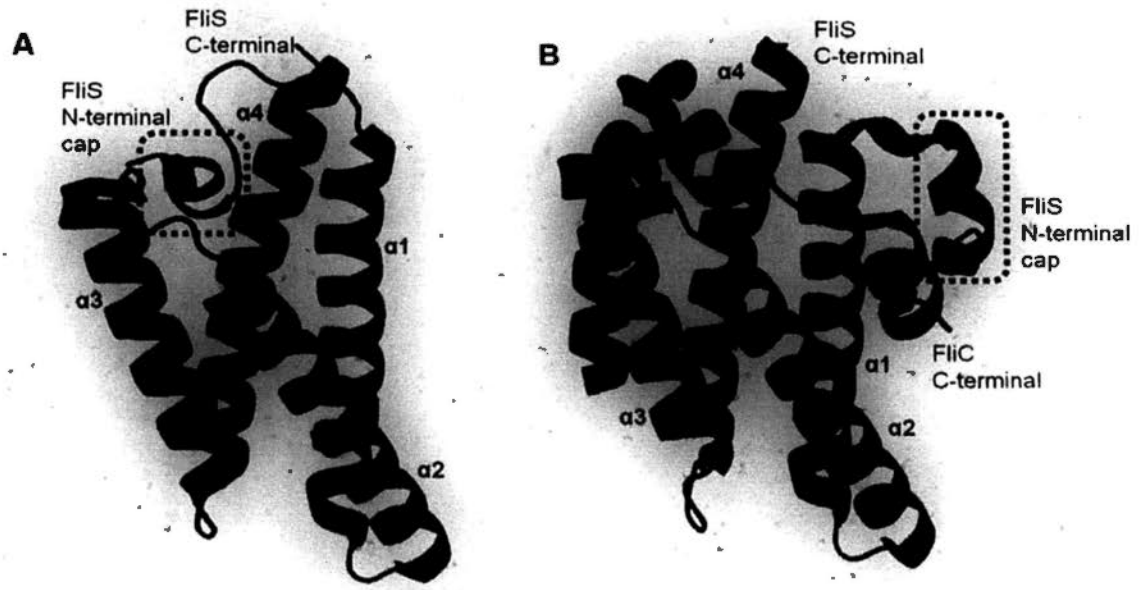

Fig.1.5 Crystal structures of free FliS and FliS/FliC complex in *A. aeolicus*
Cartoon representation of the structure of *A. aeolicus* FliS in purple color (A) and in complex with residues 464-518 of FliC fragment in blue color (B). The conformation of FliS N-terminal cap marked in red box is changed upon binding with FliC fragment.

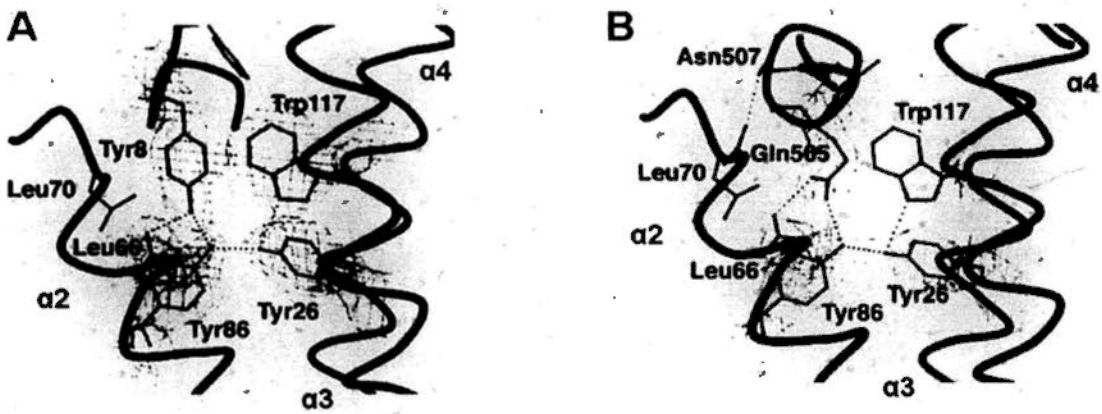

(Adapted from Evdokimov *et al.*, 2003)

Fig.1.6 Intracellular interaction of residues in binding pocket of FliS
Intracellular interaction of residues inside the binding pocket of FliS helices in free (A) form and in complex with C-terminal region of FliC (B) forming hydrogen bonding marked with dashed line is compared. The blue helices represent FliS and red helix represents C-terminal region of FliC.

1.7.1 Similarity of FliS between *H. pylori* and other bacteria

Up to now, only limited information is known for *H. pylori* FliS. Without any *in vitro* and *in vivo* experimental data, the function and structure of FliS can be analyzed by bioinformatic tools. By sequence analysis of FliS with homologue proteins with known functions, its role can be predicted (Pawlowski *et al.*, 1999).

Comparison of FliS from *Salmonella*, *E. coli*, *A. aeolicus* and *C. jejuni* (Table 1.1) reveals that *H. pylori* FliS carries similar characteristics as other FliS that it is small acid protein with about 30% of charged residues of the whole protein sequence. Moreover, *H. pylori* FliS shares about 30% identity to that of *Salmonella* and *A. aeolicus* in protein sequence alignment (Fig.1.7). All these features suggest that *H. pylori* FliS acts as a chaperone protein similar to that of *Salmonella* or *A. aeolicus* (Wattiau *et al.*, 1996; Bennett and Hughes, 2000). In addition, the residues located on *A. aeolicus* FliS protein responsible for interacting with flagellin protein (Evdokimov *et al.*, 2003) are conserved (Tyr8, Leu70, Leu82, Tyr86, Ala116 and Trp117) and highly conserved (Ile22 and Leu66) between bacteria (Fig.1.7), suggesting that *H. pylori* would interact with its substrate similarly.

FliS targets specifically to the C-terminal 40 residues as shown by the crystal structure of *A. aeolicus* FliS/FliC complex and the biochemical study of FliS from *Salmonella* (Ozin *et al.*, 2003). The C-terminal fragment of flagellin A and B

subunits are highly conserved and account for 40% sequence identity with other homologues (Table 1.2). Moreover, residues LAQANA on *A. aeolicus* FliC contacting the hydrophobic pocket on FliS (Evdokimov *et al.*, 2003) are highly conserved between flagellated bacteria. In particular, residue Gln505 responsible for hydrogen bond with Leu66 and Tyr86 in FliS is highly conserved (Fig.1.8). This high similarity of protein sequence and binding residues suggest that *H. pylori* FliS would interact with flagellin molecules in a similar mode of interaction as in *A. aeolicus* and *Salmonella*.

Table 1.1 Comparison of FliS proteins in flagellated bacteria

	Salmonella	*E. coli*	*A. aeolicus*	*H. pylori*	*C. jejuni*
Protein name	Flagellar protein	Flagellar protein	Flagellar protein	Flagellar protein	Flagellar protein
Size	135 aa	136 aa	124 aa	126 aa	128 aa
^pI	4.88	4.64	4.97	5.03	5.22
#No. of charged residues (% in whole sequence)	31 (23%)	27 (20%)	46 (37%)	32 (25%)	30 (23%)
*Protein sequence identity with *H. pylori*	31%	23%	28%	--	59%

^ pI value is calculated by Compute pI/Mw tool in ExPASy Proteomics Server (Bjellqvist *et al.*, 1993)

Charged residues are identified by ProtParam tool (Gasteiger *et al.*, 2005)

* Protein sequence alignment is performed by ClustalW (Higgins *et al.*, 1994)

Fig.1.7 Protein sequence alignment of FliS in flagellated bacteria

Protein sequences of FliS in *H. pylori*, *C. jejuni*, *Salmonella*, *E. coli* and *A. aeolicus* strains were aligned by ClustalW showing identical residues (•), highly conserved residue (:), similar residue (.), between different bacteria. And residues without any conservation are shown without any symbols. The conserved (▲) and highly conserved (Δ) and residues (○) involved in the binding with flagellin molecule are marked (Evdokimov *et al.*, 2003).

Table 1.2 Protein sequence identity of 55 residues from C-terminal of flagellin

Sequence 1	Sequence 2	Sequence identity
HPFlaA	HPFlaB	85%
HPFlaA	CJFlaB	83%
HPFlaA	CJFlaB	83%
HPFlaA	AAFliC	44%
HPFlaA	STFliC	40%
HPFlaA	ECFliC	38%

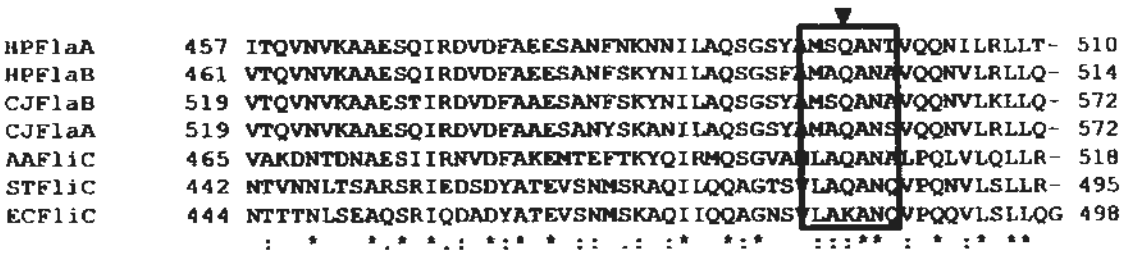

Fig.1.8 Protein sequence alignment of 55 residues from C-terminal of flagellin

Protein sequences of 55 residues from C-terminal region of flagellin in *H. pylori*, *C. jejuni*, *Salmonella*, *E. coli* and *A. aeolicus* were aligned by ClustalW showing identical residues (•), highly conserved residue (:), similar residue (.), between different bacteria. And residues without any conservation are shown without any symbols. The residues involved in binding with FliS are marked in box and the most important one is marked with (▲) (Evdokimov *et al.*, 2003).

1.7.2 Interaction map of *H. pylori* FliS

Apart from the interaction of FliS and FliC as shown in *Salmonella* and *A. aeolicus*, *H. pylori* FliS has interaction with other proteins in a yeast two-hybrid protein-protein interaction database search (Hybrigenics PimRider™ database; http://pim.hybrigenics.com/) (Rain *et al.*, 2001) (Table 1.3, upper panel). FliS is predicted to have interaction with flagellin proteins, FlaA and FlaB, and also to HP0030 (homologue of type IV secretion system subunit ComB8), hypothetical protein HP1076 and predicted S-adenosylmethionine synthetase metK with high probability represented as PIM Biological Score. From the search of FliS homologue in *C. jejuni* Interaction Database (http://itchy.med.wayne.edu/PIM2/PIM_cj.html; Parrish *et al.*, 2007), a list of high potential interaction partners including the flagellin molecules, FlaA and FlaB is obtained (Table 1.3, lower panel). *C. jejuni*

FliS interacts with other proteins like secreted protein FlaC and putative phosphate acetyltransferase pta with high confidence score. Thus, the data suggests that FliS in ε-proteobacteria not only has specific interaction with flagellin, but also has strong interaction to other proteins.

Table 1.3 Predicted interaction partners of FliS in *H. pylori* and *C. jejuni*

*H. pylori	Protein	Function	PIM Biological Score
FliS	HP0030	Homologue of type IV secretion system subunit ComB8	1e-500
	HP0115	Minor flagellin FlaB	1e-118
	HP0601	Major flagellin FlaA	1e-56
	HP1076	Hypothetical protein	1e-50
	HP0197	Predicted S-adenosylmethionine synthetase metK	1e-32

^C. jejuni	Protein	Function	Confidence Score
CJ0549	CJ1339	Major flagellin FlaA	0.998
(FliS)	CJ1338	Minor flagellin FlaB	0.949
	CJ1650	Secreted protein FlaC	0.990
	CJ0688	Putative phosphate acetyltransferase pta	0.979
	CJ0106	ATP synthase F1 sector gamma subunit atpG	0.834

* Data search from the Hybrigenics PimRider™ database

^ Data search from *Campylobacter jejuni* Interaction Database

1.8 Hypothetical protein HP1076

HP1076 is identified as one of the potential interacting partner of FliS, but little information is known about this protein as its biological role is uncharacterized. It is a cytosolic protein with molecular weight of 20 kDa and pI of 5.2. And there is no conserved domain identified and its homologue is only found in *Campylobacter*-related species but not commonly found in bacteria. HP1076 is classified in the class II gene responsible for the middle structural gene formation (rod-hook, flagellin and sheath) in the regulation of flagellar assembly system (Niehus *et al.*, 2004). Its expression is regulated under the RpoN sigma factor. In the *H. pylori* FliK null mutant (gene responsible for hook length control and export substrate specificity), the expression level of the RpoN-regulated genes including flagellin FlaB, flagellar hook and HP1076 was significantly increased (Douillard *et al.*, 2009). Moreover, the expression level of HP1076 was also up-regulated with FlaB and FlgE when the bacteria was exposed to the acidic environment at pH 5.0 (Merrell *et al.*, 2003) and even higher at pH 4.5 (Wen *et al.*, 2003). This phenotype was also observed in deletion mutant of HP0256 (a homologue of *Salmonella* FliJ) which is responsible for maintaining motility and cell envelop structure of adhesins and outer membrane proteins (Douillard *et al.*, 2010). Taken together, HP1076 may play a role in flagellar system.

Exploring the protein-protein interaction database of *H. pylori* and *C. jejuni* may provide better understanding of the biological roles. From the PimRider™ database (Table 1.4, upper panel), a list of highly possible interacting partners is identified including FliS and ClpA protein responsible for removing misfolded protein (Loughlin *et al.*, 2009). For the HP1076 homologue in *C. jejuni* (CJ1650) sharing 30% sequence identity, a possible flagellar protein and other proteins with diverse roles are identified with high confidence scores (Table 1.4, lower panel). No precise role of HP1076 is predicted from the search and the predicted interaction should be further verified to understand the biological role of HP1076.

Table 1.4 Predicted interaction partners of HP1076 in *H. pylori* and *C. jejuni*

*H. pylori	Protein	Function	PIM Biological Score
HP1076	HP0030	ATP-dependent Clp protease clpA	1e-500
	HP0753	Flagellar protein FliS	1e-50
	HP1544	Predicted toxR-activated gene tagE2	1e-26
	HP0275	ATP-dependent nuclease	1e-20
	HP0841	Predicted pantothenate metabolism flavoprotein dfp	1e-14
^C. *jejuni*	Protein	Function	Confidence Score
CJ1650 (HP1076)	CJ1313	Possible flagellar protein	0.916
	CJ1109	Putative leucyl/phenylalanyl-tRNA-protein transferase	0.872
	CJ1079	Putative periplasmic protein	0.863
	CJ0374	Hypothetical protein	0.815
	CJ0101	parB family protein	0.814

* Data search from the Hybrigenics PimRider™ database

^ Data search from *Campylobacter jejuni* Interaction Database

1.9 Objectives of the present study

Formation of functional flagella is required for *H. pylori* to colonize on gastric epithelial cells. The molecular mechanism of flagellar assembly is believed to be similar to that in enteric bacteria as protein homologues are found in *H. pylori* genome. However, more studies showed divergence of flagellar system in *H. pylori* as discussed in section 1.6. Understanding the molecular basis of the flagellar assembly pathway is emerging in particular of flagellar export mechanism. The present study focuses on the *H. pylori* export chaperone FliS which its homologue in *Salmonella*, *E. coli* and *A. aeolicus* is shown to be the bodyguard of flagellins to prevent their pre-mature polymerization in cytosol.

The molecular interaction of FliS and hypothetical protein HP1076 is studied by biochemical and structural analysis with protein X-ray crystallography. Based on the proposed broad substrate specificity of FliS as discussed in section 1.6, the interaction of FliS with flagellins and flagellar related proteins is verified with biochemical analysis. The involvement of HP1076 in that particular interaction is also examined to further elucidate the biological roles of FliS and HP1076 in the flagellar assembly pathway. For the purpose of understanding biological role of HP1076, a proteomic study of the total cell lysate of wild-type and HP1076 null

mutant of *H. pylori* is performed to characterize the protein profiling when HP1076 is knock-down.

Here, our findings have provided biochemical and biophysical roles of export chaperone FliS and HP1076 in *H. pylori*. Our results also provide more information on the divergence of flagellar system in *H. pylori* and related bacteria. In the long term, understanding of the molecular mechanism of flagellar assembly pathway would provide more insights into the export chaperones in type III secretion system and to the therapeutic therapy of the bacteria infection.

Chapter 2 Material and Methods

2.1 Molecular cloning

2.1.1 *Escherichia coli* expression vectors

pGEX-6p-3 (Amersham Biosciences, GE Healthcare) vector encodes fusion proteins with a glutathione-S-transferase (GST) tag at the N-terminal of proteins. The GST tag is removed by the PreScission™ protease which recognizes the cutting site between the GST tag and the multiple cloning sites. The vector contains ampicilin-resistant gene for selection.

pAC28m vector is modified from pET28-a vector (Novagen) that the thrombin cutting site between six polyhistidine (His_6) tag and *Nde*I site is removed and the multiple cloning site is reserved. The vector encodes a protein with a His_6 tag at the N-terminal that cannot be removed. The vector contains kanamycin-resistant gene for selection.

2.1.2 *E. coli* strains

DH5α (GIBCO) is commonly used for molecular cloning for DNA preparation. The genotype is F-φ80*lac*ZΔM15Δ(*lac*ZYA-*arg*F)U169 *rec*A1 *end*A1 *hsd*R17(rk-, mk+)*pho*A *sup*E44 *thi*-1 *gyr*A96 *rel*A1 λ-. Blue/white colony selection can be

performed as the *lac*ZΔM15 marker provides the α-complementation of the β-galactosidase gene. Replication of M13mp vectors but not plaque formation is supported with the cells. Mutation of endA1 produces higher yield of plasmid preparation and mutation of recA1 increase the insert stability. The strain does not harbor any antibiotic-resistant DNA.

Rosetta 2 (R2) (Novagen) is a BL21 derivative with the genotype as F- *ompT* *hsd*SB(RB-mB-) *gal dcm* λ(DE3 [*lac*I lacUV5-T7 gene 1 *ind*1 *sam*7 *nin*5]) pLysS-RARE (CamR). The cell is used to enhance the expression of target proteins that contains codons rarely used in *E. coli*. The cells supply seven tRNAs for the codons AUA, AGG, AGA, CUA, CCC, GGA and CGG on a compatible chloramphenicol-resistant plasmid pRARE (Novy *et al.*, 2001). The strain is chloramphenicol-resistant.

B834 (DE3) (Novagen) is the parental strain for BL21. The phenotype is F⁻ *ompT* *hsdS*$_B$ (r_B^- m_B^-) *gal dcm met* (DE3). The cell is deficient of lon and ompT protease. The cell is a lysogne of bacteriophage λDE3 which carries the T7 RNA polymerase gene under the control of lacUV5 promoter. Upon the addition of Isopropyl β-D-thiogalactoside (IPTG), the protein would be expressed. The cell is also methionine auxotroph that allows high specific labeling of the protein with selenomethionine or ^{35}S-methionine for crystallography. The strain does not harbor

any antibiotic-resistant DNA.

2.1.3 Design of primer

To amplify the target genes (full-length coding sequence of *fliS, hp1076, fliD, flgK, fliH, fliI* and fragments of *hp1076, flaAc(1255-1533bp), flaBc(1240-1545bp)*, a pair of primers is designed based on coding sequences obtained from PubMed (http://www.pubmed.com). The forward primer contains the 5' end of sequence, while reverse primer is complementary to the 3' end of sequence. The primer contains around 20-30 nucleotides with Tm (melting temperature) above 65 °C, which Tm is the temperature required to separate half of the complementary nucleotides from each other. GC content of the primer is about 50%. Specific sequences of restriction enzyme are introduced to the primers for cloning into expression vector. A flanking region of 6 random nucleotides is added to the primer to facilitate the cleavage by restriction enzymes. Primers are ordered and manufactured from Invitrogen Company.

2.1.4 Amplification of DNA by PCR (polymerase chain reaction)

The target genes were amplified from genomic DNA of *Helicobacter pylori* strain 26695 (American Type Culture Collection). The reaction was prepared in Table 2.1 and performed with thymocycler (Eppendorf) as Table 2.2 with heat lid at 105 °C to avoid evaporation of the reaction mixture. The annealing temperature was 5 °C below the Tm of primers. The time for elongation depended to length of gene to be amplified, that the polymerization rate of DNA polymerase is generally 1 kb/min. The reaction buffer and DNA polymerase were obtained from Expand® High fidelity PCR system (Roche).

Table 2.1 Composition of PCR reaction mixture

Component	**Volume**
Template (*H. pylori* strain 26695 genomic DNA)	1 µl
Forward primer (10 µM)	3 µl
Reverse primer (10 µM)	3 µl
2mM dNTPs	5 µl
10 X Reaction buffer with $MgCl_2$	5 µl
Sterilized ddH_2O	32 µl
DNA polymerase (Expand High Fidelity PCR system, 3.5 U/µl)	1 µl
Total	50 µl

Table 2.2 PCR profile

		Temperature (°C)	Time	No. of Cycle
Initial Denaturation		95	2 min	--
Thermal Cycle	Denaturation	94	50 sec	35
	Annealing	Variable	50 sec	
	Elongation	72	Variable	
Final Extension		72	10 min	--
Cooling and storage		4	∞	--

2.1.5 DNA agarose gel electrophoresis

2.1.5.1 Tris-acetate-EDTA (TAE) buffer

TAE buffer was prepared as 50X stock solution by dissolving 242 mg Tris (USB), 57.1 ml acetic acid and 100 ml 0.5 M EDTA (USB) with distilled water. The pH was adjusted to 8.0.

2.1.5.2 Preparation of agarose gels

1% agarose gel was prepared by adding 0.5 g agarose powder (USB) in 1X TAE buffer. The powder was dissolved completely with the heat in microwave oven. After cooling, ethidium bromide solution was added to a final concentration of 0.5 μg/ml before gel setting.

2.1.5.3 6X DNA loading dye

The 6X DNA loading dye was prepared by mixing 0.25 g bromophenol blue (Sigma), 0.25 g xylene cyanol FF (Sigma) and 30 ml glycerol (Sigma) with sterilized distilled water in a final volume of 100 ml. The loading dye was stored at 4 °C.

2.1.5.4 DNA gel electrophoresis

The PCR reaction mixture was mixed with appropriate amount of 6X DNA loading dye. DNA samples and 1 kb DNA ladder (Invitrogen, Favorgen) were loaded into the wells of the agarose gel in a tank containing 1X TAE buffer. The tank was connected to a power pack with a constant voltage of 120 V. The electrophoresis was stopped when the dye front reached 2/3 of the gel. The gel was placed onto a transilIluminator (wavelength of 302 nm) to visualize the ethidium bromide-stained DNA with Ultra-violet light. Gel photo was then taken.

2.1.6 DNA extraction from agarose gel

The visible band detected by Ultra-violet light was excised with a razor blade. The DNA was extracted according to standard protocol of QIAquick Gel Extraction Kit (Qiagen). Gel slice was dissolved in QG buffer in a 1.5 ml centrifuge tube at 50 °C. The dissolved gel solution was loaded to a spin column and centrifuged at 13,000 rpm for 1 min in Eppendorf bench top centrifuge Model 5415D. DNA fragments were allowed to bind to the column and flow-through was discarded. The column was washed with 0.5 ml QG buffer and later with 0.75 ml PE buffer. Residual ethanol in spin column was removed by centrifugation for additional 2 min. Finally, the DNA was eluted out by TE buffer (10 mM Tris-HCl at pH 8, 1 mM EDTA) by

centrifugation with the above condition.

2.1.7 Restriction enzyme digestion

The purified PCR product and expression vector were digested with specific enzymes (New England BioLabs Inc.) at 37 °C for 3 hr. A common buffer suitable for both enzymes was used as suggested by the manufacturer. After 2-hr digestion, alkaline phosphatase was added to the digested vector to minimize the self-annealing of vector. The reaction mixture was prepared as shown in Table 2.3. Different combination of enzymes used for each target gene was shown in Table 2.4. After digestion, the DNA was purified by QIAquick PCR Purification Kit (Qiagen) according to standard protocol. In general, 5X volume of PB buffer was mixed with the reaction mixture and filtered with a spin column. 0.75 ml PE buffer containing ethanol was applied to spin column. Residual ethanol was removed by additional centrifugation step. At last, digested DNA was eluted out with TE buffer.

Table 2.3 Composition of reaction mixture for restriction enzyme digestion

	PCR product reaction	Expression vector reaction
DNA	25 μl	10 μl
10X NEB buffer	5 μl	5 μl
10X BSA	5 μl	5 μl
Enzyme 1	1.5 μl	1.5 μl
Enzyme 2	1.5 μl	1.5 μl
Sterilized ddH_2O	12 μl	27 μl
Total	50 μl	50 μl

Table 2.4 Restriction enzymes used for target genes

Target gene	Enzyme 1	Enzyme 2	Buffer	Vector
fliS (hp0753)	*BamH*I	*Not*I	NEB buffer 3*	pGEX-6p-3
hp1076	*Nde*I	*Not*I	NEB buffer 3*	pAC28m
flaAc(hp0601)	*BamH*I	*Not*I	NEB buffer 3*	pGEX-6p-3
flaBc(hp0115)	*BamH*I	*Not*I	NEB buffer 3*	pGEX-6p-3
fliD (hp0752)	*BamH*I	*Not*I	NEB buffer 3*	pGEX-6p-3
flgK (hp1119)	*BamH*I	*Not*I	NEB buffer 3*	pGEX-6p-3
fliH (hp0353)	*BamH*I	*Not*I	NEB buffer 3*	pGEX-6p-3
fliI (hp1420)	*BamH*I	*Not*I	NEB buffer 3*	pGEX-6p-3

* NEB buffer 3: 50 mM Tris-HCl, 100 mM NaCl, 10 mM $MgCl_2$, 1 mM DTT, pH7.9

2.1.8 Construction of recombinant plasmid DNA

The digested PCR product and vector with sticky ends were ligated with T4 DNA ligase (New England BioLabs Inc.) as shown in Table 2.5. A negative control reaction was set up without the PCR product to check the effectiveness of restriction enzymes. The ligation was performed at 16 °C for 16 – 18 hr.

Table 2.5 Composition of reaction mixture for ligation

	Reaction	Negative control
PCR product	15 µl	--
Vector	2 µl	2 µl
10X T4 DNA ligase buffer*	2 µl	2 µl
T4 DNA ligase (400 U/µl)	1 µl	1 µl
Sterilized ddH_2O	--	15 µl
Total	20 µl	20 µl

* 1x T4 DNA ligase buffer: 50 mM Tris-HCl, 10 mM $MgCl_2$, 1 mM ATP, 10 mM DTT, 25 µg/ml BSA, pH7.5

2.1.9 Culture medium for *E. coli*

2.1.9.1 Luria Broth (LB) medium

LB medium was prepared by dissolving 20 g LB powder (USB) in 1 L distilled water. The medium was then autoclaved at 121 °C for 20 min.

2.1.9.2 LB agar plate

LB agar was prepared by dissolving 14 g LB agar powder (USB) in 400 ml distilled water. After autoclaved at 121 °C for 20 min, the LB agar solution was cooled down to around 50 °C. Then antibiotics, 100 µg/ml ampicillin (USB) or 33 µg/ml kanamycin or 34 µg/ml chloramphenicol were added to the agar solution. About 10-15 ml of solution was poured to a 90 mm petri dish (Kofa Enterprise Ltd.) and allowed to be solidified at room temperature.

2.1.9.3 Antibiotics

Ampicilin (USB) powder was dissolved in sterilized dd$H_2$0 at a concentration of 100 mg/ml as 1,000X stock solution. The solution was filter-sterilized with 0.2 µm filter (Sartorius) and stored at -20 °C. The stock solution was thawed at room temperature and used as 1X concentration (e.g. 1 ml stock solution to 1 L LB).

Kanamycin (Invitrogen) powder was dissolved in sterilized dd$H_2$0 at a

concentration of 33 mg/ml to prepare a 1,000X stock solution.

Chloramphenicol (Armersham) powder was dissolved in ethanol at a concentration of 34 mg/ml to prepared a 1, 000X stock solution.

2.1.10 Preparation of *E. coli* competent cells

2.1.10.1 Transformation buffers

TFB1 was prepared by dissolving 12 g RbCl, 9.9 g $MnCl_2 \cdot 4H_2O$ and 1.5 g $CaCl_2 \cdot 2H_2O$ in 700 ml sterilized ddH_2O with 30 ml 1M KOAc and 150 ml glycerol. The pH was adjusted to 5.8 with acetic acid. The solution was brought up to 1 L with ddH_2O and filter-sterilized into a sterilized container and stored at 4 °C.

TFB 2 was prepared by dissolving 1.2 g RbCl and 11 g $CaCl_2 \cdot 2H_2O$ in 700 ml sterilized ddH_2O with 150 ml glycerol. The pH was adjusted to 6.8 with NaOH and the solution was brought up to 1 L with ddH_2O and filter-sterilized.

2.1.10.2 Preparation protocol

Different competent cells used in this study were prepared with the same protocol. Frozen glycerol stock at -80 °C of DH5α and B834(DE3) was streaked on LB agar plate without antibiotics and on LB agar plate with chloramphenicol for Rosetta 2 cells. The plates were incubated at 37 °C for 16 hr. Single colony was

picked and inoculated into 5 ml LB medium with gentle shaking. About 2-hr of shaking, the OD_{600} reached about 0.3-0.5. The staring culture was inoculated into 200 ml LB medium for shaking until OD_{600} reached 0.3-0.5. The cells were harvested by centrifugation at 2,500 rpm for 15 min at 4 °C. The supernatant was discarded and the pellet was resuspended in 80 ml TFB 1 buffer. The cell suspension was chilled on ice for 15 min and pellet again with the same setting. The cell pellet was resuspended in 8 ml TFB 2 buffer and incubated on ice for 15 min. The competent cell suspension was aliquot into microfuge tube for storage at -80 °C.

2.1.11 Transformation of ligation product into *E. coli* DH5α cell

100 µl *E. coli* DH5α competent cell frozen at -80 °C was thawed on ice for 5 min. 20 µl ligation product or negative control was added and gently mixed with the cells. The cell suspension was left on ice for 20 min. The cells were heat-shocked at 42 °C for 90 sec to allow the circular plasmid DNA to enter the cells. Then the cells were chilled on ice for 1 min. 400 µl LB medium was added to the cells for recovery at 37 °C for 1 hr. After recovery, the cells were centrifuged at 8,000 rpm for 1 min. The supernatant was discarded while the pellet was resuspended with 100 µl LB medium and spread evenly on LB agar plate with appropriate antibiotic for selection. The LB agar plates were incubated at 37 °C for 16-18 hr.

2.1.12 PCR screening of colonies

The colonies on the agar plate were firstly selected by the appropriate antibiotics. The colonies grown on the plate of negative control reaction contained plasmid with incomplete enzyme digestion. The colonies grown for the ligation reactions contained the recombinant plasmid or empty vectors. In order to identify the recombinant plasmid, single colony was picked with a sterilized pipette tip and grown in 5 ml LB medium at 37 °C for 16-18 hr. The overnight-culture was used as the template for PCR check with primers specific to the target gene performed as stated in section 2.1.4. The PCR product was analyzed with agarose gel electrophoresis as stated in section 2.1.5. A band with the same size of the target gene confirmed the insertion of target gene into the vector.

2.1.13 Preparation of plasmid DNA

The recombinant plasmid DNA was prepared with QIAPREP Spin Miniprep Kit (Qiagen) with standard protocol. The cell of the positive clone was harvested from the cell culture by centrifugation at 13,000 rpm for 1 min. The cell pellet was resuspended with 250 µl chilled Buffer P1 (50 mM Tris-HCl pH 8.0, 10 mM EDTA) with RNase A. 250 µl cell lysis buffer (200 mM NaOH, 1% (w/v) SDS) was then mixed gently with cell suspension and allowed for incubation of 5 min. 350 µl

neutralization buffer (5M potassium acetate solution, pH 4.8) was added and mixed thoroughly by inverting. The mixture was centrifuged at 13,000 rpm for 10 min. The supernatant was loaded into a spin cartridge placed in a 2-ml collection tube. After centrifugation at 13,000 rpm for 1 min, the flow-through was discarded. 700 µl wash buffer (10 mM Tris-HCl pH7.5, 1 mM EDTA, 70% ethanol) was added to the spin cartridge. Residual ethanol was removed by centrifugation for another 2 min. 50 µl TE buffer (10 mM Tris-HCl pH 8, 1 mM EDTA) was added to the centre of the membrane of spin cartridge and allowed to stand for 1 min. At last, the plasmid DNA was eluted out as flow-through by centrifugation.

The purified recombinant plasmid DNA was sent out for sequencing (TechDragon Ltd.; 1st BASE sequencing, Life Scientific Health Care & Co.; BGI) to check if undesirable mutation was introduced to target genes.

2.1.14 Fragment construction of *hp1076*

The fragment of *hp1076* was designed based on the secondary structure prediction, PredictProtein (Rost *et al.*, 2004). Full-length protein sequence of HP1076 was submitted to program, a result on structural and functional prediction was generated which included PROSITE sequence motif (Bairoch *et al.*, 1997), low-complexity regions (SEG) (Wootton and Federhen, 1996), regions lacking

regular structure (NORS), predictions of secondary structure (PHDsec) (Rost and Sander, 1993), solvent accessibility (PHDacc) (Rost and Sander, 1994), globular regions (GLOBE), sub-cellular localization and functional annotations. The forward primers were designed complementary to the 5'end of the fragment and a stop codon, TAG was introduced to reverse primer if necessary. Same molecular cloning steps were followed to produce the clones.

2.1.15 Site-directed mutagenesis

Site-directed mutagenesis is a technique used for protein structure-function relationship study especially for some essential residues required for interaction or protein folding. This approach is used to make point-mutation, delete or insert amino acid to target genes on the DNA plasmid.

In this study, different mutants of GST-FliS, His_6-1076 and His_6-1076ΔN20 were created according to standard protocol of QuickChange™ Site-Directed Mutagensis Kit (Stratagene). The specific pairs of primers were designed based on some considerations, (a) the desired mutation should be located in the middle of the primer, (b) the primers should be between 25-45 bases in length with Tm greater than 70 °C, (c) The primer should be terminated with C or G bases. The reaction mixture was prepared as shown in Table 2.6. The reaction was performed with thermocycler

as stated in Table 2.7. The number of cycle was depended on type of desired mutation, 12 cycles were performed with point mutations and 16 cycles were required for single amino acid change.

The reaction mixture after the thermo-cycle was chilled on ice for 2 min to reduce the temperature to about 37 °C. 1 µl of *Dpn*I restriction enzyme (10 U/µl) (New England BioLabs Inc.) was added and incubate at 37 °C for 1 hr to digest the parental DNA plasmid. 5 µl of reaction mixture was transformed into DH5α competent cells as stated in section 2.1.11. The colonies were sent out for sequencing to confirm the mutation.

Table 2.6 Composition of reaction mixture for site-directed mutagenesis

	Reaction
DNA plasmid (5-50 ng)	~1 µl
10X reaction buffer	5 µl
Primer 1 (125 ng)	~ 1 µl
Primer 2 (125 ng)	~ 1 µl
dNTP mix	1 µl
Sterilized ddH_2O	40 µl
Pfu Turbo DNA polymerase (2.5 U/µl)	1 µl
Total	50 µl

Table 2.7 Reaction profile of site-directed mutagenesis

		Temperature (°C)	Time	No. of Cycle
Initial Denaturation		95	30 sec	--
Thermal Cycle	Denaturation	95	30 sec	12-16
	Annealing	55	1 min	
	Elongation	68	2 min/kb of plasmid length	

2.2 Protein expression

pGEX-6p-3-fliS, pAC28m-hp1076 and pAC28m-hp1076 fragments plasmids were used for the *E. coli* expression system. pGEX-6p-3-fliS was expressed as GST-tagged FliS fusion protein (GST-FliS), while pAC28m-hp1076 was expressed as His_6-tagged HP1076 fusion protein (His_6-HP1076).

2.2.1 Isopropyl β-D-thiogalactoside (IPTG)

IPTG (GE Healthcare) powder was dissolved in sterilized ddH_20 at a concentration of 0.1 M as 1,000X stock solution. The stock solution was filter-sterilized with 0.2 μm filter and stored at -20 °C.

2.2.2 Protein expression of GST-FliS, His_6-HP1076 and fragments

The plasmid was transformed into Rosetta 2 (R2) cells separately with the procedures as described in section 2.1.11. The colonies were grown on LB agar plate with appropriate antibiotics (ampicillin for pGEX-6p3-fliS and kanamycin for pAC28m-hp1076 and fragment clones) at 37 °C for 16 hr. The colonies were detached from the agar plate with LB medium supplemented with antibiotics. The cell suspension was inoculated into 4 L LB medium with antibiotics at a concentration of 5% of medium. The cells were grown at 37 °C with shaking at 250

rpm until the OD_{600} reached 0.4-0.6, which was the log phase of bacterial growth. If the expression temperature was at 37 °C, a final concentration of 0.1mM IPTG was added and the cells were shaked for additional 3-4 hr. If the expression temperature was below 25 °C, the cell culture was cooled down before addition of IPTG. And the cells were shaked for additional 16-18 hr for protein expression.

2.2.3 Protein expression of selenomethionine-substituted (SeMet) His_6-HP1076ΔN20

pAC28m-hp1076ΔN20 was transformed into *E. coli* B834 (DE3) cells and grown in LB medium at 37 °C overnight. Cells were pelleted and washed with sterilized ddH_2O for three times. Cells were then resuspened in water and inoculated to minimal medium (medium base and nutrient mix) containing selenomethionine according to manufacturer's protocol (Molecular Dimensions Limited). The cells were grown overnight at 25 °C with 0.1 mM IPTG induction.

2.2.4 Co-expression of GST-FliS and His_6-HP1076 or fragments

2 plasmids, pGEX-6p-3-fliS and pAC28m-hp1076 were co-transformed into R2 cells as described in section 2.1.11 (Kholod and Mustelin, 2001). Expression condition was the same as above.

2.3 Protein purification

Different proteins were partially purified from total cell lysate with affinity chromatography and further purified with gel filtration column. The chromatographic columns were operated manually or computationally with ÄKTAprime™ purification system (Amersham). Buffers and samples were filtered with 0.22 μm filter before loading to columns to reduce the blockage of the column system. To reduce the degradation of proteins during purification, protease inhibitors, 0.2 mM PMSF (dissolved in ethanol) and 0.2 mM benzamidine (dissolved in distilled water), were added in buffer before use and the buffer and samples should be kept on ice. The buffers used are summarized in Table 2.8. The purified proteins were used for assays or stored at -80 °C in small aliquots.

Table 2.8 Composition of buffers used in purification

Buffer name	Composition
(a) Purification of GST-FliS and FliS	
GST binding buffer	10 mM Tris, 500 mM NaCl, 2 mM DTT, 0.5 mM EDTA, pH 7.5
GST elution buffer	10 mM Tris, 500 mM NaCl, 2 mM DTT, 0.5 mM EDTA, 20 mM reduced-glutathione pH 7.5
GST low-salt buffer	10 mM Tris, 150 mM NaCl, 2 mM DTT, 0.5 mM EDTA, pH 7.5
S75 gel filtration buffer	10 mM Tris, 150 mM NaCl, 2 mM DTT, 0.5 mM EDTA, pH 7.5
(b) Purification of His_6-HP1076 or fragments or SeMet His_6-HP1076ΔN20	
Ni binding buffer	10 mM Tris, 500 mM NaCl, 20 mM imidazole, pH8.0
Ni elution buffer	10 mM Tris, 500 mM NaCl, 200 mM imidazole, pH8.0
Q sepharose binding buffer	10 mM Tris, 100 mM NaCl, 2 mM DTT, 0.5 mM EDTA, pH7.5
Q sepharose elution buffer	10 mM Tris, 1 M NaCl, 2 mM DTT, 0.5 mM EDTA, pH7.5
S75 gel filtration buffer	10 mM Tris, 150 mM NaCl, 2 mM DTT (4 mM DTT for SeMet protein), 0.5 mM EDTA, pH 7.5
(c) Purification of FliS/HP1076 complex	
Co-Ni binding buffer	10 mM Tris, 300 mM NaCl, 200 mM imidazole, pH 8.0
Co-Ni elution buffer	10 mM Tris, 300 mM NaCl, 200 mM imidazole, pH 8.0
Co-GST binding buffer	10 mM Tris, 300 mM NaCl, 2 mM DTT, 0.5 mM EDTA, pH 7.5
Co-GST low-salt buffer	10 mM Tris, 150 mM NaCl, 2 mM DTT, 0.5 mM EDTA, pH 7.5
S75 gel filtration buffer	10 mM Tris, 150 mM NaCl, 2 mM DTT, 0.5 mM EDTA, pH 7.5

2.3.1 Affinity chromatography with glutathione sepharose

The Glutathione Sepharose™ 4 Fast Flow beads (GE Healthcare) was used to purify the GST-tag fusion protein. The sepharose beads were packed in a glass Econo-Column® (BioRad) and whole purification was performed on bench. The sepharose was washed with 5 bed volumes of water and equilibrated with GST binding buffer. The filtered supernatant from total cell lysate was allowed for binding at 4 °C for 3 hr with rocking. After binding, the impurities were washed with buffer by gravity flow until no protein was detected in Bradford assay.

If untagged protein was prepared, the sepharose was then equilibrated with GST low-salt buffer. GST-tagged PreScission™ Protease was added to cleave the GST tag after overnight incubation. GST tag would bind to sepharose, while the untagged protein was eluted out. If GST-tag fusion protein was prepared, buffer supplemented with 20 mM reduced glutathione (USB) was used to elute fusion proteins.

2.3.2 Affinity chromatography with Ni-NTA sepharose

Ni-NTA (Nitrilotriacetic acid) agarose (Qiagen) was used to purify proteins with His_6-tag. NTA captured the nickel ions on the agarose and binds to the 6-histidine tag. The agarose was packed into XK16/20 column (Amersham) and washed with distilled water. The column was equilibrated with 5 bed volumes of Ni binding buffer

before sample loading. DTT and EDTA should be avoided due to strong reducing ability and metal-chelating ability respectively that affect the binding affinity of agarose. Sample was loaded to the column at 1 ml/min by a bench-top Peristaltic Pump P-1 (Amersham). 20 mM imidazole was added in binding to reduce non-specific binding. Impurities were washed away until no protein was detected in Bradford dot test. The bound proteins were then eluted out with a gradient of 20-200 mM imidazole by ÄKTAprime™ system in 10 bed volumes of elution buffer.

2.3.3 Anion exchange chromatography with Q-sepharose

Q Sepharose™ Fast Flow sepharose (GE Healthcare) was used for further purification of proteins. When the pH of buffer is higher than the pI of protein, the protein would become negatively charged. The proteins would bind to sepharose while other impurities with different pIs would be washed away. The sepharose was packed in a XK16/20 column (Amersham) and washed with distilled water. Sample was loaded with Peristaltic P-1 pump at a flow rate of 1 ml/min to equilibrated column. Unbound proteins were washed away until no protein detected by Bradford dot test assay. Proteins were eluted at a flow rate of 1 ml/min with a gradient of 0.1 – 1 M NaCl operated by ÄKTAprime™ system.

2.3.4 Size-exclusion chromatography

Proteins were separated based on the difference in size and shape. Proteins with larger size and shape would pass through the pores of resin faster than smaller and globular protein. Aggregated proteins would be eluted out in the void volume. This method was used to separate partially purified proteins from impurities. HiLoad 16/60 Superdex 75 Prep Grade (Amersham) column was connected to ÄKTA prime™ system in a cool room at 4 °C, which was firstly equilibrated with a bed-volume (120 ml) of low-salt buffer. Then partially purified protein from affinity chromatography was concentrated into around 2 ml protein solution and injected to column. Proteins were eluted at 1 ml/min for 120 ml and collected in 1-ml fraction.

2.3.5 Purification strategy of GST-FliS

4 L cell culture was harvested with centrifugation at 6,000 rpm for 15 min with Avanti® J-E Centrifuge System (Beckman). The supernatant was discarded and the pellet was resuspended with cold GST binding buffer. The cell suspension was lysed by sonication (Sonopuls) with the set-up as 30 sec per cycle, 15 sec in between each cycle and 80% of power output. The cell suspension should be kept on ice as heat was generated in the process. The total cell lysate was then centrifuged at 20,000 rpm at 4 °C for 1 hr with the same centrifugation system to remove the cell debris and

inclusion body. The supernatant was then filtered with 0.45 μm filter (Sartorius) and allowed to bind with equilibrated glutathione sepharose at 4 °C for 2 hr with rocking. GST-FliS would be bound to the sepharose and flow-through was collected to analyze the binding affinity of proteins with SDS-PAGE. The impurities were washed with binding buffer until no protein detected by Bradford dot test. Then GST elution buffer was added to collect the GST-FliS proteins in 3-ml fractions. Fractions were analyzed by SDS-PAGE, and then fractions containing the GST-FliS would be concentrated into 2-ml solution with Amicon® ultra-15 (Millipore) by centrifugation at 4,000 rpm at 4 °C. The sample was then injected into the Superdex ™ S75 column equilibrated with S75 gel filtration buffer. Fractions were collected by ÄKTA prime™ system at a flow rate of 1 ml/min and were further analyzed on SDS-PAGE to identify the purified proteins with single band. Finally, the purified proteins were concentrated for further analysis or storage at -80 °C in small aliquots.

2.3.6 Purification strategy of FliS

Purification of FliS was firstly purified with total cell lysate over-expressing GST-FliS proteins. After binding of the GST-FliS to glutathione sepharose and washing to remove impurities, the column was equilibrated with GST low-salt buffer. This step was done because PreScission™ Protease worked best at low-salt condition.

GST-tagged PreScission™ Protease was added to sepharose in about 3 ml buffer and allowed for digestion (cutting site was in between GST-tag and FliS) overnight. After digestion, the untagged FliS was collected as flow-through while the GST and Protease would be bound on sepharose. The fractions contains FliS proteins were concentrated for separation with Superdex™ S75 column. The fractions with purified FliS proteins were identified by SDS-PAGE and concentrated for assay or storage.

2.3.7 Purification strategy of His_6-HP1076 and fragments

The cells over-expressing His_6-HP1076 proteins or fragment proteins were pelleted and lysed by sonication in Ni binding buffer. The supernatant was kept on ice and loaded to equilibrated column with a bench-top Peristaltic Pump P-1 at a flow-rate of 1 ml/min. The His-tagged protein would bind on column and impurities were washed with buffer. 20 mM imidazole was added in buffer to reduce non-specific binding. The proteins were eluted with a continuous gradient of imidazole from 20-200 mM at a flow-rate of 1 ml/min with the ÄKTAprime™ system. 2 mM DTT and 0.5 mM EDTA were added to the eluted fractions to prevent protein degradation. Fractions containing His_6-HP1076 were identified by SDS-PAGE analysis and concentrated into small volume for anion-exchange chromatography. As salt concentration was the elution parameter, so the concentrated

protein in 500 mM NaCl buffer was diluted with 10 mM Tris, pH8.0 buffer to reduce the salt concentration to 50 mM NaCl. The diluted protein sample was loaded to equilibrated Q-sepharose column with the same method as Ni-NTA chromatography. Proteins were eluted with a continuous gradient of salt from 100 mM to 1 M in 1-ml fraction at a flow-rate of 1 ml/min. Fractions containing His_6-HP1076 proteins were concentrated for Superdex^{TM} 75 gel filtration. Finally, the purified protein was identified and concentrated.

2.3.8 Purification strategy of SeMet His_6-HP1076ΔN20

The cells expressing SeMet His_6-HP1076ΔN20 fragment protein were pelleted and lysed with sonication. Supernatant was loaded to Ni-NTA agarose column and eluted with a continuous gradient of imidazole from 20 to 200 mM. 4 mM DTT was added to the fractions to reduce reduction of the selenomethionine groups. The fractions containing the proteins were concentrated and further purified with Superdex^{TM} 75 gel filtration with the same setting as native protein. And again buffer containing 4 mM DTT was used for elution. The purified proteins were concentrated for crystallization.

2.3.9 Purification strategy of FliS/HP1076 complex

Pellet with expressed protein complex was lysed by sonication on ice with a buffer of 300 mM NaCl. Lower the salt concentration in binding buffer which helped to reduce chance of disturbing the protein interaction as the mode of interaction was still unknown. The supernatant was loaded to pre-equilibrated Ni-NTA column and eluted with same set-up as His_6-HP1076 proteins. His-tagged protein complex was eluted into 1 ml fraction with a gradient of imidazole. The presence of protein complex was identified by SDS-PAGE. 2 mM DTT and 0.5 mM EDTA was added to protein complex and allowed to bind with glutathione sepharose overnight at 4 °C with rocking. GST-FliS was bound on column with His_6-HP1076 and impurities were washed with buffer. PreScission™ Protease was added for digestion overnight in low-salt buffer condition. Fractions containing FliS/HP1076 complex were identified by SDS-PAGE and concentrated for Superdex™ 75 gel filtration. Fractions with purified protein complex were concentrated for crystallization.

2.4 Protein detection

2.4.1 Bradford dot test

This assay was used for general detection of presence of protein washed out during purification. Bradford assay reagent was prepared from the 5X stock of

protein assay dye reagent (BioRad). 30 µl reagent was mixed with 5 µl of testing solution on a parafilm (Whatman). The reagent was changed from brown to blue color indicating that protein was present in the solution.

2.4.2 Protein quantification with Bradford Assay

This assay was adopted to determine the concentration of purified protein or total protein in cell lysate. 1 ml of 1X Bradford assay reagent was mixed with 1 µl of protein in a 1-ml plastic cuvette and allowed to incubate at room temperature for 5 min. The Coomassie Brilliant Blue G-250 dye binds to arginine and aromatic residues and this binding would be resulted in a shirt of absorbance maximum from 470 nm to 595 nm (Bradford, 1976). The absorbance at 595 nm was measured against the blank with reagent only, the intensity of blue color was directly proportional to protein concentration.

2.4.3 Protein quantification with absorption at 280 nm

This assay was adopted to determine the concentration of purified protein in isothermal titration calorimetry. The absorbance at 280 nm depends on the content of tryptophan, tyrosine and cystine with disulfide bonds (Pace *et al.*, 1995). The extinction coefficient of protein (ε) was determined with known protein sequence by

ProtParam tool from ExPASy Server (Gasteiger *et al.*, 2005). 2 µl protein was mixed with 498 µl distilled water in quartz cuvette and absorbance at 280 nm was measured using water as blank. The concentration of protein was calculated with the following equation,

$$\text{Concentration of protein (Molar)} = \frac{\text{Absorbance at 280 nm}}{\varepsilon \cdot \text{cuvette path length}} \times \text{dilution factor}$$

2.4.4 Sodium dodecyl sulphate polyacrylamide gel electrophoresis (SDS-PAGE)

This method was used to detect the purity of proteins in purification and to analyze the results of biochemical assays. Proteins were denatured with heating and anionic detergent, SDS. SDS bound to protein with identical mass to charge ratio, making the protein become linear. Therefore, separation of the protein mixture in the gel depends on the size of protein. Proteins on the gels were visible by staining and destaining methods.

2.4.4.1 Gels for SDS-PAGE

The gel was consisted of two layers, stacking and separating gels. The upper layer was the stacking gel containing a low concentration of acrylamide and sample wells. This helped to compress the protein samples into a thin layer before entering the separating gels. The bottom layer was the separating gel that helped to separate

protein samples according to size. The resolution of separation was depended on concentration of acrylamide. A high percentage of acrylamide of 12-15% was required to separate proteins with molecular weight below 30 kDa. The components of preparation of gels are shown in Table 2.9. The apparatus were from Mini-PROTEAN® 3 system (BioRad).

Table 2.9 Composition of SDS-PAGE

Stacking gel (5 ml)		Separating gel (5 ml)			
			15 %	12 %	10 %
Distilled water	3.4 ml	Distilled water	1.1 ml	1.6 ml	1.9 ml
30% Acrylamide/bis mix	830 µl	30% Acrylamide/bis mix	2.5 ml	2 ml	1.7 ml
Tris (1 M, pH 6.8)	630 µl	Tris (1.5 M, pH 8.8)	1.3 ml	1.3 ml	1.3 ml
10% SDS	50 µl	10% SDS	50 µl	50 µl	50 µl
10% Ammonium persulfate	50 µl	10% Ammonium persulfate	50 µl	50 µl	50 µl
TEMED	5 µl	TEMED	2 µl	2 µl	2 µl

2.4.4.2 Electrophoresis buffer

Electrophoresis buffer was prepared as 10X stock solution, mixing with 30.2 g Tris, 187.6 g glycine and 100 ml 10% (w/v) SDS in 1 L distilled water. The pH of buffer was about 8.3.

2.4.4.3 5X SDS loading dye

5X SDS loading dye was prepared with 10% SDS, 0.313 M Tris-HCl (pH 6.8), 50% glycerol and 0.005% (w/v) bromophenol blue. 100 mM DTT solution was freshly added to the loading dye before use. Bromophenol blue provided the tracking of the gels during electrophoresis.

2.4.4.4 Electrophoresis

The gel cassette was assembled into the electrophoresis cell. The inner chamber was filled with fresh 1X electrophoresis buffer. Protein samples were heat at 99 °C with appropriate SDS loading dye. Protein samples and protein ladder (SeeBlue® Plus 2, Invitrogen; LMW SDS marker kit, GE Healthcare) were loaded to the wells. The electrophoresis was performed at constant voltage at 220 V for 40 min until the dye front reached the bottom of gels. The gels were then detached from the gel cassette and stained with staining solution.

2.4.4.5 Coomassie brilliant blue staining solution

Staining solution was prepared with 0.25% (w/v) coomassie blue in 450 ml distilled water, 450 ml ethanol and 100 ml acetic acid. Coomassie blue dye bound to proteins making them become visible as blue in color.

2.4.4.6 Coomassie brilliant blue destaining solution

Destaining solution was prepared with 450 ml ethanol, 450 ml distilled water and 100 ml acetic acid. This helped to remove the dye bound on the gels, making the protein bands visible.

2.4.5 Western blot analysis

2.4.5.1 Transfer buffer stock

Transfer buffer stock was prepared as 10X stock solution with 29 g glycine, 58 g Tris, 37 ml 10% SDS in 1 L distilled water. The pH of buffer was adjusted to 8.3.

2.4.5.2 1X Transfer buffer

Transfer buffer was prepared with 100 ml 10X stock solution, 200 ml methanol and 700 ml distilled water. The buffer was freshly prepared before use.

2.4.5.3 PBST

PBST was prepared as 10X stock solution with 40 g of NaCl, 1 g of KCl, 13.4 g of $Na_2HPO_4 \cdot 7\ H_2O$ and 1.2 g of KH_2PO_4 in 590 ml distilled water. 1 ml Tween-20 was added to the 1X PBST buffer.

2.4.5.4 Electro-transfer blotting

The proteins separated on SDS-PAGE were transferred to be 0.45 μm Immobilon-P® polyvinylidene fluoride (PVDF) membrane (Millipore) with the mini Trans-Blot® electrophoretic transfer cell (BioRad). The PVDF membrane was firstly activated by soaking in methanol and rehydrated in transfer buffer. The filter paper (Whatman) and filter pad were soaked in transfer buffer for rehydration. The cassette was set up as shown in Fig.2.1. Blotting was performed at a constant current, 200 mA for 1 hr in transfer buffer.

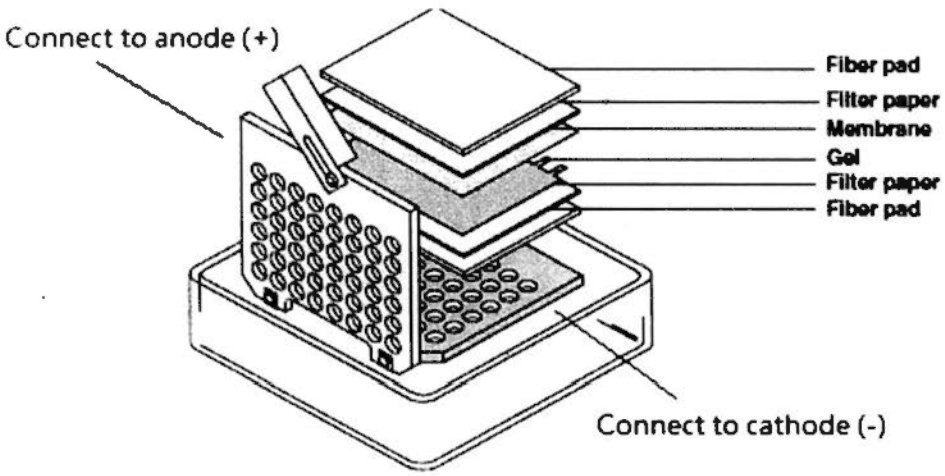

Fig.2.1 Assembly of cassette for electrophoretic transfer cell
It was modified from mini Trans-Blot® electrophoretic transfer cell Instruction Manual (Adopted from http://www.bio-rad.com/webroot/web/pdf/lsr/literature/M1703930.pdf).

2.4.5.5 Immunoblotting with antibodies

The membrane with transferred proteins was firstly soaked in 5 % (w/v) non-fat milk in PBST for 1 hr at 4 °C with rocking. Then the membrane was blotted with specific primary antibody targeting the protein of interest for 1 hr or overnight at 4

°C with rocking. The ratio of antibody used was according to the probing ratio (v/v) supplied from manufacturer. Washing steps with 3 cycles of 10 ml PBST for 10 min were carried out to remove non-specific or unbound antibody. Afterwards, horseradish peroxidase (HRP)-conjugated secondary antibody against the host of primary antibody was added for incubation for 1 hr at 4 °C. Then membrane was washed again with 3 cycles and subjected for detection.

2.4.5.6 ECL detection

The detection of bands was performed with ECL Plus Western Blotting Reagent (GE Healthcare). 1 ml of ECL solution A was mixed with 0.025 ml of solution B on a parafilm (Whatman). The membrane was immersed to the solution or 5 min for reacting with the HPR. The signal was detected with exposure to Fuji RX film (Fuji) with different time point according to the intensity of signal bands. The film was processed by film processor (Kodak).

2.5 Interaction assays

These assays aimed to study the interaction between purified FliS and HP1076 fragments. The interaction with other proteins (GST-FlaAc, GST-FlaBc, GST-FliD, GST-FlgK and GST-FliH) was performed with over-expression in cell lysate.

2.5.1 Pull-down assays

A) Purified GST-FliS and GST were immobilized on glutathione sepharose (GE Healthcare) in low-salt buffer (10 mM Tris, 150 mM NaCl, 0.2 mM PMSF, 0.2 mM benzamidine, pH 7.5) supplemented with 2 mM DTT and 0.5 mM EDTA for 1 hr, 4 ^{o}C with rocking. After washing away the unbound proteins, same molar ratio of His_6-HP1076 fragments was added for binding for additional 1 hr. Control reactions were set up with glutathione sepharose incubated with His_6-HP1076 only. After washing, proteins bound on sepharose were denatured with SDS-loading dye and heating. The result was analyzed by SDS-PAGE.

B) Similar reaction set-up was used with His_6-HP1076 fragments immobilized on Ni-NTA agarose (Qiagen) to interact with GST-FliS or GST in low-salt buffer supplemented with 20 mM imidazole to prevent non-specific binding. Control reaction was set up with Ni-NTA agarose incubated with GST-FliS only.

C) The interaction of GST-FlaAc or GST-FlaBc with FliS, HP1076 and complex was verified with pull-down assay using glutathione sepharose performed as indicated above.

2.5.2 Size exclusion chromatography assay

This method was used to compare the difference in elution property of single or protein complex. 200 μg of individual protein of FliS or His_6-HP1076 fragments was loaded to a Superdex 200 10/300 GL column (GE Healthcare) in low-salt buffer (10 mM Tris, 150 mM NaCl, 2 mM DTT, 0.5 mM EDTA, 0.2 mM PMSF, 0.2 mM benzamidine, pH 7.5). The proteins were eluted at 0.5 ml/min for 1 bed volume of 25 ml. Protein was collected at 0.5 ml-fraction and the elution profile was recorded by ÄKTA Prime™ system. While the protein mixture of FliS with His_6-HP1076 fragments was subjected for binding on ice for 30 min before injection into S200 column for separation. Same elution condition was performed. The elution volume of protein peak was compared and the fractions were analyzed by SDS-PAGE.

2.5.3 Isothermal titration calorimetry (ITC)

The ITC experiment was performed with MicroCal iTC200 calorimeter (GE Healthcare) at 25 °C. Purified proteins of FliS and His_6-HP1076ΔN20 were prepared in buffer (50 mM Tris, 50 mM NaCl, 2 mM DTT, 0.5 mM EDTA, 0.2 mM PMSF, 0.2 mM benzamidine, pH 7.5) as described in sections 2.3.6-2.3.7. The protein concentration was determined with Bradford Assay and absorption at 280 nm in duplicate. Proteins and buffer were degassed with centrifugation at 14,000 rpm for 5

min before each experiment. 25 μM FliS was loaded to the sample cell, and 390 μM His_6-HP1076ΔN20 was titrated into the cell in 20 injections of 1.5 μl with 180-sec intervals. Two blank experiments were performed; one with 250 μM His_6-HP1076ΔN20 titrated into buffer and another with buffer injected into 25 μM FliS. The heat of dilution was subtracted from experiments. Three independent experiments of FliS and His_6-HP1076ΔN20 were performed to determine the thermodynamic parameters with MicroCal Origin 7 software with fitting to one set of binding site model.

2.5.4 Co-expression and purification method

Two plasmids of wild-type or mutant protein (pGEx-6p3-fliS and pAC28m-hp1076) were co-transformed and expressed in *E. coli* R2 cells as stated in section 2.2.4. Cells over-expressing GST and His_6-HP176 were used as the control. Cells were harvested and lysed by sonication in lysis buffer (10 mM Tris, 300 mM NaCl, 0.2 mM PMSF, 0.2 mM benzamidine, pH 7.5). Cell debris was removed by centrifugation at 14,000 rpm, 4 °C for 20 min. Cell lysate was mixed with glutathione sepharose for binding at 4 °C for 2 hr. After washing with buffer, proteins bound on sepharose were eluted by 20 mM reduced glutathione and analyzed by SDS-PAGE. This method was also performed with cell lysate expressing His_6-FliS with

GST-FlaAc or GST-FlaBc or GST-FliD or GST-FlgK or GST-FliH or GST-FliI or GST to verify the interaction.

2.6 Chaperone-like activity assay

Bovine insulin (Sigma) was used as the substrate for chaperone assay as bonds between α and β chains of insulin was disrupted upon addition of DTT (Sanger, 1949), and this aggregation was reduced in the presence of chaperone proteins in the reaction mixture. This became a marker on measuring the chaperone ability of proteins. The experiment was performed according to the article of chaperone-like activity of synucleins (Souza *et al.*, 2000). Insulin was dissolved in 20 mM NaOH and diluted with 100 mM phosphate buffer, pH 7.0 to a final concentration of 0.15 mg/ml (26.5 μM). The reduction of insulin was achieved by adding 20 mM DTT in the presence or absence of different molar ratios of FliS, HP1076 or FliS/HP1076 complex. The extent of aggregation was monitored as a function of time to absorbance at 360 nm in a spectrophotometer (UV-1601, UV-visible spectrophotometer, Shimadzu) for 45 min at 25 °C.

2.7 Protein Crystallization

2.7.1 Crystallization screening

Highly purified proteins (over 90% of purity) were used for crystallization screening. The purity of proteins was determined in SDS-PAGE or size exclusion chromatography. Crystallization screening was performed with microbatch or sitting-drop methods with commercial screening kits. Index I and II (Hampton Research), Crystal screen I and II (Hampton Research) and Wizard I and II random sparse matrix crystallization screens (Emerald BioSystems) were the kits usually used which provided different combinations of salt, buffers, precipitants and pH.

Microbatch method (Fig.2.2A) allowed screening with 96 conditions on one plate. Usually 0.5 µl of protein was mixed with 0.5 µl kit solution inside a well. And the wells were covered by an oil layer which was composed of silicon oil and paraffin oil. Silicon oil was permeable which allowed evaporation of water between the atmosphere and protein droplet, while paraffin oil was non-permeable. When the water was evaporated slowly, the protein droplet became more concentrated to reach the supersaturation phase that favored the crystal formation. By adjusting the volume ratio of the two kinds of oils, the rate of water evaporation was controlled. The microbatch plates were then incubated at 16 or 20 °C.

Sitting-drop method (Fig.2.2B) was performed with 96-round well CrystalQuick

plate (Greinor Bio-One). 100 µl of kit solution was applied to the reservoir, where the protein and kit solution was mixed in different ratios in 3 wells. The plate was then sealed with Crystal Clear Sealing Tape (Hampton) and incubated at 16 or 20 °C. In this enclosed system, the concentration of kit solution in reservoir was higher than that of the protein droplets. During equilibration process, the protein concentration would increase which leaded to the movement from unsaturated phase to supersaturation phase where crystal formation may happen.

2.7.2 Optimization of crystallization conditions

When a crystal growth condition was found, the condition was optimized with crystallization buffer of different pH, precipitant concentration, salt concentration and incubation temperatures. This was performed with sitting-drop or hanging-drop vapor diffusion methods (Fig.2.2C) with Linbro plate (Hampton). Protein and crystallization buffer were mixed and added to siliconized glass circle cover slide. The cover slide was then sealed on a reservoir containing same crystallization buffer by high vacuum grease (Dow Corning).

Moreover, additive or detergent screens (Hampton) were used for optimization. A library of small molecules was provided to alter solubility and crystallization of samples, which might help to improve the quality and size of crystal.

Sometimes, microseeding method was used for improving the crystal quality (Ireton and Stoddard, 2004). Small protein crystals were transferred to a microfuge tube with crystallization buffer. Crystals were washed with buffer and pelleted at 3,000 rpm for 30 sec for two times. Then the crystal was resuspended in buffer and broken into smaller pieces as the seeds by vortexing. Crystallization plate was set-up a day before the microseeding by mixing protein and precipitant in 1:1 volume ratio with hanging-drop vapor diffusion method and incubated at the 16 °C. The seeds in 10% - 20% of total volume of droplet were transferred to the droplet pre-incubated with protein and precipitant and incubated at the same temperature.

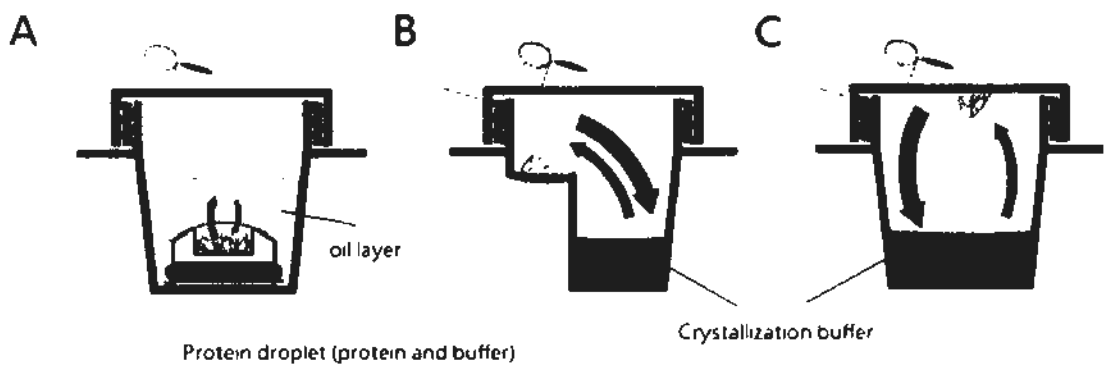

Fig.2.2 Crystallization methods in screening and optimization

(A) Microbatch method. The protein droplet was covered with oil layer. The protein concentration will be increased during evaporation of water into atmosphere. (B) Sitting-drop method. Protein droplet and crystallization buffer are in closed system. Protein concentration will be increases during equilibration process. (C) Hanging-drop vapor diffusion method. Protein droplet is hanging on coverslip in a closed system with crystallization buffer in reservoir. The figure was modified with original figure adopted from http://en.wikipedia.org/wiki/File:CrystalDrops.svg.

2.7.3 X-ray crystallography and data collection

Proteins were soaked in cryo-protectant prepared with crystallization buffer with 10-20% (v/v) of glycerol (USB) before freezing with liquid nitrogen to prevent ice ring formation during data collection.

For the FliS protein crystals, data was collected at 100 K from a frozen crystal using Rigaku Micromax 007 X-ray Generator & R.AXIS IV ++ Imaging Plate Detection Machine at the Centre of Protein Science & Crystallography, The Chinese University of Hong Kong.

For the native and selenomethionine-substituted (SeMet) His_6-HP1076ΔN20 protein crystals, a single-wavelength anomalous diffraction (SAD) and native data were collected at 100 K from frozen crystal using synchrotron radiation from the beamline HMXII at the Pohang Accelerator Laboratory (PAL) at Medical Proteomics Research Center, Korea Research Institute of Bioscience & Biotechnology, Korea with the help from Dr. Woo Eui-Jeon.

For the FliS/HP1076 complex, data was collected at 100 K from frozen crystal using x-ray with the beamline 13B1 at the National Synchrotron Radiation Research Center, Taiwan with the help from Dr. Kotaka Masayo.

2.8 Structure determination

2.8.1 Data processing

The diffraction data was firstly processed with indexing performed with Mosflm (Leslie, 1992). The diffraction spots of 2-4 images were inspected and located, the orientation of crystal space group and unit cell parameters were then determined based on the pattern of identified spots. A "Predict" was performed to determine if the predicted spots were matched with real ones. "Refine cell" was performed to refine the cell parameters and mosaicity (amount of spots to be predicted). Refinement was performed with at least 4 images and then preceded to integration of data sets. Scaling was performed with SCALA from CCP4 suite (CCP4, 1994) applied to each image to calculate a common relative scale as X-ray would cause radiation damage to crystal in long-time diffraction. Reflection file was obtained for further analysis.

2.8.2 Phase determination by molecular replacement

For the structure of FliS and FliS/HP1076 complex, the phase was solved with a known structure of a related protein as the search model by *PHASER* (McCoy *et al.*, 2005) in CCP4 suite. A good search model should share about 40% protein identity to target protein. In molecular replacement, the 3 rotation angles for orientation of

model and 3 translation parameters for position should be adjusted. Two methods, Patterson-based and likelihood method were applied for determination. Patterson-based method was dependent on Patterson-map that was a vector map showing the peaks at positions of vectors between atoms in the unit cell. The likelihood method was judgment of a better atomic model for the unknown protein structure especially for a poor search model. Electron density map was obtained.

2.8.3 Electron density map

Electron density map shows the contour representation of electron density in crystal structure and it is generated with the amplitude information obtained from experimental data and phase determined from model structure. A high resolution map can provide clear information about the positions of protein atoms.

The *Fo-Fc* and 2*Fo-Fc* map are commonly used to minimize bias from the model by subtracting the calculated structure-factor amplitude (|Fc|) from the observed structure-factor amplitude (|Fo|). The resulting electron density map of *Fo-Fc* map contains positive and negative density that shows the difference in current model. Positive density at a region shows the missing information from the current model that additional atoms should be fit into the map to generate a more precise model. Negative density shows that the atoms should be removed from the

current model. 2*Fo-Fc* map contours at certain electron densities resemble the molecular surface that the backbone and orientation of side chains can be fit into the map to improve the model.

2.8.4 Model building

Model building was performed by *COOT* (Emsley and Cowtan, 2004). This procedure helped to construct molecular models that fit into the calculated electron density map manually. Weak or unclear electron density was found for flexible or poorly diffracted regions, the contour level of the map was then reduced to show more electron density for locating the main chain atoms. The orientation of side chains could be adjusted based on the surrounding interacting residues or spatial arrangement of atoms. Sometimes alanine residue was added to the chain if the electron density map was not clear enough. By adjusting the coordinates of each atom, inserting or changing the amino acid residues, and moving the atoms or fragments, a model with the most possible configuration was obtained.

2.8.5 Structure refinement

Rigid body refinement was performed to fine-tune the orientation of molecules within the unit cells. This was followed by initial refinement with simulated annealing with the use of torsion angle dynamics to improve the structure. The atoms

were moved further apart by heating, and they would form a "native configuration" with lower internal energy when being cooled down. This reduced the degree of over-fitting the data.

Non crystallographic symmetry (NCS) averaging was applied when there is more than one copy of molecule present in the asymmetric unit of crystal. For the FliS structure, 2-fold NCS restraint was applied by setting medium restraint for main chain and loose restraint for side chain atoms in refinement program *REFMAC* in CCP4 Suite (Emsley and Cowtan, 2004) with. For FliS/HP1076 complex, NCS restraint was applied in *REFMAC* refinement in *COOT* (Emsley and Cowtan, 2004).

The initial model provided all atoms with B-factors that measured the degree of oscillation or vibration around the specific position in the model. The refinement of B-factors was carried out by group B-factor refinement CNS (Brünger *et al.*, 1998). Refinement was used to obtain a better model which provided an improved phase for generating a new electron density map. Then, another cycle of refinement was performed based on the newly model and electron density map. Most of the structure was built in the model after several rounds of refinement with acceptable R and R_{free} value, then water molecules or solvent molecules were added to the structure. Refinement was then continued until no more extra electron density was found.

2.8.6 Data processing for single-wavelength anomalous diffraction (SAD)

This was performed for a novel protein structure (HP1076) that no similar models available for molecular replacement. The data was processed by HKL2000 package (Otwinowski and Minor, 1997). A SAD diffraction data set of selenomethionine-substituted protein (SeMet) was collected and performed with local scaling to generate reference data set. The Patterson functions were then solved and the 4 selenomethionine sites were located in the asymmetric unit. This was then calculated with the native data for phase determination and improvement at 2.3 Å with the programs SOLVE (Terwilliger and Berebdze, 1999) and RESOLVE (Terwilliger, 2000) in an automatically way which resulted in a traceable electron density map. Initial model building was performed by PHENIX (Adams *et al.*, 2002) and the phase was then applied to the native data set followed by automatic model building by ARP/wARP (Langer *et al.*, 2008). The model was further subjected to modeling building and refinement using *COOT* and *REFMAC* (Emsley and Cowtan, 2004).

2.8.7 Structural validation

All these refinement would result in minimizing the R- and R-free values to obtain the closest agreement between the crystallographic model with the original

X-ray diffraction data. The calculation is based on equation, $R = \frac{\sum \| \mathbf{F}_{obs} | - | \mathbf{F}_{calc} \|}{\sum | \mathbf{F}_{obs} |}$, F_{obs} represents the amplitude of the structure-factor derived from X-ray diffraction data and F_{calc} is the structure-factor derived from crystallographic model (Blow, 2003). For a diffraction data with resolution lower than 3.0 Å, the R and R-free should be below 25% to be regarded as a good refined model. R and R-free could be reduced lower than 20% in a high resolution data set with resolution below 2.0 Å.

Moreover, stereochemistry of structural details was analyzed by the program PROCHECK (Laskowski *et al.*, 1998) which provided a Ramachandran plot. Ramachandran plot provided assessment on the most favorable region, additional allowed region, generously allowed region and disallowed region. Ideally, over 90% of the residues should be in the most favorable regions and no residue in the disallowed region.

2.9 Deletion mutant of HP1076 in *H. pylori* strain 26695

In order to investigate the biological role of HP1076, a disruption mutant of *hp1076* (ΔHP1076) of *H. pylori* was constructed. Hopefully, the mutant would show phenotypical changes or differences in any biological mechanism to provide more insights on this uncharacterized hypothetical protein.

2.9.1 Preparation of kanamycin-resistant gene (*KanR)*

The kanamycin-resistance gene (*KanR*), *aphA-3*, was determined from genomic DNA from *C. jejuni* and *C. coli* by BLASTN (NCBI) search. The conserved region was identified with multiple sequence alignment software (Higgins *et al.*, 1994) (http://www.ebi.ac.uk/clustalw/) for the design of primers. Kanamycin-resistant strain of *C. jejuni* was selected with several rounds of growth with Kanamycin. Genomic DNA was isolated by DNeasy Blood & Tissue Kit (Qiagen) for PCR amplification. The resultant PCR product of *KanR* gene contained the *BstX*1 sites on both ends, promoter regions before the coding sequence of *KanR*, which were verified by sequencing.

2.9.2 Construction of pGEM-T-Easy-hp1076:KanR

*Bst*X1 site was chosen as it was specific site on HP1076 and at both ends of *KanR* introduced by primers. The plasmid, pAC28m-hp1076 and *KanR* construct were digested with *BstX*1 restriction enzyme (New England BioLabs Inc.) separately for 3 hr as described in section 2.1.7-2.1.8. *KanR* fragment was ligated at the 344th bases on *hp1076* sequence. The colonies after transformation were selected for PCR check with HP1076-F and KanR-R primers to check if the fragment was inserted at the correct orientation. Then PCR was performed with HP1076-F and HP1076-R

primers to produce a fragment with 3' adenine-tails so as to ligate into with 3'-terminal thymidine of both ends of linearized vector, pGEM®-T-Easy vector by TA cloning according to standard protocol from manufacturer (Promega) as prepared in Table 2.10. The ligation was performed at 4 °C for 16-18 hr. 10 µl ligation reaction was transformed into DH5α competent cells and spread on LB agar supplemented with 100 µg/ml ampicillin, 0.5 mM IPTG and 80 µg/µl X-Gal (prepared with 5-bromo-4-chloro-3-indolyl-β -D-galactoside dissolved in N, N′-dimethylformamide and stored at -20 °C with aluminium foil cover) for blue/white colony screening. The white colonies containing resultant plasmid were verified by sequencing. Positive clone was prepared by QIAprep Spin Miniprep kit (Qiagen) eluted in sterilized ddH_2O performed in section 2.1.13.

Table 2.10 Composition of reaction mixture for ligation (TA cloning)

	Ligation reaction	Control reaction
pGEM-T vector (50 ng)	1 µl	1 µl
2X Rapid ligation buffer	5 µl	5 µl
PCR product	3 µl	--
Sterilized ddH_2O	--	3 µl
T4 DNA ligase (3 Weiss units/µl)	1 µl	1 µl
Total	10 µl	10 µl

2.9.3 Culture medium for *H. pylori* strain 26695

2.9.3.1 Columbia blood agar plate

The agar plate was prepared with 39 g of Columbia blood agar base (Oxoid) dissolved in 1 L of distilled water and autoclaved at 121 °C for 20 min. 5% sterilized defibrinated blood was added to the medium when it was cooled down to around 50 °C. The medium was then poured into petri dish for solidified.

2.9.3.2 Sterilized horse serum

Sterilized horse serum (Oxoid) was the extract of horse blood. It was firstly heat-inactivated at 56 °C for 15 min and stored at 4 °C before use.

2.9.3.3 Brucella broth

This was prepared by dissolving 28 g BD BBL™ brucella broth (in distilled water and autoclaved at 121 °C for 20 min. 10% heat-inactivated horse serum (Oxoid) was freshly added to broth before use.

2.9.3.4 Brucella broth agar plate

This was prepared by dissolving 28 g BD BBL™ brucella broth and 15 g BD Bact Bacto™ agar in 1 L distilled water and autoclaved at 121 °C for 20 min. 10%

heat-activated horse serum was added when the agar medium cooled down and poured into petri dish.

2.9.4 Culture of *H. pylori* strain 26695

Frozen glycerol stock of *H. pylori* strain 26695 at -80 °C was streaked on a Columbia blood agar plate. The plates were incubated at microaerophilic condition (10% CO_2, 10% H_2/N_2 stored in compressed gas cylinder) in an anaerobic jar (Oxoid) at 37 °C for 3-4 days.

2.9.5 Transformation into *H. pylori* strain 26695

The resultant plasmid was introduced into *H. pylori* by electroporation according to standard protocol (Ge and Taylor, 1997). *H. pylori* was grown on Columbia blood agar plate for 1 day and harvested in brucella broth at about 1 x 10^9 cells/ml. The cells were washed with brucella broth and centrifuged at 1,500 rpm for 3 min. Then the cells were washed with cold and sterilized electroporation buffer (272 mM Sucrose, 15% glycerol, 2.43 mM K_2HPO_4, 0.57 mM KH_2PO_4, pH 7.4) for 3 times. 5 μg of plasmid in sterilized ddH_2O and ddH_2O only were mixed separately with the cells in 50 μl electroporation buffer in a pre-chilled cuvette (gene pulser/micropulser cuvette, 0.1 cm gap, Bio-Rad) on ice. The electroporation was set

as 1.25 kV, 200 Ω with constant time of about 3-4 ms by a Gene-Pulser apparatus (Bio-Rad). Cold brucellar broth was added immediately to the cells to cool down the heat generated. The control and transformant cells were then spread on brucella broth agar plate. The plates were incubated at microaerophilic condition at 37 °C for 24 hr. The cells were harvested from agar plate and resuspended in 100 µl Phosphate buffered saline (PBS). Different serial dilutions of cell stock were spread on brucella agar plate supplemented 10 µg/ml kanamycin as selection marker and without antibiotics for control. The kanamycin-resistant transformants were detected after incubation at microaerophilic condition at 37 °C for 4-5 days.

2.9.6 Verification of ΔHP1076 in *H. pylori*

The colonies on the agar plate were sub-cultured on another agar plate with kanamycin selection. Half of the cells were harvest as glycerol stock (brucella broth, 10 % horse serum and 15 % glycerol). And another half of cells were collected for further PCR and western blot analysis.

2.9.6.1 PCR with genomic DNA extracted from *H. pylori* cells

Genomic DNA of the Wild-type (WT) and mutant strains was isolated with DNeasy Blood and Tissue Kit (Qiagen). Cells were harvested and washed with PBS

for 3 times by centrifugation at 1,500 rpm for 3 min. The cell pellet was lysed in ALT buffer and proteinase K at 56 °C for 1 hr. AL buffer was added to cell lysate together with ethanol and mixed thoroughly. Then the mixture was transferred to spin column and centrifuged at 8,000 rpm for 1 min. The filtrate was discarded and column was washed with AW1 buffer. The column was then washed with AW2 buffer and centrifuged for 8,000 rpm for 3 min to dry the membrane. The DNA bound to the column was eluted with AE buffer. The DNA extracted was used as the template for PCR with HP1076-F and HP1076-R primers as performed in section 2.1.4. The result was analyzed with DNA agarose gel electrophoresis as stated in section 2.1.5. The size of PCR product of mutant strains was larger than that of the WT as *KanR* gene was inserted into the *hp1076* gene embedded in genomic DNA.

2.9.6.2 Western blot analysis with total cell lysate

Protein level of HP1076 was further analyzed between WT and mutant strains. Harvested cells were washed with PBS and stored at -80 °C. Frozen cells were lysed on ice with Triton-X buffer (20 mM Tris, 150 mM NaCl, pH 7.5, 0.5% (v/v) Triton-X) for 1-hr incubation. The lysate was centrifuged at 14,000 rpm at 4 °C for 20 min. The concentration of total proteins in supernatant was measured by Bradford assay. About 40 μg of total proteins was loaded to each lane of SDS-PAGE and transferred to

PVDF membrane as performed in section 2.4.5. The protein level of HP0176 was detected with polyclonal rabbit anti-HP1076 antibody was produced by antibody production service of Invitrogen.

2.9.7 2-dimensonal gel electrophoresis (2-DE)

2.9.7.1 Sample preparation

The frozen cell pellet from *H. pylori* WT and mutant strains was resuspened in regeneration buffer (7 M Urea, 2 M Thio-urea, 2% CHAPS) with 20 mM DTT, 0.2 mM PMSF and 0.2 mM benzamidine. The cell suspension was incubated on ice for 1 hr and subjected for sonication with 20% power output in 6 cycles of 10 sec pulse. The cell lysate was centrifuged at 14,000 rpm at 4 °C for 15 min. The concentration of total proteins in supernatant was determined by Bradford assay. 250 µl sample solution with equal amount of proteins was prepared in RB buffer with 1.5 µl IPG buffer pH3-10 and 1 µl of 1% bromophenol blue.

2.9.7.2 First dimensional gel electrophoresis-isoelectric focusing (IEF)

This was performed with the Ettan IPGphor III Isoelectric focusing system (GE Healthcare) and 13 cm Ettan Immobiline™ drystrip gels pH3-10 (GE Healthcare). The samples with equal amount of protein were applied to the Immobiline™ Drystrip

holder (GE Healthcare) without introducing air bubbles. The dry strip gel was then overlayed with the gel facing the sample solution. Drystrip cover fluid (GE Healthcare) was loaded evenly to the top of strips to minimize sample evaporation and urea crystallization. The strip holder was covered with the lid and excess cover fluid spilled out was removed to avoid overheating of the electrode. Then it was placed on Ettan™ IPGphor™ III Isoelectric focusing unit for rehydration and focusing at constant temperature of 20 °C. The IEF profile was shown in Table 2.11. The current setting was restricted to 50 μA per strip.

Table 2.11 IEF profile for 13 cm Ettan™ Immobiline™ drystrip

Step		Voltage	Time
1	Rehydration	30 V	11 hr
2	Step and Hold	500 V	4 hr
3	Gradient	1000 V	1 hr
4	Gradient	8000 V	156, 000 Vhr

2.9.7.3 Second dimensional gel electrophoresis-SDS-PAGE

2.9.7.3.1 Strip equilibration

The isoelectrically focused strips were equilibrated with SDS equilibration buffer (6 M Urea, 75 mM Tris-HCl, pH 8.8, 29.3% (v/v) glycerol, 2% (w/v) SDS, 0.002% (w/v) bromophenol blue) containing 1% (w/v) DTT for 15 min with gentle shaking at room temperature. Strips were then equilibrated with SDS equilibration buffer with 2.5% (w/v) iodoacetamide for 15 min.

2.9.7.3.2 16 x 18 cm SDS-PAGE

12% SDS-PAGE with separating gel was prepared in gel cast with 2 sets of 16 x 18 cm glass plates separated with 1.5 mm spacers. The equilibrated strips were placed on the gels by pushing gently on the gel surface. A piece of filter paper filled with protein marker (SeeBlue®Plus2, Invitrogen) was placed at one end of the strip. The strips were then sealed with melted agarose solution (0.5% (w/v) agarose and 0.002% (w/v) bromophenol blue). The gel electrophoresis was performed with SE 600 Ruby™ Standard Dual Cooled Vertical Unit (GE Healthcare) with 1x electrophoresis buffer. The electrophoresis was set at constant current of 30 mA for 15 min to allow the samples enter gels. Then the current was set at 70 mA until the dye front reached the bottom of gel.

2.9.7.4 Detection of protein spots on gels

The gels detached from gel casts were fixed with 250 ml fixing solution (25 ml acetic acid, 100 ml methanol and 125 ml distilled water) overnight. Then the gels were stained with freshly prepared Coomassie brilliant blue staining solution for 2 hr. Coomassie brilliant blue destaining solution was then applied to allow spots to be visualized.

2.9.7.5 Identification of spots with different intensity between WT and mutant protein profiling

The gels with clear protein spots after destaining were scanned by Image Scanner™ II (GE Healthcare) with software LabScan v3.0 (GE Healthcare). The images were analyzed by ImageMaster™ 2D Platinum v7.0 (GE Healthcare) to identify the proteins with different expression level between WT and mutant strains. 3 sets of 2-DE gels were performed for data analysis to eliminate gel-to-gel variation. By the software quantifications, spots with a fold change greater than 1.5 were defined as up or down regulated spots. The corresponding spots with the range ratio (the maximum value divided by the smallest value in the sample specified) greater than 1.2 was excised for identification with mass spectrometry.

2.9.8 Mass spectrometry

2.9.8.1 Reagents for mass spectrometry

All the reagents and distilled water were freshly prepared and filtered with 0.22 μm filter before use to reduce the contamination of protein sample prepared.

Gel equilibration solution was prepared in 200 mM ammonium bicarbonate (ABC) (Sigma) was dissolved in distilled water.

Trypsin enzyme solution was prepared by dissolving lyophilized enzyme powder

(MS grade, Promega) in 25 mM ABC to a concentration of 40 ng/μl and stored at -80 °C in small aliquot.

Trypsin digestion solution was prepared by diluting gel equilibration buffer into 25 mM ABC with distilled water.

Peptide extraction solution was prepared by 50% acetonitrile (ACN) (Sigma) solution and 5% trifluoroacetic acid (TFA) (Applied Biosystems) in distilled water before use.

Resuspension solution/ equilibration solution/ washing solution were prepared by diluting 10% (v/v) TFA stock solution into 0.1% (v/v) with distilled water.

Wetting solution was mixed by 100% ACN with distilled water in 1:1 volume ratio.

Elution solution was mixed by 25% ACN and 0.5% TFA in distilled water.

Matrix solution was prepared by dissolving α-cyano-4-hydroxycinnamic acid (CHCA) (Fluka) powder in 50% ACN and 0.5% TFA until saturation and stored at -20 °C not more than 1 month.

2.9.8.2 Destaining of gel spots

The excised gel spots were cut into smaller pieces to facilitate destaining with freshly prepared and filtered destaining solution until the blue color was removed. Replacing with fresh destaining solution and vortex helps to speed up the destaining

process. When the blue color was removed, the spots were washed with distilled water for 3 times and stored at -80 °C for further analysis.

2.9.8.3 In-gel trypsin digestion

The spots were equilibrated with 100 µl gel equilibration solution for 10 min for 2 times. Then 100 µl of 100% (v/v) ACN was added to dehydrate the gel spots with 3 cycles of 5 min each. The gel spots were dried with vacuum centrifugation in SpeedVac® concentrator (Savant) for 5 min until the gels appeared as "dust-like". After that, gels were rehydrated with 6 µl of trypsin enzyme solution and incubated on ice for 30 min to allow the solution to be absorbed into the gel. Finally, 20 µl or more trypsin digestion buffer was added to cover the gels and the digestion was performed at 32 °C overnight.

2.9.8.4 Extraction of peptide mixture

The microfuge tubes containing gels were sonicated in water by Ultrasonic Cleaner for 10 min. The solution inside the tube was transferred to a new microfuge tube. Then 20 µl peptide extraction solution was added to the gels for second round of water sonication. The solution inside the tube was transfer to the same tube. 20 µl 100% ACN was added to the gel for the third round of sonication. The solution was

then pooled in the same tube. Around 60 µl pooled solution containing the peptide was dried by vacuum centrifugation by SpeedVac® for 3 hr.

2.9.8.5 Desalting and concentration of peptide mixture

Dried peptide samples were resuspended in 10 µl resuspension solution. The ZipTip® C-18 Pipette Tips (Millipore) was firstly wetted by aspiration of 10 µl wetting solution for 2 times. Some solution should be kept inside the tip to avoid drying of the tips. It was then equilibrated with 10 µl equilibration buffer for 2 times. The peptide was bound to the tip by slowly aspirating and dispensing the sample solution for 20 cycles. The tip was then washed with 10 µl washing solution for 5 times and all the solution should be dispensed completely in the last washing step. Finally, the peptide was eluted with 2 µl elution solution to a new tube by aspirating and dispensing for 20 cycles. The peptide samples were dotted on a 192 stainless steel MALDI sample plate (Applied Biosystems) with 0.5 µl each time and air-dried. 0.5 µl matrix solution was loaded to the sample dots. The plate was sent to processing by 4700 Proteomics Analyzer equipped with 4700 Explorer software (Applied Biosystems). The Proteomics Analyzer work was kindly performed by Ms Helen Tsai of Prof. Ngai's lab from Department of Biology, The Chinese University of Hong Kong.

2.9.8.6 Protein identification by MS/MS

When the data was processed, combined MS and MS/MS analysis was performed with the Mascot based GPS Explorer™ Software v3.6 (Applied Biosystems). Several parameters were set to achieve a relevant data as followed: (a) the sample peaks of contaminant from skin and hair keratin or trypsin were excluded, (b) the error tolerance rate for peptide mass was set at below 50 ppm, (c) the possible missed cleavage of trypsin was set as 1. Finally the MALDI peptide mapping was searched within the NCBInr (http://ncbi.nlm.nih.gov) databases.

2.9.9 Motility assay on soft-agar plate

This method was adopted to evaluate the motility of *H. pylori* mutant and wild-type strains according to protocol (Josenhans *et al.*, 1995; Osaki *et al.*, 2006). *H. pylori* strain 26695 and mutant strains were cultured on Columbia blood agar in microaerophilic condition for one day. Cells were harvested in brucella broth and 2 µl of cell suspension was dotted at the centre of the 0.4% soft agar (prepared from brucellar broth, 10% (v/v) horse serum and 0.3% Bacto agar). After four days of incubation under microaerophilic condition at 37 °C, the diameter of the halo will be examined and compared with wild-type strain.

2.9.10 Metronidazole susceptibility test

A disc diffusion test was performed according to protocol (DeCross *et al.*, 1993). *H. pylori* strain 26695 and mutant strains were cultured on Columbia blood agar in microaerophilic condition for three days. Cells were harvested with sterilized cotton swab, and streaked on new Columbia blood agar plate evenly. A tablet disc containing 5 μg/ml metronidazole (Oxoid) was placed at the center of plate. The plate was further incubated for three days. The zone formed (without bacteria) around the tablet disc which reflected the susceptibility of bacteria in the presence of antibiotics was measured for comparison (Chaves *et al.*, 1999; McNultya *et al.*, 2002).

2.9.11 Fractionation of bacterial cell lysate into cytosol and membrane fractions

4-day *H. pylori* cells were harvested and washed with PBS twice with centrifugation at 3,000 rpm for 2 min. The pellet was resuspended in PBS and lysed on ice with sonication with 8 cycles of 10 sec and 20% power output. The cell lysate was centrifuged at 6,000 rpm at 4°C for 10 min to remove cell debris. The supernatant was transferred to a thickwall tube 11 X 34 mm (Beckman) and centrifuged at 25,000 rpm at 4°C for 30 min by Beckman Coulter Optima TLX-120 Ultracentrifuge. The supernatant was collected for another round of

ultracentrifugation. The pellet was resuspened with PBS as the membrane fraction. And the supernatant collected after centrifugation represented the cytosol fractions. Fractions were used for western blot analysis.

2.9.12 Genetic analysis of HP1076 and FliS in Metronidazole-resistant (MtZ-R) clinical isolates

Five MtZ-R samples (10662, 10643, 10665, 10679 and 10692) were isolated from the clinical samples by the lab of Dr. Thomas Ling from Department of Microbiology, The Prince Wales of Hospital, CUHK. The cells of MtZ-R and WT strains were cultured on Columbia blood agar and harvested as stated in section 2.9.4. Cells were washed and genomic DNA was extracted as template for PCR amplification with specific primers. Forward and reverse primers targeting the *fliS* and *hp1076* genes were designed at least 100 bp upstream and downstream of target genes. The PCR amplification was performed as stated in section 2.1.4. The PCR product was analyzed on DNA agarose gel, and the band with correct size was excised for DNA extraction and followed by sequencing. The DNA sequences and translated protein sequences by Translate tool in ExPASy Server (Gasteiger *et al.*, 2005) were compared with WT gene by multiple sequence alignment, Clustal W (Higgins *et al.*, 1994).

Chapter 3

Characterization of interaction between FliS and HP1076

To investigate the interaction between FliS and HP1076, the study began on cloning the two target genes into expression vector and over-expressing and purifying the recombinant proteins. The molecular interaction was then examined by pull-down assays and size exclusion chromatography. Protein fragments and mutations of amino acid residues were constructed for the purpose of identifying the binding domains. Moreover, isothermal titration calorimetry was performed to determine the binding constant of interaction. Biochemical assays were conducted to elucidate the functional significance of FliS, HP1076 and FliS/HP1076 complex. These included chaperone-like activity and binding with other flagellar proteins.

Results and Discussion

3.1 Construction of recombinant pGEX-6p3-fliS plasmid

The target gene *fliS* (*hp 0753*) was amplified from the *H. pylori* strain 26695 genomic DNA library, and analyzed by DNA agarose gel electrophoresis. A band with size of 378 bp long was excised and purified (Fig.3.1A). The amplified DNA was digested and cloned into the expression vector, pGEX-6p-3 at the restriction

sites of *BamH*I and *Not*I. After the transformation into *E. coli* competent cell strain DH5α, three colonies were screened by PCR. The PCR products were analyzed by agarose gel electrophoresis. By examining the size of the PCR product, all the three colonies were shown to be positive (Fig.3.1B) which suggested that *fliS* was successfully cloned into pGEX-6p-3 vector. The DNA sequences of these positive clones were checked by DNA sequencing. The sequencing result was aligned with the *fliS* coding sequence obtained from NCBI by Basic Local Alignment Search Tool (BLAST) (http://blast.ncbi.nlm.nih.gov/Blast.cgi) with 100% match point.

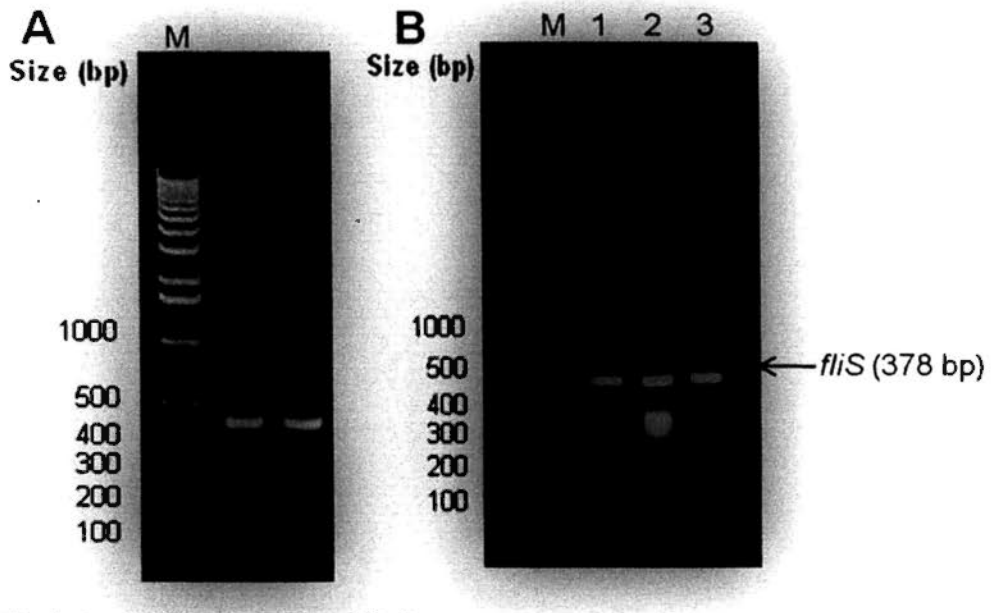

Fig.3.1 PCR products of *fliS* gene

The target gene *fliS* was amplified from *H. pylori* genomic DNA library (A) and colonies (1-3) of pGEX-6p3-fliS in PCR screening (B) showing the bands with size of around 400 bp. The PCR products were analyzed with 1% agarose DNA gel.

3.2 Construction of recombinant pAC28m-hp1076 plasmid

The full length target gene *hp1076* of 516 bp was amplified from the *H. pylori* strain 26695 genomic DNA library, and analyzed by DNA agarose gel electrophoresis (Fig.3.2A). The amplified DNA was digested and cloned into the expression vector, pAC28m at the restriction sites of *Nde*I and *Not*I. After the transformation into *E. coli* DH5α, three colonies were screened by PCR. The PCR products were analyzed by agarose gel electrophoresis. By examing the size of the PCR product, all the three colonies were shown to be positive (Fig.3.2B). Thus, full length construct of *hp1076* was successfully cloned into pAC28m vector. The DNA sequences of these positive clones were verified by DNA sequencing.

Besides constructing plasmid of full-length *hp1076* gene, different fragments of HP1076 were cloned into the same expression vector. The fragmentation design was based on secondary structure prediction from program PredictProtein (Rost *et al.*, 2004), which showed that HP1076 protein contained five helices. The molecular cloning protocol was the same as the full length construct using pAC28m-hp1076 as the template for DNA amplification. The expression plasmids with different fragments are summarized in Table 3.1 below.

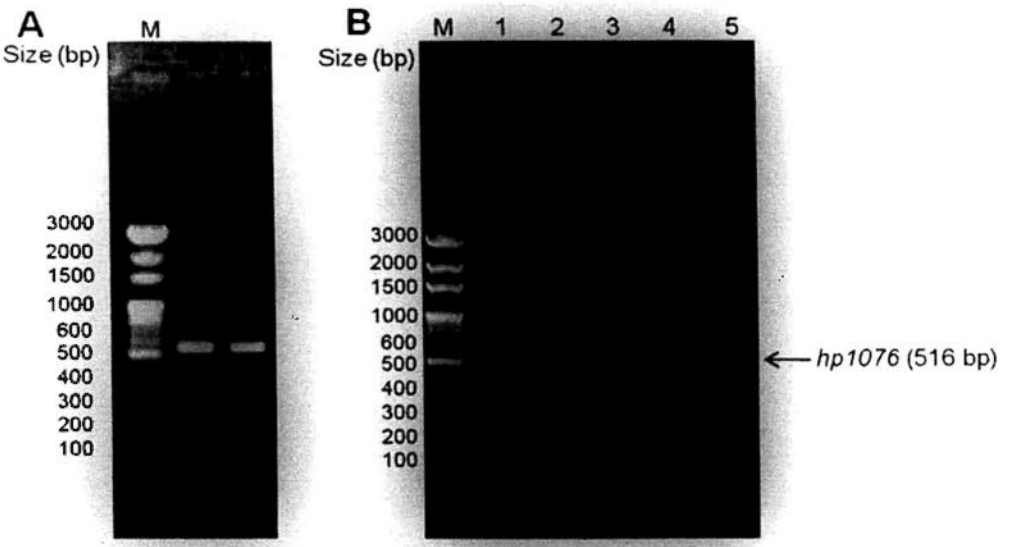

Fig.3.2 PCR products of *hp1076* gene

PCR amplification of *hp1076* was performed from *H. pylori* genomic DNA library (A) and colonies (1-5) from pAC28m-hp1076 (B) showing bands with size of 516 bp. The PCR products were analyzed with 1% agarose DNA gel.

Table 3.1 Expression plasmids of *hp1076* fragments

Expression plasmid	Length of construct	Number of residues
pAC28m-hp1076	1-516 bp	1-171 aa
pAC28m-hp1076ΔC29	1- 426 bp	1-142 aa
pAC28m-hp1076ΔN20	61-516 bp	21-171 aa
pAC28m-hp1076ΔN20ΔC29	61- 426 bp	21-142 aa
pAC28m-hp1076ΔN36	109-516bp	37-171 aa
pAC28m-hp1076ΔN36ΔC29	109- 426 bp	37-142 aa

3.3 Construction of expression plasmids for interaction assays

The full-length target genes, *fliS*, *fliD*, *flgK*, *fliH*, *fliI* and fragments of *flaAc* and *flaBc* were amplified from the *H. pylori* strain 26695 genomic DNA library (Fig.3.3) and cloned into different expression vectors, pGEX-6p-3 or pAC28m as summarized in Table 3.2.

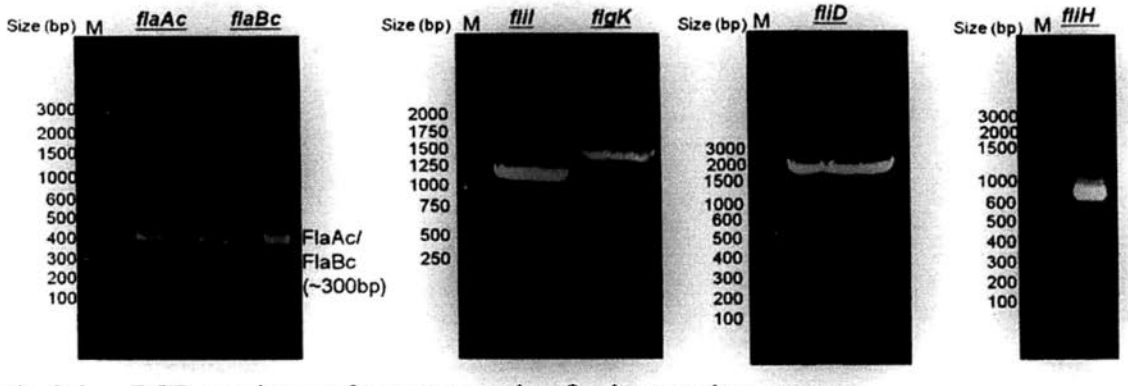

Fig.3.3 PCR products of target proteins for interaction assays
PCR amplification of *flaAc, flaBc, fliI, flgK, fliD* and *fliH* from *H. pylori* strain 26695 genomic DNA.

Table 3.2 Expression plasmids for interaction assays

Expression plasmid	Expressed protein	Length of construct	Number of residues
pAC28m-fliS	His_6-FliS	1-378 bp	1-126 aa
pGEX-6p-3-flaAc	GST-FlaAc	1255-1533 bp	418-511 aa
pGEX-6p-3-flaBc	GST-FlaBc	1240-1545 bp	413-515 aa
pGEX-6p-3-fliD	GST-FliD	1-2025 bp	1-675 aa
pGEX-6p-3-flgK	GST-FlgK	1-1821 bp	1-607 aa
pGEX-6p-3-fliH	GST-FliH	1-777 bp	1-259 aa
pGEX-6p-3-fliI	GST-FliI	1-1305 bp	1-435 aa

3.4 Purification of GST-FliS recombinant protein

The plasmid, pGEX-6p3-fliS was transformed into R2 cells and expressed at different temperatures of 37 °C, 25 °C and 16 °C to obtain the highest yield of soluble protein. About 70% of soluble GST-FliS was found in supernatant fraction after lysis (Fig.3.4). GST-FliS was expressed in a large scale with 4 L LB medium and expressed at 25 °C. The cell was pelleted and resuspended in GST binding buffer for lysis by sonication. The supernatant containing the soluble protein with size of

around 42 kDa was mixed with glutathione sepharose for binding. GST-FliS bound on sepharose was eluted with GST elution buffer as described in section 2.3.5. The eluted GST-FliS was about 80% purity with some impurities (Fig.3.5). The elution was concentrated for Superdex^{TM} S75 gel filtration for further purification. GST-FliS was eluted out at around 53 ml and most of the purities were removed. The elution fractions from E1 to E7 were pooled and an approximately 95% purity was obtained (Fig.3.6).

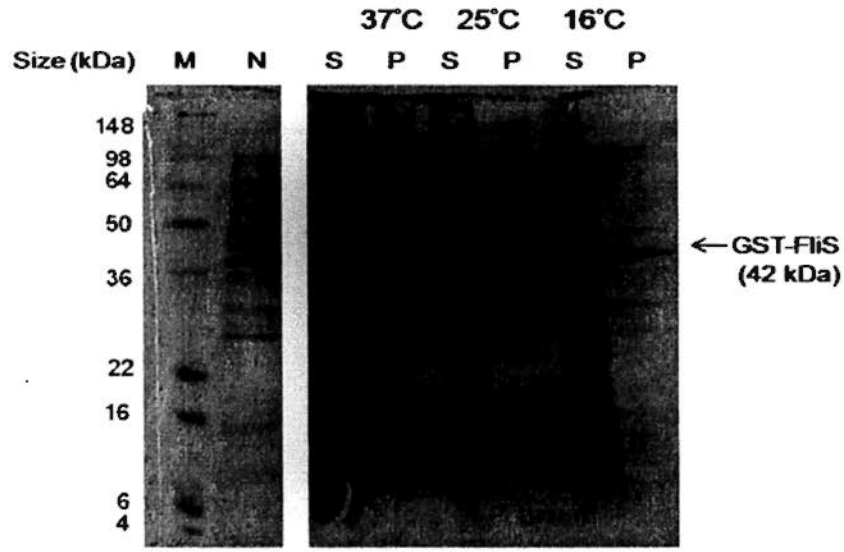

Fig.3.4 Expression of GST-FliS at different expression temperatures
Fraction before expression (N), fractions after expression with insoluble (P) and soluble (S) proteins in cell lysate were analyzed by 15% SDS-PAGE.

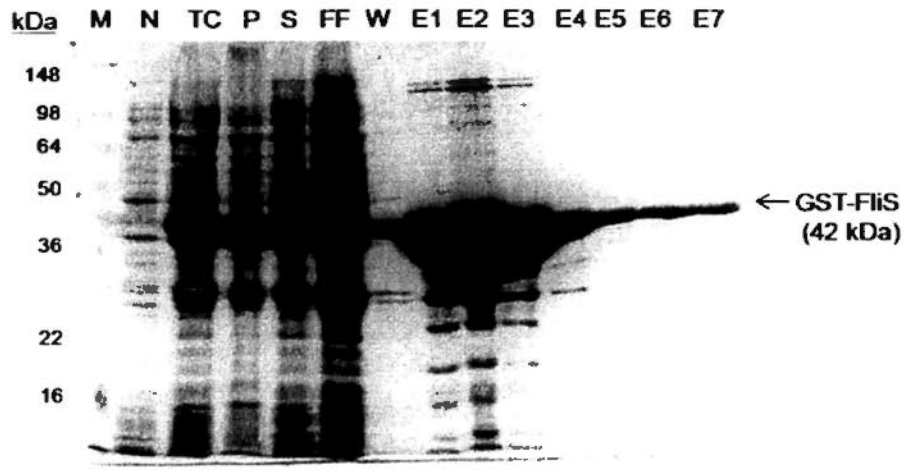

Fig.3.5 Purification of GST-FliS by glutathione sepharose
Samples of non-induced fraction (N), total cell lysate (TC), insoluble proteins (P) and soluble proteins (S) in total cell lysate, flow-through from column (FF), washing with buffer (W) and fractions eluted with GST elution buffer (E1-E7) were analyzed by 15% SDS-PAGE.

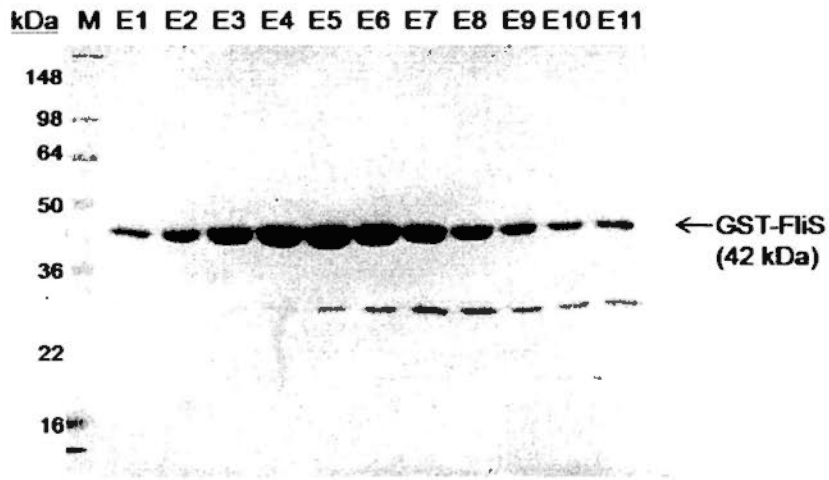

Fig.3.6 Purification of GST-FliS by Superdex^{TM} S75 column
Fractions (E1-E11) containing protein samples were analyzed by 15% SDS-PAGE.

3.5 Purification of FliS recombinant protein

Expression plasmid, pGEX-6p3-fliS was transformed into R2 cells and expressed as GST-FliS fusion protein upon IPTG induction at 25 °C. Cells were pelleted and resuspened in GST binding buffer and lysed by sonication. The soluble

protein in supernatant was subjected for binding with glutathione sepharose. The column was washed with binding buffer to remove impurities and equilibrated with GST low-salt buffer. GST-tag was removed after overnight cleavage by GST-PreScission™ Protease (PP) which worked best in low-salt buffer. The untagged FliS protein was collected as flow-through (Fig.3.7).

The partially purified FliS protein was further subjected to Superdex™ S75 gel filtration. The purified FliS protein was eluted at a sharp peak of 62 ml as shown in the elution profile while the other two peaks were impurities identified from SDS-PAGE. The fractions from 37-49 were pooled together with over 95% purity (Fig.3.8).

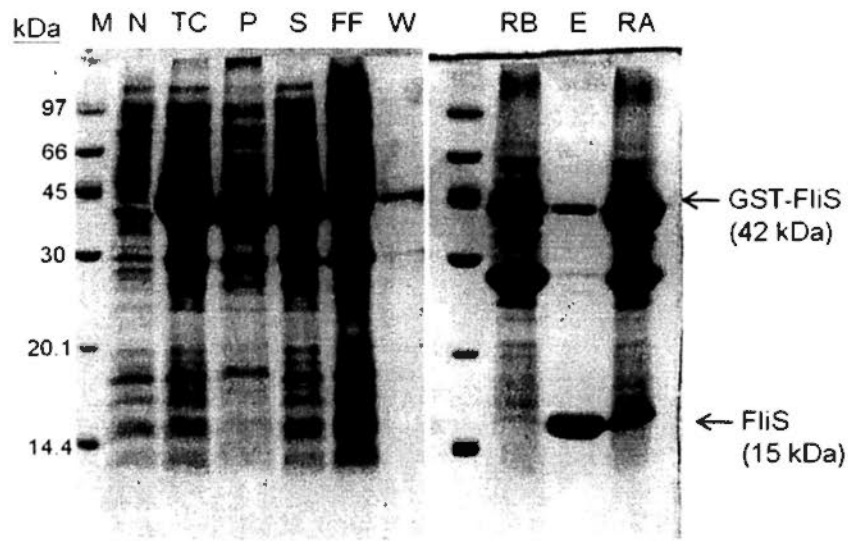

Fig.3.7 Purification of FliS by glutathione sepharose
Samples of non-induced fraction (N), total cell lysate (TC), insoluble proteins (P) and soluble proteins (S) in total cell lysate, flow-through from column (FF), washing with buffer (W), sepharose before cleavage with PP (RB), proteins eluted after digestion (E) and sepharose after elution were analyzed by 15% SDS-PAGE.

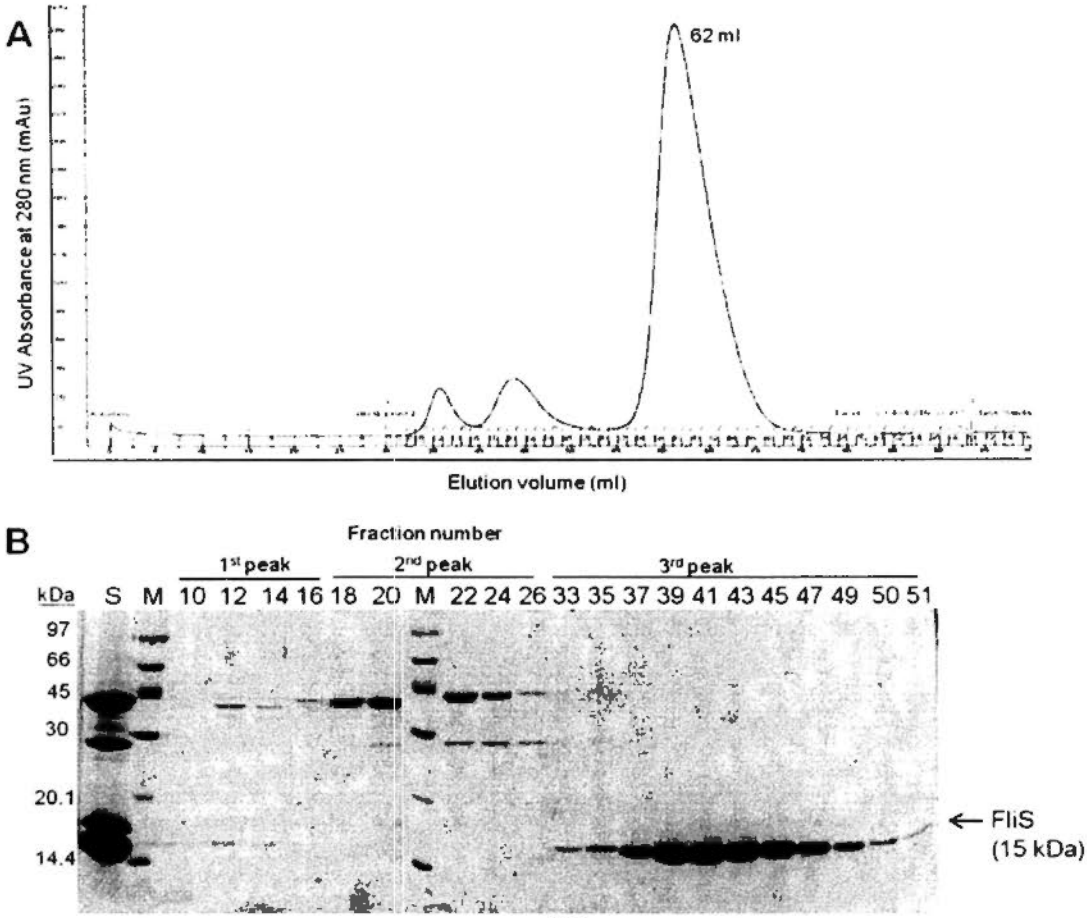

Fig.3.8 Purification of FliS by Superdex™ S75 column

Partially purified protein samples containing FliS were eluted into three peaks observed in the elution profile from ÄKTA Prime system (A). Concentrated protein sample before gel filtration and protein samples from peaks were analyzed by 15% SDS-PAGE (B).

3.6 Purification of His_6-HP1076 and fragments

The expression plasmid, pAC28m-hp1076 was transformed into R2 cells and expressed as a His_6-tagged HP1076 fusion protein (His_6-HP1076) of 20 kDa. The cell pellet was harvested and resuspened in Ni binding buffer for lysis by sonication. The soluble protein was loaded to a Ni-NTA column and impurities were washed away with buffer as stated in lanes W1 and W2. His_6-HP1076 was eluted with a

gradient of imidazole as described in section 2.3.7. About 50% purity of protein was obtained as the elution contained many impurities (Fig.3.9).

The fractions from E1-E11 (Fig.3.9) were concentrated and diluted in Q sepharose binding buffer to reduce salt concentration. The sample was loaded to Q sepharose column and eluted by increasing salt concentration in Q sepharose elution buffer. The purity of His_6-HP1076 was increased dramatically to about 80% as many impurities were removed (Fig.3.10).

The sample from E3-E9 (Fig.3.10) was further purified by Superdex^{TM} S75 gel filtration. From the SDS-PAGE analysis (Fig.3.11), purified His_6-HP1076 was eluted out at second peak while the first peak contained impurities. The protein from fractions 18-22 was pooled together and about 95% purity was obtained. Some minor bands were found which might be the degraded proteins. Other His_6-HP1076 fragments were purified with same strategies with 95% purity (Fig.3.12).

Fig.3.9 Purification of His_6-HP1076 by Ni-NTA affinity chromatography
Protein samples of flow-through collected from column (FF), washing with buffer (W1, W2) and elution by imidazole (E1-E11) were analyzed by 15% SDS-PAGE.

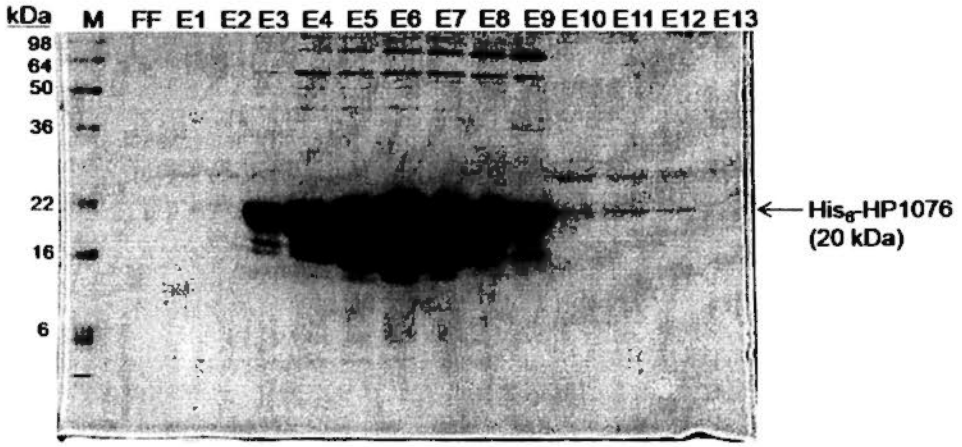

Fig.3.10 Purification of His_6-HP1076 by ion-exchange chromatography
Protein samples of flow-through collected from column (FF) and eluted fractions with increasing salt concentration were separated by 15% SDS-PAGE.

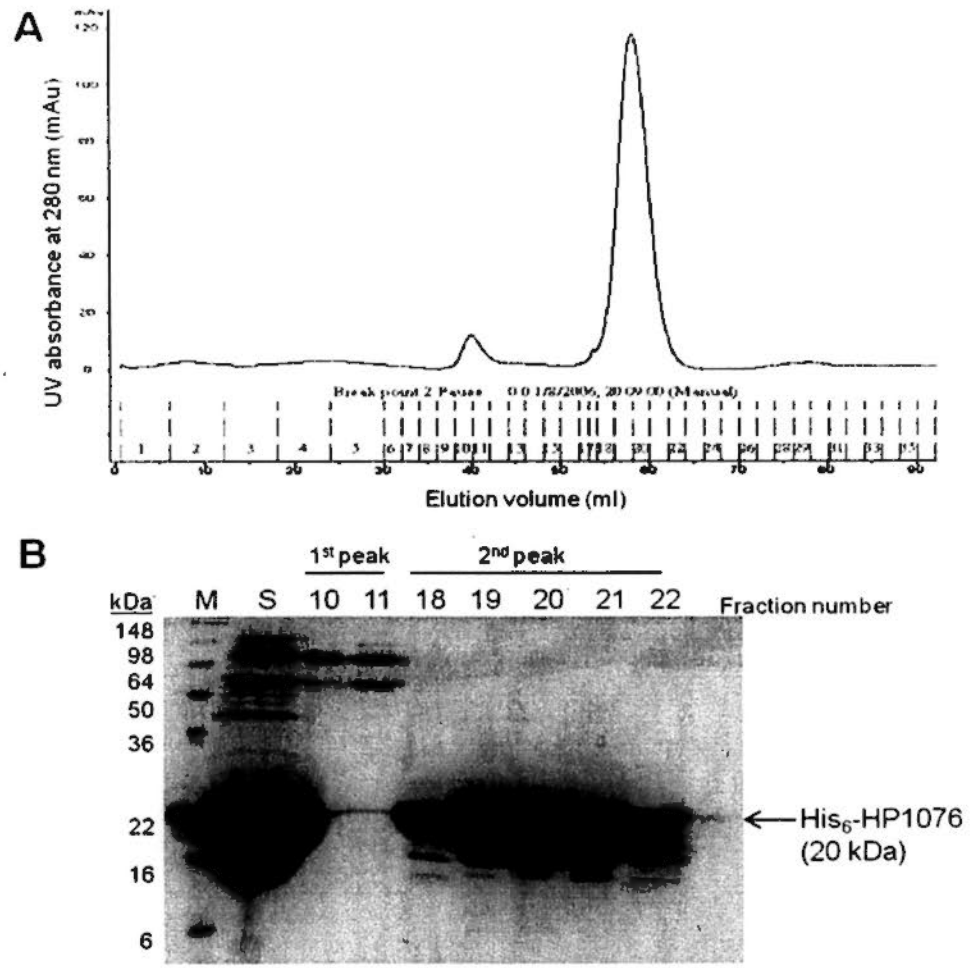

Fig.3.11 Purification of His_6-HP1076 by Superdex^{TM} S75 column
Partially purified samples containing His_6-HP1076 were eluted into two peaks in elution profile from ÄKTA Prime system (A). The fraction samples (10-22) and concentrated sample (S) were analyzed by 15% SDS-PAGE.

A

Protein fragments	Size of proteins
His_6-HP1076	20 kDa
His_6-HP1076ΔC29	15.7 kDa
His_6-HP 1076ΔN20	18 kDa
His_6-HP 1076ΔN20ΔC29	14.6 kDa
His_6-HP 1076ΔN36	16 kDa
His_6-HP 1076ΔN36ΔC29	13 kDa

B

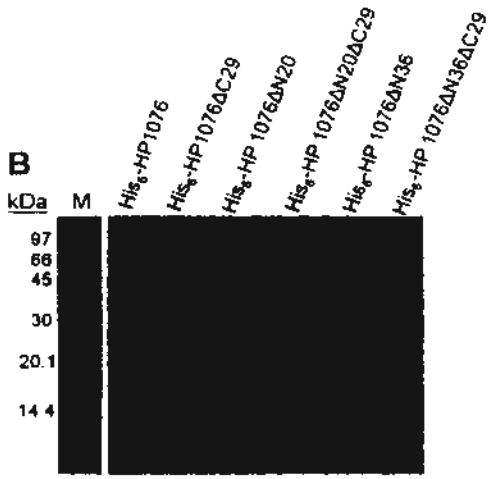

Fig.3.12 Purified protein fragments of His_6-HP1076
The purified protein fragments were summarized in table (A) and analyzed by 15% SDS-PAGE (B).

3.7 Interaction between FliS and HP1076 by pull-down assays

To confirm the interaction of FliS and HP1076 predicted from the yeast-two-hybrid analysis (Rain *et al.*, 2001), pull-down assay with affinity sepharose was performed with individual purified proteins. The minimal interaction domain on HP1076 required for FliS binding was also studied by using different HP1076 fragments (Fig.3.13). These fragments were constructed based on secondary structure prediction (Rost *et al.*, 2004) in prior to the determination of crystal structure. HP1076 was predicted to consist of five helices in the structure connected with loops, fragments were designed based on the assignment of helical structure. Deletion of one helix from the C-terminal resulted in a deletion of 29 amino acid residues from C-terminal and generated fragment ΔC29. Deletion of one helix from

N-terminal resulted in a deletion of 20 amino acid residues and generated fragment ΔN20. Moreover, deleting two helices from N-terminal was constructed in fragment ΔN36. Individual purified proteins were prepared for the interaction study.

In the pull-down assay performed with glutathione sepharose (Fig.3.14), GST-FliS or GST proteins were firstly immobilized on sepharose, and mixed with various His_6-HP1076 fragments in a 1:1 molar ratio. Control experiment was set up with His_6-HP1076 incubated with sepharose only. From Fig.3.14, full-length His_6-HP1076 was pulled out with FliS, and His_6-HP1076 was not bound to sepharose non-specifically as shown in control. The interaction of fragment ΔN20 was retained and similar to that of the full-length, so N-terminal was not involved in the interaction. However, the interaction was dramatically weakened when the 29 amino acid residues from C-terminal (ΔC29) or 36 amino acid residues from N-terminal (ΔN36) were deleted. The interaction was abolished with the fragments ΔN20ΔC29 and ΔN36ΔC29, which showed that amino acid residues 21-36 and 143-171 played a minor role in interaction. The interaction was mediated between FliS and HP1076 as no interaction was found when GST was used (Fig.3.13B). Thus, the fragment ΔN20 contained the minimal binding domain.

The interaction was further confirmed with His_6-HP1076 fragments immobilized on Ni-NTA agarose (Fig.3.15A). The interaction of FliS with full-length

and ΔN20 fragments was of similar binding affinity as similar amount of FliS was pooled out. The interaction was weakened with fragments ΔC29 and ΔN36, while the interaction was abolished with fragments ΔN20ΔC29 and ΔN36ΔC29. GST-FliS and GST showed no non-specific binding to agarose as shown in lane labeled with Crl. No similar result was obtained when GST was used instead of GST-FliS (Fig.3.15B), which confirmed that the interaction was solely occurred between FliS and HP1076 fragments. The results in Ni-NTA agarose was in line with that of glutathione sepharose, which further confirmed that the minimal binding domain was located in fragment ΔN20.

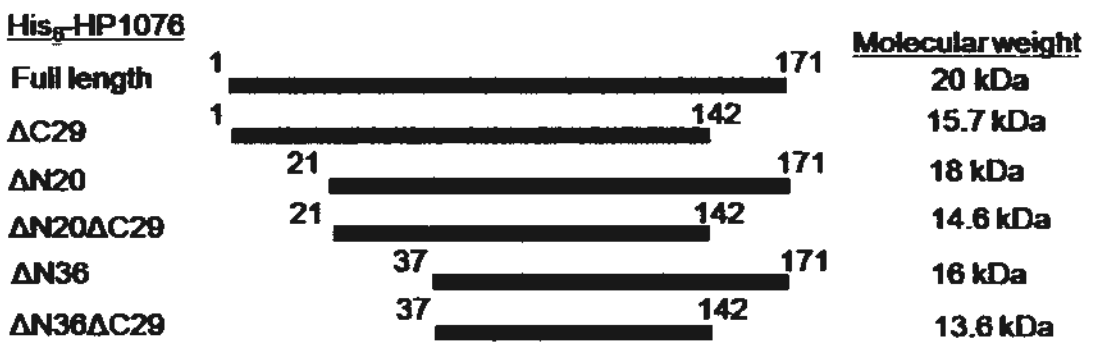

Fig.3.13 Construction of various protein fragments of His_6-HP1076

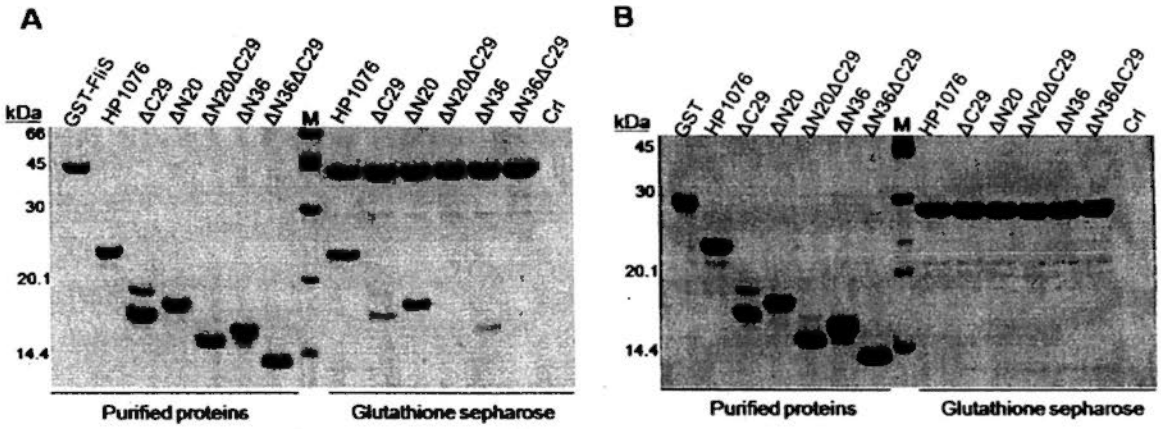

Fig.3.14 Pull-down assay performed with glutathione sepharose

Pull-down assay was performed with immobilized GST-FliS (A) or GST (B) on glutathione sepharose to test the binding of His_6-HP1076 fragments. The left panel of SDS-PAGE showed the purified proteins and the right panel showed the proteins bound to GST-FliS (A) or GST (B) immobilized sepharose after interaction. Control reactions (Crl) were set up with glutathione sepharose incubated with His_6-HP1076 only. Protein samples were analyzed in 15% SDS-PAGE.

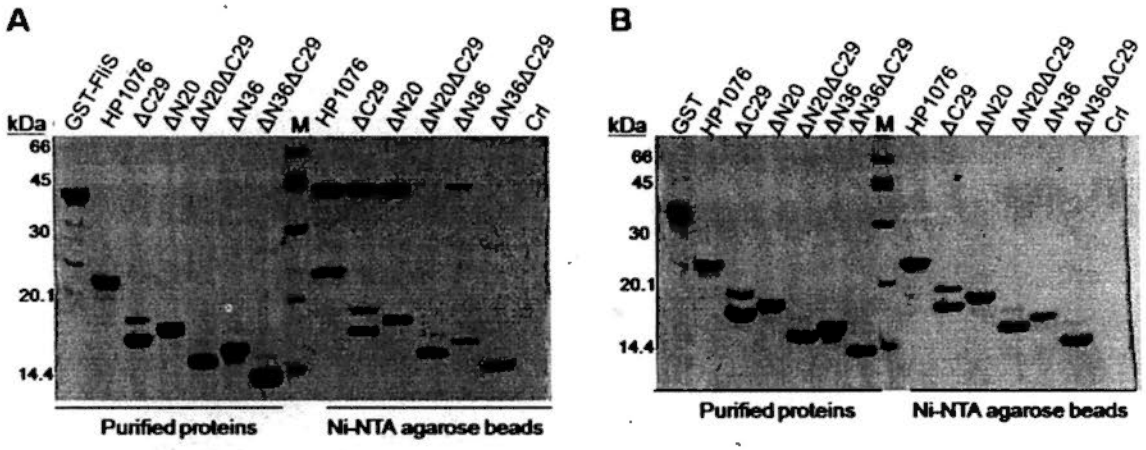

Fig.3.15 Pull-down assays performed with Ni-NTA agarose

Pull-down assay was performed with His_6-HP1076 fragments immobilized Ni-NTA agarose to test the binding to GST-FliS (A) or GST (B). The left panel of SDS-PAGE showed the purified proteins and the right panel showed the proteins bound with His_6-HP1076 fragments immobilized agarose after incubation. Control reactions were set up with GST-FliS and agarose only (A, Crl) or GST and agarose (B, Crl). Protein samples were analyzed in 15% SDS-PAGE.

3.8 Formation of stable protein complex analyzed by size exclusion chromatography

The interaction was further confirmed with size exclusion chromatography based on the size difference between single protein and protein complex. GST-FliS, GST or HP1076 fragments were analyzed by Superdex 200 10/300 GL column under the same condition as described in section 2.5.2. Various fragments of HP1076 were mixed with GST-FliS on ice for 30 min to allow interaction, then the protein mixture was subjected to gel filtration by Superdex 200. Purified GST-FliS protein was eluted out at a single peak at 12.8 ml, while HP1076 was eluted out at 14.9 ml. For the pre-mixed GST-FliS and HP1076, two peaks were obtained in the elution profile, the first peak at 11.5 ml contained protein complex of GST-FliS and HP1076 as verified in SDS-PAGE. Excess protein of HP1076 was eluted out at 14.9 ml in second peak which was the same as the elution profile of the single HP1076 protein (Fig.3.16). Thus, this showed that GST-FliS interacted with HP1076 and formed a protein complex. Another control reaction was performed by loading pre-mixed GST and HP1076, two peaks with the same elution volume of single respective proteins were observed (Table 3.3). Thus, this result further confirmed the interaction between FliS and HP1076. The results of other fragments pre-mixed with GST-FliS are summarized in Table 3.3B. By comparing the elution volumes of single proteins in

Table 3.3A, a shift of the elution profile was regarded as the presence of interaction. Thus, fragments ΔC29, ΔN20, ΔN36 and full-length protein formed stable protein complex with FliS. These findings were consistent to pull-down assays.

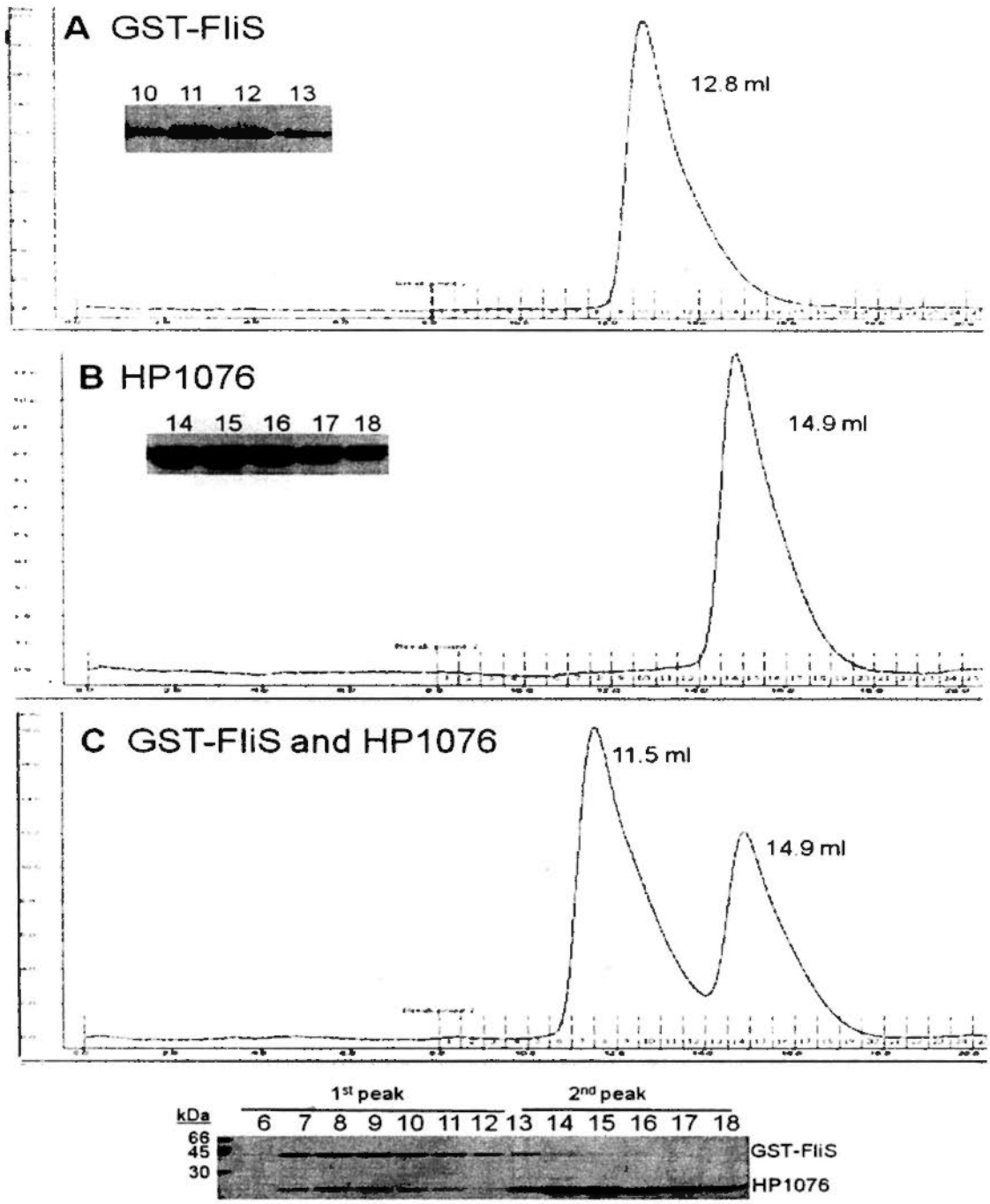

Fig.3.16 Size exclusion chromatography assay of GST-FliS and HP1076
Elution profiles of GST-FliS (A), HP1076 (B) and pre-mixed GST-FliS and HP1076 (C) were monitored by ÄKTA Prime system. The elution volume of the peaks was marked in the profile. Proteins from fractions were analyzed in 15% SDS-PAGE.

A

Sample	Elution volume
GST-FliS	12.8 ml
HP1076	14.9 ml
ΔC29	15.4 ml
ΔN20	15.3 ml
ΔN20ΔC29	15.9 ml
ΔN36	15.3 ml
ΔN36ΔC29	16.0 ml
GST	14.1 ml

B

Sample	Elution volume (1st peak)	Elution volumn (2nd peak)	Interaction (+/-)
GST-FliS and HP1076	11.5 ml	14.9 ml	+
GST-FliS and ΔC29	12.3 ml	15.4 ml	+
GST-FliS and ΔN20	12.0 ml	15.3 ml	+
GST-FliS and ΔN20ΔC29	12.8 ml	15.9 ml	-
GST-FliS and ΔN36	12.7 ml	15.3 ml	+
GST-FliS and ΔN36ΔC29	12.8 ml	16.0 ml	-
GST and HP1076	14.1 ml	14.9 ml	-

Table 3.3 Elution volumes of single or pre-mixed samples in size exclusion chromatography assay

Elution volumes of single proteins from Superdex 200 10/300 GL column are summarized in (A) and the elution volumes of pre-mixed proteins are summarized in (B) with identification of presence of interaction (+) and absence of interaction (-).

3.9 Purification of FliS/HP1076 complex

The interaction between FliS and HP1076 was demonstrated in the previous assays, isolation of over-expressed protein complex in *E. coli* expression system was examined in this section. The plasmids, pGEX-6p3-FliS and pAC28m-hp1076 were co-transformed into R2 cells and expressed at 25 °C upon IPTG induction. The cells expressing GST-FliS and His_6-HP1076 were lysed by sonication in Co-Ni binding buffer. Reducing the salt concentration helped to reduce disturbance on protein-protein interaction. The supernatant was subjected to Ni-NTA affinity chromatography first. His_6-HP1076 bound on sepharose was eluted out at 30% imidazole gradient in a single peak (Fig.3.17A). His_6-HP1076 was eluted together

with GST-FliS of about 60% purity as some impurities were found together with the elution (Fig.3.17B).

The elution fractions were pooled together and subjected to affinity chromatography with glutathione sepharose. GST-FliS bound on sepharose together with His_6-HP1076 were digested with PP to remove GST tag. GST tag stayed in the column and untagged FliS complexed with His_6-HP1076 were eluted out in fractions with 80% purity obtained (Fig.3.18).

The fractions from E1 – E4 (Fig.3.18) were subjected to Superdex^{TM} S75 gel filtration for further purification. FliS was eluted out with His_6-HP1076 as a protein complex in one single peak observed in the elution profile (Fig.3.19A). The protein complex was about 90% pure with some impurities of GST as predicted from the molecular weight from SDS-PAGE analysis (Fig3.19B). In order to remove the suspected GST, the fractions after gel filtration containing impurities were subjected to glutathione sepharose affinity chromatography. Most of the impurities were removed when compared with lanes B and E1 (Fig.3.20). Purified protein complex of about 95% purity was obtained and no degraded bands were observed from His_6-HP1076 protein (20 kDa), thus forming complex might stabilize protein.

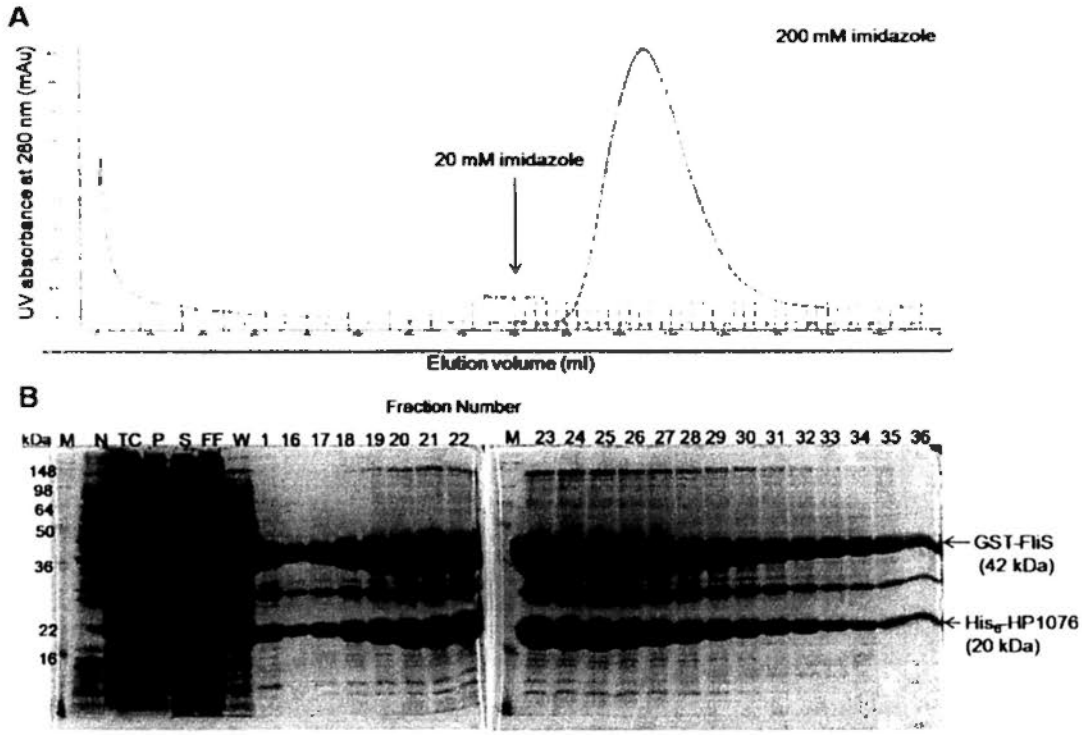

Fig.3.17 Purification of FliS/HP1076 complex by Ni-NTA sepharose

FliS/HP1076 complex was eluted in one peak observed in elution profile from nickel affinity chromatography (A). Protein samples before expression (N), total cell lysate (TC), insoluble fraction (P) and soluble fraction (S) of induced cells, flow-through collected from nickel column (FF), washing with buffer (W) and elution fractions by imidazole (1-36) were subjected to 15% SDS-PAGE.

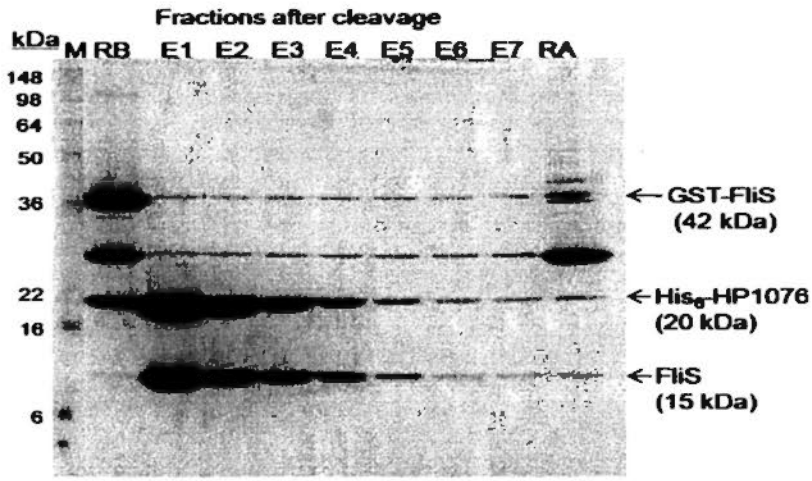

Fig.3.18 Purification of FliS/HP1076 complex by glutathione sepharose

Protein sample bound on sepharose before addition of PP (RB), eluted fractions after digestion (E1-E7) and sepharose after elution (RA) were analyzed by 15% SDS-PAGE.

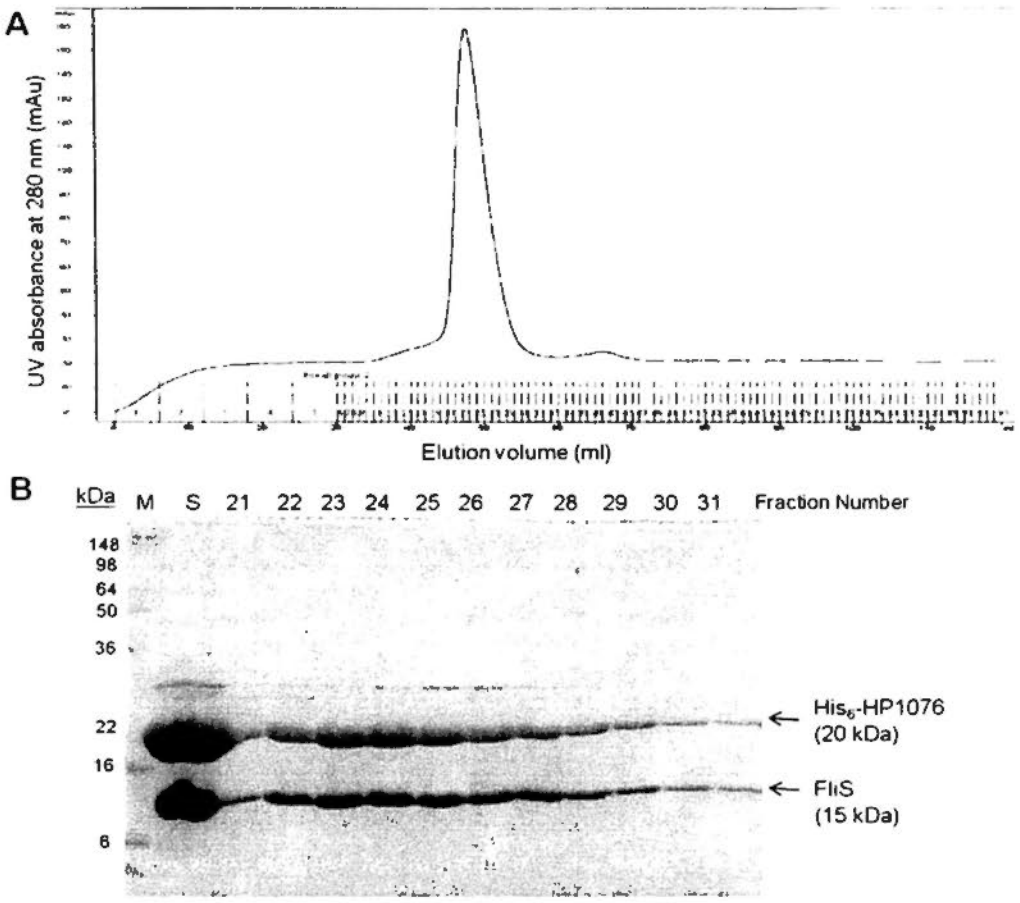

Fig.3.19 Purification of FliS/HP1076 complex by Superdex^{TM} S75 column

FliS/HP1076 complex (S) was eluted as one single peak observed in elution profile from gel filtration (A). And the corresponding fraction samples (21-31) and concentrated sample (S) were analyzed by 15% SDS-PAGE.

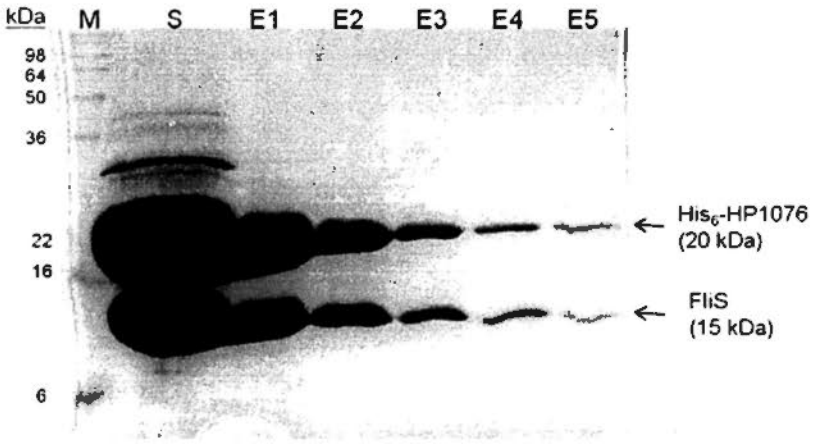

Fig.3.20 Purification of FliS/HP1076 complex by rebinding to glutathione sepharose

Protein sample from gel filtration (S) was eluted (E1-E5) after glutathione sepharose affinity chromatography and analyzed by 15% SDS-PAGE.

3.10 Binding parameters of FliS and HP1076 interaction

The binding parameters were determined with isothermal titration calorimetry (ITC), which measures the heat released or absorbed during binding events. 25 μM FliS protein was loaded to sample cell, and 390 μM His_6-HP1076ΔN20 (with minimal binding domain identified) was titrated into the cell with 20 injections of 1.5-μl portions with 180-sec intervals. The assay was performed at 25 °C with MicroCal iTC200 calorimeter. Two blank experiments, one with buffer injecting into HP1076ΔN20 and another with HP1076ΔN20 injecting into buffer in cell, were performed to determine the heat of dilution. The data was subtracted from heat of dilution so as to provide an accurate measurement of protein binding. Once the HP1076ΔN20 was injected and bound to FliS, a sharp peak was recorded as shown in upper part of Fig.3.21. The interaction was exothermic as heat measured was negative. The release of heat was gradually stopped when all the binding sites on FliS were occupied by HP1076ΔN20. The data was further integrated into a graph with MicroCal Origin 7 software with fitting to one set of binding set model as shown in lower plot of Fig.3.20. Duplicated experiment was performed to determine the kinetics parameters as association constant, $K = 1.5 \times 10^7 M^{-1}$, stoichemistry, N = 1.25, enthalpy, ΔH = -2350 kcal/mol and entropy, ΔS = 25.8 cal/mol/deg.

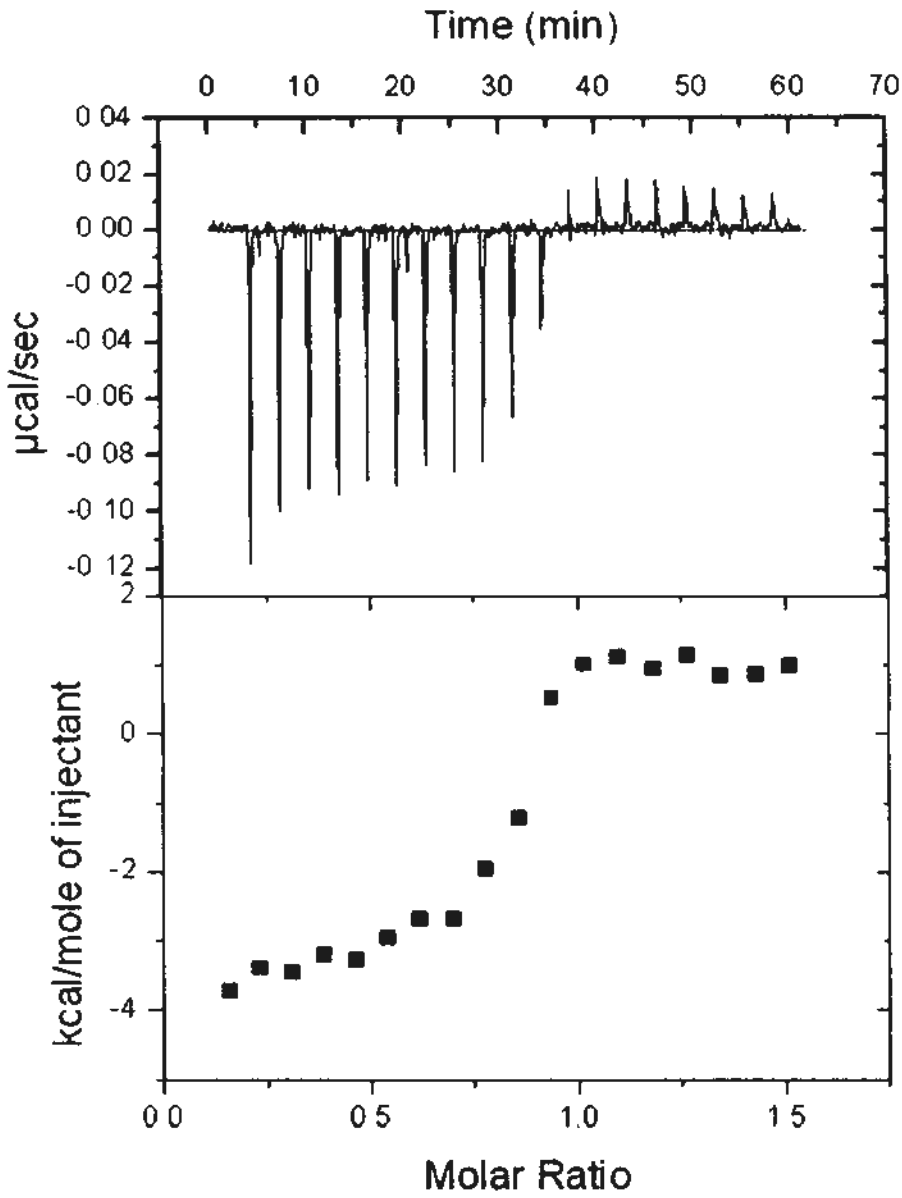

Fig.3.21 Isothermal titration calorimetry assay of FliS and HP1076

390 µM His_6-HP1076ΔN20 was titrated into 25 µM FliS proteins in 50 mM Tris, 150 mM NaCl, 2 mM DTT, 0.5 mM EDTA, 0.2 mM PMSF and 0.2 mM Benzamidine, pH7.5, at 25 °C. Total of 20 injections of 1.5 µl with 180-sec intervals were performed. The data was generated with MicroCal Origin 7 software with fitting to one set of binding set model.

3.11 Stabilization of insoluble FliS mutants by HP1076 *in vivo*

In order to investigate whether HP1076 would bind to FliS on its flagellin-binding pocket (Evdokimov *et al.*, 2003), five conserved residues (Ile24, Leu64, Leu68, Tyr79 and Leu80) located at the binding pocket were identified by protein sequence alignment of FliS in *H. pylori* and *A. aeolicus*, and these residues were mutated to alanine in GST-FliS by site-directed mutagenesis as stated in section 2.1.15. When wild-type GST-FliS (WT) and mutants (I24A, L64A, L68A, Y79A and L80A) were expressed individually, most of the mutants (I24A, L64A, L68A, L80A) were expressed as insoluble proteins in the pellet fractions after lysis (Fig.3.22A). Only Y79A was expressed as soluble protein with similar expression level to that of the WT protein. The solubility of these insoluble mutants was greatly improved when His_6-HP1076 was co-expressed (Fig.3.22B). Co-expression of GST and His_6-HP1076 was set as the control (Crl). Moreover, the GST-FliS mutants were able to form complex with His_6-HP1076 with similar binding affinity when the soluble protein fractions were subjected to pull-down assay with glutathione sepharose (Fig.3.22C). His_6-HP1076 was not pulled out when GST was expressed. Thus, the result suggested that HP1076 would stabilize the FliS protein.

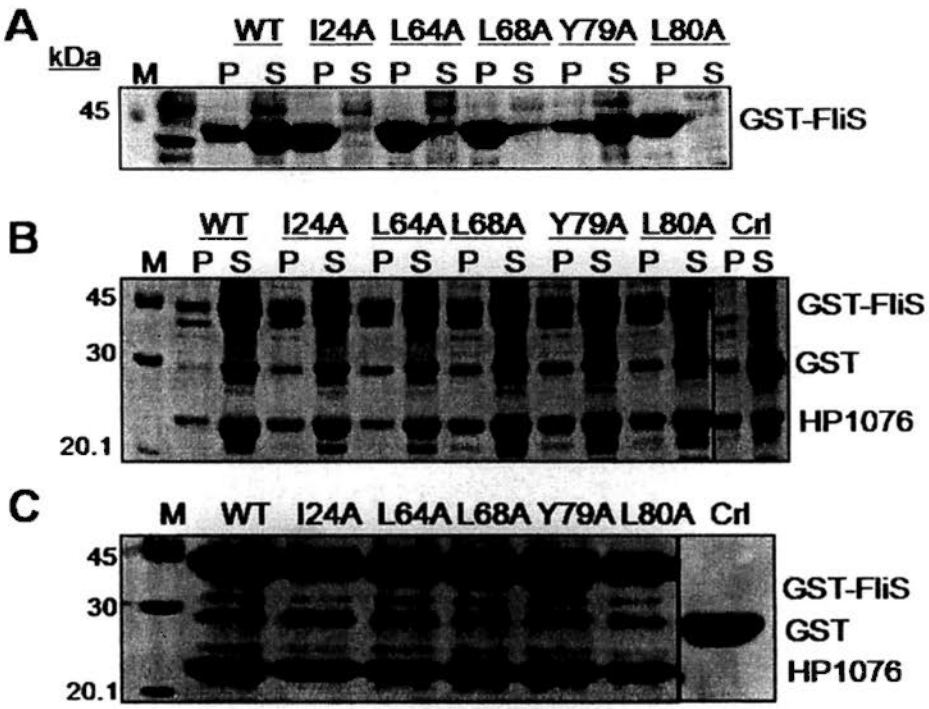

Fig.3.22 Expression profile of GST-FliS mutants with/without co-expression of HP1076

(A) Expression of wild-type GST-FliS (WT) and its mutants (I24A, L64A, L68A, Y79A, L80A) individually under the same expression condition. (B) Co-expression of GST-FliS and its mutants with HP1076 and control (Crl) set up with expressing GST and HP1076. Fractions of insoluble (P) and soluble (S) proteins after lysis were analyzed in 15% SDS-PAGE mutants in the presence of HP1076, or GST with HP1076 (Crl). (C) Pull-down assay with glutathione sepharose using soluble protein fractions from the co-expression in (B).

3.12 Chaperone-like activity of FliS and HP1076

In order to verify the proposed chaperone activity of HP1076, a reduced insulin-aggregation assay (Souza *et al.*, 2000) was performed with purified FliS, HP1076 and FliS/HP1076 complex. In this assay, the disulfide bonds between chains A and B of insulin were disrupted upon addition of DTT which led to aggregation of insulin and increase in absorbance (Sanger, 1949). The absorbance was decreased upon the addition of chaperone proteins like crystalline (Yu, 2004) and heat shock protein, Hsp26 (Haslbeck, 1999). The decrease in absorbance measured the extent of proteins on protecting insulin from denaturation. From Fig.3.23, HP1076 only exhibited a very mild chaperone activity as addition of a concentration of 30 μM of HP1076 was required to reduce the aggregation of insulin (25.6 μM) by about 20%. In contrast, 10 μM and 30 μM of FliS gave about 10 % and 40% of the anti-aggregation effect on insulin, respectively. However, the chaperone activity of FliS/HP1076 complex increased dramatically that a concentration of 10 μM was sufficient to reduce the aggregation by 35%, and 80% reduction was achieved with 30 μM of the complex. This result suggested that HP1076 may act as a chaperone to FliS to assist the chaperone activity by stabilizing FliS.

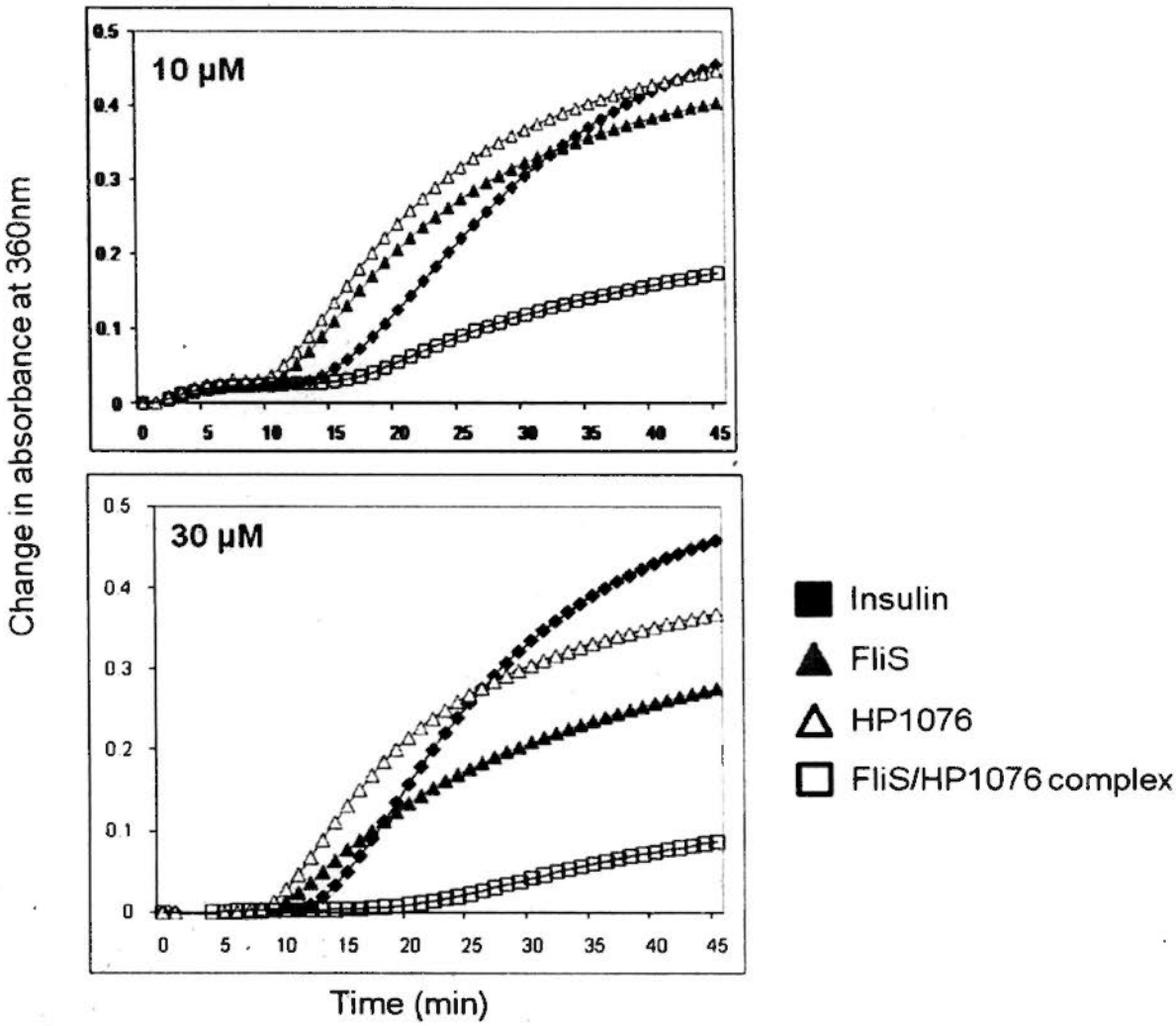

Fig.3.23 Chaperone-like activity assay performed with denatured insulin
Aggregation was initiated using DTT in phosphate buffer at 25°C with 25.6 μM insulin (■) and in the presence of 10 μM, or 30 μM of FliS (▲), HP1076 (Δ) or FliS/HP1076 complex (□).

3.13 Interaction of FliS to C-terminal fragments of flagellin A and B

Flagellin molecules form the filament structure by polymerization of flagellin monomers exported from the cytosol. Before the flagellar assembly, flagellin monomers are bound with the flagellar chaperone FliS in order to prevent pre-mature polymerization in *Salmonella* (Auvray *et al.*, 2001) and *A. aeolicus* (Evdokimov *et al.*, 2003). The C-terminal end of flagellin fragment was shown to be essential for

binding with FliS when the protein structure of the complex of flagellin and FliS was solved (Evdokimov *et al.*, 2003). To verify whether such interaction also occurs in the *H. pylori* system, a binding assay between FliS and C-terminal fragments of flagellin was performed with co-expression method. The cells co-expressed with His_6-FliS and GST or GST-FlaAc or GST-FlaBc were lysed and analyzed on SDS-PAGE (Fig.3.24A). All the proteins were over-expressed but the GST-FlaAc and GST-FlaBc were found mainly in insoluble fractions as the flagellin protein is highly hydrophobic. The C-terminal is highly disordered and previously was shown to be stabilized by FliS in *Salmonella* (Ozin *et al.*, 2003). Equal amount of soluble fractions determined from Bradford assay were subjected to pull-down assays using glutathione sepharose and Ni-NTA agarose beads. The proteins bound on the affinity sepharose through the GST- or His_6-tags were analyzed by SDS-PAGE (Fig.3.24B). His_6-FliS was successfully pulled the GST-FlaAc and GST-FlaBc fragments but not the GST protein, suggesting that FlaAc or FlaBc could bind to FliS.

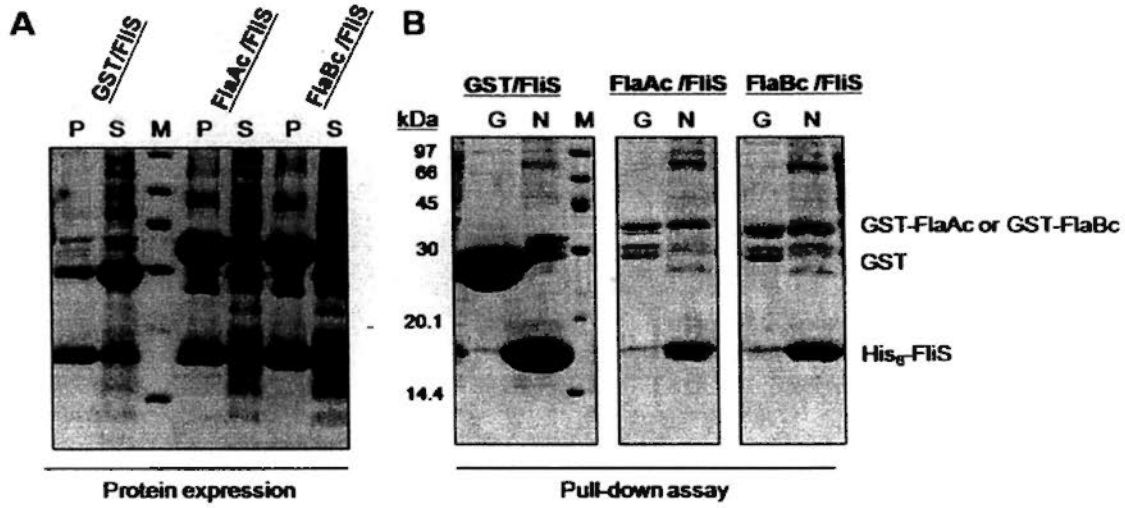

Fig.3.24 Co-expression and pull-down of FlaAc and FlaBc with FliS
(A) Expression profile of co-expressed proteins under the same expression condition, showing the insoluble (P) and soluble (S) protein fractions after cell lysis.
(B) Pull-down assays with glutathione sepharose (G) and Ni-NTA agarose beads (N) with cell lysate from co-expression. The protein samples were separated by 15% SDS-PAGE analysis.

3.14 Interaction of FliS with C-terminal fragments of flagellin A and B is not inhibited by HP1076

The C-terminal fragments of FlaA and FlaB were shown to have interaction with FliS, and HP1076 would bind tightly to FliS with an association constant of $1.5 \times 10^7\ M^{-1}$. The effect of HP1076 on flagellin-FliS binding was studied in this experiment. The over-expressed GST-FlaAc or GST-FlaBc or GST (Control) proteins in soluble fractions of lysate were immobilized on glutathione sepharose to verify the binding with FliS, HP1076 and FliS/HP1076 complex. The immobilization of GST-FlaAc was not satisfied as the amount of soluble protein was low. The sequence

identity of C-terminal regions of FlaA and FlaB is 74% in the sequence alignment (Fig.3.25). Thus, the binding of FliS to FlaAc is believed to be similar to that of FlaBc. In Fig.3.26, FliS bound on FlaBc, this is consistent with the results in co-expression and pull-down assays. HP1076 had no interaction with FlaBc, and it did not inhibit or enhance the interaction between FliS and FlaBc. This was further verified by subsequent incubation of FliS followed by HP1076 (FliS, HP1076) or vice versa (HP1076, FliS) to immobilized GST-FlaBc, no difference of FliS binding to FlaBc was observed. All these results indicated that HP1076 did not enhance or inhibit the binding between FliS and FlaBc and different binding sites on FliS were utilized for HP1076 and FlaBc.

```
HP0601(FlaA)    VTTLRGAMVVIDIAESAMKMLDKVRSDLGSVQNQMISTVNNISITQVNVKAAESQIRDVD 273
HP0115(FlaB)    VTSLKGAMIVMDMADSARTQLDKIRSDMGSVQMELVTTINNISVTQVNVKAAESQIRDVD 277
                **:*:***:*:*:*:** . ***:***:**** ::::*:****:****************

HP0601(FlaA)    FAEESANFNKNNILAQSGSYAMSQANTVQQNILRLLT 510
HP0115(FlaB)    FAEESANFSKYNILAQSGSFAMAQANAVQQNVLRLLQ 514
                ********.* ********:**:***:****:****
```

Fig.3.25 Protein sequence alignment of FlaAc and FlaBc in *H. pylori*
Identical residue is represented as *, highly conserved residue is represented as:, similar residue is represented as ., residues without any conservation are without any symbols.

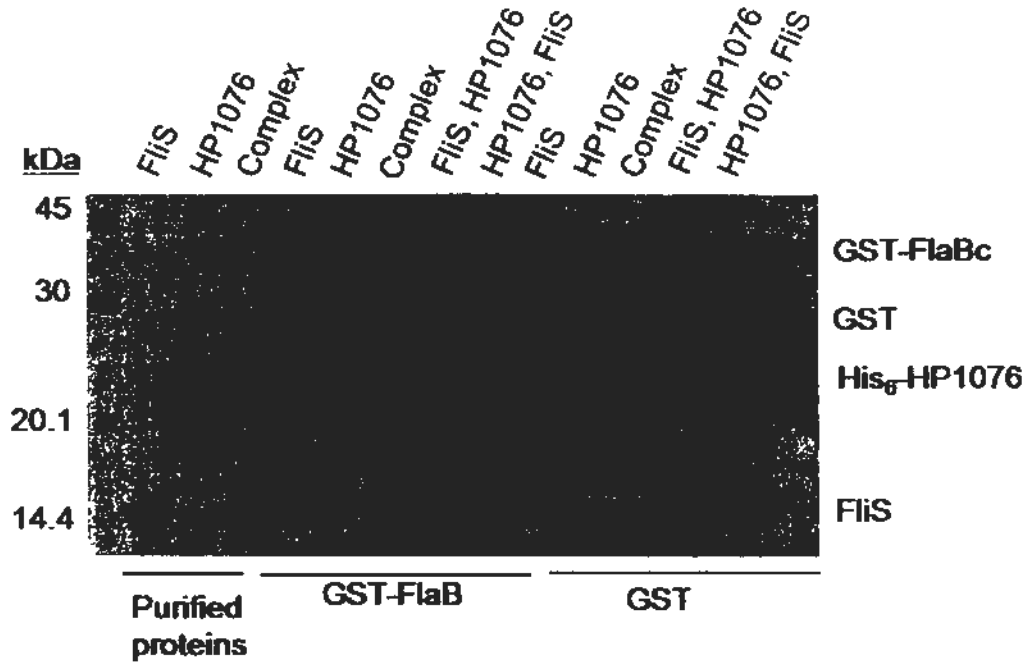

Fig.3.26 Pull-down assay of GST-FlaBc with FliS, HP1076 and FliS/HP1076
Pull-down assay was performed with immobilized GST-FlaBc on glutathione sepharose to verify the binding with purified proteins of FliS, HP1076, complex or subsequent addition of FliS or HP1076. Control reaction was performed with GST proteins. Protein samples were analyzed on 15% SDS-PAGE.

3.15 Interaction of FliS with flagella-related proteins

The result of the DTT-induced insulin aggregation assay described in section 3.12 suggested that FliS possessed a general chaperone activity. In *H. pylori*, there are no homologous chaperones of FlgN and FliT, specific to FlgK/FlgL and FliD, respectively (Fraser *et al.*, 1999; Bennett *et al.*, 2001; Imada *et al.*, 2010) identified so far. Moreover, FliS in *H. pylori* is predicted to have interaction with proteins not restricted to flagellins (Rain *et al.*, 2001). Thus, we hypothesized that FliS may have a broad substrate binding ability.

To test this hypothesis, flagellar proteins, FliD, FlgK, FliI and FliH were over-expressed with FliS (Fig.3.27A). Pull-down assay with Ni-NTA sepharose was adopted to verify their interaction (Fig.3.27B). Flagellar capping protein FliD and flagellar hook associated protein FlgK were pulled together with His_6-FliS. A control experiment was performed with expressed GST and His_6-FliS which showed no interaction. This suggested that FliS would bind to other flagellar associated proteins. Moreover, some components in the export machinery were also tested for binding with FliS. FliI is a membrane-associated ATPase involved in secretion of flagellar subunits coupled with ATP hydrolysis in *Salmonella* (Auvray *et al.*, 2002) and its regulator FliH binds to FliI to inhibit the enzymatic activity of ATPase regulating the export of substrates. FliI was expressed as insoluble protein in Fig.3.27A, thus, the interaction with FliS could not be verified with this method. In the future, by changing the tagging system of FliI or constructing fragment to remove unstructured coil (Lane *et al.*, 2005) or even expressing with its interacting partner FliH may help to improve the solubility of protein. For FliH, it showed over-expression and interaction with FliS. Thus, this preliminary screening method showed that FliS would bind to flagellar associated proteins, FliD and FlgK and regulator of ATPase, FliH. But it is not clear if the binding is through the flagellin- or HP1076-binding pockets on FliS.

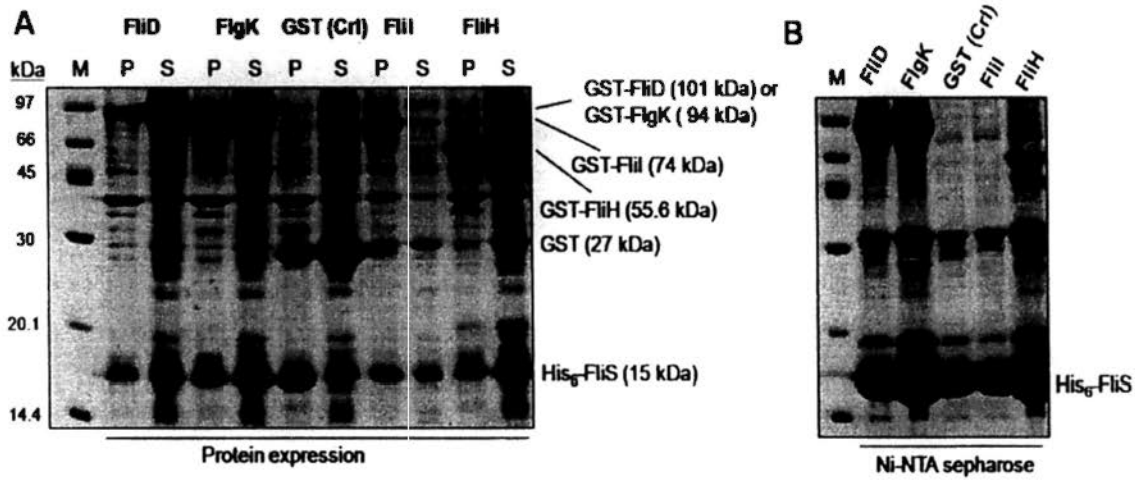

Fig.3.27 Co-expression and pull-down assays of FliS and flagellar protein substrates (A) Expression profile of co-expressed proteins with insoluble (P) and soluble (S) protein fractions analyzed on 15% SDS-PAGE.
(B) Pull-down assays were performed with Ni-NTA agarose beads using soluble fractions of cell lysate.

3.16 Conclusion

In the present study, the recombinant proteins of FliS and H1076 fragments were purified up to 95% purity for subsequent assays. The interaction between FliS and HP1076 confirmed the prediction from the yeast two-hybrid interaction study in PimRider™ database (Rain *et al.*, 2001). The minimal binding domain on HP1076 was mapped to 20-171 residues. Their association was very strong with Ka = 1.5×10^7 M^{-1} which was similar to that of *Salmonella* FliS and FliC fragment with Ka = 1.9×10^7 M^{-1} (Muskotál *et al.*, 2006). HP1076 did not bind to flagellin-binding pocket on FliS as mutants of residues involved in flagellin-binding showed interaction with HP1076. Moreover, HP1076 displayed co-chaperone activity on FliS as it prevented

the insoluble FliS mutants to form inclusion body by promoting the protein folding. It also enhanced the chaperone activity of FliS. However, HP1076 did not enhance or inhibit the binding of C-terminal fragment of flagellin to FliS. The detailed mechanism on co-chaperone activity of HP1076 remains verified in future.

The results of the chaperone activity of FliS and interaction with FlgK, FliD and FliH suggested that *H. pylori* FliS functions as general chaperone with broad substrate specificity not restricted to flagellins. In addition, various interacting partners are identified from database and the reduced expression level of flagellar proteins (flagellins FlaA and FlaB and hook protein subunit FlgE) in *H. pylori* *fliS*-deletion mutant (Allan *et al.*, 2000) further suggests that FliS is likely a general chaperone. This finding account for a new view of the flagellar system in *H. pylori* and this will be a starting point for further investigation of the different mechanism in flagellar system.

Chapter 4

Crystal structures of FliS, HP1076 and FliS/HP1076 complex

In order to obtain more molecular details of the interaction between FliS and HP1076, the crystal structures of FliS, HP1076 and FliS/HP1076 complex were determined by crystallography. The structure details would be discussed in this chapter.

Results and Discussion

4.1 Crystallization of FliS

Purified protein in a concentration of 7 or 9 mg/ml was used for crystallization screening with commercial kits in microbatch method. Protein and crystallization kit reagents were mixed in 1:1 volume ratio in the droplet which was covered by a layer of oil containing silicon oil and paraffin oil. After 2-day incubated at 20 °C, crystals were found in condition containing 0.2 M NaCl, 0.1 M HEPES at pH 7.5 and 21% (w/v) PEG-3000 (Fig.4.1). This condition was further optimized in order to obtain large single crystal for X-ray data collection. PEG-3350 was used as PEG-3000 was out of stock during optimization, and this change would not affect the crystallization of FliS. The buffer pH of HEPES at 7.3, 7.5 and 7.7 was tested, and the amount of

PEG-3350 ranged from 21 to 27% (w/v) was used. In different combinations of precipitant conditions, crystals were formed with different sizes as shown in Fig.4.2.

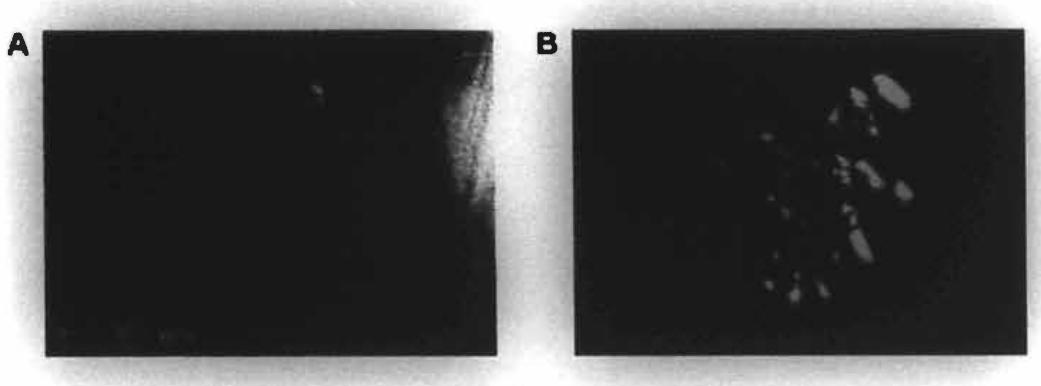

Fig.4.1 Crystals of FliS in microbatch screening trials
(A) 7 mg/ml FliS was crystallized into rod-like crystals with a size of about 0.1mm.
(B) 9 mg/ml FliS was crystallized into smaller crystals with size less than 0.1mm.

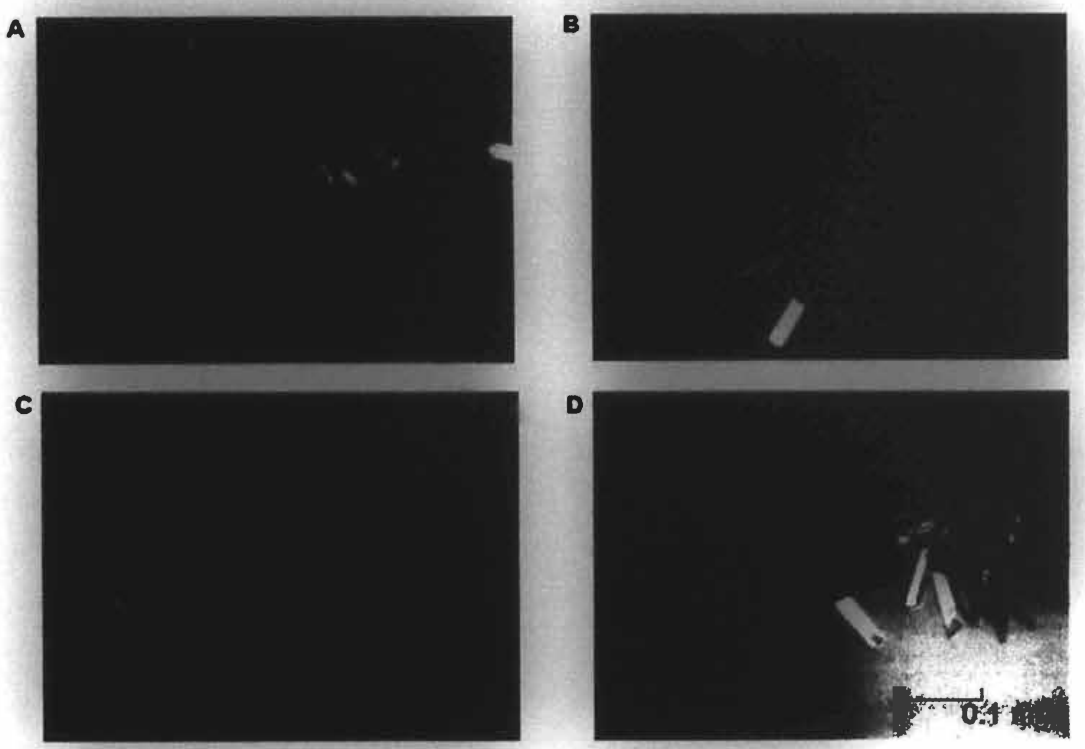

Fig.4.2 Crystallization optimization of FliS in hanging-drop vapour diffusion method
(A) 9 mg/ml of FliS was crystallized in 0.2 M NaCl, 23% (w/v) PEG-3350, 0.1 M HEPES, pH 7.7. (B) 7 mg/ml FliS was crystallized in 0.2 M NaCl, 25% (w/v) PEG-3350, 0.1 M HEPES pH 7.5. (C) 7 mg/ml FliS was crystallized in 0.2 M NaCl, 21% (w/v) PEG-3350, 0.1 M HEPES pH 7.3. (D) 7 mg/ml FliS was crystallized in 0.2 M NaCl, 21% (w/v) PEG-3350, 0.1 M HEPES pH 7.7.

4.2 Crystallization of His_6-HP1076 and HP1076ΔN20 fragment

5 mg/ml of purified full-length His_6-HP1076 was used for crystallization screening with commercial kits with sitting-drop method. Protein was mixed with reagents in 1:1 ratio. The plates were incubated at 16 and 25 °C, no crystals were formed after a 6-month of incubation. Only clear droplet and heavy precipitate were obtained (Fig.4.3). Thus, a truncated fragment was used for the screening.

5 mg/ml of purified His_6-HP1076ΔN20 was screened with commercial kits with sitting-drop method similar to full-length protein. Crystals were found in a condition containing 0.1 M Bis-Tris, pH 6.5, 25% (w/v) PEG-3350 and 0.2 M lithium sulfate at 16 °C (Fig.4.4A). This was further optimized by varying the pH and concentrations of precipitant in hanging-drop vapor diffusion method. Larger crystals were formed in an optimized condition of 0.1 M Bis-Tris, pH6.5, 27% (w/v) PEG-3350, 0.2 lithium sulfate (Fig.4.4B).

In order to solve the phasing problem of this novel protein without any similar 3D structure found in the Protein Data Bank, selenomethionine-substituted (SeMet) protein was prepared. The SeMet proteins were purified with the same condition as the native protein except 4 mM DTT was added in the storage buffer to reduce oxidation of selenomethionine. 5 mg/ml purified SeMet His_6-HP1076ΔN20 fragment was crystallized in the same condition of native protein. Crystals were formed at 16

°C with similar shape as the native protein (Fig.4.4C) with hanging-drop vapor diffusion method.

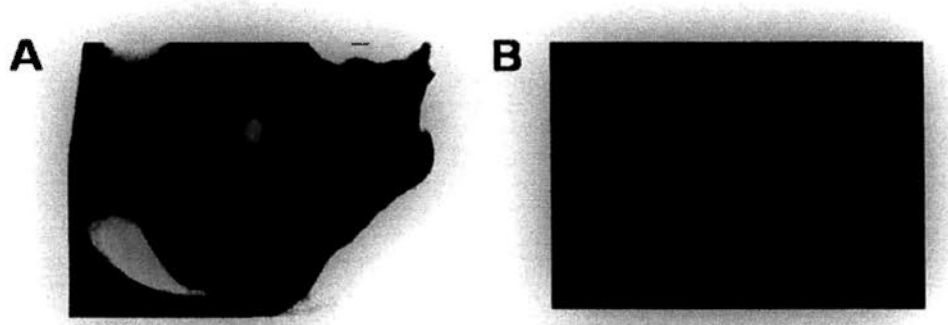

Fig.4.3 Crystallization results of full-length His_6-HP1076 protein
(A) HP1076 protein was heavily precipitated with precipitant
(B) A clear droplet was remained after 6-month incubation

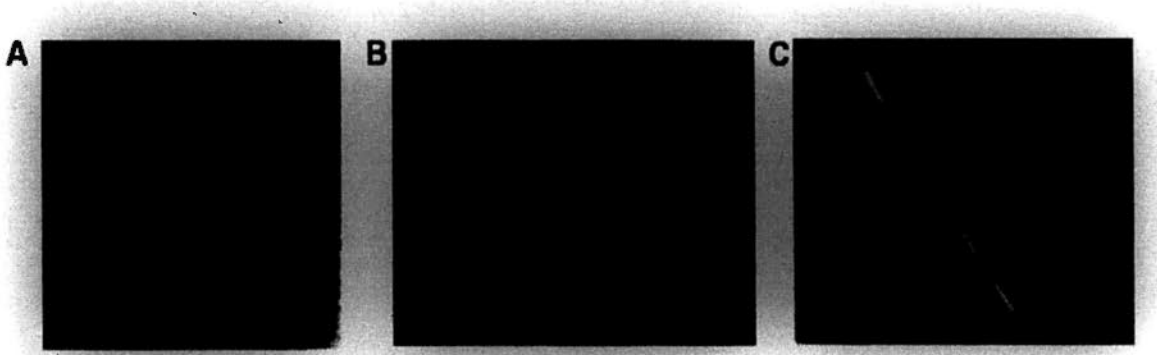

Fig.4.4 Crystals of His_6-HP1076ΔN20 fragment
(A) 5 mg/ml His_6-HP1076ΔN20 fragment was crystallized with in 0.1 M Bis-Tris, pH 6.5, 25% (w/v) PEG-3350 and 0.2 M lithium sulfate
(B) 5 mg/ml His_6-HP1076ΔN20 fragment was crystallized in an optimized condition containing 0.1 M Bis-Tris, pH 6.5, 27% (w/v) PEG-3350 and 0.2 M lithium sulfate
(C) 5 mg/ml SeMet His_6-HP1076ΔN20 fragment was crystallized in 0.1 M Bis-Tris, pH 6.5, 27% (w/v) PEG-3350 and 0.2 M lithium sulfate

4.3 Crystallization of FliS/HP1076 complex

Purified protein complex was used for screening with commercial kits in sitting-drop methods. Protein crystals were formed at 16 °C in some conditions, but most of them showed big crystals together with small crystals (Fig.4.5A-C). Only

tiny single crystal was formed in a condition containing 0.1 M MES, pH 6.0, 10% (v/v) 2-propanol, and 0.2 M calcium acetate (Fig.4.5D). So this condition was further optimized in hanging-drop vapor diffusion method. Unfortunately, no significant improvement was obtained as only slightly bigger crystals were obtained with an optimized condition containing 0.1 M MES, pH 5.7, 3% (v/v) 2-propanol, and 0.2 M calcium acetate (Fig.4.6A). Thus, microseeding method was adopted to optimize crystal quality (Ireton and Stoddard, 2004). Crystallization plate was set up by mixing 6.5 mg/ml protein complex and precipitant (0.1 M MES, pH 5.7, 3% (v/v) 2-propanol, and 0.2 M calcium acetate) in 1:1 ratio and incubated at 16 °C for one day. Protein crystals obtained from previous plate (Fig.4.5D) were washed with precipitant by centrifugation at low speed to remove any excess protein in droplet. Then the crystals were resuspended in precipitant and broken into smaller pieces by vortexing to prepare the seed mixture. The seed mixture was added in a droplet that occupied 10% of the total volume of droplet. Larger and single crystals were formed on the plate after 7-day incubation (Fig.4.6B, C).

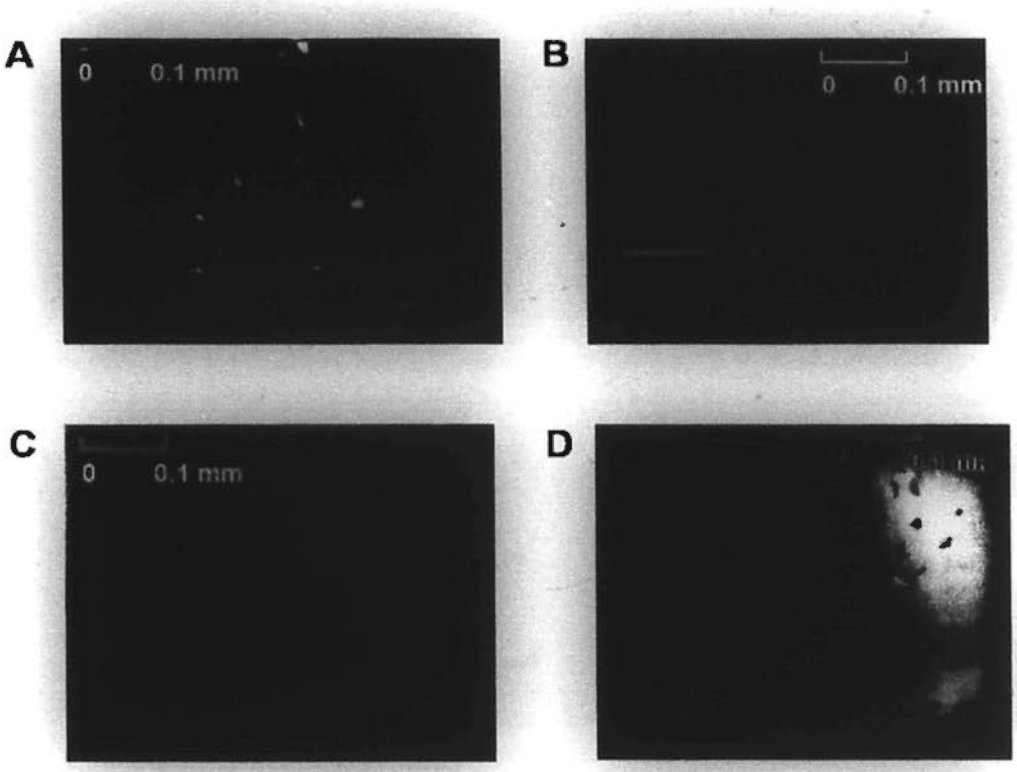

Fig.4.5 Crystals of FliS/HP1076 complex in crystallization screening

5 mg/ml protein complex was crystallized with sitting-drop method in the following conditions: (A) 0.1 M Tris, pH 8.5, 25% (w/v) PEG-3350, (B) 0.2 M Sodium malonate, pH 7.0, 20% (w/v) PEG-3350, (C) 0.2 M Sodium citrate tribasic dehydrate, 20% (w/v) PEG-3350, (D) 0.1 M MES, pH 6.0, 10% (v/v) 2-propanol, and 0.2 M calcium acetate.

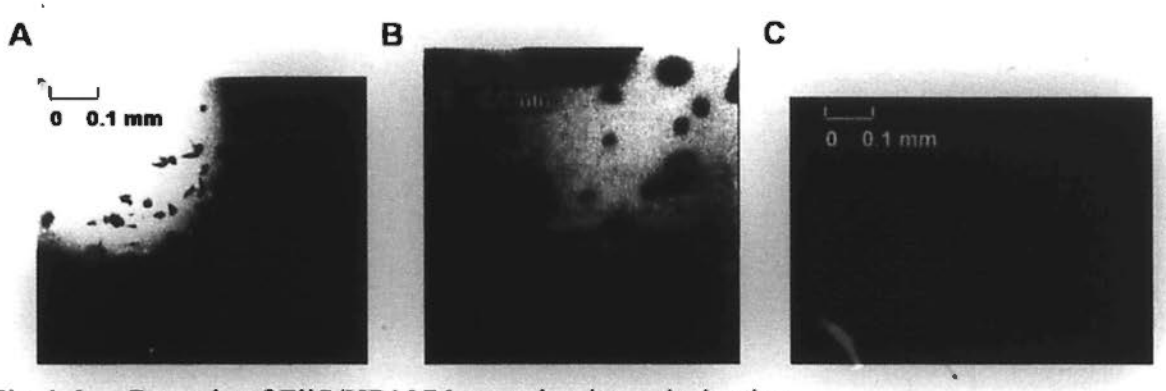

Fig.4.6 Crystals of FliS/HP1076 complex in optimization

(A) 6.5 mg/ml protein complex was crystallized in an optimized condition containing 0.1 M MES, pH 5.7, 3% (v/v) 2-propanol, and 0.2 M calcium acetate.

(B, C) Crystals formed by microseeding with 10% crystal seeds added in droplet pre-mixing with 6.5 mg/ml protein and precipitant (0.1 M MES, pH 5.7, 3% (v/v) 2-propanol, and 0.2 M calcium acetate) in 1:1 volume ratio.

4.4 Structure determination and refinement of FliS

A single FliS crystal (Fig.4.2D) was mounted for X-ray diffraction and diffracted up to 2.7 Å. Representative diffraction image is shown in Fig.4.7 which shows the pattern of reflection. After auto-indexing by Mosflm (Leslie, 1992), the protein was found to be crystallized in the space group $I4_122$, with unit-cell dimensions a=b= 92.54 Å, c = 144.92 Å, $\alpha = \beta = \gamma = 90°$. Statistics for data collection are summarized in Table 4.1. The structure was solved by molecular replacement (Rhodes, 2000) using *A. aeolicus* FliS (PDB ID code 1ORJ) as the search model in *PHASER* (McCoy *et al.*, 2005). With the phase determined, electron density map was then constructed for model building. Helices of the model were fit into the electron density map (Fig.4.8A) and the side chains of residues were also clearly shown in the map (Fig.4.8B). After rounds of refinement performed by *REFMAC* in CCP4 Suite (Emsley and Cowtan, 2004) to fine-tune the orientation of atoms within the unit cells, the R and R_{free} of the current model were refined to 23.78 and 28.38% respectively.

The Ramachandran plot produced by *PROCHECK* (Laskowski *et al.*, 1993) (Fig.4.9) shows the stereochemical quality of a protein structure. For the 119 residues in the FliS solved structure, 92.7% residues were found in the most favored allowed region and 7.3% were in additional allowed region, which showed that the structure

was in a good quality.

The final model of FliS consisted of 18-126 residues forming four-helix up-and-down bundle structure (Fig.4.10A). The helices were labeled as α1-4 from the N-terminal. There was no clear electron density for the N-terminal 17 residues and this region appeared to be disordered. Only 3-12 residues were traced with electron density and marked with coil region occupying the groove created by the helices at the bottom of structure. When the surface electrostatic potential was analyzed (Fig.4.10B), a more electronegative surface patch was found at the top and α2-α4 face, electropositive and hydrophobic surface were scattered around the whole structure. The residues Tyr3 and His12 were modeled as alanine as no density was observed for the side chains. The coordinates have been deposited in Protein Data Bank (PDB ID 3IQC).

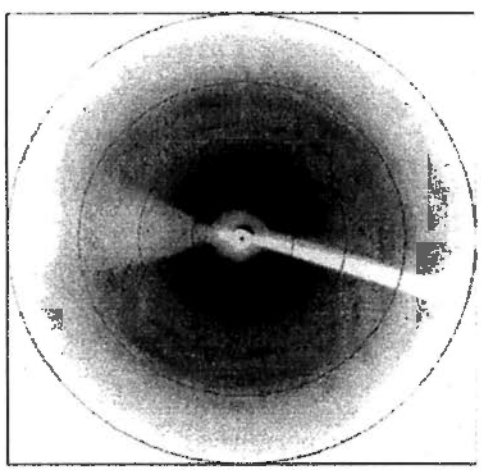

Fig.4.7 Representative X-ray diffraction image of FliS crystal
The resolution shells from the outer shell to inner shell were 2.5, 3.4, 5.1, 10.1 Å respectively.

Table 4.1 Data analysis and refinement statistics of FliS

Data Collection	
Space group	$I4_122$
Unit cell dimensions	
a, *b*, *c* (Å)/ α, β, γ(°)	92.5,92.5,144.9/ 90.0, 90.0, 90.0
Resolution (Å)	42.7-2.7 (2.85-2.7)
R_{merge}	0.038 (0.499)
$I / \sigma I$	24.4 (3.0)
Completeness (%)	97.6 (100.0)
Redundancy	5.0 (5.1)

Refinement	
Resolution (Å)	42.7-2.7
Number of reflections	8287
R / R_{free}	23.78/28.38
No of atoms refined	
Protein	1,776
Water	11
B-factors	
Protein	56.53
Water	44.34
Rmsd bond lengths(Å)	0.026
Rmsd bond angles (°)	1.922
Ramachandran plot	92.7/7.3/0/0

(Values in parentheses are for the highest-resolution shell.)

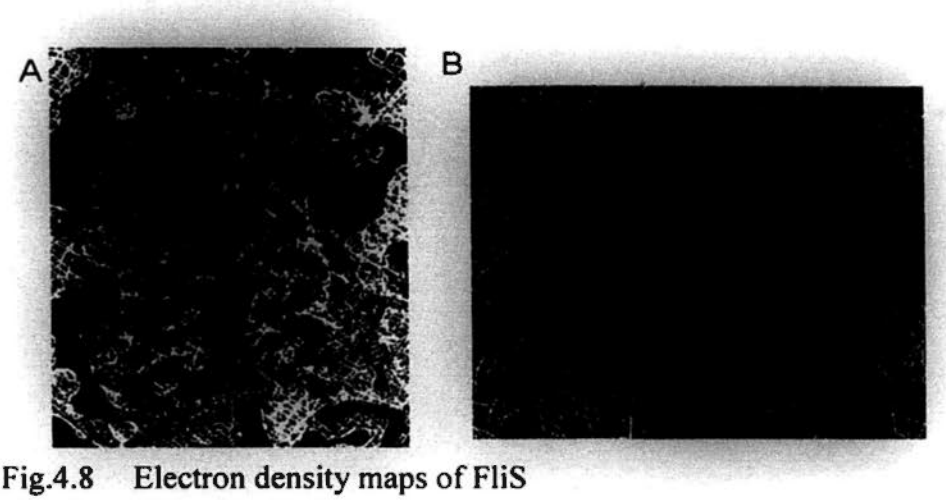

Fig.4.8 Electron density maps of FliS

The 2Fo-Fc density maps at 1 σ contour level are shown with well fitted two helical structures (α3-4) presented as pink ribbon in A and amino acid residues labeled as sticks with carbon, oxygen and nitrogen atoms colored as pink, red and blue respectively in B.

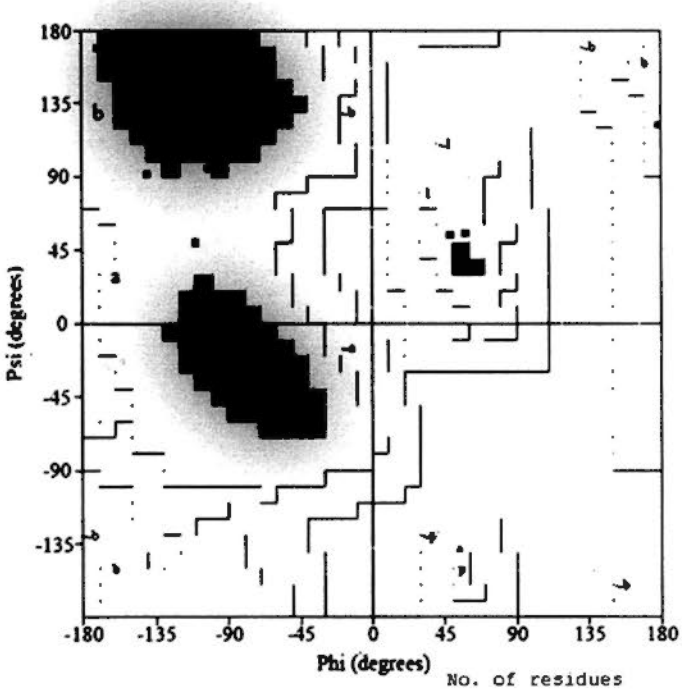

		No. of residues	
Most favoured regions	[A,B,L]	101	92.7%
Additional allowed regions	[a,b,l,p]	8	7.3%
Generously allowed regions	[~a,~b,~l,~p]	0	0.0%
Disallowed regions	[XX]	0	0.0%
Non-glycine and non-proline residues		109	100.0%
End-residues (excl. Gly and Pro)		4	
Glycine residues (shown as triangle)		5	
Proline residues		1	
Total number of residues		119	

Fig.4.9 Ramachandran plot of FliS structure

For the total 119 residues, 92.7% residues were in the most favored region marked as red and 7.3% residues were within the additional allowed region marked as yellow.

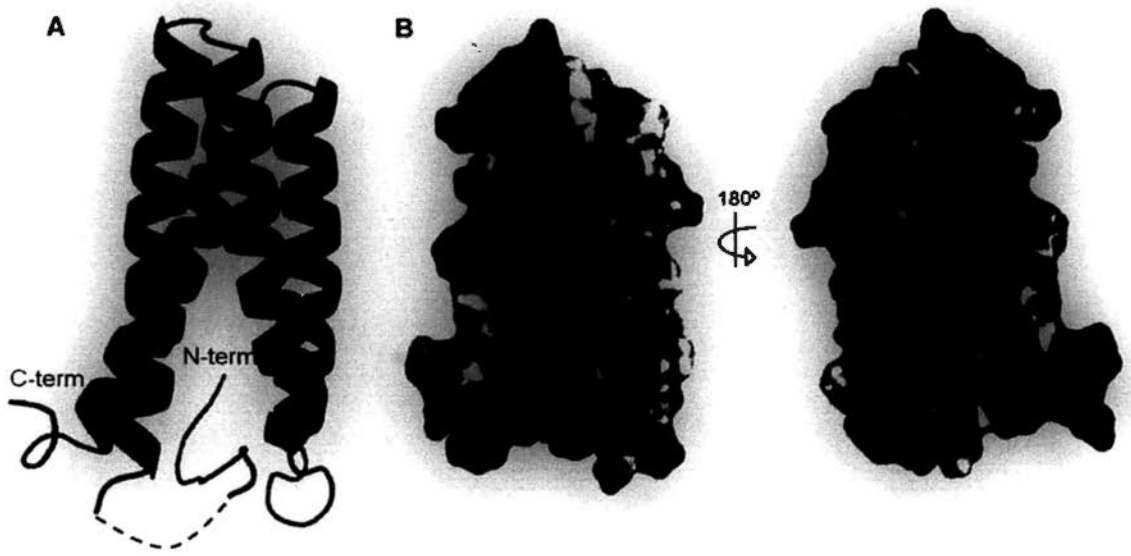

Fig.4.10 Crystal structure of FliS

(A) Cartoon representation of FliS structure. The four helices were labeled as α1-α4 from the N-terminal. The disordered N-terminal region was modeled from unclear electron density map as represented as a coil region. The residues without identity were represented by a dashed line connecting the disordered N-terminal to α1 helix.

(B) Molecular surface of FliS colored by electrostatic potential with contour level of ±5 kT, acidic and basic residues were colored red and blue respectively.

4.5 Structural comparison of *H. pylori* FliS with *A. aeolicus* FliS

DaliLite server (Holm and Park, 2000) was used to identify related structures deposited in Protein Data Bank similar to *H. pylori* FliS. The result revealed the highest similarity was *A. aeolicus* FliS with a rmsd (root mean square deviation) of 1.9 Å over 113 residues with Z-score of 16.4 suggesting that the two FliS structures were probable homologous. When the two FliS were superimposed, the helices were well fit together with similar topology (Fig.4.11A). Only the loops connecting α2-α3 and α3-α4 showed large difference marked in red boxes in Fig.4.11B. The amino acid residues in this region are in low sequence identity (Fig.4.12). Moreover, the side

chains of the conserved residues involved in the flagellin-binding pocket showed similar orientation to that of *A. aeolicus* FliS (Fig.4.11C, Fig.4.12). The flexible N-terminal region occupying the flagellin-binding pocket is likely to be stabilized in the same way as *A. aeolicus* FliS (Fig.4.11D) through hydrogen bonds of conserved Tyr10, Tyr28 and Tyr84 residues (Fig.4.12). The C-terminal regions of flagellin molecules of FliC involved in FliS binding are highly conserved with that of FlaA or FlaB of about 40% sequence identity (Fig.1.8). From the molecular surface of the *A. aeolicus* FliS (Fig.4.13), a groove was formed spanning the bottom part of the helices which was well fitted with flagellin fragment. The conserved residues on the enteric bacteria FliS were localized on the bottom part which were involved in binding flagellin C-terminal region through conserved residues (Fig.4.13). Thus, this suggested that the interaction of FliS and flagellin was conserved in *H. pylori* and the flexible N-terminal controlled the entry of flagellin for binding. The binding mode of FliS-FlaA/FlaB in *H. pylori* resembled that of the FliS-FliC in enteric bacteria and this binding was evolutionary conserved.

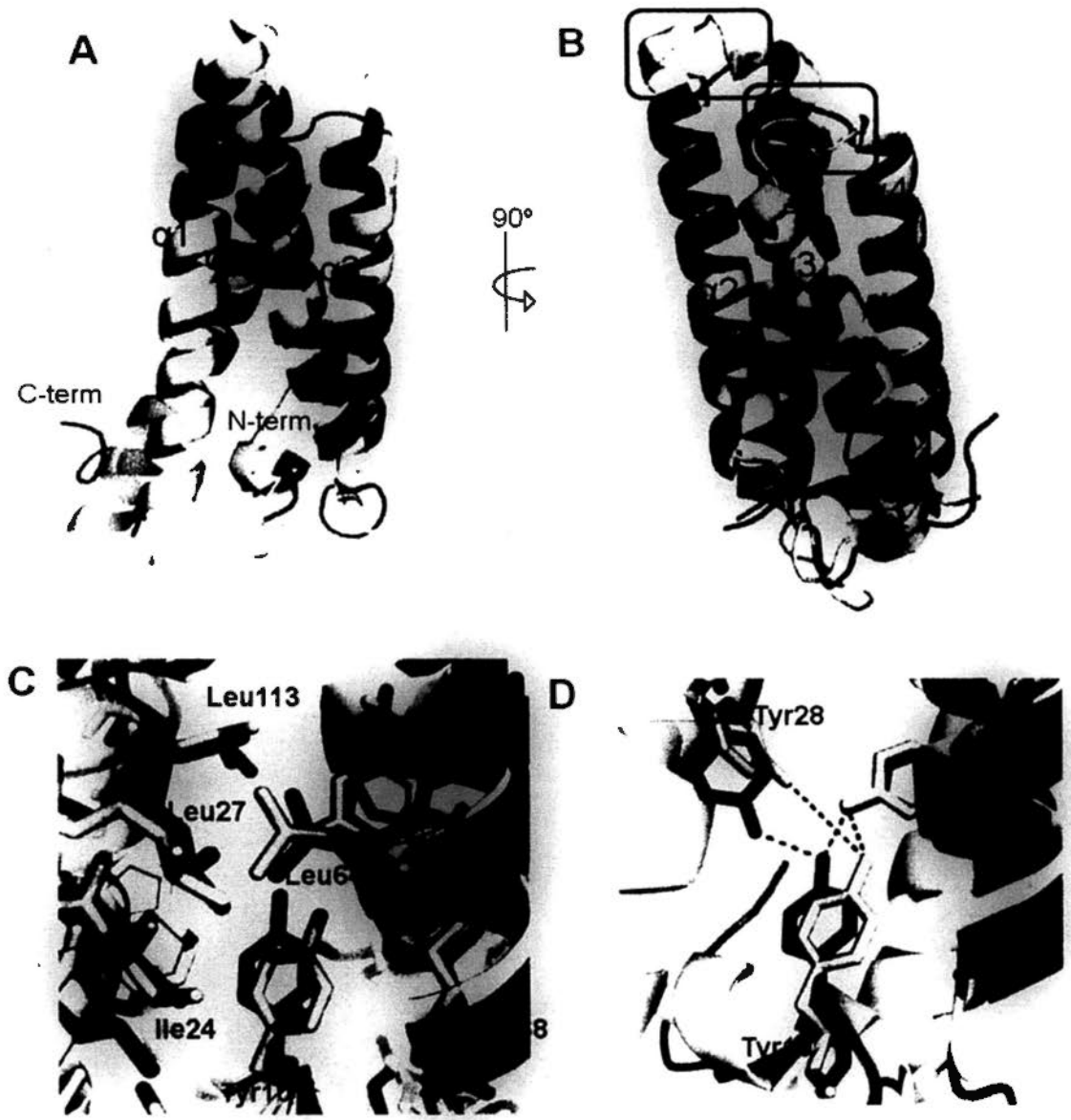

Fig.4.11 Superimposition of FliS structure of *H. pylori* and *A. aeolicus*
(A) *H. pylori* FliS (purple) is superimposed to *A. aeolicus* FliS (white) with good alignment of helices. (B) The largest structural differences are marked in red boxes. (C) The flagellin-binding pocket showing the similarity of residues involved in binding to flagellin. (D) Conserved tyrosine residues involved in stabilizing flexible N-terminal region.

```
                                  α1                  α2
                  *
H.pylori          MQYANAYQAYQHNRVS----VESPAKLIEMLYEGILRFSSQAKRCIENEDIEKK----IY 52
C.jejuni          MQNNLAYNAYSQNQVG----IESPQKLIEMLYEGILRFCARAKVAIRNEDIEQR----VY 52
Salmonella        MYTASGIKAYAQVSVESAVMSASPHQLIEMLFDGANSALVRARLFLEQGDVVAK----GE 56
E.coli            MYAAKGTQAYAQIGVESAVMSASQQQLVTMLFDGVLSALVRASLFMQDNNQQGK----GV 56
A.aeolicus        --MRNIAEAYFQNMVET----ATPLEQIILLYDKAIECLERAIEIYDQVNELEKRKEFVE 54
                                  α3                  α4
H.pylori          YINRVTDIFTELLNI-LDYEKGGEVAVYLTGLYTHQIKVLTQANVENDASKIDLVLNVAR 111
C.jejuni          FVKRTTAIFIELINT-LNYEKGGEVAHYLSGLYTREIQLLSLANLENNEDRINEVINVTK 111
Salmonella        ALSKAINIIDNGLKAGLDQEKGGEIATNLSELYDYMIRRLLQANLRNDAQAIEEVEGLLS 116
E.coli            SLSKAINIIENGLRVSLDEESKDELTQNLIALYSYMVRRLLQANLRNDVSAVEEVEALMR 116
A.aeolicus        NIDRVYDIIS-ALKSFLDHEKGKEIAKNLDTIYTIILN--TLVKVDKTKEELQKILEILK 111

H.pylori          GLLEAWREIHSDELA----- 126
C.jejuni          GLLEAWREVHNNETVAQ--- 128
Salmonella        NIAEAWKQISPKASFQESR- 135
E.coli            NIADAWKESLLSPSLIQDPV 136
A.aeolicus        DLREAWEEVKKKV------- 124
```

Fig.4.12 Multiple sequence alignment of FliS from various bacteria

Secondary structures are shown as grey boxes above the sequence alignment. Triangles represent the residues involved in flagellin interaction. Tyrosine residues involved in stabilizing the flexible N-terminal region are marked with (*).

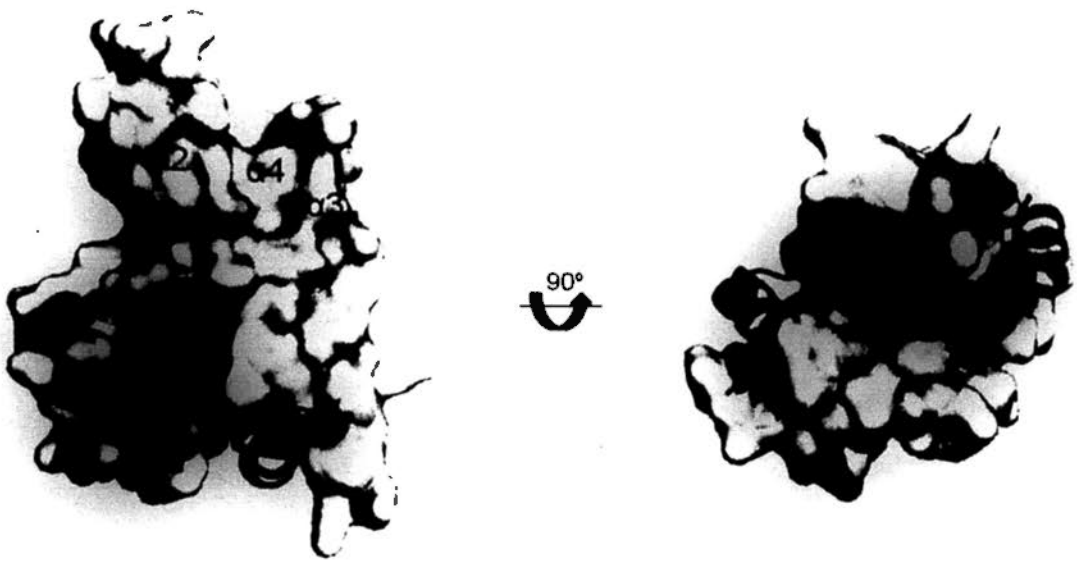

Fig.4.13 Molecular surface of *A. aeolicus* FliS/FliC complex

Molecular surface of FliS (white) with conserved residues colored in red is shown in complex of FliC fragment (light blue) with conserved residues colored in dark blue.

4.6 Structural determination and refinement of HP1076

Diffraction data of native crystal of HP1076ΔN20 was collected up to 1.74 Å (Table 4.2). A 2.33 Å single-wavelength anomalous diffraction (SAD) dataset was collected from a SeMet crystal. The four selenomethionine sites were located and provided information to calculate the phase to a resolution of 2.33 Å. Traceable electron density map was resulted and used for refinement with native dataset by ARP/wARP (Langer *et al.*, 2008) to current model with R and R_{free} values of 21.01% and 23.31%, respectively. HP1076 was found to be crystallized in space group of $C222_1$ with unit cell dimensions of a=58.9, b=87.2, c=60.8 Å, $\alpha = \beta = \gamma = 90$ °. The refinement statistics are summarized in Table 4.2. The model was well fitted into the electron density with helical and β-strand structures (Fig.4.14). As the data was collected to a good resolution, the electron density showed more details in the side chains for constructing a more precise structure. Ramachandran plot of HP1076 structure showed that the structure was in good quality that 95.3% and 4.7% of total 115 residues were in the most favored region and additional allowed region respectively (Fig.4.15).

HP1076 structure consisted of 33-147 residues and adopted a bundle-like fold with 3 helices (α1-α3), short helices (η1-η2) and anti-parallel β sheet (β1-β3) (Fig.4.16A). The secondary structures were arranged as β1-α1-η1-α2-β2-β3-η2-α3

from N-terminal. The β sheet localized on one edge of bundle and the short helices localized on the top of the bundle. The short helices (η1-η2) were 3/10 helices which occurred due to kinks at Gly63 in α1 and Glu119 in front of α3. When η1 and η2 helices were packed together with other 3 helices, the overall structure resembled 4-helix bundle structure. When the electrostatic potential surface of HP1076 was calculated (Fig.4.16B), a highly electronegative charged residues was localized on the surface of α3 and the β sheets. An electropositive surface and hydrophobic surface were localized between α1-α2 helices on the opposite side of the structure. The coordinates have been deposited in Protein Data Bank (PDB ID 3K1H).

Table 4.2 Data analysis and refinement statistics of HP1076

Data collection	**Native HP1076ΔN20**	**SeMet HP1076ΔN20**
Space group	$C222_1$	$C222_1$
Unit cell dimensions		
a, b, c (Å)	58.9, 87.2, 60.8	57.5, 88.6, 60.4
α, β, γ(°)	90.0, 90.0, 90.0	90.0, 90.0, 90.0
Resolution (Å)	26.1-1.74 (1.8-1.74)	50.0-2.33 (2.41-2.33)
R_{merge}	0.056 (0.443)	0.136 (0.476)
$I / \sigma I$	45.8 (3.6)	16.7 (2.7)
Completeness (%)	98.5 (90.4)	91.5 (70.3)
Redundancy	7.4 (6.1)	12.0 (8.0)
Refinement		
Resolution (Å)	26.06-1.74	
No. reflections	16,258	
R / R_{free}	21.01/23.31	
No. atoms		
Protein	906	
Water	83	
B-factors		
Protein	23.34	
Water	32.13	
Rmsd bond lengths(Å)	0.010	
Rmsd bond angles (°)	1.169	
Ramachandran plot	95.3/4.7/0/0	

(Values in parentheses are for the highest-resolution shell.)

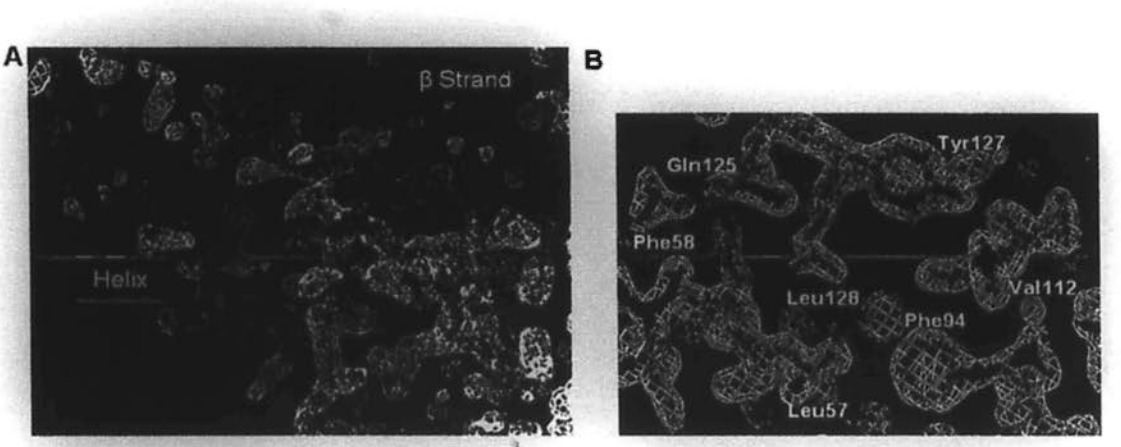

Fig.4.14 Electron density maps of HP1076

The 2Fo-Fc density maps at 1 σ contour level are shown with well fitted helical structures and β-strands presented as blue ribbon (A) and amino acid residues labeled as sticks with carbon, oxygen and nitrogen atoms colored as blue, red and light blue respectively (B).

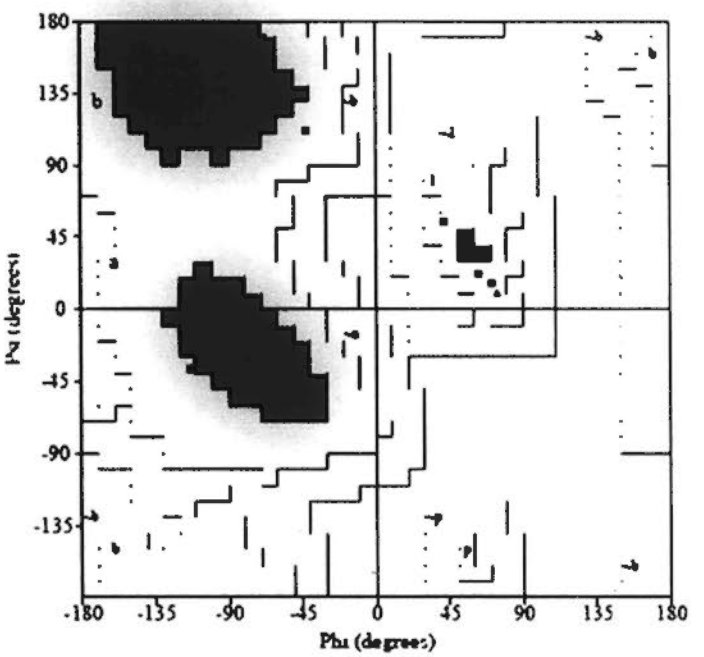

		No. of residues	
Most favoured regions	[A,B,L]	102	95.3%
Additional allowed regions	[a,b,l,p]	5	4.7%
Generously allowed regions	[~a,~b,~l,~p]	0	0.0%
Disallowed regions	[XX]	0	0.0%
Non-glycine and non-proline residues		107	100.0%
End-residues (excl. Gly and Pro)		2	
Glycine residues (shown as triangles)		4	
Proline residues		3	
Total number of residues		115	

Fig.4.15 Ramachandran plot of HP1076 structure

For the total 115 residues, 95.3% residues are in the most favored region marked as red and 4.7% residues are within the additional allowed region marked as yellow.

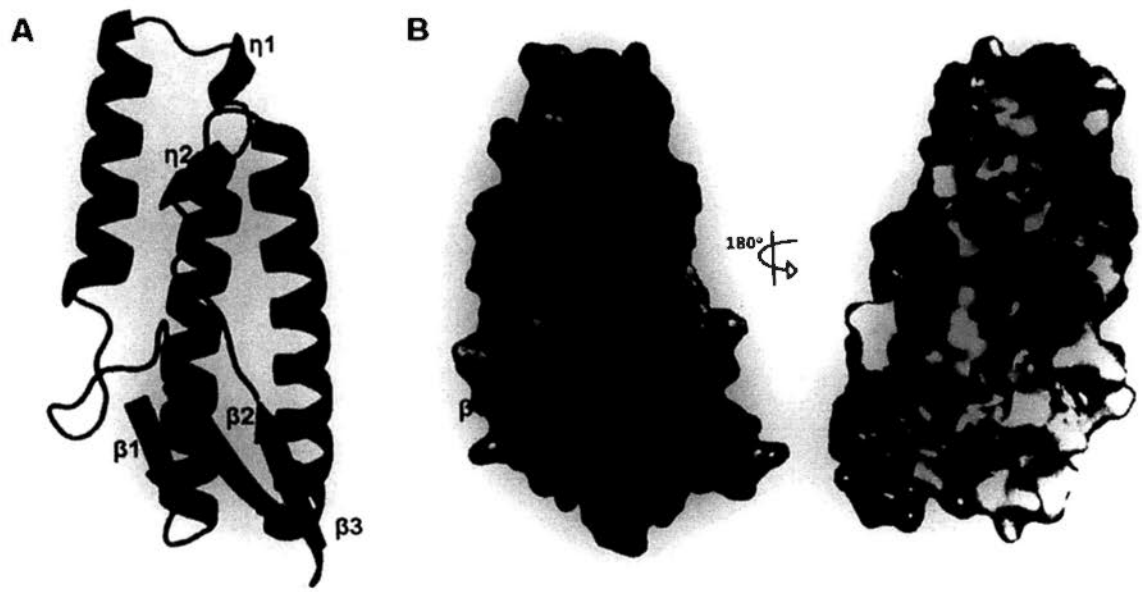

Fig.4.16 Crystal structure of HP1076
(A) Cartoon representation of HP1076 with helices and short helices labeled as α1-α3 and η1-η2 respectively. Strands are represented by arrows and labeled as β1-β3. (B) Molecular surface of HP1076 colored by electrostatic potential with contour level of ±5 kT, acidic and basic residues are colored red and blue, respectively.

4.7 Structural similarity search of HP1076

DALI structural homology search (Holm and Sander, 1996) of HP1076 revealed hits with flagellar related proteins included flagellin homologue P5, flagellar hook-associated protein 3 (HAP3) and flagellar protein with a significant Z score above 5 which meant the structures were probably homologous (Table 4.3). The rmsd showed the average deviation of distance of aligned alpha carbons, that the homologues were in good alignment. The homologues were in low protein sequence identity of <15%. However when the structures are superimposed (Fig.4.17), the α1-α3 helices of HP1076 were overlapped well with the homologues. The β sheet

was not aligned so well with that in flagellin homologue P5 and HAP3 and also large insertion of structures with unrelated homology were found. HP1076 was aligned better with FliS to certain extent. Moreover, HP1076 was found to be structurally homologous to phase 1 flagellin and invasin IPAD which is a needle tip protein in type III secretion system (Steele-Mortimer *et al.*, 2002). These results suggested that HP1076 was structurally related to proteins in flagellar system and type III secretion system.

Table 4.3 Result of structure homologues from DALI search

Protein structure	**Species**	**Z score**	**Rmsd**	**% sequence identity**	**PDB code**
Flagellin homolog P5	*Sphinogmonas sp. A1*	11.9	2.3 Å	11	2ZBI
Flagellar hook-associated protein 3	*Salmonella typhimurium*	10.0	2.0 Å	10	2D4X
Flagellar protein FliS	*Aquifex aeolicus*	7.1	2.9 Å	13	1ORJ
Phase 1 flagellin	*Salmonella typhimurium*	7.0	2.3 Å	13	1UCU
Invasin IPAD	*Shigella flexneri*	6.7	2.8 Å	10	2J0O

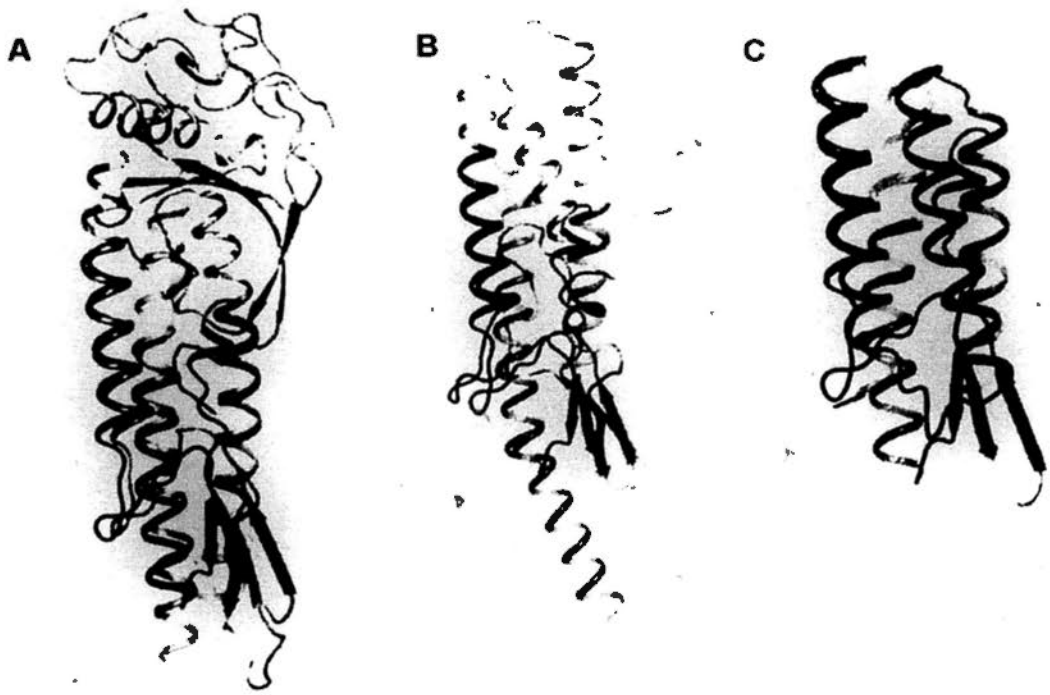

Fig.4.17 Superimposition of HP1076 with structural homologues from DALI search HP1076 colored in blue is superimposed with flagellin homologue P5 colored in orange (A), hook-associated protein 3 colored in red (B) and flagellar protein FliS colored in pink (C). The structure without any homology is colored in yellow.

4.8 Structural determination and refinement of FliS/HP1076 complex

Crystal of full length FliS/HP1076 complex was diffracted to 2.7 Å. The structure was determined by molecular replacement using solved FliS and HP1076 in this study as the search models. In the 2Fo-Fc electron density map, the helices of FliS and HP1076 were well fitted into the map (Fig.4.18). The complex was crystallized in space group of $P4_1$ with unit cell dimension, a=b=50.3 Å, c=242Å and $\alpha = \beta = \gamma = 90$ °. The current model was refined to R and R_{free} values of 25.83 and 29.87%, respectively. The other refinement statistics are summarized in Table 4.4. A Ramachandran plot of FliS/HP1076 complex showed that for the total 449 residues,

90.9% residues, 8.4% residues and 0.7% residues were found in the most favored region, additional allowed region and generously allowed regions, respectively (Fig.4.19). The structure was in a good quality as above 90% residues were within the most favored regions. The coordinates have been deposited in Protein Data Bank (PDB ID 3K1I).

Two HP1076 and two FliS were found in one asymmetric unit. The current model consisted of 20-124 residues of FliS and 28-146 residues of HP1076. The missing part was due to the absence of electron density for model building. The interaction was mainly mediated by α2-α3 interface of FliS to an extended α1 helix rearranged from β1 strand from HP1076 (Fig.4.20).

Table 4.4 Data analysis and refinement statistics of FliS/HP1076 complex

Data collection	
Space group	$P4_1$
Unit cell dimensions	
a, *b*, *c* (Å)/ α, β, γ(°)	50.3, 50.3, 242.0/ 90.0,90.0,90.0
Resolution (Å)	30.0 – 2.69 (2.8-2.69)[a]
R_{merge}	0.083 (0.474)
$I / \sigma I$	21.5 (3.6)
Completeness (%)	95.6 (98.7)
Redundancy	4.7 (4.7)

Refinement	
Resolution (Å)	19.33-2.70
No. reflections	14883
R / R_{free}	25.83/29.87
No. atoms	
Protein	3591
Water	16
B-factors	
Protein	44.79
Water	29.38
Rmsd bond lengths(Å)	0.015
Rmsd bond angles (°)	1.442
Ramachandran plot	90.6/8.6/0.7/0

(Values in parentheses are for the highest-resolution shell.)

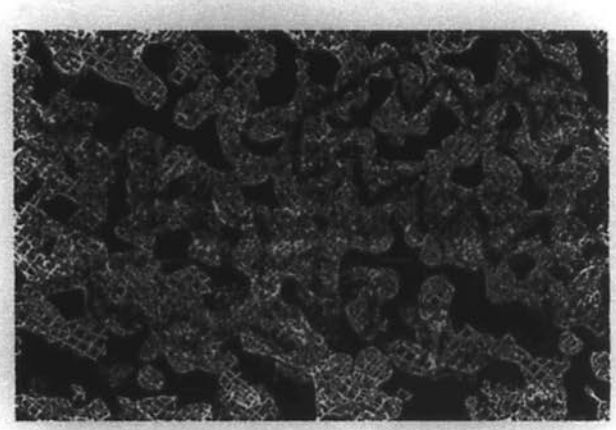

Fig.4.18 Electron density map of FliS/HP1076 complex

The 2Fo-Fc density maps at 1 σ contour level is shown with well fitted helical structures of FliS colored in purple and HP1076 colored in blue at the interface.

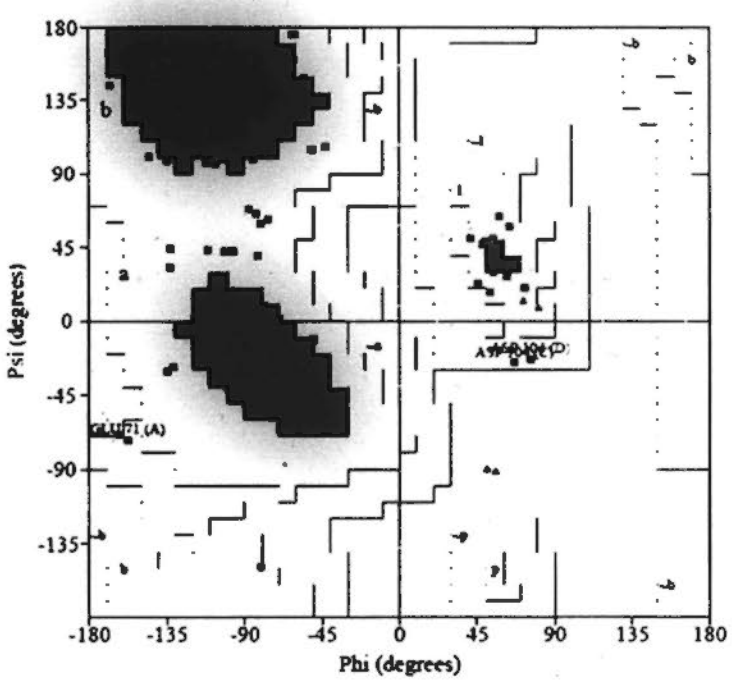

		No. of residues	
Most favoured regions	[A,B,L]	379	90.9%
Additional allowed regions	[a,b,l,p]	35	8.4%
Generously allowed regions	[~a,~b,~l,~p]	3	0.7%
Disallowed regions	[XX]	0	0.0%
Non-glycine and non-proline residues		417	100.0%
End-residues (excl. Gly and Pro)		8	
Glycine residues (shown as triangles)		18	
Proline residues		6	
Total number of residues		449	

Fig.4.19 Ramachandran plot of FliS/HP1076 complex structure

For the total 449 residues, 90.9% residues are in the most favored region marked as red and 8.4% residues are within the additional allowed region marked as yellow and only 0.7% residues are in generously allowed regions colored in light yellow.

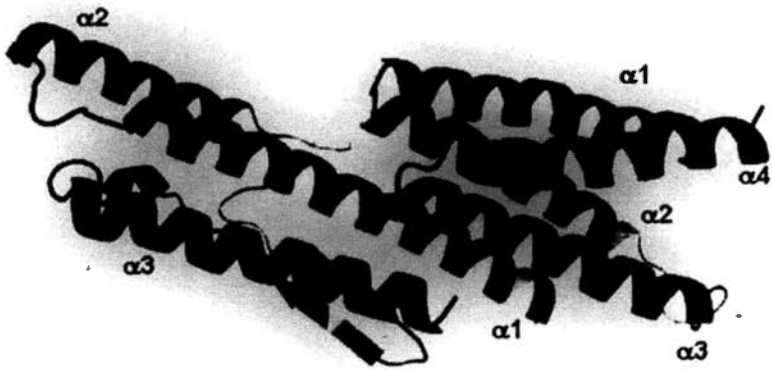

Fig.4.20 Crystal structure of FliS/HP1076 complex
HP1076 is colored in blue in complex with FliS colored in pink with helices.

4.9 Conformational change in FliS/HP1076 complex

Structural rearrangement was observed when HP1076 was in complex with FliS, a protein structural alignment was performed in DaliLite server (Holm and Park, 2000). When complex was superimposed with FliS, rmsd of Cα value of 0.7 Å was obtained over the whole structure which suggested that there was no significant change in the helical structure (Fig.4.21A). Superimposition of complex with HP1076 revealed rmsd of Cα value of 1.2 Å over 109/115 residues. Moreover, a significant conformational change of HP1076 was observed that the β1 strand was unfolded into an extended α1 helix creating a larger interface for binding with FliS (Fig.4.21B). The structural movement was mediated mainly by the Lys38 residue on HP1076 that favored hydrogen bonds formation with Asn55 and Asp59 residues on FliS and further stabilization by hydrogen and hydrophobic interaction between the α2-α3 interface of FliS and extended helix of HP1076 (Fig.4.21C) which will be

further discussed in next section. This conformational change is essential as this creates increased surface for binding with FliS.

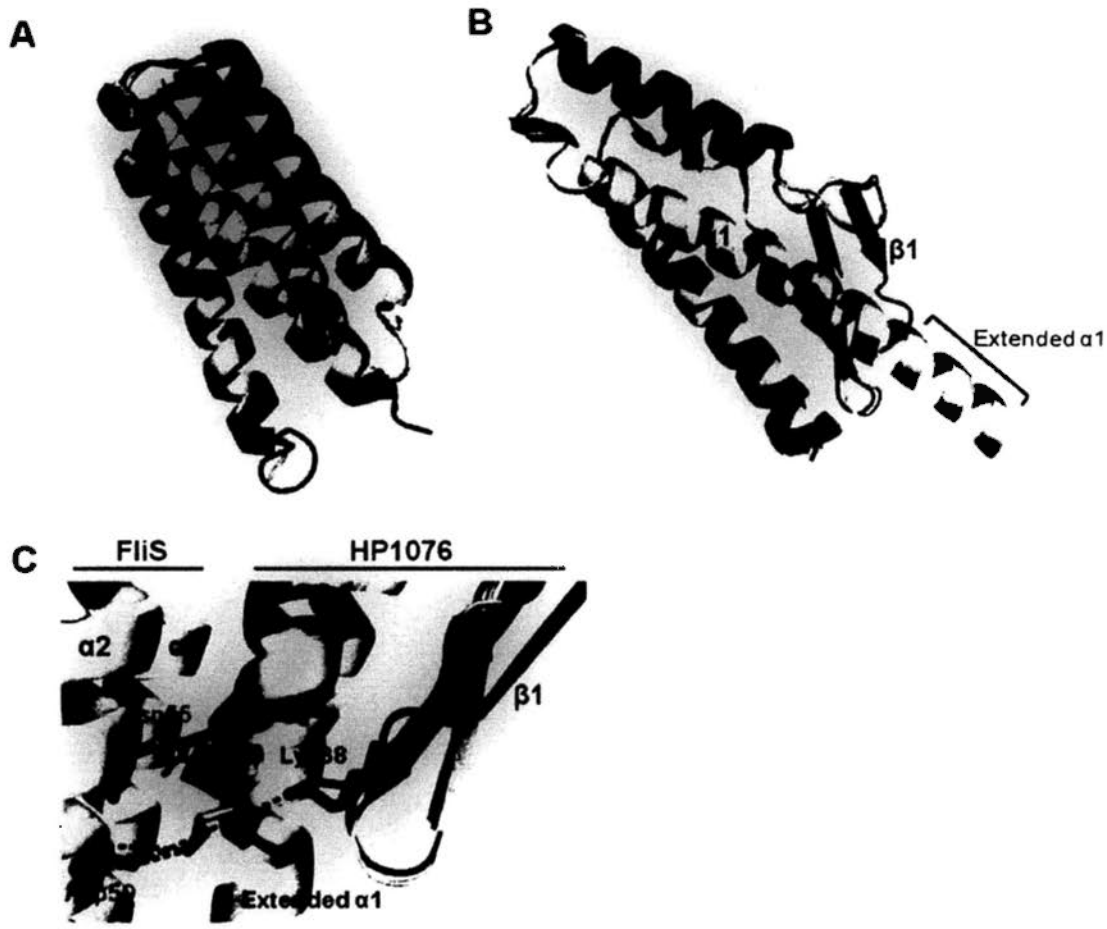

Fig.4.21 Superimposition of complex with free FliS and HP1076

The relevant FliS and HP1076 in complex structure colored in yellow is superimposed with FliS in green (A) and HP1076 in blue (B) revealed conformational change of β1 strand into extended α1 helix in HP1076 probably mediated by Lys38 residue on HP1076 (C) forming hydrogen bonding (pink dashed lines) for stabilization.

4.10 The FliS/HP1076 interface

The binding interface was localized on the electropositive and hydrophobic surface composed of extended α1 helix and C-terminal end of α3 of HP1076 with the interface between α2-α3 helices of FliS (Fig.4.22A). The interaction was mediated mainly with hydrogen and hydrophobic interactions between 15 residues from HP1076 and 18 residues from FliS which occupied 906 $Å^2$ of the protein surface (Fig.4.22B-C). Eight extensive hydrogen bonds and salt bridges forming on the interface (Table 4.5) stabilized the α2 and α3 helices of FliS in position that might be essential for the protein folding and chaperone activity enhanced by co-chaperone HP1076. This observation agreed with the previous findings described in section 3.12. Moreover, the previous interaction assays identified 21-171 residues of HP1076 were essential in interaction, this was further supported from the interface analysis that Ile30, Phe33, Ser34, Lys38, Leu42 and Ser143, Ser145, Leu146 from N-terminal and C-terminal respectively were required for stable complex formation.

Multiple sequence alignment of HP1076 from *Campylobacter*-related species revealed that the 15 residues required in interaction consisted of 5 totally conserved and 5 highly conserved residues (Fig.4.23A). Moreover, two totally conserved residues, Asn41 and Gln48 on α1 of HP1076 were fitted perfectly to the groove formed from α2-α3 on FliS (Fig.4.23B). This suggested that the association of FliS

and HP1076 was in similar mode from *Campylobacter*-related species. When HP1076-bound FliS was superimposed on the FliS in complex with C-terminal flagellin fragment from *A. aeolicus* (Fig. 4.22C), HP1076 interacted with FliS at a distant site from flagellin-binding pocket, which was consistent to the experimental data of interaction assay. FliS consisted of a highly conserved flagellin-binding pocket instead of HP1076. These further suggest that the association of FliS to flagellin is evolutionary conserved in enteric bacteria while the association of FliS to HP1076 is unique in ε-proteobacteria especially in *Campylobacter*-related species.

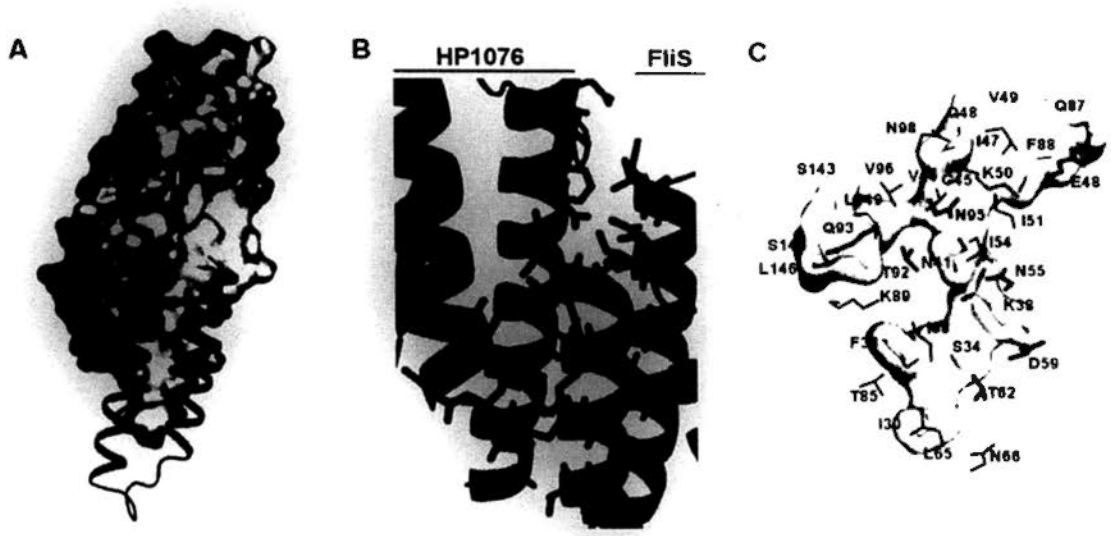

Fig.4.22 Molecular interaction of FliS and HP1076

(A) HP1076 is colored by electrostatic potential with a contour level of ±5 kT, with acidic and basic residues colored in red and blue respectively. Cartoon representation of α2-α3 helices of FliS colored in pink in complex with HP1076. (B) The binding interface showing the residues in association between HP1076 (blue) and FliS (pink). (C) Enlarged view of binding interface between HP1076 (white) showing residues of HP1076 (blue) and FliS (pink) involved in association. Residues involved in hydrogen bond formation are represented as sticks.

Table 4.5 Hydrogen bonds and salt bridge formation between FliS and HP1076

	FliS	**HP1076**	**Distance (Å)**
Hydrogen bond	OεGlu48	NεGln87	3.13
	OδAsn55	NδAsn41	2.93
	NδAsn55	OLys38	3.03
	OδAsp59	NζLys38	3.05
	OγThr62	OγSer34	3.09
	OγThr92	OδAsn41	3.12
	NδGln93	OLeu146	2.33
	NδAsn95	OδAsn41	2.96
Salt bridge	OδAsp59	NζLys38	3.05
	OδAsp59	NζLys38	3.65

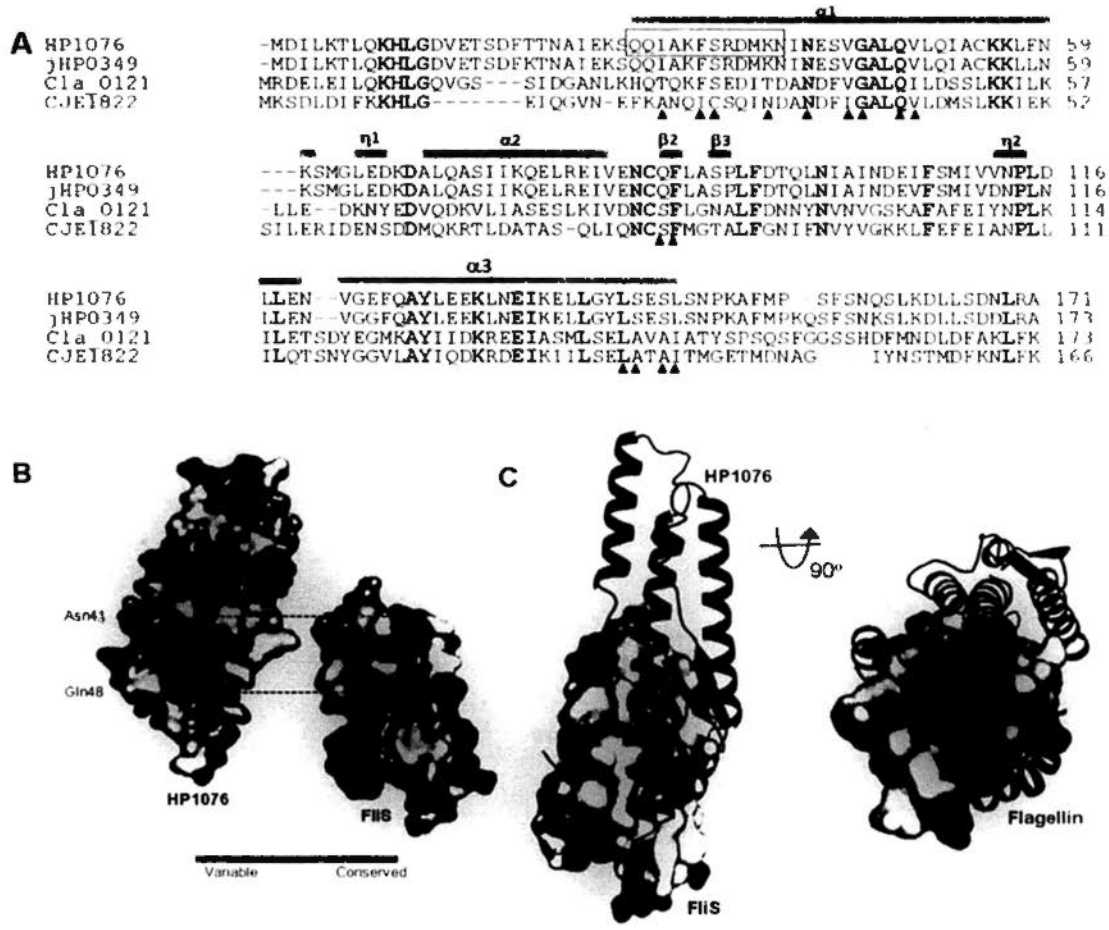

Fig.4.23 Sequence alignment of HP1076 and molecular interaction of FliS and HP1076

(A) Multiple sequence alignment of HP1076 from *H. pylori* strain 26695 (HP1076), *H. pylori* strain J99 (jHP0349), *Campylobacter lari* (Cla_0121) and *C. jejuni* (CJE1822). Box was the residues required in extension of α1 and triangles indicated the residues involved in FliS association. Secondary structures are indicated as grey boxes. Totally conserved residues are bolded.

(B) Surface representation of FliS and HP1076 colored according to conservation of sequence showing totally conserved residues in dark blue color. Conserved residues Asn41 and Gln48 on HP1076 are well fitting into the groove on FliS indicated by dashed lines.

(C) Surface representation of FliS (white) with conserved residues colored in pink is in complex with flagellin fragment (green) and HP1076 (blue) showing the conservation of binding pockets.

4.11 Verification of molecular interaction of FliS and HP1076 by pull-down assay

To verify the interface of FliS and HP1076 observed from the crystal structure, different HP1076 mutants were constructed using His_6-HP1076ΔN20 as template. Mutants of N41AQ48AF88A, K38AN41A and F33AK38E were created which included the top, middle and bottom interface (Fig.4.24A). Pull-down assay (Fig.4.24B) showed that mutants N41AQ48AF88A and K38AN41A did not bind with FliS and mutant F33AK38E showed reduced binding affinity when compared with wild-type His_6-HP1076ΔN20 (WT). These results were correlated to the structure that those residues were essential in interaction especially those located at the top and middle interface. Disruption of hydrogen bonds of Lys38 would interfere the association of FliS and HP1076, the interaction was even abolished when this mutant was combined with N41A. These suggested that the middle interface was critical for association. The result of mutant N41AQ48AF88A was further illustrated with single and double mutants. The pull-down assays (Fig.4.24C) showed that the single mutant N41A and double mutant N41AQ48A did not bind with FliS, while the binding with FliS of Q48A was reduced to about one-third when compared with WT, and the mutant F88A did not inhibit the binding. This suggested that hydrogen bond of Asn41 was critical in interaction, Gln48 might play a supplementary role in

stabilizing the complex formation and Phe88 was less important in association. Thus, the interaction is likely initiated by the Asn41 at the middle interface that captures FliS in the position and Gln48 plays supplementary role on stabilizing the complex formation, while Lys38 plays a role in creating an additional binding surface for Phe33 to form hydrophobic bonds with FliS.

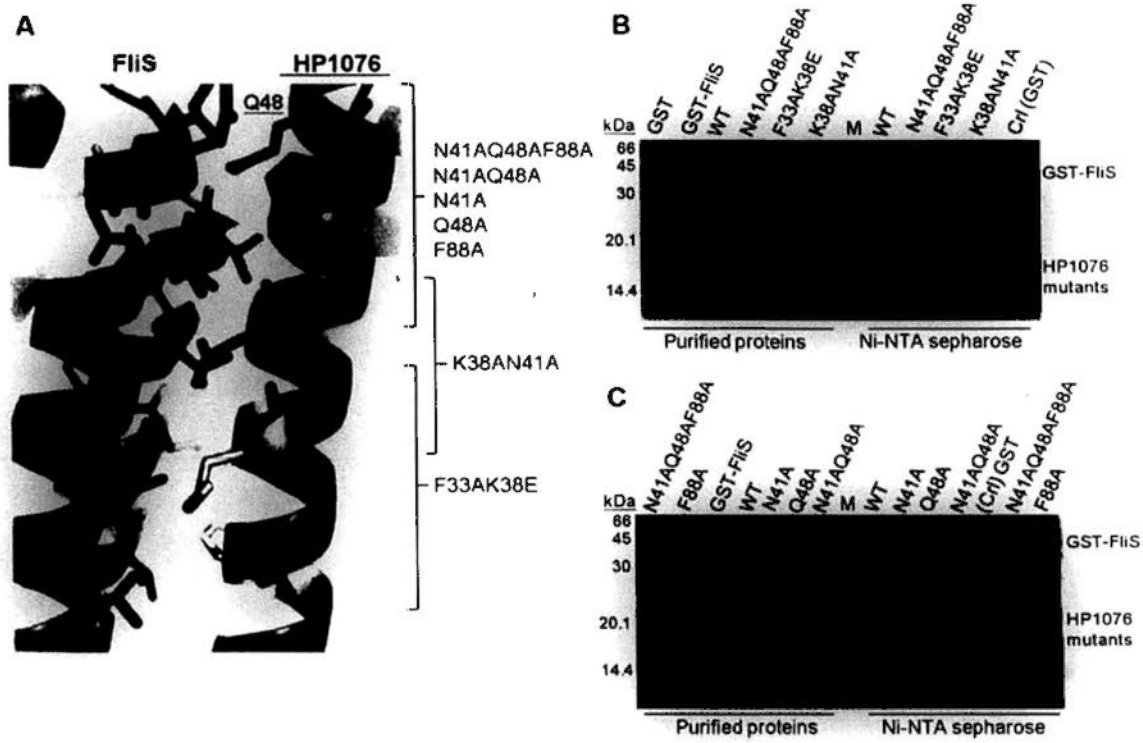

Fig.4.24 Verification of binding interface on HP1076

(A) Structure represented the different His_6-HP1076ΔN20 mutants constructed. Totally conserved residues are bolded.

(B, C) Pull-down assays were performed using Ni-NTA agarose immobilized with different His_6-HP1076ΔN20 mutants to examine the binding with GST-FliS. Control (Crl) was set up with wild-type His_6-HP1076ΔN20 (WT) and GST only. The left panel of SDS-PAGE shows the purified proteins and right panel is the proteins bound on sepharose.

4.12 Conclusion

In the present study, the crystal structure of flagellar protein FliS from *H. pylori* was determined at 2.7 Å. *H. pylori* FliS adopts a four helical bundle structure and assembles the protein folding with homologues from *A. aeolicus* that the association with flagellin is evolutionary conserved in enteric bacteria and ε-proteobacteria through highly conserved flagellin-binding pocket.

The novel crystal structure of hypothetical protein HP1076 was determined at 1.74 Å. HP1076 adopts a similar bundle structure as FliS, and consists of three helices, two 3/10 helices and three β-strands. It is structurally related to the proteins in flagellar and type III secretion systems including flagellin homologue P5, flagellar hook-associated protein 3, FliS and invasin protein. HP1076 displays electropositive and hydrophobic surface required for interacting with FliS, and electronegative surface with unknown function.

The crystal structure of binary complex of FliS and HP1076 was also determined at 2.7 Å. A conformational change on HP1076 was observed when in complex with FliS that β1 strand was refolded into extended α1 helix creating increased binding surface. The interface was located at extended α1 and C-terminal end of α3 on HP1076 and surface between α2-α3 of FliS. Such interaction was mediated by extensive hydrogen and hydrophobic interactions between 18 and 15

residues from FliS and HP1076 respectively. Asn41 from HP1076 was the critical residues involved in interaction, while Gln48 and Lys38 play supplementary role in stabilizing the complex formation. The association of FliS and HP1076 was suggested to be conserved in ε-proteobacteria especially in *Campylobacter*-related species.

Chapter 5 Characterization of HP1076 null mutant in *Helicobacter pylori*

In order to investigate the biological roles of uncharacterized HP1076 in *H. pylori*, a deletion mutant was constructed in which the gene *hp1076* was disrupted by kanamycin-resistant gene. The difference in protein expression profiles of wild-type (WT) and mutant was compared by 2-dimensonal gel electrophoresis (2-DE) analysis to provide more insights into the possible roles of HP1076. Several assays including motility assay and drug susceptibility test were performed to study the effect on deletion of HP1076. Moreover, FliS and HP1076 proteins may be varied or mutated in different drug-resistant strains, the result provides a preliminary data on the gene diversity.

Results and Discussion

5.1 Construction of a deletion plasmid, pGEM-T-Easy-hp1076:KanR

The kanamycin-resistant gene, *KanR* and the plasmid pAC28m-hp1076 were digested with restriction enzyme *BstX*I. Then, *KanR* was inserted to *BstX*I site located at 344th bases of *hp1076* construct. And the insertion of *KanR* gene into *hp1076* was confirmed by PCR screening with HP1076-F and HP1076-R primers. A

correct insertion of *KanR* DNA would produce a PCR product of 1,700 bp long, while no insertion would produce a band size of around 500 bp only (Fig.5.1A). The positive clone was further confirmed by sequencing and used as the template for the PCR amplification to generate a construct of *hp1076:KanR*, and ligated into linearized pGEM-T-Easy vector by TA cloning. The final clones were confirmed by PCR screening indicates successful ligation to produce the resultant plasmid, pGEM-T-Easy-hp1076:KanR (Fig.5.1B).

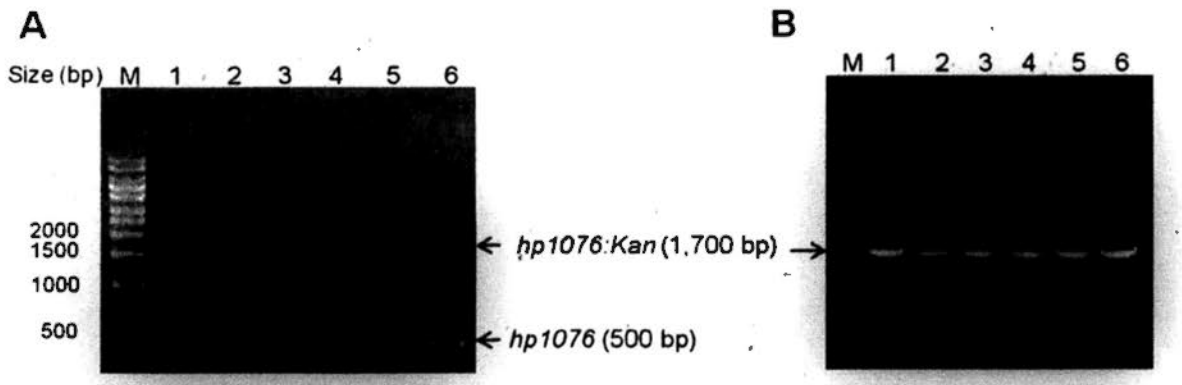

Fig.5.1 PCR screening of *hp1076:KanR* construct
(A) PCR screening of clones (1-6) with insertion of *KanR* into *hp1076* construct in plasmid, pAC28m-hp1076:KanR. PCR product with band size of 1,700 bp indicates positive results, a band size of 500 bp indicates negative result.
(B) PCR screening of clones (1-6) of resultant plasmid, pGEM-T-Easy-hp1076:KanR. PCR products were analyzed with 1% DNA agarose gel.

5.2 Verification of ΔHP1076 mutant in *H. pylori*

The deletion plasmid, pGEM-T-Easy-hp1076:KanR dissolved in ddH_2O was transformed into *H. pylori* strain 26695 by electroporation as described in section 2.9.5. Transformation using ddH_2O to the bacteria acts as a control to generate

wild-type transformant. The transformants with *HP1076:KanR* were selected with kanamycin, and that with ddH_2O was grown on agar plate without kanamycin. The cells were collected after sub-culture for PCR and western blotting analysis to verify the deletion of HP1076.

The genomic DNA of WT and ΔHP1076 mutant bacteria extracted as stated in section 2.9.6.1 was used as the template for PCR amplification with HP1076 primers complementary to the upstream and downstream of the gene. A 516-bp PCR product was produced in WT strain and 1,700-bp PCR products were generated in the mutant (Fig.5.2). This confirmed that the gene *hp1076* of genomic DNA was successfully replaced by the deletion constructed.

Next, the protein expression level of HP1076 in total cell lysate was verified by western blot analysis. HP1076 protein on PVDF membrane was detected by polyclonal rabbit anti-HP1076 antibody and then with Donkey anti-rabbit IGG-HRP antibody. A specific band of HP1076 was identified in the WT compared with the control, while no protein was detected from the mutant strain (Fig.5.3). This suggested that HP1076 was not expressed in the mutant strain.

All these verification results suggested that the deletion mutant ΔHP1076 in *H. pylori* was successfully constructed and could be used for further analysis.

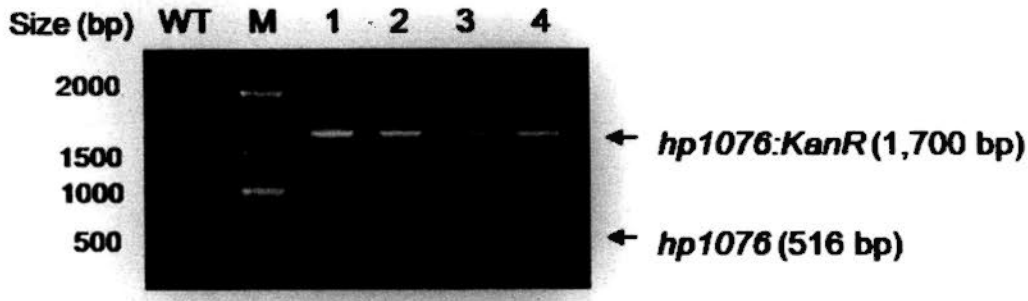

Fig.5.2 PCR amplification from genomic DNA of *H. pylori* WT and ΔHP1076 mutant

PCR product from WT strain (WT) and mutant strains (1-4) were analyzed in 1% DNA agarose gel.

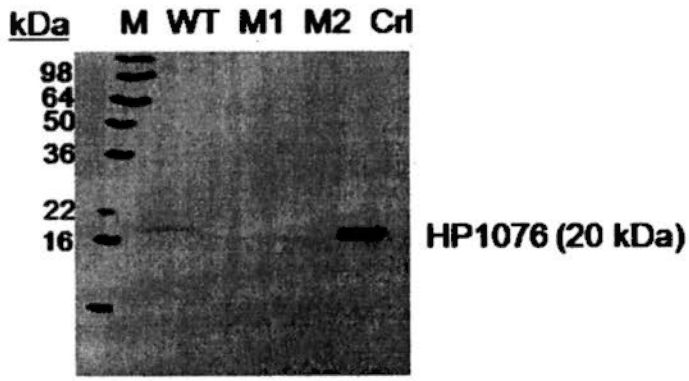

Fig.5.3 Western blot analysis of HP1076 in WT and ΔHP1076 mutant

Proteins on PVDF membrane were probed with primary and secondary antibody in a ratio of 1:100,000 and 1:5,000 respectively. The signal was detected by 10-sec exposure. Protein level of HP1076 in total cell lysate from wild-type (WT) and mutant (M1 and M2) strains were compared with the positive control (Crl) using 0.1 μg purified His_6-HP1076 protein.

5.3 Expression level of FliS and flagellin

Our previous experiments show that HP1076 works as a co-chaperone to FliS and binds specifically to FliS without interfering its binding with flagellin. HP1076 is shown to be related to the flagellar system with regulatory role (Niehus *et al.*, 2004). It would be interested to study the direct effect on flagellin and FliS in the deletion mutant of HP1076. A western blot analysis was performed to study the protein expression level of FliS and flagellin in total cell lysate.

Equal amount of total proteins from WT and mutant strains was separated in SDS-PAGE and transferred to PVDF membrane. FliS is detected by polyclonal rabbit anti-FliS antibody and then with Donkey anti-rabbit IGG-HRP antibody. From Fig.5.4, a specific band of FliS was detected with expected size as compared with the control (Crl). The protein level of FliS was calculated by the software ImageJ 1.43u (National Institutes of Health, USA; Abramoff *et al.*, 2004), FliS in mutant was reduced to 0.85 fold when compared with that of WT, suggesting that FliS level was inhibited slightly. This was consistent with previous result on the co-chaperone activity of HP1076, that HP1076 was important in stabilization of FliS and thus regulating FliS level inside the cells. But more experiments should be performed in the future when the mechanism of the co-chaperone activity of HP1076 is elucidated.

From Fig.5.4, flagellin was detected by mouse monoclonal 54 kDa antigen

antibody and then with Donkey anti-mouse IGG-HRP antibody. The protein level of flagellin did not show any difference between WT and mutant strains, suggesting that deleting HP1076 would not affect the flagellin level. This agreed with our previous data that HP1076 showed no binding with flagellin and did not inhibit the interaction of FliS and flagellin. The protein level of flagellin remained unchanged, however it is possible that the flagellin molecules in the mutant remained inside the cytosol and not exported out for the filament formation as in the WT strain. This cannot be explained from the present study as total proteins were detected and this can be achieved by separation of the bacteria cell lysate into cytosol and membrane fractions by ultracentrifugation.

The total cell lysate of WT and mutant strains were lysed on ice with sonication, cell debris was removed by low-speed centrifugation. The supernatant was further separated into cytosol (supernatant) and membrane (pellet) fractions after ultracentrifugation. Proteins of cytosol (S) and membrane (P) fractions were detected by specific anti-flagellin antibody as stated before. From Fig.5.5, flagellin proteins of both strains were found mainly in membrane fraction, and there was a faint band in the cytosol fraction of deletion mutant. This initial result suggested that some flagellin molecules remained inside the cytosol in the mutant strain.

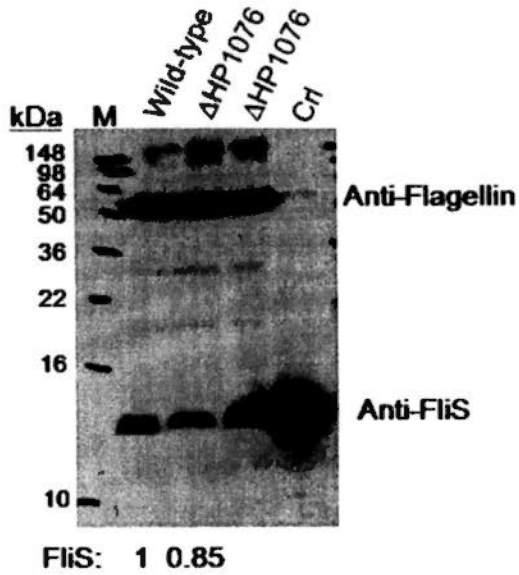

Fig.5.4 Western blot analysis of FliS and flagellin in WT and ΔHP1076 mutant

Proteins on PVDF membrane were probed with primary anti-FliS and secondary anti-rabbit antibody in a ratio of 1:100,000 and 1:5,000 respectively. Flagellin protein is detected with primary anti-flagellin and secondary anti-mouse antibody in a ratio of 1:5,000. The signal was detected by 10-sec exposure. Lane M: Invitrogen SeeBlue® Plus 2 pre-stained protein standard. Protein level of FliS and flagellin in total cell lysate from wild-type (WT) and ΔHP1076 mutant strains were compared with the positive control (Crl) using 0.1 μg purified FliS protein. The fold change of protein level of FliS was marked at the bottom of the figure.

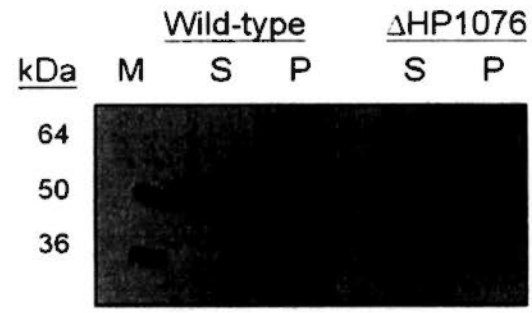

Fig.5.5 Western blot analysis of flagellin in cytosol and membrane fractions of WT and ΔHP1076 mutant

The protein level of flagellin in cytosol (S) and membrane (P) fractions were detected by primary anti-flagellin and secondary anti-mouse antibody in a ratio of 1: 5,000. The signal was detected by 15-sec exposure.

5.4 Motility assay of WT and ΔHP1076 mutant in *H. pylori*

The motility of bacteria is a virulence factor for infection and HP1076 is one of the genes categorized in class II under the RpoN sigma factor which is responsible for regulating the middle flagellar structure with unknown mechanism (Niehus *et al.*, 2004). Previous analysis in section 5.3 showed that the amount of flagellin inside the cytosol was increased in mutant strain. It would be interesting to investigate if deleting HP1076 would have any effect on the bacterial motility. Both WT and mutant cells were harvested in brucella broth and small aliquots were dotted on the 0.3% soft agar. The plates were incubated under microaerophilic condition at 37 °C for four days. The growth of bacteria formed a halo at the centre and its diameter was measured for comparison. From Fig.5.6, both WT and mutant showed growth on the agar plate, but the halo size of the WT strain was 12 mm which was larger than that of the ΔHP1076 which was 8 mm. This indicated that the motility was impaired in the mutant strain. This finding further implied that HP1076 was involved in the motility pathways.

	Zone Size
WT HP 26695	12 ± 0.2 mm
ΔHP1076	8 ± 0.3 mm

Fig.5.6 Motility assay of WT and ΔHP1076 mutant in *H. pylori*
One-day *H. pylori* cells were collected and dotted on a 0.3% soft agar plate. After incubation in a microaerophilic condition for 4 days at 37℃, the halo size was measured. The assay had been performed for three times.

5.5 Proteomic study of wild-type and ΔHP1076 mutant in *H. pylori*

Deleting *hp1076* may have altered the protein profiling in mutant strain. It was anticipated that proteins shown to be differentially expressed in the mutant strain would link to HP1076 directly or indirectly. Identification of these proteins and their roles would provide better understand about the biological significance of HP1076.

5.5.1 2-dimensonal gel electrophoresis (2-DE) analysis

The total cell lysate of WT (*H. pylori* strain 26695) and ΔHP1076 mutant was prepared for 2-DE analysis. Equal amounts of total protein were separated on pH strip ranging from pI3-10 and then SDS-PAGE for molecular masses ranging from 10 to 250 kDa. The protein spots were visualized by Coomassie brilliant blue staining. By analysis with ImageMaster™ 2D Platinum v7.0 (GE Healthcare) software, the spots differed in intensity between WT and mutant strains were identified (Fig.5.7) showing a list of spot pairs. The spots with a fold change in intensity (ratio) of 1.5 or above were selected for further analysis with mass spectrometry. The spots can also be visualized in a 3-dimensional view for a better understanding of the nature of spots as it may contain some less intense peaks forming a dense peak when visualized in a 2-dimensional view (Fig.5.7, 3D View). Three independent samples were applied in this 2-DE analysis to provide comparable

results. All together, 40 differential spots including 17 down-regulated (D) and 23 up-regulated (U) were found (Fig.5.8).

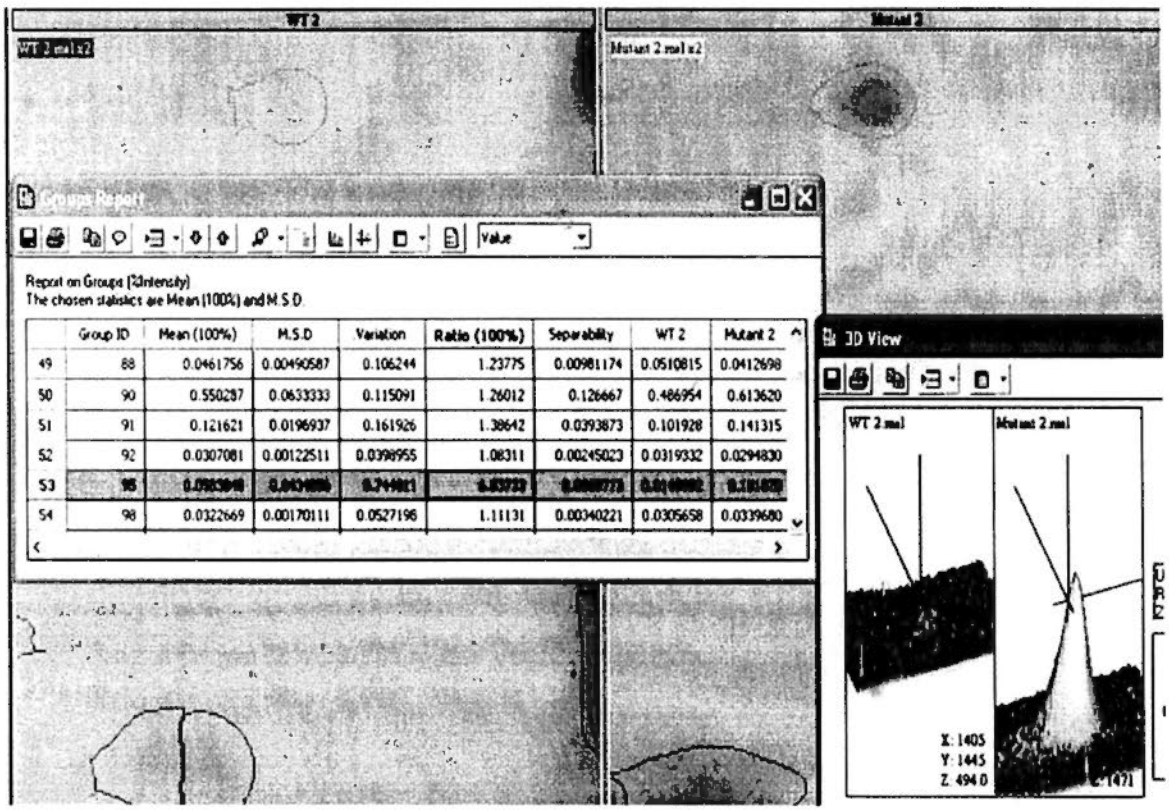

Fig.5.7 Spot detection and analysis by ImageMaster™ 2D Platinum software
The spots with different intensity between WT and ΔHP1076 mutant are outlined in green. The ratio of the difference in intensity and the statistics of mean squared deviation (M.S.D.) are shown in the Groups Report, here showing the spot pairs with 6.83 folds change in expression level as an example. The 3D view of the spots is shown in the right hand corner.

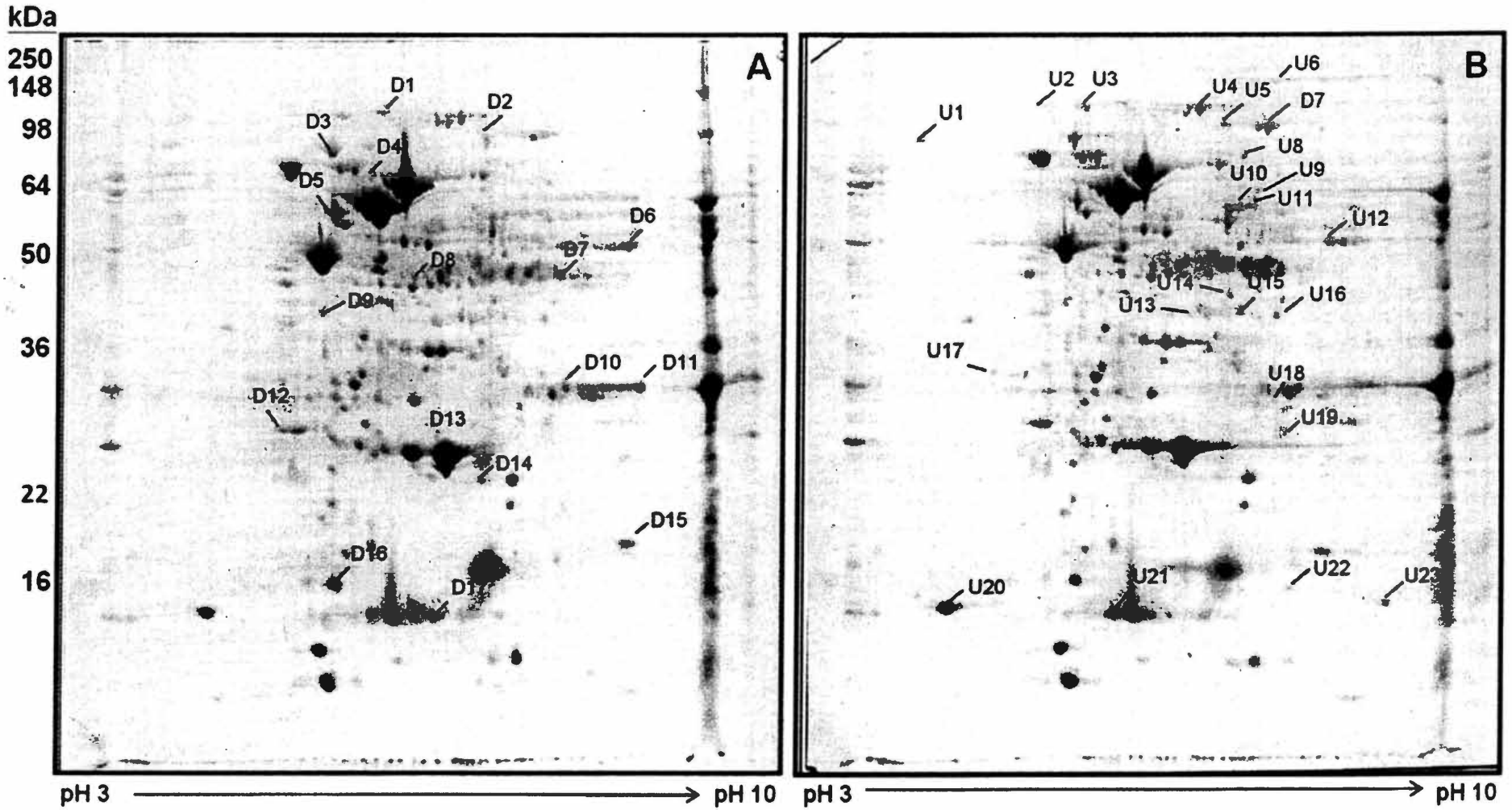

Fig.5.8 Representative 2-DE image of total cell lysate from *H. pylori* WT and ΔHP1076 mutant

Protein samples were analyzed with IEF using 13-cm Immobiline™ strip pH 3-10 followed by 12% SDS-PAGE analysis. (A) is the gel of WT sample; and (B) is the gel of ΔHP1076 mutant. Spots with up-(U) or down-(D) regulated expression level are marked on figure.

5.5.2 Identification of proteins by mass spectrometry

Spots with different expression level were digested into peptide by in-gel digestion with trypsin and the peptide was crystallized with the matrix solution and sent to peptide mass fingerprint (PMF) analysis by matrix-assisted laser desorption ionization time-of-flight mass spectrometry (MALDI-TOF MS). The PMF raw data for the peptide fragment was searched against the protein database of NCBInr by the Mascot based GPS Explorer™ Software v3.5. The background noise produced from the MS and MS/MS peaks of skin keratin and trypsin was filtered before protein identification.

The accuracy of the protein identification was determined by the Protein Score and Protein Score C.I. % (confidence interval) that should be above 80% as illustrated as green and pink spots in MALDI plate (Fig.5.9), and also the number of peptide matched is better to be greater than 4 to provide significant results. The residue on peptide was determined from the mass difference between each single peak (Fig.5.9, lower panel). The list of proteins identified for at least two times in three independent 2-DE analysis are summarized in Table 5.1. The corresponding changes in the intensity of selected spots on are illustrated in Fig.5.10 and Fig.5.11.

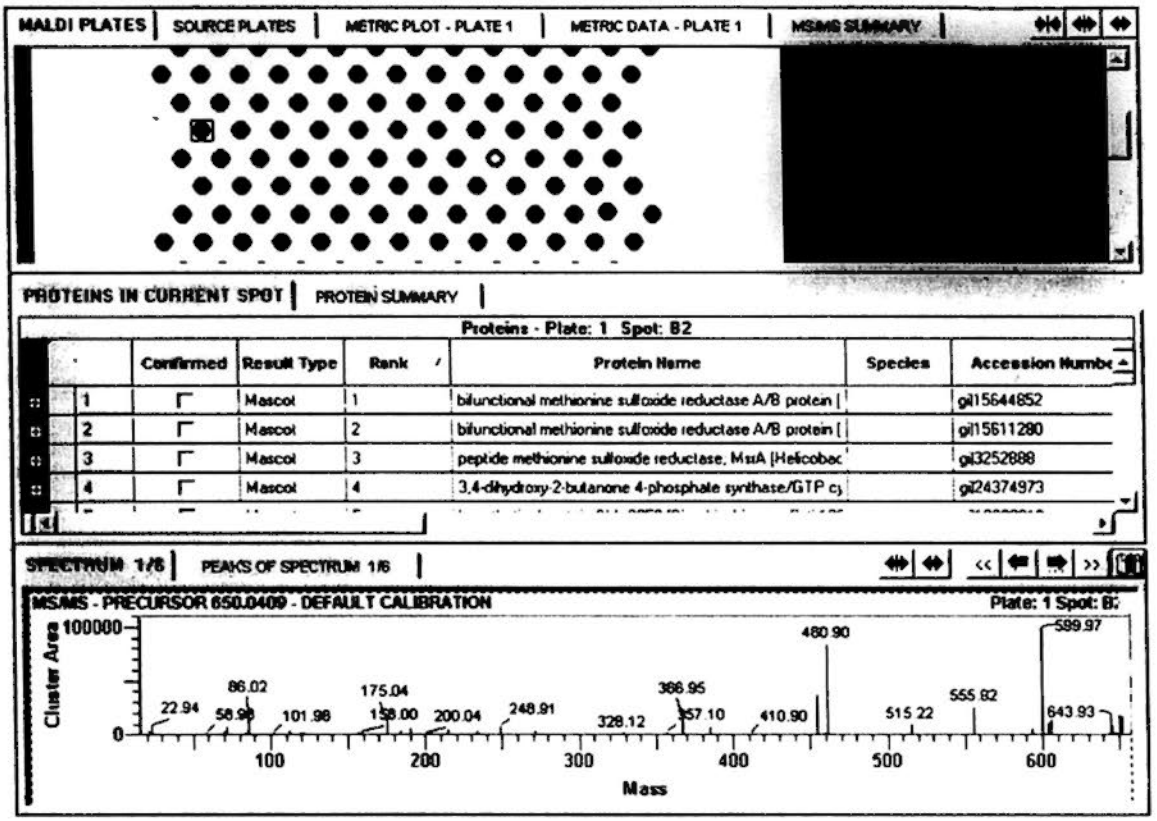

Fig.5.9 The peptide search result by GPS Explorer™ software

The upper panel shows the % CI value (confidence score), green spots are in 100% CI, pink spots are in % CI value around 80 and yellow spots are in low % CI values. The summary of the protein identified is shown in middle panel. The lower panel shows the spectrum peak with corresponding mass.

Table 5.1 List of proteins with differential expression level after the deletion of HP1076 in *H. pylori* strain 26695
Proteins were analyzed by MALDI-TOF MS/MS protein mass fingerprinting.

Up-regulated							
Identity	gi	MW (kDa)	pI	Pep count	Protein Score	% C.I.	Function
2-Hydroxyacid dehydrogenase	gi15644726	34774.6	6.56	7	154	100	Oxidation and reduction
Aspartyl-tRNA synthetase (AspS)	gi15645242	65560.2	6.45	9	180	100	tRNA synthesis
ATP-dependent protease binding subunit (ClpB)	gi15644892	96623.4	6.02	13	139	100	Heat shock protein involved in stress
Bifunctional aconitate hydratase 2/2-methylisocitrate dehydratase	gi15611783	92682.9	6	7	59	74.68	Metabolism
Bifunctional methionine sulfoxide reductase A/B protein (MsrA/B)	gi15644852	41249	7.16	13	270	100	Anti-oxidation
Cag pathogenicity island protein (Cag 26)	gi15645173	132305.8	8.82	11	94	99.992	Effector protein in infection
Cinnamyl-alcohol dehydrogenase ELI3-2 (Cad)	gi15645718	38620.6	6.96	1	59	75.337	Aldehyde reduction
FAD-dependent thymidylate synthase (ThyX)	gi15646141	27013.9	8.56	3	56	50.792	Pyrimidine metabolism
Flavodoxin (FldA)	gi15645775	17481.7	4.45	5	359	100	Electron transport
Fumarate reductase flavoprotein subunit (FrdA)	gi15644821	80070.5	6.87	16	313	100	Electron transport
Hypothetical protein HP0318	gi15644946	28489.5	7.27	8	175	100	Heme oxygenase in iron metabolism
Leucyl aminopeptidase (LAP)	gi15645195	54398.6	6.66	10	87	99.962	Protein turnover
Neutrophil activating protein (NapA/Bacterioferritin)	gi15644871	16922.7	5.59	7	157	100	Survival and pathogenesis
Polynucleotide phosphorylase/	gi15645827	76836.2	5.47	10	200	100	RNA processing

Polyadenylase							
Putative neuraminyllactose-binding hemagglutinin homolog (HpaA)	gi15645038	28330.9	7.88	12	294	100	Adhesion
Quinone-reactive Ni/Fe hydrogenase, small subunit (HydA)	gi15645255	42327	6.36	7	62	86.447	Activation of hydrogenase and urease
Quinone-reactive Ni/Fe hydrogenase, large subunit (HydB)	gi15645256	64356.1	6.82	11	163	100	Accessory subunit on activation of hydrogenase and urease
Response regulator (OmpR)	gi15644795	25839.6	5.2699	8	147	100	Transcription regulation
Thioredoxin reductase (TrxB)	gi15645778	35963.7	6.42	4	154	100	Enzyme in oxidation and reduction

Down-regulated							
Identity	gi	MW (kDa)	pI	Pep count	Protein Score	% C.I.	Function
2-oxoglutarate-acceptor oxidoreductase subunit (OorA)	gi15645214	41482.3	5.98	5	65	93.641	Oxidation and reduction
2-Oxoglutarate-acceptor oxidoreductase subunit (OorB)	gi15645215	30394.9	7.59	6	404	100	Oxidation and reduction
Alkyl hydroperoxide reductase (AhpC)	gi15646170	22221.4	5.88	5	364	100	Oxidation and reduction
Alkyl hydroperoxide reductase C22 protein	gi29150161	20293.4	5.76	5	317	100	Oxidation and reduction
Co-chaperonin GroES	gi15611080	12982.5	6.1199	7	366	100	Nickel binding, chaperone
Elongation factor G	gi15645809	76972.2	5.25	13	243	100	Translocation of ribosome in translation
Elongation factor Tu	gi15645819	43620.4	5.17	12	302	100	Translocation of ribosome in translation
F0F1 ATP synthase subunit alpha	gi15645748	55108.8	5.2899	11	122	100	Metabolism
Preprotein translocase subunit SecA	gi15645405	99022.1	5.62	19	416	100	Protein secretion/ translocation

Pyruvate flavodoxin oxidoreductase subunit gamma	gi15645722	20952	8.52	5	138	100	Oxidation and reduction
Urease accessory protein (UreG)	gi15644698	21941.2	5.03	2	58	69.558	Nickel insertion to urease
Urease UreA	gi21637178	18209.5	7.01	11	310	100	Urea hydrolysis
bifunctional urease subunit gamma/beta	gi15611139	26550.9	8.47	11	149	100	Urea hydrolysis
Urease UreB	gi21637179	40171.9	5.03	8	224	100	Urea hydrolysis

Up-regulated proteins

Wild-type	Δ HP1076 mutant	Wild-type	Δ HP1076 mutant

a. 2-Hydroxyacid dehydrogenase

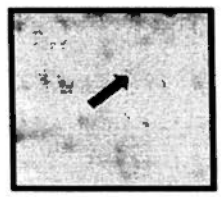
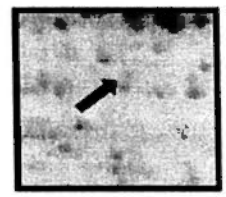

b. Aspartyl-tRNA synthetase

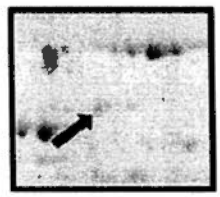
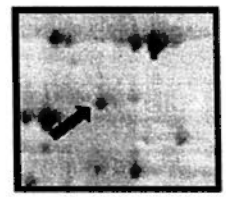

c. ATP-dependent protease binding subunit (ClpB)

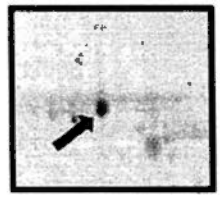
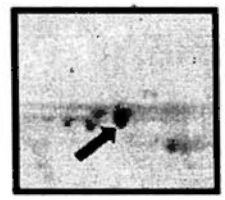

d. Bifunctional aconitate hydratase 2/2-methylisocitrate dehydratase

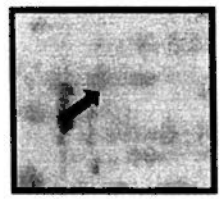
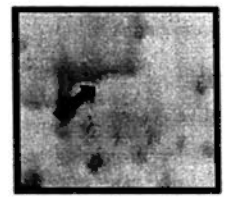

e. Bifunctional methionine sulfoxide reductase A/B protein (MsrA)

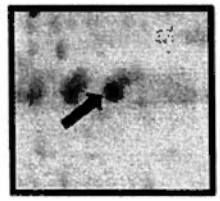
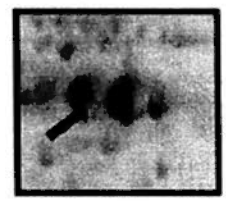

f. Cag pathogenicity island protein (Cag 26)

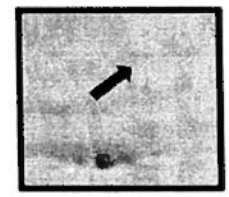
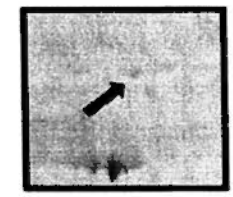

g. Cinnamyl-alcohol dehydrogenase ELI3-2 (Cad)

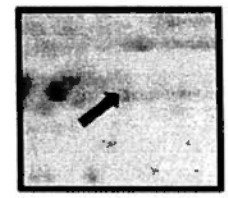


h. FAD-dependent thymidylate synthase

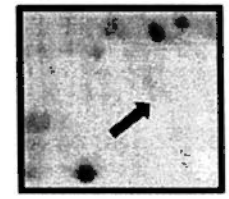
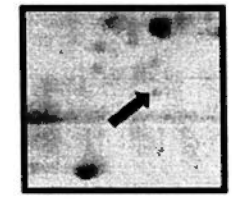

i. Flavodoxin

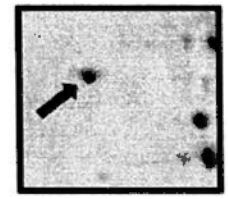


j. Fumarate reductase flavoprotein subunit

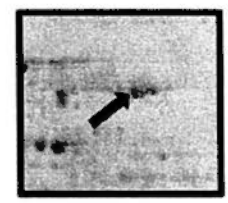
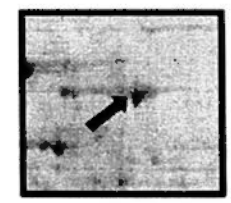

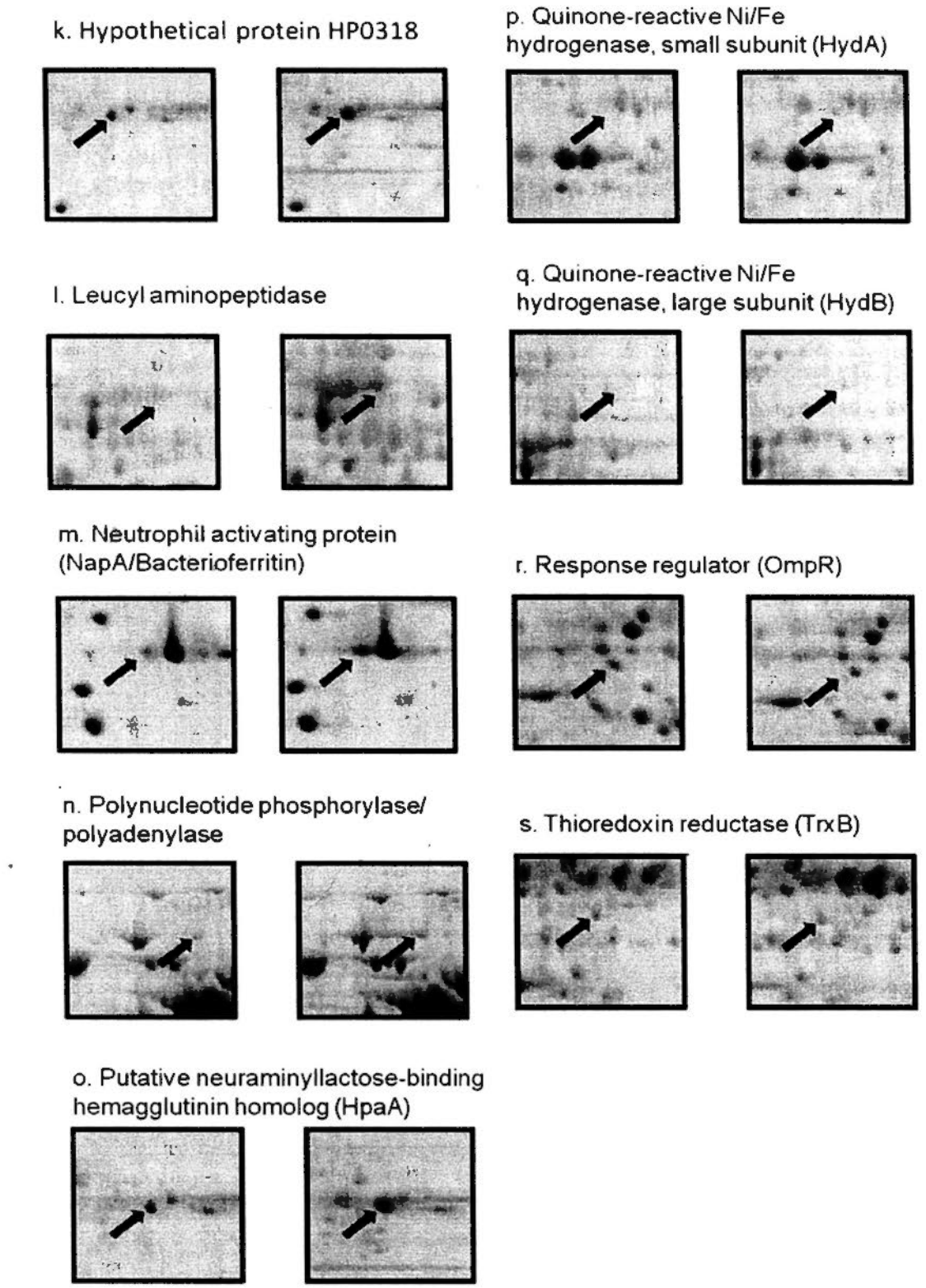

Fig.5.10 Comparison of the increased protein expression level of selected spots in ΔHP1076 mutant compared with WT strain
The differential spots on stained 2-DE were analyzed by ImageMaster™ 2D Platinum v7.0 software and marked by arrows. The protein identity (a-s) was matched in the NCBI database.

Down-regulated proteins

Wild-type Δ HP1076 mutant Wild-type Δ HP1076 mutant

a. 2-oxoglutarate-acceptor oxidoreductase subunit (OorA)

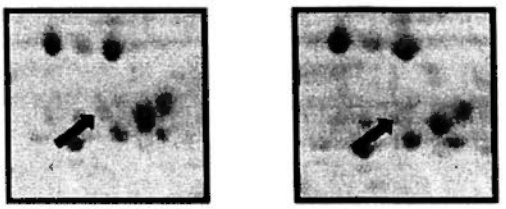

b. 2-oxoglutarate-acceptor oxidoreductase subunit (OorB)

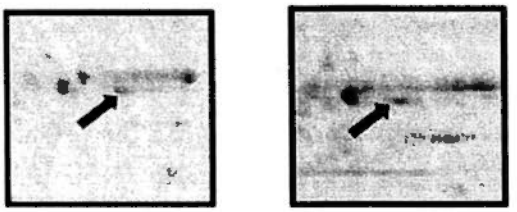

c. Alkyl hydroperoxide reductase (AhpC) Alkyl hydroperoxide reductase C22 protein

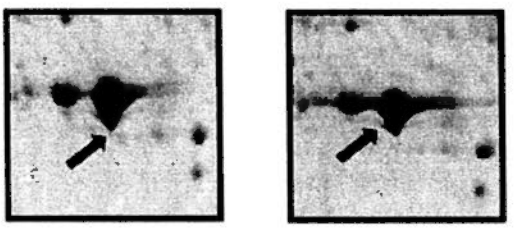

d. Co-chaperonin GroES

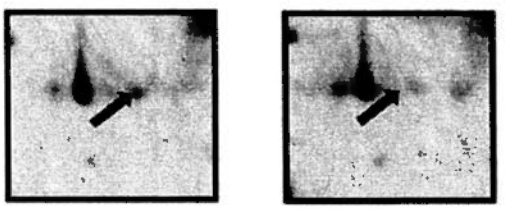

e. Elongation factor G

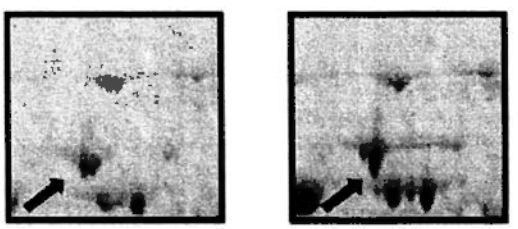

f. Elongation factor Tu

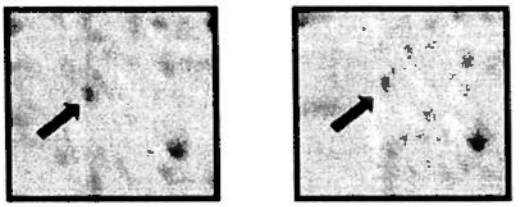

g. F0F1 ATP synthase subunit alpha

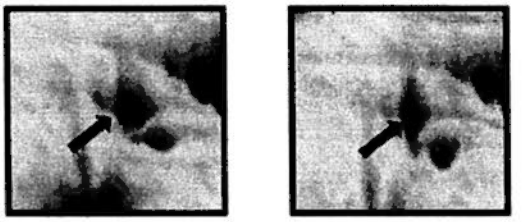

h. Preprotein translocase subunit SecA

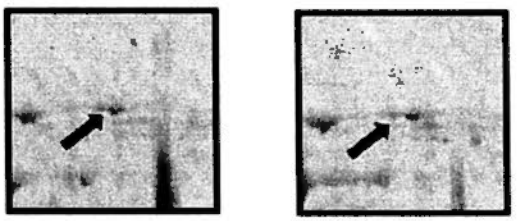

i. Pyruvate flavodoxin oxidoreductase subunit gamma

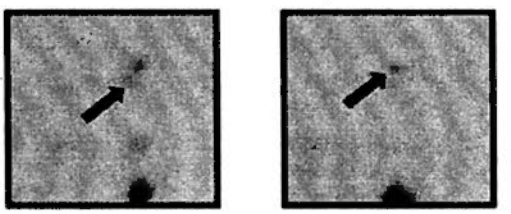

j.Urease accessory protein (UreG)

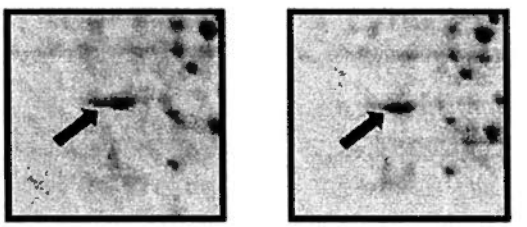

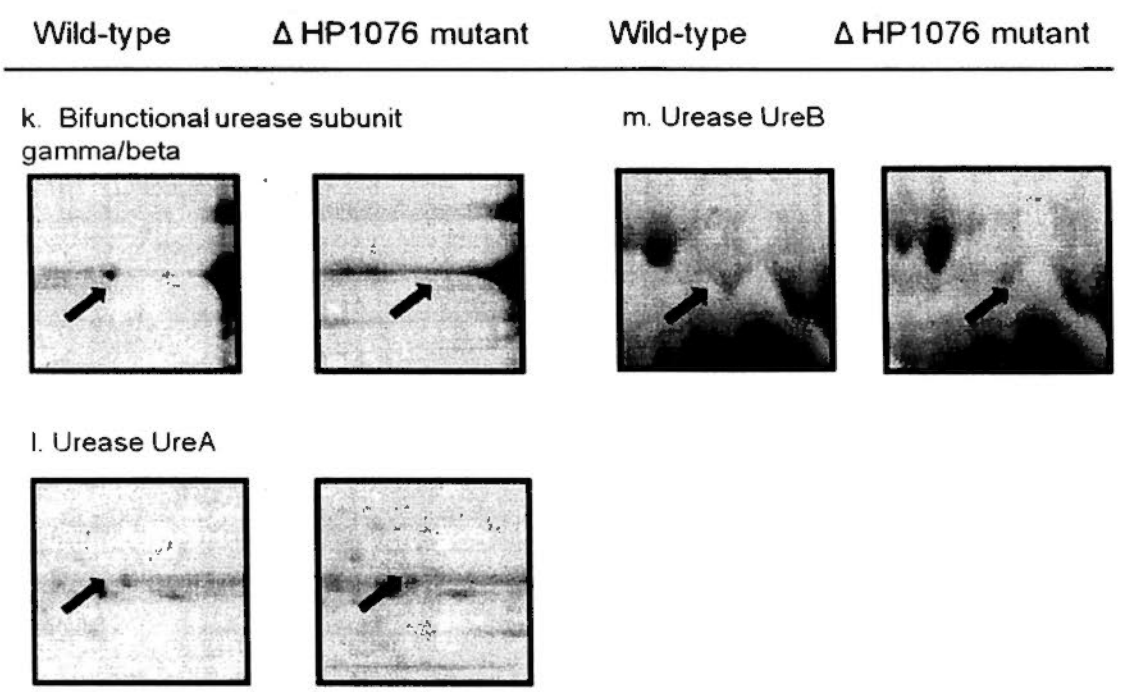

Fig.5.11 Comparison of the decreased protein expression level of selected spots in ΔHP1076 mutant compared with WT strain
The differential spots on stained 2-DE were analyzed by ImageMaster™ 2D Platinum v7.0 software and marked by arrows. The protein identity (a-l) was matched in the NCBI database.

5.5.3 Highlight of the identified proteins

5.5.3.1 2-Hydroxyacid dehydrogenase (Up-regulated)

2-Hydroxyacid dehydrogenase is an enzyme of the oxidoreductase family which catalyses the redox reaction with the binding of NAD or NADH as acceptor. It is newly identified to carry thioredoxin-like protein folding and classified as thiol:disulfide oxidoreductase (Kaakoush *et al.*, 2007) resembling the uncharacterized Dsb system in *H. pylori* which influences the colonization of bacteria (Godlewska *et al.*, 2006) . The oxidoreductase is involved in the catalyzing the formation of disulfide bond and proper protein folding of the components of type III secretion system, secreted proteins and toxins for pathogenesis resembling the Dsb system in other bacteria (Yamanaka *et al.*, 1994; Yu and Kroll, 1999).

5.5.3.2 Aspartyl-tRNA synthetase (AspS) (Up-regulated)

AspS belongs to the non-discriminating subtype of the enzyme essential in the protein synthesis which targets two types of tRNA synthesis, $tRNA^{Asp}$ and $tRNA^{Asn}$ (Chuawong and Hendrickson, 2006). AspS works on linking carboxyl group of aspartate molecules to ATP and directing attachment of the aminoacyl-adenylate to corresponding tRNA according the genetic code (Ibba and Söll, 2000).

5.5.3.3 ATP-dependent protease binding subunit (ClpB) (Up-regulated)

ClpB is stress-induced protein when cells are exposed to change in temperature (Allan *et al.*, 1998). It is essential for bacterial infection and survival during heat stress when exposed to the host (Squires *et al.*, 1991). It has activation and disaggregation effect on the heat-inactivated proteins in ATP-dependent manner working synergistically to DnaK chaperone system (Doyle *et al.*, 2007). It also

regulates the degradation of the irreversibly denatured proteins. Reactivation of the denatured proteins helps to enhance survival of the cells. ClpB is also identified as an antigen which is specifically detected by the sera from patient with positive *H. pylori* infection (Haas *et al.*, 2002).

5.5.3.4 Bifunctional aconitate hydratase 2/2-methylisocitrate dehydratase (Up-regulated)

It is a metabolic enzyme catalyzing the conversion of citrate into cis-aconitate and isocitrate involved in TCA cycle (Jordan *et al.*, 1999). Iron determines the roles of enzyme that iron-bound form is important for binding of substrate while iron-unbound form acts as transcriptional regulator in *E. coli* (Tang *et al.*, 2005). It also enhances the level of superoxide dismutase to cope with the oxidative stress (Tang *et al.* 2002). Oxidative stress would promote the formation of iron unbound form in *Salmonella* that facilitates the binding to cell division protein ftsH transcript to reduce the level of stress responsive FtsH protease and ultimately leads to reduced level of flagellin molecules (Tang *et al.*, 2004).

5.5.3.5 Bifunctional methionine sulfoxide reductase A/B protein (MsrA/B) (Up-regulated)

It is an antioxidant enzyme required to reduce the oxidized methionine to restore the active state of methione for protein synthesis, which methionine is easily oxidized by reactive oxygen species into methionine sulfoxide (Hoshi and Heinemann, 2001). Msr enzyme is essential for the survival and colonization of *H. pylori* especially in high-oxidative environment (Alamuri *et al.*, 2004). Msr enzyme is associated to the aging of animal models that over-expression in the cell would

increase the life span (Stadtman *et al.*, 2005).

5.5.3.6 Cag pathogenicity island protein (Cag 26) (Up-regulated)

Cag26 is also called CagA which is an antigen recognized by the sera of patient with *H. pylori* infection (Jungblut *et al.*, 2000; Haas *et al.*, 2002). It is the virulence factor that CagA-positive strain is correlated to the increased risk on developing gastric disease (Blaser *et al.*, 1995). It is the effector protein that is secreted into gastric epithelial cells through the type IV secretion system upon the attachment with *H. pylori* (Odenbreit *et al.*, 2000). CagA binds externalized phosphatidylserine on the epithelial cells to initiate the entry into the host cells (Murata-Kamiya *et al.*, 2010). Injected CagA is phosphorylated and interferes the signaling transduction pathway of epithelial cells resulted in enhancing cell proliferation, apoptosis and production of reactive oxygen species which damages DNA which ultimately causes the gastric carcinogenesis (Stabile and Smith, 2005; Zhong *et al.*, 2007). The expression level of CagA is increased in acidic exposure (Karita *et al.*, 1996; Merrell *et al.*, 2003), whereas more CagA proteins are transported to the membrane for the export through type IV secretion system in acidic environment (Wu *et al.*, 2005). It is also reported that bacteria strain with CagA is more susceptible to the low pH environment than that lack of CagA which accounts for the survival ability (Karita and Blaser, 1998).

5.5.3.7 Cinnamyl-alcohol dehydrogenase ELI3-2 (Cad) (Up-regulated)

The expression of Cad is significantly increased when exposure to the acidic environment (Ang *et al.*, 2001). Cad is an enzyme that catalyses the reversible conversion of aldehyde in cells into corresponding alcohol, e.g. benzaldehyde dismutation into benzyl alcohol and benzoic acid (Mee *et al.*, 2005). Ethanol

metabolism provides energy for bacteria in low-oxygen environment. The aldehyde formation accounts for the pathogenesis of bacteria that the toxic substance inhibits gastric epithelial cell proliferation and mucosal protecting to the cells (Matysiak-Budnik *et al.*, 1995).

5.5.3.8 FAD-dependent thymidylate synthase (ThyX) (Up-regulated)

Synthesis of thymidylate (dTMP) is required for the replication of DNA in organism and catalyzed by thymidylate synthase on methylation of the deoxyuridine 5'-monophosphate (dUMP) or by thymidine kinase on synthesis from thymidine compound of growth medium (Neuhard and Kelln, 1996). However, *H. pylori* lacks the mentioned enzymes which a protein ThyX without any sequence homology is identified for compensation (Myllykallio *et al.*, 2002). ThyX catalyses the conversion of dUMP and methylenetetrahydrofolate into dTMP and tetrahydrofolate with enhanced activity with FAD.

5.5.3.9 Flavodoxin (FldA) (Up-regulated)

Flavodoxin is flavin mononucleotide (FMN) that carries protein required in electro transfer reaction in various mechanisms. The pyruvate oxidoreductase (Por) catalyzes the oxidative decarboxylation of the pyruvate into acetyl-coenzyme A (acetyl-CoA) and electron transfer to flavodoxin (Hughes *et al.*, 1995). Flavodoxin is required for the growth of bacteria as it facilitates the only pyruvate decarboxylating mechanism essential for the entry of Krebs cycle in *H. pylori* (Marais *et al.*, 1999; Tomb *et al.*, 1997). *H. pylori* flavodoxin is highly stable even at pH 5.0 which accounts for the survival of bacteria in the acid environment (Cremade *et al.*, 2007). FldA is identified as secreted protein in a 2-DE analysis on the extracellular protein

(Bumann *et al.*, 2002) which acts as an antigen associated to the development of gastric mucosa-associated lymphoid tissue lymphoma (MALToma) in stomach as detected from the sera of patient (Chang *et al.*, 1999) and gastric ulcer patient (Jungblut *et al.*, 2000).

5.5.3.10 Fumarate reductase flavoprotein subunit (FrdA) (Up-regulated)

FrdA is the enzyme catalyzing the conversion of succinate into fumarate in the presence of other subunits FrdB and FrdC in the Krebs cycle (Marais *et al.*, 1999). It is related to the energy production in anaerobic respiration as fumarate is the terminal electron acceptor in the mechanism (Ge, 2002). It is reported that FrdA is essential in the colonization of *H. pylori* as the deletion mutant has no detected colonization in mice model (Ge *et al.*, 2000) and it is also recognized by the sera from infected patient which acts as antigen (Haas *et al.*, 2002). The Frd activity is crucial for function of NH_3/H_2 pump to repose to acidic environment and neutralize the acid for survival of *H. pylori* (Bhattacharyya *et al.*, 2001).

5.5.3.11 Hypothetical protein HP0318 (Up-regulated)

HP0318 is the conserved hypothetical protein and is recognized as antigen by the sera from infected patient (Haas *et al.*, 2002) and in infected human gastric adenocarcinoma epithelial cell line (Backert *et al.*, 2005). It is newly identified as a functional heme oxygenase HugZ that degrades heme into biliverdin with the release of iron (Guo *et al.*, 2008) that heme might be acquired by the iron-dependent outer membrane receptors (Worst *et al.*, 1995). Iron is essential to maintain colonization of *H. pylori* in mini-mature pig model (Koga *et al.*, 2002) that retaining a suitable level of iron in cytoplasm is needed. Moreover, the deletion mutant has poor growth when

hemoglobin added as the iron source in the growth medium (Guo *et al.*, 2008). Thus, HP0318 is essential on the iron metabolism that is required for the colonization and growth of *H. pylori*.

5.5.3.12 Leucyl aminopeptidase (LAP) (Up-regulated)

LAP is enzyme catalyzing the removal of N-terminal amino acid from various peptide and protein which is necessary for regular protein turnover, maturation and removal of unsubstituted amino acids (Lazdunski, 1989). LAP is only identified aminopeptidase in *H. pylori* which shows broad substrate specificity on various polypeptides to release amino acid to maintain life cycle of bacteria (Dong *et al.*, 2005). It is reported that the growth of *H. pylori* is dramatically inhibited when potent LAP inhibitor, Bestatin (Morty and Morehead, 2002) is added in the culture which further shows that LAP activity is required for the growth of *H. pylori*.

5.5.3.13 Neutrophil activating protein (NapA/Bacterioferritin) (Up-regulated)

NapA is reported to be related to the pathogenesis and survival of *H. pylori*. NapA attracts leukocytes to the site of infection and activates the production of reactive oxygen intermediate (Satin *et al.*, 2000). And it also attracts the neutrophils to the site of infection by promoting adhesion to the epithelial cells (Yoshida *et al.*, 2003). The production and secretion of T helper (Th) 1 polarizing cytokines, IL-12 and IL-23 from neutrophils, macrophage and dendritic cells is also stimulated. This helps to drive to the Th1 immune response which is related to more severe damage of inflammation and gastric disease (D'Elios *et al.*, 2005).

NapA is also a virulence factor essential for colonization and pathogenesis. It is involved in iron uptake and storage required for survival of *H. pylori* (Waidner *et al.*,

2002) as iron is the nutrient for growth. It is an oxidative stress protein which is up-regulated as compensation to the diminished stress resistance factors in *H. pylori* (Olczak *et al.*, 2005). NapA can bind DNA to protect damage from toxic free radicals (Bijlsma *et al.*, 2000).

5.5.3.14 Polynucleotide phosphorylase/ Polyadenylase (Up-regulated)

It is enzyme in RNA processing that affects the cell viability but the protein is not well characterized in *H. pylori*. It was reported that addition of poly (A) tails to transcripts (polyadenylation) targeted the RNA decay but this increased the stability of polynucleotide phosphorylase/polyadenylase transcript and slightly increased the protein level in *E. coli*. Polyadenylation of RNA transcript would increase the degradation assisted by polynucleotide phosphorylase/polyadenylase (Mohanty and Kushner, 2002). When the protein in *E. coli* was inactivated, the activity of two major exonucleases was increased to replace the loss of the enzyme but more mRNA decay intermediates were accumulated. And the deletion mutant showed a significant decrease effect on the growth rate and mRNA decay mechanism (Mohanty and Kushner, 2003).

5.5.3.15 Putative neuraminyllactose-binding hemagglutinin homolog (HpaA) (Up-regulated)

HpaA is recognized by the sera of infected patient (Haas *et al.*, 2002). This is identified as lipoprotein acting as potential receptor for *N*-acetylneuraminyllactose (NANA) on mammalian cells with *H. pylori* CCUG 17874 (Evans *et al.*, 1988; O'Toole *et al.*, 1995). *H. pylori* HpaA is identified as adhesin through the fetuin-binding activity and contains conserved amino acids in the sialic-binding

motif in *E. coli* which is responsible for colonization (Evans *et al.*, 1993). A more recent study has shown that the localization of HpaA is in flagella sheath structure recognized by specific antibody and the adherence ability to gastric mucosal cells between deletion mutant and wild-type strains 11637 is similar (Jones *et al.*, 1997). The adhesion ability of HpaA is still controversial which its ability is strain-specific as different strains had been used in the above experiments.

5.5.3.16 Quinone-reactive Ni/Fe hydrogenase, small subunit (HydA) and Quinone-reactive Ni/Fe hydrogenase, large subunit (HydB) (Up-regulated)

HydA and HydB are the accessory proteins on properly incorporation of nickel ions to the membrane-associated hydrogenase protein complex and also urease required for full activity. Double mutant of proteins would be resulted in no hydrogenase and decreased urease activity with similar expression level of urease A and UreB proteins but not functional as lack of nickel ions (Olson *et al.*, 2001). HydA contains nickel and iron required for the full activity of hydrogenase (Benoit and Maier, 2008). Deletion mutant of HydB has shown that HydB has binding sites for nickel ions that required for activation of hydrogenase with GTP activity (Jacobi *et al.*, 1992; Maier *et al.*, 1995). Deletion mutant of HydB also abolishes the colonization to mucosal cells (Olson and Maier, 2002).

The conversion of fumarate into succinate is catalyzed by the hydrogenase, fumarate reductase and menaquinone which is the lipid component of the bacterial electron transport chain used in anaerobic respiration with hydrogen as energy source (Hazell and Mendz, 1997). The hydrogenase formed with hydA, hydB and hydC proteins in anaerobic bacterium *Wolinella succinogenes* that catalyzes the reduction of menaquinone with hydrogen in anaerobic respiration (Dross *et al.*, 2005) and the

hydrogenase complex formed with hydABCDE is believed to catalyze similar pathway (Benoit *et al.*, 2004).

5.5.3.17 Response regulator (OmpR) (Up-regulated)

Deletion of OmpR is lethal to the *H. pylori* (Beier and Frank, 2000) and its expression level of OmpR is reduced upon acidic exposure (Bury-Moné *et al.*, 2004). It was reported that the response regulator system of OmpR and histidine kinase regulates the expression of genes for the bacterial viability, adaption and survival of *H. pylori* inside the host. OmpR acts as the effector protein that is phosphorylated by the sensor protein histidine kinase upon changes in environment, which phosphorylated-OmpR regulates target genes with unknown functions responsible for colonization in mice model (Panthel *et al.*, 2003). OmpR is identified as virulence factor by the sera from gastric cancer patient (Lin *et al.*, 2006).

5.5.3.18 Thioredoxin reductase (TrxB) (Up-regulated)

TrxB is one of the enzymes in thioredoxin system to repair the non-functional oxidized proteins so as to remove the oxidative stress in *H. pylori* (Comtois *et al.*, 2003). The localization of TrxB is altered from the cytosol to medium broth if the bacteria are under biological, physical or chemical stress that initiates the reduction of the target proteins for protection (Windle *et al.*, 2000). TrxB destabilizes immunoglobin IgG and IgA by reducing the disulfide bond of the heavy chains which resulted in reduced complement activation (Brekke *et al.*, 1993) and mucosal secretion (Mackinnon and Hooper, 1994) respectively which results in facilitating the evasion from the immune system during infection. Moreover, TrxB reduces the disulfide bond at the region required for cross-linking of mucin monomer which alter

the gel-like structure of the mucus layer which enhance colonization of bacteria (Dekker *et al.*, 1991).

5.5.3.19 2-Oxoglutarate-acceptor oxidoreductase subunit, OorA and OorB and pyruvate flavodoxin oxidoreductase subunit gamma (PorD) (Down-regulated)

POR catalyzes the decarboxylation of pyruvate to form acetyl-CoA with the reduction of electron acceptor flavodoxin, to compensate the lack of other pyruvate dehydrogenase and pyruvate formate-lyase in *H. pylori* (Hughes *et al.*, 1995; Tomb *et al.*, 1997). OOR enzyme catalyzes the oxidative decarboxylation of 2-oxoglutarate into succinyl-CoA which is an intermediate in TCA cycle, with the reduction of electron acceptor ferredoxin (Hughes *et al.*, 1998). Reduced flavodoxin and ferredoxin serve as the intermediate electron acceptor that donate electron to NADP into NADPH which then enter the electron transport chain for energy production (Hughes *et al.*, 1998). Both enzymes are active only in the low oxygen concentration that contributes to the microaerophilic phenotype of *H. pylori*. Inhibition of the enzyme by oxygen is lethal to the cells. Both enzymes are failed to be inactivated which suggests that they are essential for the cell viability (Hughes *et al.*, 1998). Moreover, both enzymes are related to the activation of the antibiotics Metronidazole from a pro-drug form into an active form with the electron transfer (Edwards, 1993). The protein expression level of pyruvate ferredoxin oxidoreductase (HP1110) and 2-oxoglutarate-acceptor oxidoreductase (HP0591) is reduced in the metronidazole-resistant strain of *H. pylori* strain HER 126 V1 identified in 2-DE analysis (Kaakoush *et al.*, 2009).

5.5.3.20 Alkyl hydroperoxide reductase (AhpC) and alkyl hydroperoxide reductase C22 protein (Down-regulated)

Alkyl hydroperoxide reductase C22 is the c subunit of AhpC, which serves as antioxidant enzyme catalyzing the reduction of organic hydroperoxides including hydrogen peroxide into corresponding alcohols (Wood *et al.*, 2003). AhpC is thioredoxin dependent on the antioxidant pathway (Wang *et al.*, 2006). Reduced level of AhpC leads to the induction of NapA expression to protect *H. pylori* from oxidative stress (Olczak *et al.*, 2005). Alkyl hydroperoxide reductase is related to the colonization as deletion mutant of strain SS1 cannot be recovered from the infected mice model (Olczak *et al.*, 2003). AhpC is also detected from the serum from infected gerbil model (Yan *et al.*, 2001). AhpC exists as two forms with different stress condition, low molecular weight oligomer serves as reduction of organic peroxide in normal stress, and high molecular oligomers serve as chaperone to prevent aggregation of unfolded protein in severe stress condition that favor the formation of stress-induced unfolding of protein (Chuang *et al.*, 2006).

5.5.3.21 Co-chaperonin GroES (Down-regulated)

GroES works together with GroEL to refold the non-native proteins that GroES help to encapsulate the unfolded protein in the hydrophobic cavity of GroEL (Thirumalai and Lorimer, 2001). GroES is identified as virulence factor as detected specifically by the sera from patient with infected *H. pylori* or gastric cancer (Jungblut *et al.*, 2000). GroES is a secreted protein that induced inflammation by inducing production of pro-inflammatory cytokines IL-8, IL-6, GM-CSF, IL-1β and TNF-α in gastric cell which the cytokines would leads to progression of damage of gastric cells into gastric cancer. Moreover, GroES enhances expression of proteins

related to proliferation and inhibits the apoptosis-resistant pathway, which in turns promoting abnormal growth of the gastric cells and ultimately into malignancy (Jungblut *et al.*, 2000). GroES is newly identified to have Ni-binding activity which serves as chaperone of nickel essential in nickel homeostasis, metal detoxification and maturation of Quinone-reactive Ni/Fe hydrogenase in anaerobic respiration (Cun *et al.*, 2008; Schauer *et al.*, 2010).

5.5.3.22 Elongation factor G and Elongation factor Tu (down-regulated)

Elongation factor is essential in the translation step by ribosome. Elongation factor Tu (EF-Tu) is a GTP binding protein that mediates the entry of corresponding aminoacyl tRNA into the A-site of ribosome in a correct manner according to the message on mRNA (Grunberg-Manago, 1996). Elongation factor G (EF-G) is a GTPase that promotes the movement of the tRNA and mRNA after each round of peptide bond formation by GTP hydrolysis (Rodnina *et al.*, 1997) and it also helps in recycling the ribosome (Ramakrishnan, 2002). EF-G and EF-Tu are identified as antigen detected by the serum from the patient with *H. pylori* infection which exist as surface bound protein to elicit immune response (Haas *et al.*, 2002; Lin *et al.*, 2007). The expression level of EF-Tu increases under stress by bile has been reported in the *H. pylori* (Shao *et al.*, 2008) and *C. jejuni* (Fox *et al.*, 2007). EF-G and EF-Tu also display chaperone property on protecting aggregation of protein induced by stress and restoring their native forms (Caldas *et al.*, 1998; Caldas *et al.*, 2000).

5.5.3.23 F0F1 ATP synthase subunit alpha (Down-regulated)

ATPase is the enzyme localized on cytoplasmic membrane required for synthesis of ATP and regulation of intracellular pH homeostasis with the

transmembrane electrochemical proton gradient for synthesis and hydrolysis of ATP which help in intracellular pH homeostasis (Futai and Kanazawa, 1983). ATPase is a multicomplex formed by a soluble catalytic domain (F1) with α, β, ε, γ and δ subunit and a transmembrane domain with a, b and c subunit for translocation of H+ ions. The catalytic subunit of ATPase is formed by the $\alpha_3\beta_3$ hexamer (Miwa and Yoshida, 1989). ATP-binding motif is determined on α and β subunits and they are essential in the catalysis (McGowan *et al.*, 1997). The α subunit is linked to δ subunit by cysteine bonding that anchor on the membrane (Ogilvie *et al.*, 1997). The survival of *H. pylori* at pH6.0 is affected when the F0F1 ATP synthase is specifically inhibited (Futai and Kanazawa, 1983). F0F1 ATPase synthase subunit alpha forming of the catalytic subunit of functional ATPase is associated to energy production and pH homeostasis of *H. pylori*.

5.5.3.24 Preprotein translocase subunit SecA (Down-regulated)

SecA is one of the components of the Sec protein translocation apparatus across the inner membrane which serves as the ATP hydrolysis in assisting the translocation of proteins across the membrane (Duong *et al.*, 1997a; Thanassi and Hultgren, 2000). Its protein level is induced upon the exposure of the acid environment (Ang *et al.*, 2001). In *E. coli* model, SecA is localized in the cytosol that it binds to the precursor unfolded preprotein through specific signal peptide domain and then the Sec-preprotein complex is bound to the core subunit of apparatus. ATP is bound assisting the translocation of about 30 residues of the preprotein across the inner membrane. The preprotein is released from the SecA upon hydrolysis of ATP. The cycle of bound and unbound form of SecA assists the translocation of preprotein by ATP hydrolysis (Duong and Wickner, 1997b; van der Wolk *et al.*, 1997; Eichler *et*

al., 1998). While the secreted proteins with putative signal peptide in *H. pylori* are identified as vacuolating cytotoxin VacA for cell killing, cell binding factor for cell envelope structure and glutamyltranspeptidase for synthesis of cofactors in the 2-DE analysis of the secreted proteins (Bumann *et al.*, 2002).

5.5.3.25 Urease accessory protein (UreG), Urease UreA/ bifunctional urease subunit gamma/beta and UreB (Down-regulated)

Urease is the known virulence factor and is crucial for the survival of *H. pylori* inside the stomach as it hydrolyzes urea into ammonium and carbon dioxide to neutralize the acidic environment (Mobley *et al.*, 1988, Marais *et al.*, 1999) that expression level is stimulated by acidic exposure (Bury-Moné *et al.*, 2004). Urease stimulates the secretion of inflammatory cytokines (Harris *et al.*, 1996) and also the urease activity is toxic to the gastric epithelial cells by the formation of monochloramine with enhanced cytotoxicity to gastric cells (Smoot *et al.*, 1990; Suzuki *et al.*, 1992). Urease is essential for the colonization as disruption mutant fails to be recovered from infected piglet model (Eaton *et al.*, 1991). It is also reported that disruption mutant of UreB reduces the motility of the bacteria across the mucous layer (Nakamura *et al.*, 1998). Urease binds to the Class II MHC exposed on the gastric epithelial cell for adhesion (Fan *et al.*, 2000). UreB binds to the CD74 on the gastric epithelial cells which the complex would stimulate the production of IL-8 and activation of NF-κB (Beswick *et al.*, 2006).

Urease is an enzyme complex consisting of membrane-associate subunit of UreA/UreB complex associated with acid-gated urea channel UreI and an accessory subunit of UreE-H (Voland *et al.*, 2003). UreI is required for the localization of the urease from cytoplasmic to membrane bound in acidic exposure (Hong *et al.*, 2003).

Disruption mutant of UreG abolishes the urease activity as UreG is required to incorporate nickel ions to apoenzyme which is required for functional activity. Its ability on GTP hydrolysis is believed to promote the formation and stabilization of the accessory protein subunit and apoenzyme UreA/UreB subunit. Maturation of urease is also dependent on the HydB protein that mobilizes the nickel ions from storage proteins to apoenzyme mediated by GTP hydrolysis (Mehta *et al.*, 2003; Voland *et al.*, 2003).

UreA and UreB are the antigens recognized by the sera from the patients with infected *H. pylori* or gastric disease from extensive 2-DE analysis (Jungblut *et al.*, 2000; Haas *et al.*, 2002; Lin *et al.*, 2006). UreG is newly identified with UreA and UreB as up-regulated expression in the infected human gastric adenocarcinoma epithelial cell line (Backert *et al.*, 2005).

5.5.4 Significance of the identified proteins in pathogenesis of *H. pylori*

In summary, most of the identified proteins play significant roles in pathogenesis of *H. pylori* which are summarized in Table 5.2.

Table 5.2 Significance of the identified proteins in pathogenesis of *H. pylori*

Identified proteins	Expression level in ΔHP1076
Acts as antigen	
ATP-dependent protease binding subunit (ClpB)	+
Cag pathogenicity island protein (Cag26)	+
Flavodoxin (FldA)	+
Fumarate reductase flavoprotein subunit (FrdA)	+
Hypothetical protein (HP0318)	+
Putative neuraminyllactose-binding hemagglutinin homolog (HpaA)	+
Response regulator (OmpR)	+
Co-chaperonin (GroES)	-
Elongation factor G (EF-G)	-
Elongation factor (EF-Tu)	
Urease (UreA)	-

Urease (UreB)	-
Urease accessory protein (UreG)	-

Bacterial survival	
ATP-dependent protease binding subunit (ClpB)	+
Bifunctional aconitate hydratase 2/2-methylisocitrate dehydratase	+
Bifunctional methionine sulfoxide reductase A/B protein (MsrA/B)	+
Hypothetical protein (HP0318)	+
Leucyl aminopeptidase (LAP)	+
Neutrophil activating protein (NapA/Bacterioferritin)	+
Polynucleotide phosphorylase/ Polyadenylase	+
Response regulator (OmpR)	+
Thioredoxin reductase (TrxB)	+
2-oxoglutarate-acceptor oxidoreductase subunit (OorA, OorB)	-
Pyruvate flavodoxin oxidoreductase subunit gamma (PorD)	-
F0F1 ATP synthase subunit alpha	-
Urease (UreA)	-
Urease (UreB)	-
Urease accessory protein (UreG)	-

Bacterial colonization	
2-Hydroxyacid dehydrogenase	+
Fumarate reductase flavoprotein subunit (FrdA)	+
Bifunctional methionine sulfoxide reductase A/B protein (MsrA/B)	+
Hypothetical protein (HP0318)	+
Neutrophil activating protein (NapA/Bacterioferritin)	+
Putative neuraminyllactose-binding hemagglutinin homolog (HpaA)	+
Quinone-reactive Ni/Fe hydrogenase, small subunit (HydA)	+
Quinone-reactive Ni/Fe hydrogenase, large subunit (HydB)	+
Thioredoxin reductase (TrxB)	+
Alkyl hydroperoxide reductase (AhpC)	-
Urease (UreA)	-
Urease (UreB)	-
Urease accessory protein (UreG)	-

Infection of *H. pylori*	
ATP-dependent protease binding subunit (ClpB)	+
Cag pathogenicity island protein (Cag26)	+
Cinnamyl-alcohol dehydrogenase ELI3-2 (Cad)	+
Neutrophil activating protein (NapA/Bacterioferritin)	+
Co-chaperonin (GroES)	-
Preprotein translocase subunit SecA	-
Urease (UreA)	-
Urease (UreB)	-
Urease accessory protein (UreG)	-

(+) represents up-regulation and (-) represents down-regulation in ΔHP1076 mutant

5.5.5 Verification of up-regulation of Cag pathogenicity island protein (Cag 26)

As discussed previously, CagA is essential for the pathogenesis of the *H. pylori* to gastric mucosal cells that disrupts the signal transduction pathways of the host and enhances the cell proliferation. Before performing the detailed study on the effect of the HP1076 over the CagA mechanism, the increased expression of protein should be confirmed with the immunoblotting analysis. CagA protein in the total cell lysate was detected by specific rabbit polyclonal anti-CagA antibody and then with Donkey anti-rabbit IGG-HRP antibody. The protein level of CagA in ΔHP1076 strain was significantly increased by 2.6 folds using WT as the control for comparison (Fig.5.12). This result was consistent with the result in 2-DE analysis.

However, the mechanism of HP1076 on enhancing the expression of CagA is still not known. Enhanced CagA protein level in the bacterial cytosol is not reported as CagA elicits toxic effect once it is translocated into the host cells. More experiments should be performed in the future to elucidate the detailed mechanism. The localization of CagA in the cytosol should be compared as it is reported that CagA is normally distributed over the cytosol of bacteria, and it is extensively localized near the bacterial membrane where the type IV secretion apparatus is located upon acidic exposure (Wu *et al.*, 2005). If more CagA is localized for the secretion in the deletion mutant which suggests that the toxic effect on mucosal cells may be enhanced by the secreted CagA. The infection rate or adhesion ability of the bacteria with deletion mutant can be studied.

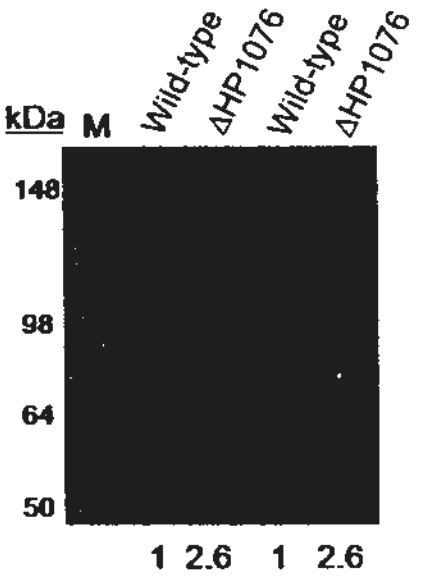

Fig.5.12 Western blot analysis of CagA in WT and ΔHP1076 mutant
Proteins on PVDF membrane were probed with primary anti-CagA and secondary anti-rabbit antibody in a ratio of 1:10,000 and 1:5,000 respectively. Lane M: Invitrogen SeeBlue® Plus 2 pre-stained protein standard. The signal was detected with 1-min exposure. The fold change of protein level of CagA was calculated by ImageJ and marked at the bottom of the figure.

5.5.6 Verification of down-regulation of Urease UreA and UreB

Urease is the key enzyme essential for the survival, colonization and pathogenesis of *H. pylori* inside host stomach. An immunoblotting analysis was performed to verify the reduced expression of the UreA and UreB in the cell lysate from WT and deletion mutants. UreA and UreB were detected separately by specific rabbit polyclonal anti-UreA antibody and rabbit polyclonal anti-UreB antibody and then by Donkey anti-rabbit IGG-HRP antibody. In the expression of UreA, the protein level of mutant strain was reduced to 0.8 fold when compared with WT while that of UreB was reduced to 0.5 fold in deletion mutant (Fig.5.13). A faint band of size around 64 kDa was found which might be the dimer formation of the UreA subunit. This result supports the reduced expression of the UreA and UreB identified in the 2-DE analysis. However, the mechanism of HP1076 on controlling the protein level remains to be elucidated.

In the future, the urease activity should be measured between the WT and deletion mutant as it is reported that urease activity of UreG-deletion mutant is reduced even the protein levels of UreA and UreB remained constant (Mehta *et al.*, 2003). And UreG protein level is reduced in 2-DE analysis that may affect the urease activity as it is required in maturation of functional urease enzyme. Moreover, the adherence ability to gastric epithelial cells will be studied which provide more direct effect on the infection of *H. pylori* with ΔHP1076 mutant.

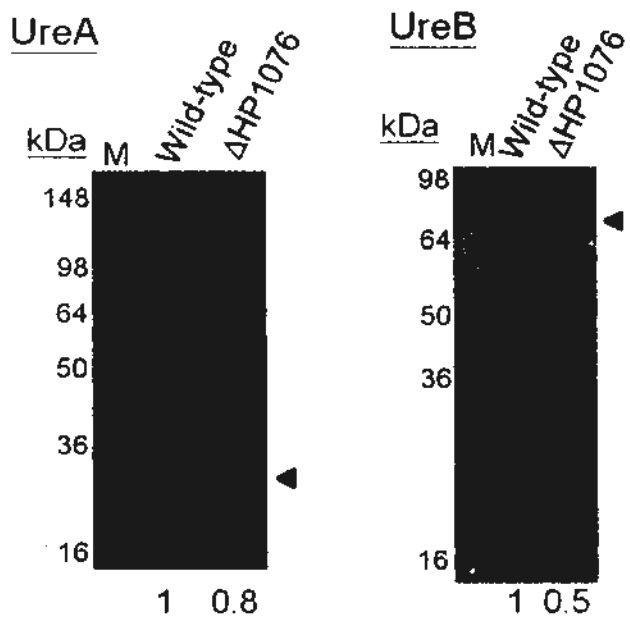

Fig.5.13 Western blot analysis of UreA and UreB in WT and ΔHP1076 mutant
Proteins on PVDF membrane were probed with primary anti-UreA or anti-UreB and secondary anti-rabbit antibody in a ratio of 1:10,000 and 1:5,000 respectively. Lane M: Invitrogen SeeBlue® Plus 2 pre-stained protein standard. The signal was detected with 1-min exposure. The fold change of protein level of UreA or UreB was calculated by ImageJ and marked at the bottom of the figure.

5.6 Metronidazole susceptibility test

Metronidazole (MtZ) is commonly used in a combined treatment to eradicate *H. pylori* (Edwards *et al.*, 1993). It is a pro-drug that diffuses into the bacteria and requires the activation by the bacterial enzymes in low-oxygen level. The nitro group is reduced by accepting one electron and converted into nitro-radical intermediate

that causes damage to DNA. The electron transfer is mediated from the flavodoxin or ferrodoxin which are reduced by the 2-oxoglutarate-acceptor oxidoreductase Oor and pyruvate flavodoxin oxidoreductase POR (Mendz, 1993; Hoffman *et al.*, 1996; Jorgensen *et al.*, 1998).

From the result of 2-DE analysis, the expression level of 2-oxoglutarate-acceptor oxidoreductase subunit, OorA and OorB and pyruvate flavodoxin oxidoreductase subunit gamma (PorD) were reduced in the deletion mutant which might affect the activation of MtZ and gain resistant to it.

In order to investigate whether the mutant strains would alter the antibiotic resistance of the bacteria, a disc diffusion test with metronidazole (MtZ) antibiotic was employed (DeCross *et al.*, 1993). A 5 μg/ml MtZ disc was placed at the centre of the Columbia blood agar plate streaked with *H. pylori* strain 26695. If the bacterium is resistant to MtZ drug, bacteria would grow evenly on the whole agar plate as observed as the grey layer. If the bacterium is sensitive to MtZ drug, no cell would be grown around the disc, the diameter of the zone will be measured as a sign of susceptibility. For the zone size smaller than 16 mm, the cells are resistant to the drug tested, while a zone size larger than 21 mm is regarded as susceptible (Chaves *et al.*, 1999; McNultya *et al.*, 2002). Three bacteria strains of WT, ΔHP1076 and MtZ-R were tested and the results of three trials are summarized in Table 5.3. The zone size of WT strain was 25 mm which was sensitive to MtZ, while control MtZ-R strain has no visible zone appeared on agar plate (Fig.5.14). The zone size of ΔHP1076 was 15.3 mm which was resistant to MtZ. This suggested that deleting HP1076 reduced the protein level of subunits of Oor and POR which further inhibited the pro-drug activation of MtZ inside the bacteria. Thus, HP1076 may be essential for the action of the commonly used nitroimidazole drugs.

Fig.5.14 Metronidazole susceptibility test on blood agar plates
Test performed with wild-type (A) and ΔHP1076 mutant (B) with visible zone formed around drug disc, and MtZ-R strain (C) with no visible zone formed around.

Table 5.3 Results of Metronidazole susceptibility test

Bacterial strain	**Zone size (mm)**			
	Trial 1	Trial 2	Trial 3	Average
Wild-type	25	25-26	25	25
ΔHP1076	15	16	15	15.3
MtZ-R	0	2	0	0.7

5.7 Genomic analysis of HP1076 and FliS in Metronidazole-resistant (MtZ-R) clinical isolates

In attempt to investigate the involvement of FliS and HP1076 in the infection of *H. pylori*, the conservation of target genes in MtZ-R was analyzed with the wild-type strains. Metronidazole is an antibiotic used in the combined drug treatment of *H. pylori*, but the resistant rate is reported to increase worldwide (Alarcón *et al.*, 1999; Ching *et al.*, 1996; Banatvala *et al.*, 1994). Our 2-DE analysis showed that deletion of the gene, *hp1076* would be resulted in MtZ-R, so it would be interested to investigate the differences in DNA and protein sequences between wild-type and MtZ-R samples.

The clinical isolates were obtained from our collaborator, Dr. Thomas Ling from the Department of Microbiology in the Prince of Wales Hospital. The genomic DNA of WT and MtZ-R samples were isolated and used as template for PCR amplification with specific primers producing PCR products with 100-bp upstream or downstream

of target genes. This helped to provide a full analysis of the whole genes and the mutations were analyzed by protein sequence alignment software, ClustalW with translated DNA sequence results. At least three independent isolates were used for the analysis.

For the protein sequence alignment of FliS (Fig.5.15), the protein sequences of WT and MtZ-R were totally identical, which indicated that FliS is conserved among the strains. This is consistent to the fact that FliS is an essential gene required for gastric colonization (Kavermann *et al.*, 2003) and required for flagellar assembly. And the MtZ-R samples were isolated from the patients with infected bacteria that the FliS isolated should be a functional one.

For the protein sequence alignment of HP1076 (Fig.5.16), the protein sequences of MtZ-R strains were highly similar to WT with above 94% identity (Table 5.4). Four residues in WT strain, Thr20, Val112, Val121 and Gln159 were mutated into Lys20, Asp112, Ala121, Lys159 in all MtZ-R samples. The T→K and V→A changes were similar with their nature of side chain, polar threonine residue was changed into a basic residue, lysine, with a longer side chain and a non-polar residue valine was changed into a non-polar alanine residue. The Q→ K change was highly similar in polarity of side chain, but the charge changed into a basic one. The V→D change was not conserved, as non-polar and neutral valine residue was changed into the acidic and polar aspartic acid.

To further study the relationship of the mutated HP1076 on FliS-binding, V112D, V121A and Q159K single mutants were constructed by site-directed mutagenesis of the expression plasmids, pAC28m-hp1076. The T20K mutant was not constructed as this residue was not located in the minimal binding domain of ΔN20 fragment shown in molecular interaction assays of HP1076 fragments and FliS.

The single mutant or WT plasmids, pAC28m-hp1076 were co-expressed with GST-FliS under the same expression level of soluble proteins (Fig.5.17A). When the cell lysate was subjected for pull-down assays with glutathione (G) or Ni-NTA (N) sepharose (Fig.5.17B), the HP1076 mutants displayed similar binding affinity to FliS as the WT HP1076. Thus, the specific point mutations in HP1076 in MtZ-R samples were not inhibited the binding with FliS. However the mutation effect may be on other proteins in other metabolic pathways that need further investigation.

```
26695          MQYANAYQAYQHNRVSVESPAKLIEMLYEGILRFSSQAKRCIENEDIEKKIYYINRVTDI 60
10662          MQYANAYQAYQHNRVSVESPAKLIEMLYEGILRFSSQAKRCIENEDIEKKIYYINRVTDI 60
10643          MQYANAYQAYQHNRVSVESPAKLIEMLYEGILRFSSQAKRCIENEDIEKKIYYINRVTDI 60
10665          MQYANAYQAYQHNRVSVESPAKLIEMLYEGILRFSSQAKRCIENEDIEKKIYYINRVTDI 60
10679          MQYANAYQAYQHNRVSVESPAKLIEMLYEGILRFSSQAKRCIENEDIEKKIYYINRVTDI 60
10692          MQYANAYQAYQHNRVSVESPAKLIEMLYEGILRFSSQAKRCIENEDIEKKIYYINRVTDI 60
               ************************************************************

26695          FTELLNILDYEKGGEVAVYLTGLYTHQIKVLTQANVENDASKIDLVLNVARGLLEAWREI 120
10662          FTELLNILDYEKGGEVAVYLTGLYTHQIKVLTQANVENDASKIDLVLNVARGLLEAWREI 120
10643          FTELLNILDYEKGGEVAVYLTGLYTHQIKVLTQANVENDASKIDLVLNVARGLLEAWREI 120
10665          FTELLNILDYEKGGEVAVYLTGLYTHQIKVLTQANVENDASKIDLVLNVARGLLEAWREI 120
10679          FTELLNILDYEKGGEVAVYLTGLYTHQIKVLTQANVENDASKIDLVLNVARGLLEAWREI 120
10692          FTELLNILDYEKGGEVAVYLTGLYTHQIKVLTQANVENDASKIDLVLNVARGLLEAWREI 120
               ************************************************************

26695          HSDELA 126
10662          HSDELA 126
10643          HSDELA 126
10665          HSDELA 126
10679          HSDELA 126
10692          HSDELA 126
               ******
```

Fig.5.15 Protein sequence alignment of FliS between WT and MtZ-R clinical isolates

Protein sequences of WT (26695) and MtZ-R clinical isolate samples (10662, 10643, 10665, 10679 and 10692) were aligned by ClustalW showing totally matches (•) of all residues between different strains.

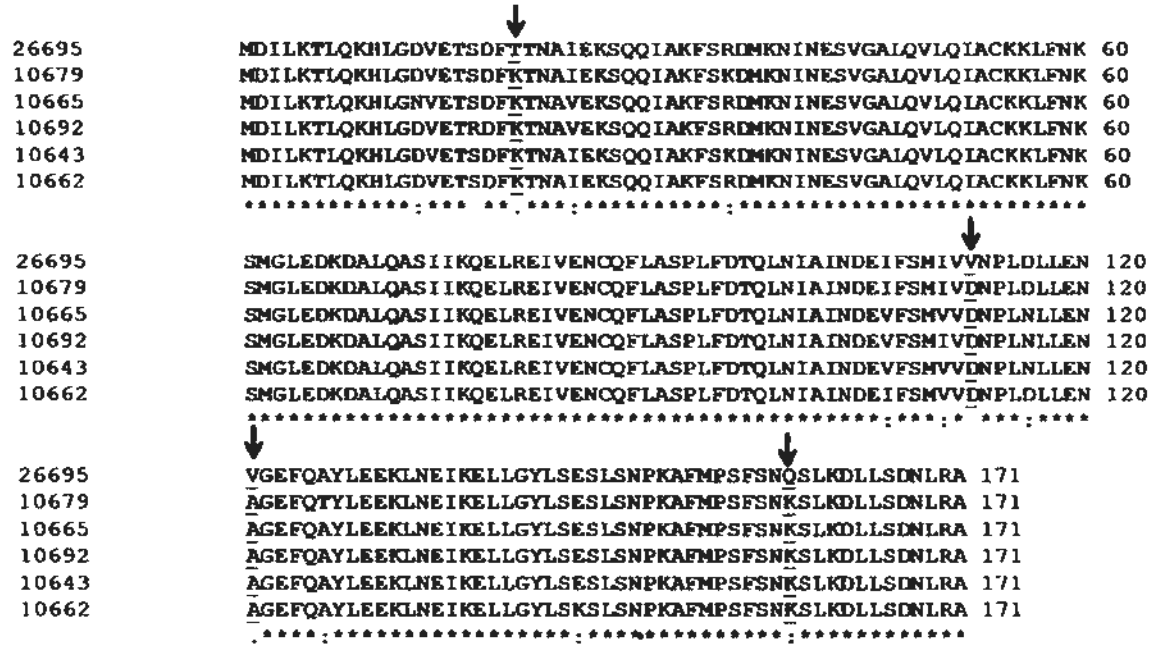

Fig.5.16 Protein sequence alignment of HP1076 between WT and MtZ-R clinical isolates

Protein sequences of WT (26695) and MtZ-R clinical isolate samples (10662, 10643, 10665, 10679 and 10692) were aligned by ClustalW showing identical residues (•), highly conserved residue (:), similar residue (.), between different strains. And residues without any conservation are shown without any symbols. Mutated residues in MtZ-R strains are underlined and marked with arrows.

Table 5.4 Protein sequence identity and mutations of HP1076 between WT and MtZ-R clinical isolates

MtZ-R clinical isolate	Sequence identity to WT	Mutation in HP1076
10662	96%	T20K, I100V, V112D, V121A, E144K, Q159K
10679	96%	T20K,R35K,V112D,V121A, A126T, Q159K
10643	95%	T20K, R35K, I96V, I100V, V112D, D116N, V121A, Q159K
10692	95%	S17R, T20K, I24V, I96V, V112D, D116N, V121A, Q159K
10665	94%	D13N, T20K, I24V, I96V, I100V, V112D, D116N, V121A, Q159K

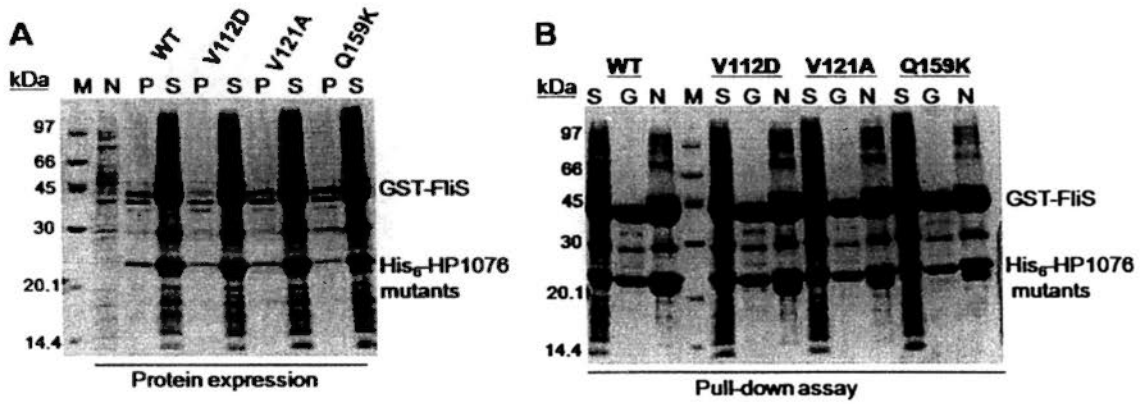

Fig.5.17 Co-expression and pull-down assays of HP1076 mutants in MtZ-R clinical isolates with GST-FliS
(A) Expression profile of co-expressed proteins with insoluble (P) and soluble (S) protein fractions of wild-type (WT) and mutants (V112D, V121A and Q159K) of HP1076 analyzed on 15% SDS-PAGE.
(B) Pull-down assays were performed with glutathione sepharose (G) Ni-NTA agarose beads (N) using soluble fractions of cell lysate (S).

5.8 Conclusion

HP1076 was successfully disrupted by the insertion of kanamycin-resistant gene and a deletion mutant in *H. pylori* strain 26695 (ΔHP1076) was constructed. The mutant strain and WT strain were cultured for analysis. In the immunoblotting analysis, the protein level of FliS in the mutant was slightly reduced which further supported the co-chaperone activity on stabilizing FliS in cytosol. While the total flagellin protein level was similar, there was more flagellin found in cytosol fraction in mutant strain suggesting that the filament formation on bacterial membrane was inhibited. This result further confirmed with the motility assay that mutant strain was less motile on soft agar plate than that of WT strain. Based on the preliminary results of the ΔHP1076 mutant strain, HP1076 is essential in the motility system that HP1076 is needed to stabilize and retain a proper level of FliS in cytosol. This subsequently would assist the chaperone activity of FliS on protecting flagellin molecules from aggregation inside cytosol or promote export of flagellin on the FliS/flagellin complex as HP1076 showed binding with that complex. HP1076 may

function similarly with the hook-associated protein FlgK and flagellar capping protein FliD which will be verified in future. Simile mode of interaction of co-chaperone to chaperone (PseE-PseG) has been found in type III secretion system in *Pseudomonas aeruginosa*, which the co-chaperone PseE stabilizes export chaperone PseG on binding with the type III needle component PseF and a stable complex of PseE/PseG/PseF has formed (Quinaud *et al.*, 2005; Plé *et al.*, 2010).

Various interacting partners of HP1076 were identified together with FliS (PimRider™, Rain *et al.*, 2001) which proposed that HP1076 might function in other pathways. A proteomic study of the WT and mutant strains was performed to aid in this purpose. 40 differentially expressed proteins were found with 19 up-regulated and 14 down-regulated proteins identified by mass spectrometry. About 7 samples were identified with poor result of confidence score below 50% or even not identified from the database search. The reasons for the poor result might be due to poor experimental skills in preparing the peptide or the amount of peptide prepared is low that only a small portion of whole protein sequence is identified which is resulted in low confidence score. This can be improved with a more careful preparation or loading more samples to increase the intensity of each spot.

A broad range of proteins were identified with the deletion of HP1076 as shown in Table 5.1-5.2, that involved in (1) anti-oxidant defense system that is required for microaerophilic *H. pylori* as it can only survive with low oxygen level (Bury-Moné *et al.*, 2006). Anti-oxidant system also allows persistent colonization in human stomach in removing large amount of toxic reactive oxygen species generated and repairing cell damage of *H. pylori* induced from the inflammatory response (Wang *et al.*, 2006). (2) Metabolism, energy production, and protein and DAN synthesis systems that allow the survival of bacterium. (3) Iron or nickel mechanism and pH

homeostasis system allows growth of bacterium inside the stomach. Iron is required in functional activation of metabolic enzymes and regulation of gene expression (Fassbinder *et al.*, 2000) that the acquiring and storage system is tightly regulated (Marais *et al.*, 1999). Nickel is required in catalytically activation of essential urease enzyme (Cussac *et al.*, 1992) and GroES serves as the nickel storage (Kansau *et al.*, 1996). Ammonium is produced by urease to neutralize the acidic environment required for long-term colonization. (4) Adhesion, binding of *H. pylori* to the exposed surface of gastric epithelial cells allows the colonization and infection inside stomach. (5) Pathogenesis, secreted effector CagA disrupts the signaling pathway of the epithelial cells and induces proliferation of the cells. The secretion of pro-inflammatory cytokines is stimulated by NapA, urease and GroES. Moreover, most of the proteins identified acts as immunogens that are recognized by the sera from patient with infection and gastric cancer. 3 identified proteins with essential role in infection were further verified to confirm the increased and reduced expression level of CagA, urease UreA and UreB respectively.

Deletion mutant displays resistance to antibiotic drug Metronidazole (MtZ) in disc diffusion test, that is very likely due to the reduced expression POR and Oor enzymes required in electron transfer system in deletion mutant. Thus, HP1076 is probably associated to the stabilization of POR and Oor enzymes for the activation pathway of common nitroimidazole drug for eradication. In the MtZ-R clinical isolate samples, FliS is found to be totally conserved while HP1076 showed some mutations. From the crystal structure showed in this project and the pull-down assay with FliS, the mutations on HP1076 are not essential for the binding with FliS, but they may cause defect on binding with other interacting partners.

The results in this chapter provide preliminary information to understand the

biological role of HP1076 in *H. pylori*, that HP1076 may be involved in motility system, pathogenesis, survival and colonization of *H. pylori* inside human stomach.

Chapter 6

General Conclusion and Future perspective

Flagellar assembly pathway in enteric bacteria requires macromolecule structure and chaperone proteins to assist on stabilizing export substrates inside cytosol or targeting to the export apparatus (Macnab, 2003; Wilharm *et al.*, 2007). *H. pylori* possess homologues to most of the flagellar proteins, but more studies have shown that the flagellar system differs from that of *E. coli* and *Salmonella* (Tomb *et al.*, 1997; Galkin *et al.*, 2008). Only one export chaperone FliS is identified in *H. pylori* that is required in filament formation, while escort general chaperone FliJ (Evans *et al.*, 2006) and other export chaperones FliT and FlgN in *Salmonella* (Fraser *et al.*, 1999; Bennett *et al.*, 2001) has not been identified in *H. pylori*. The present study focuses on investigation of association and biological roles of flagellar protein FliS from *H. pylori* which is the bodyguard of flagellin molecules inside cytosol and a hypothetical protein HP1076.

The association of FliS and HP1076 was demonstrated, which was consistent with the prediction in *H. pylori* (Rain *et al.*, 2001). The minimum binding domain was determined on residues 21-171 of HP1076 and stable complex was formed in solution. The strength of interaction was strong with association constant, Ka = 1.5 x 10^7 M^{-1}.

The association of FliS with C-terminal region of flagellin was demonstrated in pull-down assay and this binding was not inhibited with the binding of HP1076, suggesting that HP1076 and flagellin bind at different sites on FliS. This was further supported by the crystal structure of FliS/HP1076. FliS displayed general chaperone

activity on inhibiting aggregation of reduced insulin and stabilized HP1076 from degradation when in complex as less degraded bands with lower molecular weight was observed during purification (Fig.3.11 and Fig.3.19). FliS was demonstrated to interact with hook-associated protein FlgK, flagellar capping protein FliD and ATPase regulator FliH at the first time. This suggests that FliS is likely a general chaperone on protecting export substrates flagellin molecules, FlgK and FliD from aggregation and facilitates the export by directing them to the export apparatus FliH coupled with ATP hydrolysis by FliI. These findings offer evidence on the divergence in flagellar export mechanism in *H. pylori*.

Moreover, HP1076 displayed co-chaperone activity on FliS by stabilizing protein folding of insoluble FliS with mutations in residues for flagellin-binding, and by enhancing the chaperone activity of FliS on preventing insulin from aggregation. HP1076 also exhibits properties of type III chaperones that they are small acidic proteins dominated with helical structures (Wattiau *et al.*, 1996; Bennett and Hughes, 2000) which was observed from crystal structure.

The structure determination of FliS, HP1076 and their complex provided more detailed study on molecular interaction and functional role of HP1076. The crystal structure of *H. pylori* FliS was determined which adopts a four helical up-and-down bundle resembling that of *A. aeolicus*. The association of flagellin is evolutionary conserved in bacteria as the flagellin-binding pocket is highly conserved. Moreover, the crystal structure of HP1076 was shown to be structurally related to proteins in flagellar and type III secretion system which further supported the involvement of HP1076 in assisting FliS in flagellar assembly pathway. A highly electronegative surface was found localized oppositely to the binding surface with FliS. This region

may bind to export apparatus mediated the flagellar protein export, which this mechanism has been proposed with FliJ in *Salmonella* (Minamino *et al.*, 2000b).

The structure of FliS/HP1076 complex showed that the chaperone-co-chaperone association is mediated by extensive hydrogen and hydrophobic bonds between helical structures. Asn41 on HP1076 was demonstrated as critical for binding as substitution with alanine would abolish the interaction with FliS. In addition, Lys38 would induce a conformational change on HP1076 to create an increased binding surface. This chaperone-co-chaperone association of FliS/HP1076 is new in the flagellar export mechanism, but similar assembly has been demonstrated in type III secretion system for virulence factor in *Pseudomonas aeruginosa* and *Yersinia pestis* (Quinaud *et al.*, 2005; Quinaud *et al.*, 2007; Sun *et al.*, 2007; Plé *et al.*, 2010). *Pseudomonas* PscF and *Yersinia* YscF are the injection needle proteins to be secreted for cytotoxicity that resembles the *H. pylori* flagellin molecules which are protected by chaperone PscG or YscG or FliS inside cytosol respectively. The interaction of PscG/PscF or YscG/YscF resembles that of FliS/FliC through hydrophobic interaction and the chaperone is further stabilized by co-chaperone PscE or YscE. But the interaction between helices of chaperone-co-chaperone association is different from that of FliS/HP1076. The association of FliS and HP1076 is unique in ε-proteobacteria especially in *Campylobacter*-related species.

For the HP1076 deletion mutant in *H. pylori*, initial results showed that motility of bacteria in soft-agar test was reduced when compared with wild-type strain that might be due to the reduced level of FliS as demonstrated in immunoblotting analysis. This further supported that HP1076 plays a role in stabilizing FliS to a proper level in cytosol. Thus, HP1076 might play essential role in infection as motility is a virulence

factor for infection.

From the proteomice study of mutant and WT strains, differentially expressed proteins were identified by mass spectrometry. A broad range of proteins identified (Table 5.1-5.2) involved in (1) anti-oxidant defense mechanism that allows persistent colonization of bacteria inside human stomach on removing reactive oxygen species generated during infection (Wang *et al.*, 2006), (2) metabolism to allow survival of bacteria inside stomach, (3) metal metabolism and pH homeostasis system that allows activation of urease enzymes for long-term colonization, (4) adhesion to enhance infection and colonization, (5) pathogenesis that elicits toxic effect on signal transduction pathway of gastric epithelial cells or enhances secretion of pro-inflammatory cytokines during infection. Some of the identified proteins are antigens in the infection of *H. pylori*. Three proteins CagA, urease UreA and UreB were confirmed by immunoblotting analysis from which the results were in line with the proteomic analysis with respective enhanced and reduced expression level.

Interestingly, deletion mutant displayed resistance to antibiotic drug metronidazole in drug susceptibility test. This is very likely related to the reduced expression of 2-oxoglutarate-acceptor oxidoreductase and pyruvate flavodoxin oxidoreductase that are required for activation of pro-drug inside bacteria. In the genetic study of the metronidazole-resistant clinical isolates, mutations on HP1076 were observed but FliS was totally conserved. Those mutations on HP1076 were not essential in binding with FliS from the pull-down assay and crystal structure.

In conclusion, the association of FliS with HP1076 was demonstrated. *H. pylori* FliS was shown to interact with flagellar related protein not restricted in flagellin. Moreover, FliS and HP1076 displayed chaperone activity which HP1076 acts as

co-chaperone to FliS. The chaperone-cochaperone association was firstly reported in flagellar export system. HP1076 plays important role in flagellar system on motility, and possibly survival, colonization and infection of *H. pylori* and antibiotic resistant pathway of metronidazole.

In future, further experiments can be carried out to provide more information to understand the biological roles of FliS and HP1076 in flagellar system or other infection mechanisms.

A. Study on flagellar system

For the interaction of FliS with FlgK, FliH and FliD, the effect of co-chaperone HP1076 on these bindings will be investigated. Although HP1076 showed no enhancing effect on binding with FlaBc, HP1076 may promote binding for other proteins. It would be interested to investigate the binding sites on newly identified FliS interacting partners that they may compete with FlaBc for the flagellin-binding pocket. Moreover, association of FliS with FliH may promote protein export or acts as cycling mechanism of the unloaded FliS chaperone, assays on binding with FliS and loaded FliS chaperone will be studied with FliH and HP1076. Hopefully, a more detailed molecular mechanism of the flagellar export will be elucidated.

B. Study on HP1076

It would be interested to investigate the highly electronegative surface of HP1076 crystal structure opposite to the FliS-binding site which may assist the binding of FliS/HP1076 to other flagellar export proteins which similar mechanism has been proposed in *Salmonella* FliJ. Preliminary X-ray structural data of FliJ from

Salmonella has been reported (Ibuki *et al.*, 2009), but the coordinates were not deposited in Protein Data Bank. A structural comparison would be performed to obtain a better understanding of the export mechanism. The differential expression level of CagA and urease UreA and UreB in HP1076 null mutant prompts us to investigate the effect of HP1076 on infection system. The infection rate and urease activity of the mutant strain would be measured. The association of HP1076 to drug resistance is also interested to investigate as more antibiotic-resistant strains are reported that may lead to failure on eradication of *H. pylori* and more serious illness.

Appendices

1. Vector Maps of Expression Vector

(a) pGEX-6p-3 vector

pGEX-6P-1 (27-4597-01)

PreScission™ Protease

Leu Glu Val Leu Phe Gln↓Gly Pro Leu Gly Ser Pro Glu Phe Pro Gly Arg Leu Glu Arg Pro His
CTG GAA GTT CTG TTC CAG GGG CCC CTG GGA TCC CCG GAA TTC CCG GGT CGA CTC GAG CGG CCG CAT
BamH I EcoR I Sma I Sal I Xho I Not I

pGEX-6P-2 (27-4598-01)

PreScission™ Protease

Leu Glu Val Leu Phe Gln↓Gly Pro Leu Gly Ser Pro Gly Ile Pro Gly Ser Thr Arg Ala Ala Ala Ser
CTG GAA GTT CTG TTC CAG GGG CCC CTG GGA TCC CCA GGA ATT CCC GGG TCG ACT CGA GCG GCC GCA TCG
BamH I EcoR I Sma I Sal I Xho I Not I

pGEX-6P-3 (27-4599-01)

PreScission™ Protease

Leu Glu Val Leu Phe Gln↓Gly Pro Leu Gly Ser Pro Asn Ser Arg Val Asp Ser Ser Gly Arg
CTG GAA GTT CTG TTC CAG GGG CCC CTG GGA TCC CCG AAT TCC CGG GTC GAC TCG AGC GGC CGC
BamH I EcoR I Sma I Sal I Xho I Not I

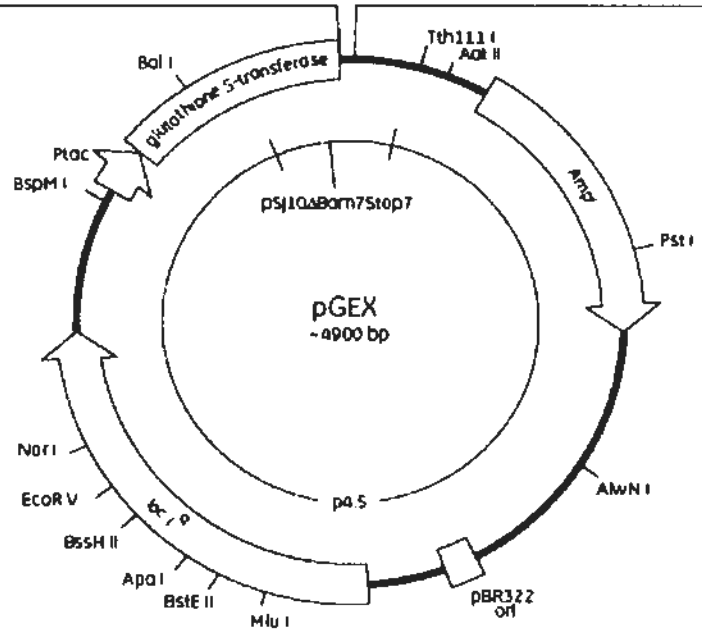

(b) pET-28-a vector

pET-28b(+) sequence landmarks	
T7 promoter	370-386
T7 transcription start	389
His•Tag coding sequence	270-287
T7•Tag coding sequence	207-239
Multiple cloning sites	
(*BamH* I - *Xho* I)	158-203
His•Tag coding sequence	140-157
T7 terminator	26-72
lacI coding sequence	773-1852
pBR322 origin	3286
Kan coding sequence	3995-4807
f1 origin	4903-5358

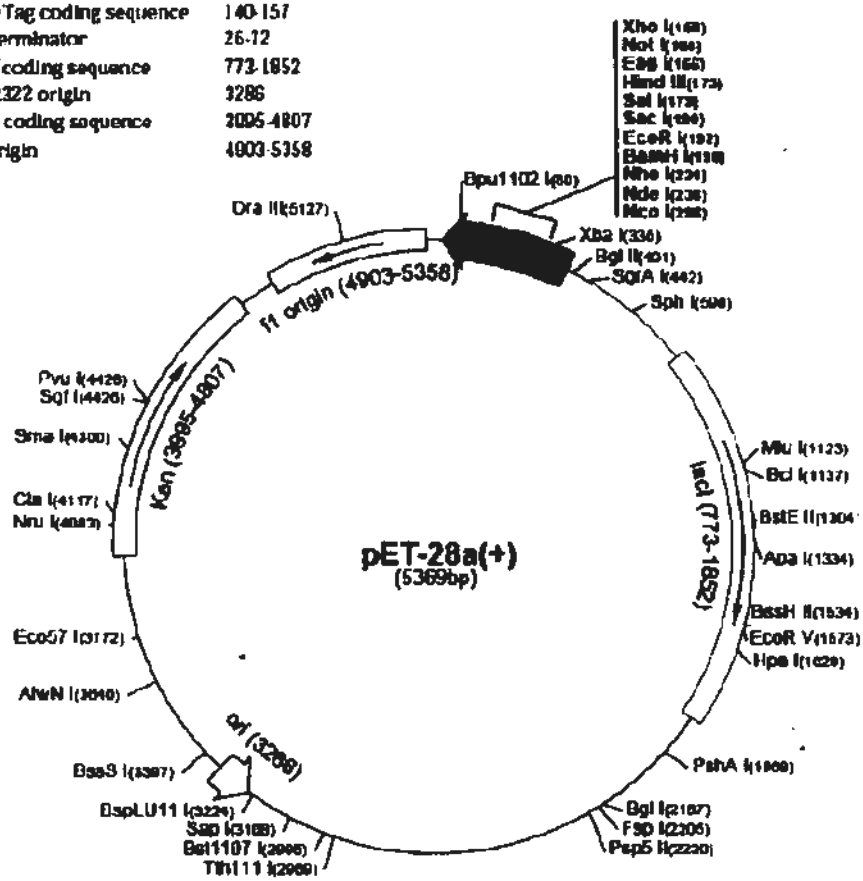

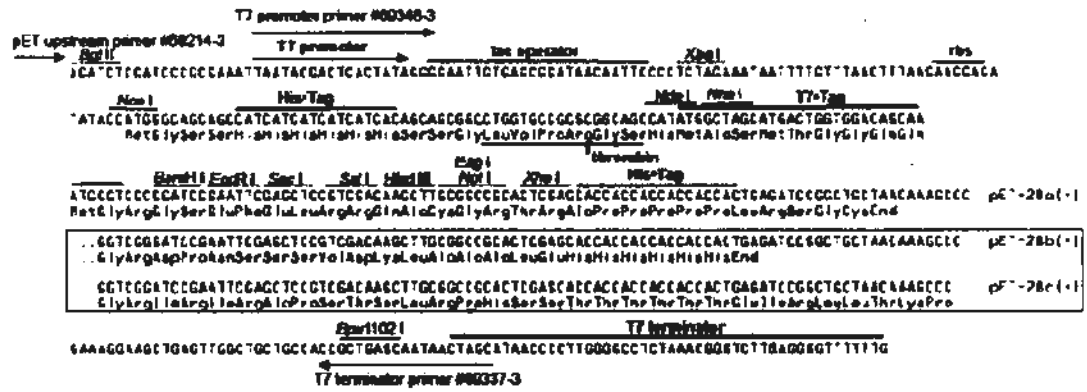

pET-28a-c(+) cloning/expression region

(c) pGEM-T-Easy vector

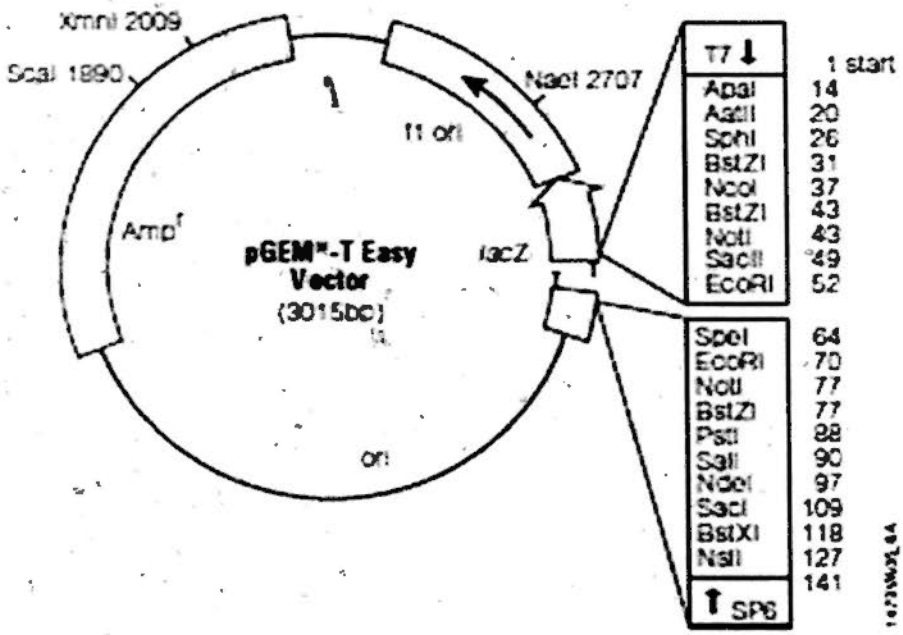

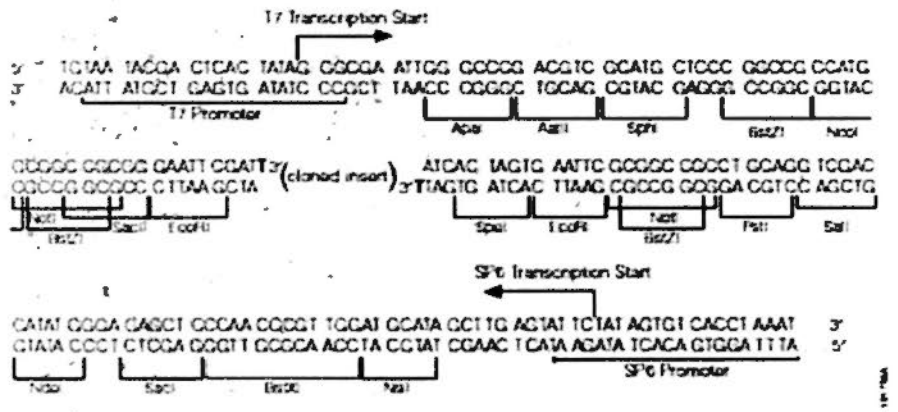

2. DNA sequences of studied proteins

fliS (hp0753) 1-378 bp

ATGCAATACGCTAACGCTTATCAAGCTTACCAGCATAACCGAGTGAGTGTGGASTRAINCCGGCAAAACTCA
TTGAAATGCTTTATGAAGGGATTTTGAGATTTTCTTCGCAAGCCAAACGCTGTATTGAAAATGAAGACAT
TGAAAAAAAGATTTATTATATTAATAGGGTTACGGATATTTTCACGGAATTGTTGAATATTTTAGATTAT
GAAAAAGGGGGGGAAGTGGCGGTGTATCTTACGGGCTTATACACCCATCAAATCAAAGTTTTAACGCAGG
CCAATGTGGAAAATGATGCGAGTAAGATTGATTTGGTGTTGAATGTGGCTAGAGGGTTATTAGAAGCATG
GAGGGAASTRAINATTCAGATGAACTCGCCTAA

hp1076 1-516 bp

ATGGATATTTTAAAAACTCTTCAAAAACATTTGGGCGATGTTGAAACAAGCGATTTTACAACCAATGCGA
TAGAAAASTRAINCAACAAATCGCTAAATTCAGTAGGGACATGAAAAATATAAACGAGAGCGTTGGAGCGTT
ACAAGTCTTGCAAATCGCTTGCAAAAAGCTTTTCAATAAGAGCATGGGTTTAGAAGATAAAGACGCTTTG
CAAGCTTCTATCATCAAACAGGAATTGCGAGAAATTGTAGAAAATTGCCAGTTTTTAGCCTCCCCTTTGT
TTGACACTCAGCTCAACATTGCAATCAATGATGAAATTTTTTCCATGATTGTGGTTASTRAINGTTGGATTT
ATTGGAAAATGTGGGCGAGTTTCAAGCTTATTTGGAAGAAAAATTAAACGAAATTAAGGAATTATTAGGT
TATTTGAGTGAAAGCCTTTCAAACCCTAAAGCCTTCATGCCAAGTTTTTCAAATCAAAGCCTTAAAGATT
TATTAAGCGATAATTTGAGGGCTTAG

flaAc (hp0601) 1255-1533 bp

GGTGCGATGGTGGTGATTGACATTGCCGAGTCTGCGATGAAAATGTTGGATAAAGTCCGATCTGATTT
AGGTTCTGTGCAAAATCAAATGATTAGCACCGTGAATAACATCAGCATCACTCAAGTGAATGTTAAAG
CGGCTGAATCTCAAATCAGGGATGTGGATTTTGCTGAAGAGAGCGCGAATTTCAATAAAAACAACATT
TTGGCACAATCAGGTAGCTATGCGATGAGTCAAGCCAACACCGTTCAACAAAATATCTTAAGGCTTTT
AACTTAG

*flaBc (hp0115)*1240-1545 bp

ATCTTGAGCGGCTTGAACGGCTTTGGTTTTAATGGTGTCTAAGATTTTGATTTGCTCSTRAINATCGC
TTTATCTGCGGTTTGAACCATACCAATAGCGTCATTGGCGTTGCGGATCGCTTGACCCAAATTCGCGC
TTTGACTCCTTAAGCTATCAGCGATCGCCSTRAINCACTAGAATCGTCAGCGGCTTTATTGSTRAINT
AAGCCCTGAGCTTAACTTTTCAAGCGAGCTTGAAAGGTCTCTGTTGTTTTGAACCCCTACCGCATGAG
AAGTTAAAGCGGCGATATTGGTATTTSTRAINTAAAACTCAT

fliI (hp1420) 1-1305 bp

TTATCTTAAGATTTCTTCTAATTGCTGAAAGCTTGTTTCAAAAGGCTGCAAAGCGTTTTCATCTTGCGCT
AAAAATTGCTCCATTAGAGCCTTTTTCTTAATCGCTTCATCAAGCTCTTTATCGTTCCCCATTTGATAAG
STRAINGATGCGAATGAGCATTTCATTTTCTTTCAATAACGCATACAAACGGCGGAATTTTCTCGCGCAAAG
GTTTTGAGACTCGCTGATGATGTCTTTAGCCACCCTTGATGCGGAGTTTAAAATATTAATAGGCGGGTAG
STRAINCATAATCGGTCAATTCCCTGCTTAAGACGATATGCCCGTCTAAAATACTCCTGGTCTGATCGGCTA
TGGGATCGCTCAAATCATCGCCCTCTACTAGCACGCTAAAAAAAGCCGTAATGCTCCCCTTATTTTCTTC
CTTACCCGCTCTCTCCATCAATTGAGGCAATAAGGAAAGCGCGGATGGGGGGTAGCCTTTGGAAGTGGGC
GGTTCGCCTAAGGCTAAGCCGATTTCTCTTTGAGCCATAGCGAAACGAGTCACTGASTRAINATGATAAACA
ACACGTCTAGCCCTTGGTTTTTAAAATACTCCGCCACGCTCATCGCGCAAAAGGCCCCGTATTTCCGCAT
CAAAGGGCTATCATCGCTCGTAGCGACCACCAACACGCAAGAGCTTAASTRAINCCTTTTAAGTTTTTCTCT
ATAAATTCAGGGATTTCTCTGCCCCTTTCCCCAATCAAAGCGATCACTTTAATAGGCGCTAAGCAACCCC
TAGTGATCATGCCCATTAGCGTGGATTTACCCACCCCAGAGCCGGCAAAAATGCCCAGTTTTTGCCCCTT
ACCGCAAGTCAAAAGCCCATCAATGCTCTTCACCCCCACGCTAAAAATCTCATCAATCAAGCCTCTTTTT
AAAGGGGCTATAGGCGTTGTAATGACAGGCGCTAATCGTTCATAATCTAGCGCCCCCTTATTGTCAATGA
CTTGCCCTAAAGGGTTAAGCACCCTCCCTAAAAGATTACGGCCCACAGGAAAATTCAACCCCTCTTTTAA
AAACAGCACCTTATCGCCAGCCCTAGCCCCCTCTATAAAGTTAAAGGGCGTAAAACCAAACTGCTCTTTT
TCTGCCACCACCACCATTCCCACGCATTCGCTGCCATCGCTTTTTTCAATCTTCACCACATCGCCCACAG
ACGGGTTAAAACCSTRAINGCATAAACGATATTGGGCATGATTTTTTTCACGCTCCCATAGCGAGGCGATAG
ATCAAAATGCTGATTCAAGCGGTTTTTTAAGGATTTTAGGGGCAT

flgK (hp1119) 1-1821 bp

TTATTGTTTASTRAINCCAATAAAGTGTCTATCSTRAINGATCAATAGCGGTAATGACTTTAGCGTTAGCCG
CATAGCCGCTTTGAAACTTGATCAAATTCACCATTTCTTCSTRAINACGCTCACTTGCGAAATAGAGAGTTG
CTCTTTTTTAATGGTTTCTAACATGCTCTTTTTAGTGTCCAAAATACGCCCGGATTTTTCAGCGTCCGTGTT
GATTTTACCGGTTAAAAATTGATAAAACTCGCTGATTTTCATTGGTTTAATGTCAAACTTATCGTTATAA
AASTRAINACGCTATCGTATTGCAATTGCTGCATCATGTTCGCCACATCAAAATTCCCATTAATGGGAGCAA
GCCATGGGCGGATAGTGGTAGGCTCTTTTTTGTATTCCTTATTCAAGCTGATATTAGAAGCGTCATCGCC
TTGAAAAAAAAGGGTTGAGTTTTAACGCTCCCATAAAATTCGTGCCGTTATCTTTCATAGAGACAAACAAC
CCTTGCGAAGCGTTTTTAGGCTGGATAACAAACTTTTTAGTCTCATTGTTAAAGCCCGCTGTGAAATAAT
CATCAAAATCGTTTTCGGTGTTATTGTCCTGATTGTCATCAGTGTTAGCGTTAATGGCTTGGATAATATC
GTTCATGGTTGTAATGGGCGTGATAGCAATGGTTTTTCTAGCGATTTCTTTACCATCGGTGTTGTAAGCG
ATTAAGTCAAACGAGCCGTTTTTGATATTGTAGTTAGTGTCTTTAAAGGCTTCATCGCTATTAAACTCCA
CCGGCTCGCCCTCAATATAATGACTCGCGCTTTGAGCGTAAATCGCATTAGTGGATTCTATCAAACCCTT
AGCAAAAGASTRAINAACAAATCAATATAATCTTGTAATTTGCCCTTTAAAGTCCCGTTAGAGCCGTCATTA
TACACATTCAATAACGCCCCCACTCTTCCCTGATTGAGCTTGTCAGTAATATTAGTAACCTTAAAATCAT
CGCTTTGAAAATAAACCTGGTTCAAACCCCCTTTATTTTCGGATTCTTTAACCACTAAAGGATGGAAAAT
AGAGCCATCAATGATATTGAACCCATGCCCGATATTAAGGTTATAGCTCTCATCAAASTRAINGCTGAGTCT
TTATCGGTGAGCGAATGAGTCTTAATGCTGCTTTTAAAAACATTCCCCCCTAAAAGCTCTCGCAAATGGA
ATTCCAATTCATCTCGCTTSTRAINCTTAATTCGTTCGCATGCTTTAAACTCTTGTTGTTTTCCACTTCTTT
AATGCGTTTGTTAATCTCAGCGATTTGAGAACCCAAGCTATTGACTTCTTTAATGACGCTTTTTAATTCT
TCACTCGCCTTGTGCTGTAAGGTCGTTAACCTCTCTCTGGTGTCTTTAATGTTGTGCGTTAAAGCTTCTG
TTTTTTGAGCGAGAGCCTGTTTTTGAGCGGAGTCTTTGGCGTTTTTAGACAATTCTTTCCATGAATTAAA
ATAATCTTGCAASTRAINGTAAAAAGGCTCGCTTCATCAATGTCCGGAAAATACGCGCTCGCTTCTTTTAAA
TGCGAAAATTCTGTATCGTAATAAGTGTTTTCGTAATTAGCTTTCGTGTAACGAGCAAAAACAAACTCAT
CATGCACCCTTTCAATGGCTTCCACSTRAINACGCCCATATTCACGTTTTTAGTGCCATACATATAGGCCGC
TTGGGGCTTTGCAATCACGCGCTGGCGGCTATAAAATTCATCGCTAGCGTTAGAAATATTATTCCCGGTA
ACSTRAINACCATGCTCTGATGGGCTTGAAGGCCGGTGTAAGAAGTGTTGAGTGAAGATAAGATTCCGCCCA
T

fliD (hp0752) 1-2025 bp

ATGGCAATAGGTTCATTAAGCTCATTAGGGCTTGGCAGTAAGGTTTTGAATTACGATGTGATTGACAAGC
TTAAGGACGCTGATGAAAAGGCGTTAATCGCCCCCTTAGACAAGAAAATGGAGCAAAATGTTGAAAAACA
AAAAGCCCTTGTAGAAATTAAAACGCTCCTTTCAGCTCTAAAAGGCCCGGTTAAAACGCTTTCAGATTAT
TCCACTTATATCAGCCGAAAAAGCAATGTTACAGGCGATGCGTTGAGTGCGAGCGTGGGGGTTGGCGTGC
CTATTCAAGATATTAAAGTGGATGTGCAAAATTTAGCGCAAGGCGATATTAACGAATTGGGGGCGAAATT
TTCTTCAAGAGACGATATTTTTAGCCAAGTGGATACCACGCTCAAGTTTTACACACAAAACAAAGACTAC
GCCGTTAATATTAAAGCAGGAATGACTTTAGGCGATGTGGCTCAAAGCATCACGGACGCTACCAATGGCG
AAGTGATGGGTATTGTGATGAAAACAGGAGGGAATGACCCCTACCAATTAATGGTGAATACCAAAAACAC
CGGCGAAGACAACCGAGTCTATTTTGGCTCACACCTCCASTRAINACGCTCACTAACAAAAACGCCCTTTCT
TTGGGGGTTGATGGGAGCGGAAAAAGTGAAGTGAGTTTGAATTTAAAGGGGGCTGATGGGAACATGCATG
AAGTCCCCATCATGCTAGAACTCCCTGAAAGCGCTTCTATCAAACAAAAAAACACCGCASTRAINAAAAAGC
GATGGAGCAGGCTTTAGAAAATGACCCTAATTTTAAAAATTTGATCGCTAATGGGGATATTTCCATAGAC
ACTCTTCATGGAGGGGAATCTTTAATCATTAATGACAGGCGTGGGGGAAACATTGAAGTTAAAGGGAGTA
AGGCTAAAGAGCTTGGGTTTTTACAAACCACCACCCAAGAAAGCGATTTATTAAAAAGCTCTCGCACGAT
AAAAGAGGGTAAATTAGAAGGGGTGGTCAGTTTGAATGGCCAAAAACTGGATTTGAGTGCTTTAACCAAA
GAGAGCAACACCAGTGAAGAAAACACAGACGCTATCATTCAAGCGATCAACGCTAAGGAAGGCTTGAGTG
CGTTCAAAAACGCCGAAGGCAAGCTTGTGATCAATTCTAAAACCGGAATGCTAACGATTAAGGGCGAGGA
CGCTTTAGGCAAGGCCAGTTTGAAAGATTTGGGTTTAAATGCTGGCATGGTGCAATCTTATGAAGCTTCA
CAAAACACGCTTTTTATGTCTAAAAATTTGCAAAAAGCGAGCGATTCAGCATTCACTTATAATGGGGTGA
GCATCACACGCCCCACTAATGAGGTCAATGATGTGATTAGTGGGGTTAATATCACTTTGGAGCAAACCAC
AGAGCCTAATAAACCTGCCATTATCAGCGTGAGTAGGGACAATCAAGCCATTATAGACAGCCTTACTGAA
TTTGTCAAAGCCTATAATGAGCTTSTRAINCTAAACTGGATGAAGACACTCGTTATGACGCTGACACTAAAA
TCGCTGGGATTTTTAACGGCGTGGGCGATATTCGCGCGATTCGATCTTCTCTTAATAATGTGTTTTCTTA
TAGCGTGCATACGGATAATGGGGTAGAAAGCTTGATGAAATACGGGCTTAGTTTAGACGATAAGGGCGTG
ATGAGTTTGGATGAGGCTAAATTGAGTAGTGCGCTAAATTCTAACCCTAAAGCGACTCAAGATTTTTTCT
ATGGGAGTGATAGTAAGGATATGGGGGGCAGAGAASTRAINACCAAGAGGGCATTTTTTCTAAATTCAATCA
AGTCATCGCTAATCTCATAGATGGAGGGAACGCTAAATTAAAGATTTATGAAGATTCCCTAGACAGAGAC
GCTAAAAGCCTGACTAAAGACAAAGAAAACGCTCAAGAGCTTTTAAAAACCCGCTACAACATTATGGCGG
ACGTTTTGCCGCTTATGATAGCCAAATCTCTAAAGCCAATCAAAAATTCAATTCCGTGCAAATGA

fliH (hp0353) 1-777 bp

ATGTCATTGAATAGCCGTAAGAACTTGATTCAAAAAGATCATTTGAATAAGCATGACATTCAAAAATACG
AATTTAAAAACATGGCAAACTTACCCCCTAAAACTASTRAINTAATAGCGCGTCTTTAGAAACGCCTAACCT
AGAAGAGCCTTTGGAAAAAAAAGCGATAGAAAACGATTTGATTGATTGCTTGTTGAAAAAAACCGATGAG
CTTTCAAGCCATTTAGTGAAATTGCAAATGCAGTTTGAAAAAGCCCAAGAAGAGAGTAAAGTTTTGATTG
AAAACGCTAAAAACGACGGCTATAAAATCGGCTTTAAAGAGGGCGAAGAAAAAATGCGTAACGAACTCAC
TCACAGCGTGAATGAAGAAAAAAACCAGCTTTTGCATGCGATCACCACTTTAGATGAAAAAATGAAAAAA
TCAGAAGATCATTTAATGGCTTTAGAAAAGGAATTGAGCGCGATTGCGATAGATATAGCTAAAGAAGTGA
TCCTTAAAGAAGTGGAAGACAACAGCCAAAAAGTAGCCCTTGCTTTGGCTGAAGAGCTTTTAAAAAACGT
TTTAGACGCAACGGATATTCATTTAAAAGTCASTRAINCTTGGATTACCCTTATTTAAACGAGCGTTTGCAA
AACGCTTCTAAAATCAAATTAGAGAGCAATGAGGCTATTTCTAAAGGAGGCGTTATGATCACTAGCTCTA
ATGGGAGCCTTGATGGGAATTTAATGGAGCGCTTTAAAACGCTCAAAGAAAGCGTGTTGGAAAATTTTAA
GGTGTGA

3. Primers used in this study

Primer for amplifying from genomic DNA (5' → 3')		Enzymatic site
FliS-F	TCCATTGGSTRAINATGCAATACGCTAACGCTTATCAAGC	*BamH*I
FliS-R	TCCATTGCCGCCGCTTAGGCGAGTTCATCTGAATGGATTT	*Not*I
FlaAc-F	TCCATTGGSTRAINAATTTAACCTTAAATGGGATTCATTTGG	*BamH*I
FlaAc-R	TCCATTGCGGCCGCCTAACTCAAACTTCCTGACTGGAC	*Not*I
FlaBc-F	TCCATTGGSTRAINATAGGGGCTGGGGTAACAAGCCT	*BamH*I
FlaBc-R	TCCATTGCGGCCGCTTATTGTAAAAGCCTTAAGACATT	*Not*I
FliD-F	TCCATTGGSTRAINATGGCAATAGGTTCATTAAGCTC	*BamH*I
FliD-R	TCCATTGCGGCCGCTCATTTGCACGGAATTGAATT	*Not*I
FlgK-F	TCCATTGGSTRAINATGGGCGGAATCTTATCTTC	*BamH*I
FlgK-R	TCCATTGCGGCCGCTTATTGTTTASTRAINCCAATAAAGTG	*Not*I
FliI-F	TCCATTGGSTRAINATGCCCCTAAASTRAINTTAAAA	*BamH*I
FliI-R	TCCATTGCGGCCGCTTATCTTAAGATTTCTTCTAATTGCTG	*Not*I
FliH-F	GGGGGGGGSTRAINATGTCATTGAATAGCCGTAAGAACTTGAT T	*BamH*I
FliH-R	GGGGGGGCGGCCGCTCACACCTTAAAATTTTCCAACACGCTT TC	*Not*I
Primers for truncations of HP1076		
HP1076-F	TCCATTCATATGGATATTTTAAAAACTCTTCAAAAACATTT	*Nde*I
HP1076-R	TCCATTGCGGCCGCCTAAGCCCTCAAATTATCGGT	*Not*I
ΔN20-F	TCCATTCATATGACCAATGCGATAGAAAASTRAINCAAC	*Nde*I
ΔN36-F	TCCATTCATATGATGAAAAATATAAACGAGAGCGTTGG	*Nde*I
ΔC39-R	TCCATTGCGGCCGCTTACAAATAACCTAATAATTCCTTAATTC G	*Not*I
Primers for amplifying KanR gene for HP1076 null mutant construction		
KanR-F	AACCATGATTGTGGTATATTGACAATACTGATAA	*Bst*X1
KanR-R	AACCATGATTGTGGGAGTATGGACAGTTGCGG	*Bst*X1

Mutagenesis Primers	
Mutation of residues on HP1076ΔN20 for interaction	
N41AQ48A-F	GAAAAATATAGCCGAGAGCGTTGGAGCGTTAGCAGTCTTGCAAA
N41AQ48A-R	TTTGCAAGACTGCTAACGCTCCAACGCTCTCGGCTATATTTTTC
F88A-F	GAAAATTGCCAGGCTTTAGCCTCCCCTT
F88A-R	AAGGGGAGGCTAAAGCCTGGCAATTTTC
F33AK38A-F	AATCGCTAAAGCCAGTAGGGACATGGCAAATATAAACG
F33AK38A-R	CGTTTATATTTGCCATGTCCCTACTGGCTTTAGCGATT
K38AN41A-F	AGTAGGGACATGGCAAATATAGCCGAGAGCGTTG
K38AN41A-R	CAACGCTCTCGGCTATATTTGCCATGTCCCTACT
N41A-F	ACATGAAAAATATAGCCGAGAGCGTTGGAGC
N41A-R	GCTCCAACGCTCTCGGCTATATTTTTCATGT
Q48A-F	GCGTTGGAGCGTTAGCAGTCTTGCAAATCG
Q48-R	CGATTTGCAAGACTGCTAACGCTCCAACGC
Mutations of residues of HP1076 in MtZ-R clinical isolate	
V112D-F	TTTTTTCCATGATTGTGGATASTRAINGTTGGATTTATTGG
V112D-R	CCAATAASTRAINAACGGATTSTRAINACAATCATGGAAAAAA
V121A-F	GATTTATTGGAAAATGCGGGCGAGTTTCAAGCTTATT
V121A-R	AATAAGCTTGAAACTCGCCCGCATTTTCCAATAAATC
Q159K-F	TCATGCCAAGTTTTTCAAATAAAAGCCTTAAAGATTTATTAAG
Q159K-R	CTTAATAAATCTTTAAGGCTTTTATTTGAAAAACTTGGCATGA

Primers for genetic analysis of WT and MtZ-R strains	
GFliS-F	GTCATCGCTA ATCTCATAGATGGAGG
GFliS-R	CCTTAAGGCTTAAAAGCGCATCTAAAT
GHP1076-F	CGCATGCAAAAACACCCAAGAACACAAGCCCCACACTAA
GHP1076-R	AAAGCCTGGAATTTACAGACTTGGGCTATTACTTGGTGG

4. Electrophoresis markers

1 kb DNA ladder (Invitrogen)

Structure of Fragments in 1-Kb Increments:

5'-GATCC——— G
G ——— CCTAG-5'
(996 bp)$_n$

Notes:
During 1% agarose gel electrophoresis with Tris-acetate (pH 7.5) as the running buffer, bromophenol blue migrates together with the 500 bp band.

The 1650 bp band is generated from pUC. The bands smaller than 1000 bp are derived from lambda DNA.

1 Kb Plus DNA Ladder
0.7 µg/lane
0.9% agarose gel
stained with ethidium bromide

Favorgen 100 bp DNA marker and Favorgen 250 bp DNA marker

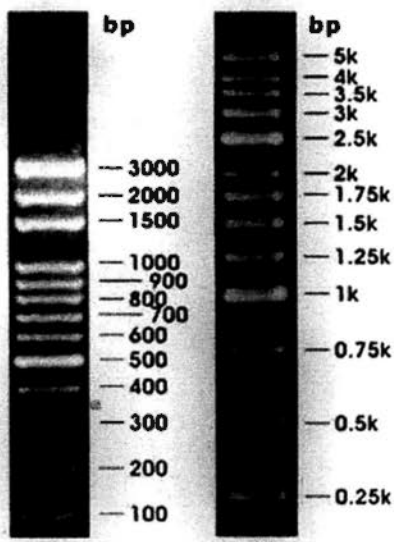

100bp DNA Ladder

1. 4% Agarose electrophoresis
2. 5ul per load
3. 500bp, 1.5Kbp, 2 Kbp, and 3Kbp are more intensive
4. Cat. No.: FALA100

250bp DNA Ladder Plus

1. 1% Agarose electrophoresis
2. 2.5ul per load
3. 1Kbp and 2.5Kbp are more intense than other bands
4. Cat. No.: FALA250

Invitrogen Seeblue® Plus 2 pre-stained protein standard

Protein	Approximate Molecular Weights (kDa)				
	Tris-Glycine	Tricine	NuPAGE® MES	NuPAGE® MOPS	NuPAGE® Tris-Acetate
Myosin	250	210	188	191	210
Phosphorylase	148	105	98	97	111
BSA	98	78	62	64	71
Glutamic Dehydrogenase	64	55	49	51	55
Alcohol Dehydrogenase	50	45	38	39	41
Carbonic Anhydrase	36	34	28	28	n/a
Myoglobin Red	22	17	17	19	n/a
Lysozyme	16	16	14	14	n/a
Aprotinin	6	7	6	n/a	n/a
Insulin, B Chain	4	4	3	n/a	n/a

NuPAGE® Novex
Bis-Tris 4-12% Gel

GE Healthcare LMW SDS Marker

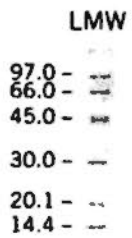

LMW: A 3-µl aliquot of a two-fold dilution of LMW Marker Kit was separated on a 15% T, 2.7% C polyacrylamide gel.

References

Abramoff, M. D., Magelhaes, P. J., and Ram, S. J. (2004). Image processing with ImageJ. *Biophotonics International, 11*(7), 36-42.

Adams, P. D., Grosse-Kunstleve, R. W., Hung, L. W., Ioerger, T. R., McCoy, A. J., Moriarty, N. W., Read, R. J., Sacchettini, J. C., Sauter, N. K., and Terwilliger, T. C. (2002). PHENIX: Building new software for automated crystallographic structure determination. *Acta Crystallographica.Section D, Biological Crystallography, 58*(Pt 11), 1948-1954.

Alamuri, P., and Maier, R. J. (2004). Methionine sulphoxide reductase is an important antioxidant enzyme in the gastric pathogen *Helicobacter pylori*. *Molecular Microbiology, 53*(5), 1397-1406.

Alarcon, T., Domingo, D., and Lopez-Brea, M. (1999). Antibiotic resistance problems with *Helicobacter pylori*. *International Journal of Antimicrobial Agents, 12*(1), 19-26.

Aldridge, P., and Hughes, K. T. (2002). Regulation of flagellar assembly. *Current Opinion in Microbiology, 5*(2), 160-165.

Aldridge, P., Karlinsey, J., and Hughes, K. T. (2003). The type III secretion chaperone FlgN regulates flagellar assembly via a negative feedback loop containing its chaperone substrates FlgK and FlgL. *Molecular Microbiology, 49*(5), 1333-1345.

Allan, E., Dorrell, N., Foynes, S., Anyim, M., and Wren, B. W. (2000). Mutational analysis of genes encoding the early flagellar components of *Helicobacter pylori*: Evidence for transcriptional regulation of flagellin A biosynthesis. *Journal of Bacteriology, 182*(18), 5274-5277.

Allan, E., Mullany, P., and Tabaqchali, S. (1998). Construction and characterization of a *Helicobacter pylori* clpB mutant and role of the gene in the stress response. *Journal of Bacteriology, 180*(2), 426-429.

Andersen-Nissen, E., Smith, K. D., Strobe, K. L., Barrett, S. L., Cookson, B. T., Logan, S. M., and Aderem, A. (2005). Evasion of toll-like receptor 5 by flagellated bacteria. *Proceedings of the National Academy of Sciences of the United States of America, 102*(26), 9247-9252.

Ando, T., Goto, Y., Maeda, O., Watanabe, O., Ishiguro, K., and Goto, H. (2006). Causal role of *Helicobacter pylori* infection in gastric cancer. *World Journal of Gastroenterology : WJG, 12*(2), 181-186.

Ang, S., Lee, C. Z., Peck, K., Sindici, M., Matrubutham, U., Gleeson, M. A., and Wang, J. T. (2001). Acid-induced gene expression in *Helicobacter pylori*: Study in genomic scale by microarray. *Infection and Immunity, 69*(3), 1679-1686.

Asahi, M., Azuma, T., Ito, S., Ito, Y., Suto, H., Nagai, Y., Tsubokawa, M., Tohyama, Y., Maeda, S., Omata, M., Suzuki, T., and Sasakawa, C. (2000). *Helicobacter pylori* CagA protein can be tyrosine phosphorylated in gastric epithelial cells. *The Journal of Experimental Medicine, 191*(4), 593-602.

Auvray, F., Ozin, A. J., Claret, L., and Hughes, C. (2002). Intrinsic membrane targeting of the flagellar export ATPase FliI: Interaction with acidic phospholipids and FliH. *Journal of Molecular Biology, 318*(4), 941-950.

Auvray, F., Thomas, J., Fraser, G. M., and Hughes, C. (2001). Flagellin polymerisation control by a cytosolic export chaperone. *Journal of Molecular Biology, 308*(2), 221-229.

Backert, S., Gressmann, H., Kwok, T., Zimny-Arndt, U., Konig, W., Jungblut, P. R., and Meyer, T. F. (2005). Gene expression and protein profiling of AGS gastric epithelial cells upon infection with *Helicobacter pylori*. *Proteomics, 5*(15), 3902-3918.

Bairoch, A., Bucher, P., and Hofmann, K. (1997). The PROSITE database, its status in 1997. *Nucleic Acids Research, 25*(1), 217-221.

Banatvala, N., Davies, G. R., Abdi, Y., Clements, L., Rampton, D. S., Hardie, J. M., and Feldman, R. A. (1994). High prevalence of *Helicobacter pylori* metronidazole resistance in migrants to east london: Relation with previous nitroimidazole exposure and gastroduodenal disease. *Gut, 35*(11), 1562-1566.

Bennett, J. C., and Hughes, C. (2000). From flagellum assembly to virulence: The extended family of type III export chaperones. *Trends in Microbiology, 8*(5), 202-204.

Bennett, J. C., Thomas, J., Fraser, G. M., and Hughes, C. (2001). Substrate complexes and domain organization of the *Salmonella* flagellar export chaperones FlgN and FliT. *Molecular Microbiology, 39*(3), 781-791.

Beswick, E. J., Pinchuk, I. V., Minch, K., Suarez, G., Sierra, J. C., Yamaoka, Y., and Reyes, V. E. (2006). The *Helicobacter pylori* urease B subunit binds to CD74 on gastric epithelial cells and induces NF-kappaB activation and interleukin-8 production. *Infection and Immunity, 74*(2), 1148-1155.

Bhattacharyya, S., Ge, Z., Krishnamurthy, P., Chambers, T. J., Phadnis, S. H., and Fox, J. G. (2001). *Helicobacter pylori* required fumarate reductase for acid resistance. *Gastroentology, 120*(Supp 1.1), A655.

Bjellqvist, B., Hughes, G. J., Pasquali, C., Paquet, N., Ravier, F., Sanchez, J. C., Frutiger, S., and Hochstrasser, D. (1993). The focusing positions of polypeptides in immobilized pH gradients can be predicted from their amino acid sequences. *Electrophoresis, 14*(10), 1023-1031.

Blaser, M. J., Perez-Perez, G. I., Kleanthous, H., Cover, T. L., Peek, R. M., Chyou, P. H., Stemmermann, G. N., and Nomura, A. (1995). Infection with *Helicobacter*

pylori strains possessing cagA is associated with an increased risk of developing adenocarcinoma of the stomach. *Cancer Research, 55*(10), 2111-2115.

Blow, D. (2003). Outline of crystallography for biologist. (2nd ed., pp. 1-228). New York: Oxford University Press.

Bradford, M. M. (1976). A rapid and sensitive method for the quantitation of microgram quantities of protein utilizing the principle of protein-dye binding. *Analytical Biochemistry, 72*, 248-254.

Brahmachary, P., Dashti, M. G., Olson, J. W., and Hoover, T. R. (2004). *Helicobacter pylori* FlgR is an enhancer-independent activator of sigma54-RNA polymerase holoenzyme. *Journal of Bacteriology, 186*(14), 4535-4542.

Brekke, O. H., Michaelsen, T. E., Sandin, R., and Sandlie, I. (1993). Activation of complement by an IgG molecule without a genetic hinge. *Nature, 363*(6430), 628-630.

Brunger, A. T., Adams, P. D., Clore, G. M., DeLano, W. L., Gros, P., Grosse-Kunstleve, R. W., Jiang, J. S., Kuszewski, J., Nilges, M., Pannu, N. S., Read, R. J., Rice, L. M., Simonson, T., and Warren, G. L. (1998). Crystallography and NMR system: A new software suite for macromolecular structure determination. *Acta Crystallographica.Section D, Biological Crystallography, 54*(Pt 5), 905-921.

Bumann, D., Aksu, S., Wendland, M., Janek, K., Zimny-Arndt, U., Sabarth, N., Meyer, T. F., and Jungblut, P. R. (2002). Proteome analysis of secreted proteins of the gastric pathogen *Helicobacter pylori*. *Infection and Immunity, 70*(7), 3396-3403.

Bury-Mone, S., Kaakoush, N. O., Asencio, C., Megraud, F., Thibonnier, M., De Reuse, H., and Mendz, G. L. (2006). Is *Helicobacter pylori* a true microaerophile? *Helicobacter, 11*(4), 296-303.

Bury-Mone, S., Thiberge, J. M., Contreras, M., Maitournam, A., Labigne, A., and De Reuse, H. (2004). Responsiveness to acidity via metal ion regulators mediates virulence in the gastric pathogen *Helicobacter pylori*. *Molecular Microbiology, 53*(2), 623-638.

Caldas, T., Laalami, S., and Richarme, G. (2000). Chaperone properties of bacterial elongation factor EF-G and initiation factor IF2. *The Journal of Biological Chemistry, 275*(2), 855-860.

Celli, J. P., Turner, B. S., Afdhal, N. H., Keates, S., Ghiran, I., Kelly, C. P., Ewoldt, R. H., McKinley, G. H., So, P., Erramilli, S., and Bansil, R. (2009). *Helicobacter pylori* moves through mucus by reducing mucin viscoelasticity. *Proceedings of the National Academy of Sciences of the United States of America, 106*(34), 14321-14326.

Censini, S., Lange, C., Xiang, Z., Crabtree, J. E., Ghiara, P., Borodovsky, M., Rappuoli, R., and Covacci, A. (1996). Cag, a pathogenicity island of *Helicobacter pylori*, encodes type I-specific and disease-associated virulence factors. *Proceedings of the National Academy of Sciences of the United States of America, 93*(25), 14648-14653.

Chadsey, M. S., and Hughes, K. T. (2001). A multipartite interaction between *Salmonella* transcription factor sigma28 and its anti-sigma factor FlgM: Implications for sigma28 holoenzyme destabilization through stepwise binding. *Journal of Molecular Biology, 306*(5), 915-929.

Chang, C. S., Chen, L. T., Yang, J. C., Lin, J. T., Chang, K. C., and Wang, J. T. (1999). Isolation of a *Helicobacter pylori* protein, FldA, associated with mucosa-associated lymphoid tissue lymphoma of the stomach. *Gastroenterology, 117*(1), 82-88.

Chaves, S., Gadanho, M., Tenreiro, R., and Cabrita, J. (1999). Assessment of metronidazole susceptibility in *Helicobacter pylori*: Statistical validation and error rate analysis of breakpoints determined by the disk diffusion test. *Journal of Clinical Microbiology, 37*(5), 1628-1631.

Chen, L., and Helmann, J. D. (1994). The *bacillus subtilis* sigma D-dependent operon encoding the flagellar proteins FliD, FliS, and FliT. *Journal of Bacteriology, 176*(11), 3093-3101.

Ching, C. K., Leung, K. P., Yung, R. W., Lam, S. K., Wong, B. C., Lai, K. C., and Lai, C. L. (1996). Prevalence of metronidazole resistant *Helicobacter pylori* strains among chinese peptic ulcer disease patients and normal controls in hong kong. *Gut, 38*(5), 675-678.

Chuang, M. H., Wu, M. S., Lo, W. L., Lin, J. T., Wong, C. H., and Chiou, S. H. (2006). The antioxidant protein alkylhydroperoxide reductase of *Helicobacter pylori* switches from a peroxide reductase to a molecular chaperone function. *Proceedings of the National Academy of Sciences of the United States of America, 103*(8), 2552-2557.

Chuawong, P., and Hendrickson, T. L. (2006). The nondiscriminating aspartyl-tRNA synthetase from *Helicobacter pylori*: Anticodon-binding domain mutations that impact tRNA specificity and heterologous toxicity. *Biochemistry, 45*(26), 8079-8087.

CCP4 (1994). The CCP4 suite: Programs for protein crystallography. *Acta Crystallographica.Section D, Biological Crystallography, 50*(Pt 5), 760-763.

Cremades, N., Bueno, M., Neira, J. L., Velazquez-Campoy, A., and Sancho, J. (2008). Conformational stability of *Helicobacter pylori* flavodoxin: Fit to function at pH 5. *The Journal of Biological Chemistry, 283*(5), 2883-2895.

Crew, K. D., and Neugut, A. I. (2006). Epidemiology of gastric cancer. *World Journal of Gastroenterology : WJG, 12*(3), 354-362.

Cun, S., Li, H., Ge, R., Lin, M. C., and Sun, H. (2008). A histidine-rich and cysteine-rich metal-binding domain at the C terminus of heat shock protein A from *Helicobacter pylori*: Implication for nickel homeostasis and bismuth susceptibility. *The Journal of Biological Chemistry, 283*(22), 15142-15151.

Cussac, V., Ferrero, R. L., and Labigne, A. (1992). Expression of *Helicobacter pylori* urease genes in escherichia coli grown under nitrogen-limiting conditions. *Journal of Bacteriology, 174*(8), 2466-2473.

DeCross, A. J., Marshall, B. J., McCallum, R. W., Hoffman, S. R., Barrett, L. J., and Guerrant, R. L. (1993). Metronidazole susceptibility testing for *Helicobacter pylori*: Comparison of disk, broth, and agar dilution methods and their clinical relevance. *Journal of Clinical Microbiology, 31*(8), 1971-1974.

Dekker, J., Aelmans, P. H., and Strous, G. J. (1991). The oligomeric structure of rat and human gastric mucins. *The Biochemical Journal, 277 (Pt 2)*(Pt 2), 423-427.

D'Elios, M. M., Amedei, A., Benagiano, M., Azzurri, A., and Del Prete, G. (2005). *Helicobacter pylori*, T cells and cytokines: The "dangerous liaisons". *FEMS Immunology and Medical Microbiology, 44*(2), 113-119.

Dong, L., Cheng, N., Wang, M. W., Zhang, J., Shu, C., and Zhu, D. X. (2005). The leucyl aminopeptidase from *Helicobacter pylori* is an allosteric enzyme. *Microbiology (Reading, England), 151*(Pt 6), 2017-2023.

Douillard, F. P., Ryan, K. A., Hinds, J., and O'Toole, P. W. (2009). Effect of FliK mutation on the transcriptional activity of the {sigma}54 sigma factor RpoN in *Helicobacter pylori*. *Microbiology (Reading, England), 155*(Pt 6), 1901-1911.

Douillard, F. P., Ryan, K. A., Lane, M. C., Caly, D. L., Moore, S. A., Penn, C. W., Hinds, J., and O'Toole, P. W. (2010). The HP0256 gene product is involved in motility and cell envelope architecture of *Helicobacter pylori*. *BMC Microbiology, 10*, 106.

Doyle, S. M., Hoskins, J. R., and Wickner, S. (2007). Collaboration between the ClpB AAA+ remodeling protein and the DnaK chaperone system. *Proceedings of the National Academy of Sciences of the United States of America, 104*(27), 11138-11144.

Duong, F., Eichler, J., Price, A., Leonard, M. R., and Wickner, W. (1997a). Biogenesis of the gram-negative bacterial envelope. *Cell, 91*(5), 567-573.

Duong, F., and Wickner, W. (1997b). The SecDFyajC domain of preprotein translocase controls preprotein movement by regulating SecA membrane cycling. *The EMBO Journal, 16*(16), 4871-4879.

Eaton, K. A., Brooks, C. L., Morgan, D. R., and Krakowka, S. (1991). Essential role of urease in pathogenesis of gastritis induced by *Helicobacter pylori* in gnotobiotic piglets. *Infection and Immunity, 59*(7), 2470-2475.

Eaton, K. A., Morgan, D. R., and Krakowka, S. (1992). Motility as a factor in the colonisation of gnotobiotic piglets by *Helicobacter pylori*. *Journal of Medical Microbiology, 37*(2), 123-127.

Edwards, D. I. (1993). Nitroimidazole drugs--action and resistance mechanisms. I. mechanisms of action. *The Journal of Antimicrobial Chemotherapy, 31*(1), 9-20.

Eichler, J., Rinard, K., and Wickner, W. (1998). Endogenous SecA catalyzes preprotein translocation at SecYEG. *The Journal of Biological Chemistry, 273*(34), 21675-21681.

El-Omar, E. M., Carrington, M., Chow, W. H., McColl, K. E., Bream, J. H., Young, H. A., Herrera, J., Lissowska, J., Yuan, C. C., Rothman, N., Lanyon, G., Martin, M., Fraumeni, J. F.,Jr, and Rabkin, C. S. (2000). Interleukin-1 polymorphisms associated with increased risk of gastric cancer. *Nature, 404*(6776), 398-402.

El-Omar, E. M., Rabkin, C. S., Gammon, M. D., Vaughan, T. L., Risch, H. A., Schoenberg, J. B., Stanford, J. L., Mayne, S. T., Goedert, J., Blot, W. J., Fraumeni, J. F.,Jr, and Chow, W. H. (2003). Increased risk of noncardia gastric cancer associated with proinflammatory cytokine gene polymorphisms. *Gastroenterology, 124*(5), 1193-1201.

Emsley, P., and Cowtan, K. (2004). Coot: Model-building tools for molecular graphics. *Acta Crystallographica.Section D, Biological Crystallography, 60*(Pt 12 Pt 1), 2126-2132.

Evans, L. D., Stafford, G. P., Ahmed, S., Fraser, G. M., and Hughes, C. (2006). An escort mechanism for cycling of export chaperones during flagellum assembly. *Proceedings of the National Academy of Sciences of the United States of America, 103*(46), 17474-17479.

Evdokimov, A. G., Phan, J., Tropea, J. E., Routzahn, K. M., Peters, H. K., Pokross, M., and Waugh, D. S. (2003). Similar modes of polypeptide recognition by export chaperones in flagellar biosynthesis and type III secretion. *Nature Structural Biology, 10*(10), 789-793.

Fan, X., Gunasena, H., Cheng, Z., Espejo, R., Crowe, S. E., Ernst, P. B., and Reyes, V. E. (2000). *Helicobacter pylori* urease binds to class II MHC on gastric epithelial cells and induces their apoptosis. *Journal of Immunology (Baltimore, Md.: 1950), 165*(4), 1918-1924.

Fassbinder, F., van Vliet, A. H., Gimmel, V., Kusters, J. G., Kist, M., and Bereswill, S. (2000). Identification of iron-regulated genes of *Helicobacter pylori* by a modified fur titration assay (FURTA-hp). *FEMS Microbiology Letters, 184*(2), 225-229.

Figura, N., Guglielmetti, P., Rossolini, A., Barberi, A., Cusi, G., Musmanno, R. A., Russi, M., and Quaranta, S. (1989). Cytotoxin production by *campylobacter pylori* strains isolated from patients with peptic ulcers and from patients with chronic gastritis only. *Journal of Clinical Microbiology, 27*(1), 225-226.

Fox, E. M., Raftery, M., Goodchild, A., and Mendz, G. L. (2007). *Campylobacter jejuni*response to ox-bile stress. *FEMS Immunology and Medical Microbiology, 49*(1), 165-172.

Fox, J. G., Correa, P., Taylor, N. S., Lee, A., Otto, G., Murphy, J. C., and Rose, R. (1990). *Helicobacter mustelae*-associated gastritis in ferrets. an animal model of *Helicobacter pylori* gastritis in humans. *Gastroenterology, 99*(2), 352-361.

Foynes, S., Dorrell, N., Ward, S. J., Stabler, R. A., McColm, A. A., Rycroft, A. N., and Wren, B. W. (2000). *Helicobacter pylori* possesses two CheY response regulators and a histidine kinase sensor, CheA, which are essential for chemotaxis and colonization of the gastric mucosa. *Infection and Immunity, 68*(4), 2016-2023.

Fraser, G. M., Bennett, J. C., and Hughes, C. (1999). Substrate-specific binding of hook-associated proteins by FlgN and FliT, putative chaperones for flagellum assembly. *Molecular Microbiology, 32*(3), 569-580.

Fraser, G. M., Gonzalez-Pedrajo, B., Tame, J. R., and Macnab, R. M. (2003). Interactions of FliJ with the *Salmonella* type III flagellar export apparatus. *Journal of Bacteriology, 185*(18), 5546-5554.

Futai, M., and Kanazawa, H. (1983). Structure and function of proton-translocating adenosine triphosphatase (F0F1): Biochemical and molecular biological approaches. *Microbiological Reviews, 47*(3), 285-312.

Galkin, V. E., Yu, X., Bielnicki, J., Heuser, J., Ewing, C. P., Guerry, P., and Egelman, E. H. (2008). Divergence of quaternary structures among bacterial flagellar filaments. *Science (New York, N.Y.), 320*(5874), 382-385.

Gasteiger, E., Hoogland, C., Gattiker, A., Duvaud, S., Wilkins, M. R., Appel, R. D., and Bairoch, A. (2005). Protein identification and analysis tools on the ExPASy server. In J. M. Walker (Ed.), *The proteomics protocols handbook* (pp. 571-607) Humana Press.

Ge, Z., and Taylor, D. E. (1997). *Helicobacter pylori* DNA transformation by natural competence and electroporation. In C. L. Clayton, and H. L. Mobley (Eds.), *Helicobacter pylori protocols* (pp. 145-152). Totowa, N.J.: Humana Press.

Ge, Z. (2002). Potential of fumarate reductase as a novel therapeutic target in *Helicobacter pylori* infection. *Expert Opinion on Therapeutic Targets, 6*(2), 135-146.

Ge, Z., Feng, Y., Dangler, C. A., Xu, S., Taylor, N. S., and Fox, J. G. (2000). Fumarate reductase is essential for *Helicobacter pylori* colonization of the mouse stomach. *Microbial Pathogenesis, 29*(5), 279-287.

Geis, G., Suerbaum, S., Forsthoff, B., Leying, H., and Opferkuch, W. (1993). Ultrastructure and biochemical studies of the flagellar sheath of *Helicobacter pylori*. *Journal of Medical Microbiology, 38*(5), 371-377.

Godlewska, R., Dzwonek, A., Mikula, M., Ostrowski, J., Pawlowski, M., Bujnicki, J. M., and Jagusztyn-Krynicka, E. K. (2006). *Helicobacter pylori* protein oxidation influences the colonization process. *International Journal of Medical Microbiology : IJMM, 296*(4-5), 321-324.

Grunberg-Manago, M. (1996). Regulation of the expression of aminoacyl-tRNA synthetases and translation factors. In F. C. Neidhardt (Ed.), *Escherichia coli and Salmonella: Cellular and molecular biology* (2nd ed., pp. 1432-1457). Washington, D.C: ASM Pres.

Guo, Y., Guo, G., Mao, X., Zhang, W., Xiao, J., Tong, W., Liu, T., Xiao, B., Liu, X., Feng, Y., and Zou, Q. (2008). Functional identification of HugZ, a heme oxygenase from *Helicobacter pylori*. *BMC Microbiology, 8*, 226.

Gwack, J., Shin, A., Kim, C. S., Ko, K. P., Kim, Y., Jun, J. K., Bae, J., Park, S. K., Hong, Y. C., Kang, D., Chang, S. H., Shin, H. R., and Yoo, K. Y. (2006). CagA-producing *Helicobacter pylori* and increased risk of gastric cancer: A nested case-control study in korea. *British Journal of Cancer, 95*(5), 639-641.

Haas, G., Karaali, G., Ebermayer, K., Metzger, W. G., Lamer, S., Zimny-Arndt, U., Diescher, S., Goebel, U. B., Vogt, K., Roznowski, A. B., Wiedenmann, B. J., Meyer, T. F., Aebischer, T., and Jungblut, P. R. (2002). Immunoproteomics of *Helicobacter pylori* infection and relation to gastric disease. *Proteomics, 2*(3), 313-324.

Harris, P. R., Mobley, H. L., Perez-Perez, G. I., Blaser, M. J., and Smith, P. D. (1996). *Helicobacter pylori* urease is a potent stimulus of mononuclear phagocyte activation and inflammatory cytokine production. *Gastroenterology, 111*(2), 419-425.

Haslbeck, M., Walke, S., Stromer, T., Ehrnsperger, M., White, H. E., Chen, S., Saibil, H. R., and Buchner, J. (1999). Hsp26: A temperature-regulated chaperone. *The EMBO Journal, 18*(23), 6744-6751.

Helicobacter and Cancer Collaborative Group. (2001). Gastric cancer and *Helicobacter pylori*: A combined analysis of 12 case control studies nested within prospective cohort. *Gut, 49*, 347-353.

Hoffman, P. S., Goodwin, A., Johnsen, J., Magee, K., and Veldhuyzen van Zanten, S. J. (1996). Metabolic activities of metronidazole-sensitive and -resistant strains of *Helicobacter pylori*: Repression of pyruvate oxidoreductase and expression of isocitrate lyase activity correlate with resistance. *Journal of Bacteriology, 178*(16), 4822-4829.

Holm, L., and Park, J. (2000). DaliLite workbench for protein structure comparison. *Bioinformatics (Oxford, England), 16*(6), 566-567.

Holm, L., and Sander, C. (1996). Alignment of three-dimensional protein structures: Network server for database searching. *Methods in Enzymology, 266*, 653-662.

Hong, W., Sano, K., Morimatsu, S., Scott, D. R., Weeks, D. L., Sachs, G., Goto, T., Mohan, S., Harada, F., Nakajima, N., and Nakano, T. (2003). Medium pH-dependent redistribution of the urease of *Helicobacter pylori*. *Journal of Medical Microbiology, 52*(Pt 3), 211-216.

Hoshi, T., and Heinemann, S. (2001). Regulation of cell function by methionine oxidation and reduction. *The Journal of Physiology, 531*(Pt 1), 1-11.

Hughes, N. J., Chalk, P. A., Clayton, C. L., and Kelly, D. J. (1995). Identification of carboxylation enzymes and characterization of a novel four-subunit pyruvate:Flavodoxin oxidoreductase from *Helicobacter pylori*. *Journal of Bacteriology, 177*(14), 3953-3959.

Hughes, N. J., Clayton, C. L., Chalk, P. A., and Kelly, D. J. (1998). *Helicobacter pylori* porCDAB and oorDABC genes encode distinct pyruvate:Flavodoxin and 2-oxoglutarate:Acceptor oxidoreductases which mediate electron transport to NADP. *Journal of Bacteriology, 180*(5), 1119-1128.

Ibba, M., and Soll, D. (2000). Aminoacyl-tRNA synthesis. *Annual Review of Biochemistry, 69*, 617-650.

Ibuki, T., Shimada, M., Minamino, T., Namba, K., and Imada, K. (2009). Crystallization and preliminary X-ray analysis of FliJ, a cytoplasmic component of the flagellar type III protein-export apparatus from *Salmonella* sp. *Acta Crystallographica.Section F, Structural Biology and Crystallization Communications, 65*(Pt 1), 47-50.

Ikeda, T., Homma, M., Iino, T., Asakura, S., and Kamiya, R. (1987). Localization and stoichiometry of hook-associated proteins within *Salmonella typhimurium* flagella. *Journal of Bacteriology, 169*(3), 1168-1173.

Imada, K., Minamino, T., Kinoshita, M., Furukawa, Y., and Namba, K. (2010). Structural insight into the regulatory mechanisms of interactions of the flagellar type III chaperone FliT with its binding partners. *Proceedings of the National Academy of Sciences of the United States of America, 107*(19), 8812-8817.

Ireton, G. C., and Stoddard, B. L. (2004). Microseed matrix screening to improve crystals of yeast cytosine deaminase. *Acta Crystallographica.Section D, Biological Crystallography, 60*(Pt 3), 601-605.

Iwamoto, H., Czajkowsky, D. M., Cover, T. L., Szabo, G., and Shao, Z. (1999). VacA from *Helicobacter pylori*: A hexameric chloride channel. *FEBS Letters, 450*(1-2), 101-104.

Jaiswal, M., LaRusso, N. F., and Gores, G. J. (2001). Nitric oxide in gastrointestinal epithelial cell carcinogenesis: Linking inflammation to oncogenesis. *American Journal of Physiology.Gastrointestinal and Liver Physiology, 281*(3), G626-34.

Johensans, C., Labigne, A., and Suerbaum, S. (1995). Reporter gene analyses show that expression of both *H. pylori* flagellins is dependent on the growth phase. *Gut, 41*, A246.

Jordan, P. A., Tang, Y., Bradbury, A. J., Thomson, A. J., and Guest, J. R. (1999). Biochemical and spectroscopic characterization of *Escherichia coli* aconitases (AcnA and AcnB). *The Biochemical Journal, 344 Pt 3*, 739-746.

Jorgensen, M. A., Manos, J., Mendz, G. L., and Hazell, S. L. (1998). The mode of action of metronidazole in *Helicobacter pylori*: Futile cycling or reduction? *The Journal of Antimicrobial Chemotherapy, 41*(1), 67-75.

Josenhans, C., Labigne, A., and Suerbaum, S. (1995). Comparative ultrastructural and functional studies of *Helicobacter pylori* and *Helicobacter mustelae* flagellin mutants: Both flagellin subunits, FlaA and FlaB, are necessary for full motility in helicobacter species. *Journal of Bacteriology, 177*(11), 3010-3020.

Jungblut, P. R., Bumann, D., Haas, G., Zimny-Arndt, U., Holland, P., Lamer, S., Siejak, F., Aebischer, A., and Meyer, T. F. (2000). Comparative proteome analysis of *Helicobacter pylori*. *Molecular Microbiology, 36*(3), 710-725.

Kaakoush, N. O., Asencio, C., Megraud, F., and Mendz, G. L. (2009). A redox basis for metronidazole resistance in *Helicobacter pylori*. *Antimicrobial Agents and Chemotherapy, 53*(5), 1884-1891.

Kaakoush, N. O., Kovach, Z., and Mendz, G. L. (2007). Potential role of thiol:Disulfide oxidoreductases in the pathogenesis of *Helicobacter pylori*. *FEMS Immunology and Medical Microbiology, 50*(2), 177-183.

Kansau, I., Guillain, F., Thiberge, J. M., and Labigne, A. (1996). Nickel binding and immunological properties of the C-terminal domain of the *Helicobacter pylori* GroES homologue (HspA). *Molecular Microbiology, 22*(5), 1013-1023.

Karita, M., and Blaser, M. J. (1998). Acid-tolerance response in *Helicobacter pylori* and differences between cagA+ and cagA- strains. *The Journal of Infectious Diseases, 178*(1), 213-219.

Karita, M., Tummuru, M. K., Wirth, H. P., and Blaser, M. J. (1996). Effect of growth phase and acid shock on *Helicobacter pylori* cagA expression. *Infection and Immunity, 64*(11), 4501-4507.

Karlinsey, J. E., Lonner, J., Brown, K. L., and Hughes, K. T. (2000b). Translation/secretion coupling by type III secretion systems. *Cell, 102*(4), 487-497.

Karlinsey, J. E., Tanaka, S., Bettenworth, V., Yamaguchi, S., Boos, W., Aizawa, S. I., and Hughes, K. T. (2000a). Completion of the hook-basal body complex of the *Salmonella typhimurium* flagellum is coupled to FlgM secretion and fliC transcription. *Molecular Microbiology, 37*(5), 1220-1231.

Kavermann, H., Burns, B. P., Angermuller, K., Odenbreit, S., Fischer, W., Melchers, K., and Haas, R. (2003). Identification and characterization of *Helicobacter pylori* genes essential for gastric colonization. *The Journal of Experimental Medicine, 197*(7), 813-822.

Kawagishi, I., Muller, V., Williams, A. W., Irikura, V. M., and Macnab, R. M. (1992). Subdivision of flagellar region III of the escherichia coli and *Salmonella typhimurium* chromosomes and identification of two additional flagellar genes. *Journal of General Microbiology, 138*(6), 1051-1065.

Kholod, N., and Mustelin, T. (2001). Novel vectors for co-expression of two proteins in *E. coli*. *BioTechniques, 31*(2), 322-3, 326-8.

Kim, J. S., Chang, J. H., Chung, S. I., and Yum, J. S. (1999). Molecular cloning and characterization of the *Helicobacter pylori* fliD gene, an essential factor in flagellar structure and motility. *Journal of Bacteriology, 181*(22), 6969-6976.

Koga, T., Shimada, Y., Sato, K., Takahashi, K., Kikuchi, I., Okazaki, Y., Miura, T., Katsuta, M., and Iwata, M. (2002). Contribution of ferrous iron to maintenance of the gastric colonization of *Helicobacter pylori* in miniature pigs. *Microbiological Research, 157*(4), 323-330.

Kostrzynska, M., Betts, J. D., Austin, J. W., and Trust, T. J. (1991). Identification, characterization, and spatial localization of two flagellin species in *Helicobacter pylori* flagella. *Journal of Bacteriology, 173*(3), 937-946.

Kutsukake, K., Ikebe, T., and Yamamoto, S. (1999). Two novel regulatory genes, fliT and fliZ, in the flagellar regulon of *Salmonella*. *Genes and Genetic Systems, 74*(6), 287-292.

Labigne, A., and de Reuse, H. (1996). Determinants of *Helicobacter pylori* pathogenicity. *Infectious Agents and Disease, 5*(4), 191-202.

Lane, M. C., O'Toole, P. W., and Moore, S. A. (2006). Molecular basis of the interaction between the flagellar export proteins FliI and FliH from *Helicobacter pylori*. *The Journal of Biological Chemistry, 281*(1), 508-517.

Langer, G., Cohen, S. X., Lamzin, V. S., and Perrakis, A. (2008). Automated macromolecular model building for X-ray crystallography using ARP/wARP version 7. *Nature Protocols, 3*(7), 1171-1179.

Laskowski, R. A., MacArthur, M. W., Moss D.S., and Thornton, J. M. (1993). *PROCHECK*: A program to check the stereochemical quality of protein structures. *J. Appl. Cryst, 26*, 283-291.

Lazdunski, A. M. (1989). Peptidases and proteases of escherichia coli and *Salmonella typhimurium*. *FEMS Microbiology Reviews, 5*(3), 265-276.

Leslie, A. G. W. (1992). Recent changes to the MOSFLM package for processing film and image plate data. *Joint CCP4 + ESF-EAMCB Newsletter on Protein Crystallography, 26*

Lin, Y. F., Wu, M. S., Chang, C. C., Lin, S. W., Lin, J. T., Sun, Y. J., Chen, D. S., and Chow, L. P. (2006). Comparative immunoproteomics of identification and characterization of virulence factors from *Helicobacter pylori* related to gastric cancer. *Molecular and Cellular Proteomics : MCP, 5*(8), 1484-1496.

Liu, R., and Ochman, H. (2007). Stepwise formation of the bacterial flagellar system. *Proceedings of the National Academy of Sciences of the United States of America, 104*(17), 7116-7121.

Logan, S. M., and Trust, T. J. (1983). Molecular identification of surface protein antigens of *Campylobacter jejuni*. *Infection and Immunity, 42*(2), 675-682.

Loughlin, M. F., Arandhara, V., Okolie, C., Aldsworth, T. G., and Jenks, P. J. (2009). *Helicobacter pylori* mutants defective in the clpP ATP-dependant protease and the chaperone clpA display reduced macrophage and murine survival. *Microbial Pathogenesis, 46*(1), 53-57.

Machado, J. C., Pharoah, P., Sousa, S., Carvalho, R., Oliveira, C., Figueiredo, C., Amorim, A., Seruca, R., Caldas, C., Carneiro, F., and Sobrinho-Simoes, M. (2001). Interleukin 1B and interleukin 1RN polymorphisms are associated with increased risk of gastric carcinoma. *Gastroenterology, 121*(4), 823-829.

Mackinnon, L. T., and Hooper, S. (1994). Mucosal (secretory) immune system responses to exercise of varying intensity and during overtraining. *International Journal of Sports Medicine, 15 Suppl 3*, S179-83.

Macnab, R. M. (2003). How bacteria assemble flagella. *Annual Review of Microbiology, 57*, 77-100.

Marais, A., Mendz, G. L., Hazell, S. L., and Megraud, F. (1999). Metabolism and genetics of *Helicobacter pylori*: The genome era. *Microbiology and Molecular Biology Reviews: MMBR, 63*(3), 642-674.

Marshall, B. J., and Warren, J. R. (1984). Unidentified curved bacilli in the stomach of patients with gastritis and peptic ulceration. *Lancet, 1*(8390), 1311-1315.

Matysiak-Budnik, T., Karkkainen, P., Methuen, T., Roine, R. P., and Salaspuro, M. (1995). Inhibition of gastric cell proliferation by acetaldehyde. *The Journal of Pathology, 177*(3), 317-322.

McCoy, A. J., Grosse-Kunstleve, R. W., Storoni, L. C., and Read, R. J. (2005). Likelihood-enhanced fast translation functions. *Acta Crystallographica.Section D, Biological Crystallography, 61*(Pt 4), 458-464.

McGowan, C. C., Cover, T. L., and Blaser, M. J. (1997). Analysis of F1F0-ATPase from *Helicobacter pylori*. *Infection and Immunity, 65*(7), 2640-2647.

McNulty, C., Owen, R., Tompkins, D., Hawtin, P., McColl, K., Price, A., Smith, G., Teare, L., and PHLS Helicobacter Working Group. (2002). *Helicobacter pylori* susceptibility testing by disc diffusion. *The Journal of Antimicrobial Chemotherapy, 49*(4), 601-609.

Mee, B., Kelleher, D., Frias, J., Malone, R., Tipton, K. F., Henehan, G. T., and Windle, H. J. (2005). Characterization of cinnamyl alcohol dehydrogenase of *Helicobacter pylori*, an aldehyde dismutating enzyme. *The FEBS Journal, 272*(5), 1255-1264.

Mehta, N., Benoit, S., and Maier, R. J. (2003). Roles of conserved nucleotide-binding domains in accessory proteins, HypB and UreG, in the maturation of nickel-enzymes required for efficient *Helicobacter pylori* colonization. *Microbial Pathogenesis, 35*(5), 229-234.

Mendz, G. L., and Megraud, F. (2002). Is the molecular basis of metronidazole resistance in microaerophilic organisms understood? *Trends in Microbiology, 10*(8), 370-375.

Merrell, D. S., Goodrich, M. L., Otto, G., Tompkins, L. S., and Falkow, S. (2003). pH-regulated gene expression of the gastric pathogen *Helicobacter pylori*. *Infection and Immunity, 71*(6), 3529-3539.

Minamino, T., Chu, R., Yamaguchi, S., and Macnab, R. M. (2000b). Role of FliJ in flagellar protein export in *Salmonella*. *Journal of Bacteriology, 182*(15), 4207-4215.

Minamino, T., and Macnab, R. M. (1999). Components of the *Salmonella* flagellar export apparatus and classification of export substrates. *Journal of Bacteriology, 181*(5), 1388-1394.

Minamino, T., and MacNab, R. M. (2000a). Interactions among components of the *Salmonella* flagellar export apparatus and its substrates. *Molecular Microbiology, 35*(5), 1052-1064.

Minamino, T., and Namba, K. (2004). Self-assembly and type III protein export of the bacterial flagellum. *Journal of Molecular Microbiology and Biotechnology, 7*(1-2), 5-17.

Minohara, Y., Boyd, D. K., Hawkins, H. K., Ernst, P. B., Patel, J., and Crowe, S. E. (2007). The effect of the cag pathogenicity island on binding of *Helicobacter pylori* to gastric epithelial cells and the subsequent induction of apoptosis. *Helicobacter, 12*(6), 583-590.

Miwa, K., and Yoshida, M. (1989). The alpha 3 beta 3 complex, the catalytic core of F1-ATPase. *Proceedings of the National Academy of Sciences of the United States of America, 86*(17), 6484-6487.

Mobley, H. L., Cortesia, M. J., Rosenthal, L. E., and Jones, B. D. (1988). Characterization of urease from *Campylobacter pylori*. *Journal of Clinical Microbiology, 26*(5), 831-836.

Molinari, M., Salio, M., Galli, C., Norais, N., Rappuoli, R., Lanzavecchia, A., and Montecucco, C. (1998). Selective inhibition of ii-dependent antigen presentation by *Helicobacter pylori* toxin VacA. *The Journal of Experimental Medicine, 187*(1), 135-140.

Morty, R. E., and Morehead, J. (2002). Cloning and characterization of a leucyl aminopeptidase from three pathogenic leishmania species. *The Journal of Biological Chemistry, 277*(29), 26057-26065.

Murata-Kamiya, N., Kikuchi, K., Hayashi, T., Higashi, H., and Hatakeyama, M. (2010). *Helicobacter pylori* exploits host membrane phosphatidylserine for delivery, localization, and pathophysiological action of the CagA oncoprotein. *Cell Host and Microbe, 7*(5), 399-411.

Muskotal, A., Kiraly, R., Sebestyen, A., Gugolya, Z., Vegh, B. M., and Vonderviszt, F. (2006). Interaction of FliS flagellar chaperone with flagellin. *FEBS Letters, 580*(16), 3916-3920.

Myllykallio, H., Lipowski, G., Leduc, D., Filee, J., Forterre, P., and Liebl, U. (2002). An alternative flavin-dependent mechanism for thymidylate synthesis. *Science (New York, N.Y.), 297*(5578), 105-107.

Nakamura, H., Yoshiyama, H., Takeuchi, H., Mizote, T., Okita, K., and Nakazawa, T. (1998). Urease plays an important role in the chemotactic motility of *Helicobacter pylori* in a viscous environment. *Infection and Immunity, 66*(10), 4832-4837.

Neuhard, J., and Kelln, R. A. (1996). Biosynthesis and conversions of pyrimidines. In F. C. Neidhardt (Ed.), *Escherichia coli and Salmonella: Cellular and molecular biology* (2nd ed., pp. 580-599). Washington, DC: ASM Press.

Niehus, E., Gressmann, H., Ye, F., Schlapbach, R., Dehio, M., Dehio, C., Stack, A., Meyer, T. F., Suerbaum, S., and Josenhans, C. (2004). Genome-wide analysis of transcriptional hierarchy and feedback regulation in the flagellar system of *Helicobacter pylori*. *Molecular Microbiology, 52*(4), 947-961.

Niehus, E., Ye, F., Suerbaum, S., and Josenhans, C. (2002). Growth phase-dependent and differential transcriptional control of flagellar genes in *Helicobacter pylori*. *Microbiology (Reading, England), 148*(Pt 12), 3827-3837.

Novy, R., Drott, D., Yaeger, K., and Mierendorf, R. (2001). Overcoming the codon bias of *E. coli* for enhanced protein expression. *InNovations, 12*, 1-3.

Odenbreit, S., Puls, J., Sedlmaier, B., Gerland, E., Fischer, W., and Haas, R. (2000). Translocation of *Helicobacter pylori* CagA into gastric epithelial cells by type IV secretion. *Science (New York, N.Y.), 287*(5457), 1497-1500.

Ogilvie, I., Aggeler, R., and Capaldi, R. A. (1997). Cross-linking of the delta subunit to one of the three alpha subunits has no effect on functioning, as expected if delta is a part of the stator that links the F1 and F0 parts of the *Escherichia coli* ATP synthase. *The Journal of Biological Chemistry, 272*(26), 16652-16656.

Olczak, A. A., Seyler, R. W.,Jr, Olson, J. W., and Maier, R. J. (2003). Association of *Helicobacter pylori* antioxidant activities with host colonization proficiency. *Infection and Immunity, 71*(1), 580-583.

Olczak, A. A., Wang, G., and Maier, R. J. (2005). Up-expression of NapA and other oxidative stress proteins is a compensatory response to loss of major *Helicobacter pylori* stress resistance factors. *Free Radical Research, 39*(11), 1173-1182.

Osaki, T., Hanawa, T., Manzoku, T., Fukuda, M., Kawakami, H., Suzuki, H., Yamaguchi, H., Yan, X., Taguchi, H., Kurata, S., and Kamiya, S. (2006). Mutation of luxS affects motility and infectivity of *Helicobacter pylori* in gastric mucosa of a mongolian gerbil model. *Journal of Medical Microbiology, 55*(Pt 11), 1477-1485.

O'Toole, P. W., Lane, M. C., and Porwollik, S. (2000). *Helicobacter pylori* motility. *Microbes and Infection / Institut Pasteur, 2*(10), 1207-1214.

Ottemann, K. M., and Lowenthal, A. C. (2002). *Helicobacter pylori* uses motility for initial colonization and to attain robust infection. *Infection and Immunity, 70*(4), 1984-1990.

Otwinowski, Z., and Minor, W. (1997). Processing of X-ray diffraction data collected in oscillation mode. *Methods in Enzymology, 276*, 307-326.

Ozin, A. J., Claret, L., Auvray, F., and Hughes, C. (2003). The FliS chaperone selectively binds the disordered flagellin C-terminal D0 domain central to polymerisation. *FEMS Microbiology Letters, 219*(2), 219-224.

Pace, C. N., Vajdos, F., Fee, L., Grimsley, G., and Gray, T. (1995). How to measure and predict the molar absorption coefficient of a protein. *Protein Science : A Publication of the Protein Society, 4*(11), 2411-2423.

Parrish, J. R., Yu, J., Liu, G., Hines, J. A., Chan, J. E., Mangiola, B. A., Zhang, H., Pacifico, S., Fotouhi, F., DiRita, V. J., Ideker, T., Andrews, P., and Finley, R. L.,Jr. (2007). A proteome-wide protein interaction map for *Campylobacter jejuni*. *Genome Biology, 8*(7), R130.

Parsot, C., Hamiaux, C., and Page, A. L. (2003). The various and varying roles of specific chaperones in type III secretion systems. *Current Opinion in Microbiology, 6*(1), 7-14.

Pawlowski, K., Zhang, B., Rychlewski, L., and Godzik, A. (1999). The *Helicobacter pylori* genome: From sequence analysis to structural and functional predictions. *Proteins, 36*(1), 20-30.

Penn, C. W., and Luke, C. J. (1992). Bacterial flagellar diversity and significance in pathogenesis. *FEMS Microbiology Letters, 79*(1-3), 331-336.

Pereira, L., and Hoover, T. R. (2005). Stable accumulation of sigma54 in *Helicobacter pylori* requires the novel protein HP0958. *Journal of Bacteriology, 187*(13), 4463-4469.

Peter, S., and Beglinger, C. (2007). *Helicobacter pylori* and gastric cancer: The causal relationship. *Digestion, 75*(1), 25-35.

Ple, S., Job, V., Dessen, A., and Attree, I. (2010). Cochaperone interactions in export of the type III needle component PscF of *Pseudomonas aeruginosa*. *Journal of Bacteriology, 192*(14), 3801-3808.

Plummer, M., van Doorn, L. J., Franceschi, S., Kleter, B., Canzian, F., Vivas, J., Lopez, G., Colin, D., Munoz, N., and Kato, I. (2007). *Helicobacter pylori* cytotoxin-associated genotype and gastric precancerous lesions. *Journal of the National Cancer Institute, 99*(17), 1328-1334.

Portal-Celhay, C., and Perez-Perez, G. I. (2006). Immune responses to *Helicobacter pylori* colonization: Mechanisms and clinical outcomes. *Clinical Science (London, England : 1979), 110*(3), 305-314.

Quinaud, M., Chabert, J., Faudry, E., Neumann, E., Lemaire, D., Pastor, A., Elsen, S., Dessen, A., and Attree, I. (2005). The PscE-PscF-PscG complex controls type III secretion needle biogenesis in *Pseudomonas aeruginosa*. *The Journal of Biological Chemistry, 280*(43), 36293-36300.

Quinaud, M., Ple, S., Job, V., Contreras-Martel, C., Simorre, J. P., Attree, I., and Dessen, A. (2007). Structure of the heterotrimeric complex that regulates type III secretion needle formation. *Proceedings of the National Academy of Sciences of the United States of America, 104*(19), 7803-7808.

Rain, J. C., Selig, L., De Reuse, H., Battaglia, V., Reverdy, C., Simon, S., Lenzen, G., Petel, F., Wojcik, J., Schachter, V., Chemama, Y., Labigne, A., and Legrain, P. (2001). The protein-protein interaction map of *Helicobacter pylori*. *Nature, 409*(6817), 211-215.

Ramakrishnan, V. (2002). Ribosome structure and the mechanism of translation. *Cell, 108*(4), 557-572.

Rhodes, G. (2000). *Crystallography mage crystal clear: A guide for users of macromolecule models* (2nd ed.). USA: Academic Press.

Rodnina, M. V., Savelsbergh, A., Katunin, V. I., and Wintermeyer, W. (1997). Hydrolysis of GTP by elongation factor G drives tRNA movement on the ribosome. *Nature, 385*(6611), 37-41.

Rost, B., and Sander, C. (1993). Prediction of protein secondary structure at better than 70% accuracy. *Journal of Molecular Biology, 232*(2), 584-599.

Rost, B., and Sander, C. (1994). Conservation and prediction of solvent accessibility in protein families. *Proteins, 20*(3), 216-226.

Rost, B., Yachdav, G., and Liu, J. (2004). The PredictProtein server. *Nucleic Acids Research, 32*(Web Server issue), W321-6.

Sanger, F. (1949). Fractionation of oxidized insulin. *The Biochemical Journal, 44*(1), 126-128.

Satin, B., Del Giudice, G., Della Bianca, V., Dusi, S., Laudanna, C., Tonello, F., Kelleher, D., Rappuoli, R., Montecucco, C., and Rossi, F. (2000). The neutrophil-activating protein (HP-NAP) of *Helicobacter pylori* is a protective antigen and a major virulence factor. *The Journal of Experimental Medicine, 191*(9), 1467-1476.

Schauer, K., Muller, C., Carriere, M., Labigne, A., Cavazza, C., and De Reuse, H. (2010). The *Helicobacter pylori* GroES cochaperonin HspA functions as a specialized nickel chaperone and sequestration protein through its unique C-terminal extension. *Journal of Bacteriology, 192*(5), 1231-1237.

Shao, C., Zhang, Q., Sun, Y., Liu, Z., Zeng, J., Zhou, Y., Yu, X., and Jia, J. (2008). *Helicobacter pylori* protein response to human bile stress. *Journal of Medical Microbiology, 57*(Pt 2), 151-158.

Smith, K. D., Andersen-Nissen, E., Hayashi, F., Strobe, K., Bergman, M. A., Barrett, S. L., Cookson, B. T., and Aderem, A. (2003). Toll-like receptor 5 recognizes a conserved site on flagellin required for protofilament formation and bacterial motility. *Nature Immunology, 4*(12), 1247-1253.

Smoot, D. T., Mobley, H. L., Chippendale, G. R., Lewison, J. F., and Resau, J. H. (1990). *Helicobacter pylori* urease activity is toxic to human gastric epithelial cells. *Infection and Immunity, 58*(6), 1992-1994.

Souza, J. M., Giasson, B. I., Lee, V. M., and Ischiropoulos, H. (2000). Chaperone-like activity of synucleins. *FEBS Letters, 474*(1), 116-119.

Squires, C. L., Pedersen, S., Ross, B. M., and Squires, C. (1991). ClpB is the *Escherichia coli* heat shock protein F84.1. *Journal of Bacteriology, 173*(14), 4254-4262.

Stabile, B. E., Smith, B. R., and Weeks, D. L. (2005). *Helicobacter pylori* infection and surgical disease--part II. *Current Problems in Surgery, 42*(12), 796-862.

Stadtman, E. R., Van Remmen, H., Richardson, A., Wehr, N. B., and Levine, R. L. (2005). Methionine oxidation and aging. *Biochimica Et Biophysica Acta, 1703*(2), 135-140.

Steele-Mortimer, O., Brumell, J. H., Knodler, L. A., Meresse, S., Lopez, A., and Finlay, B. B. (2002). The invasion-associated type III secretion system of *Salmonella enterica* serovar typhimurium is necessary for intracellular

proliferation and vacuole biogenesis in epithelial cells. *Cellular Microbiology, 4*(1), 43-54.

Suerbaum, S., Josenhans, C., and Labigne, A. (1993). Cloning and genetic characterization of the *Helicobacter pylori* and *Helicobacter mustelae* flaB flagellin genes and construction of H. pylori flaA- and flaB-negative mutants by electroporation-mediated allelic exchange. *Journal of Bacteriology, 175*(11), 3278-3288.

Sun, P., Tropea, J. E., Austin, B. P., Cherry, S., and Waugh, D. S. (2008). Structural characterization of the *Versinia pestis* type III secretion system needle protein YscF in complex with its heterodimeric chaperone YscE/YscG. *Journal of Molecular Biology, 377*(3), 819-830.

Suzuki, M., Miura, S., Suematsu, M., Fukumura, D., Kurose, I., Suzuki, H., Kai, A., Kudoh, Y., Ohashi, M., and Tsuchiya, M. (1992). *Helicobacter pylori*-associated ammonia production enhances neutrophil-dependent gastric mucosal cell injury. *The American Journal of Physiology, 263*(5 Pt 1), G719-25.

Tang, Y., Guest, J. R., Artymiuk, P. J., and Green, J. (2005). Switching aconitase B between catalytic and regulatory modes involves iron-dependent dimer formation. *Molecular Microbiology, 56*(5), 1149-1158.

Tang, Y., Guest, J. R., Artymiuk, P. J., Read, R. C., and Green, J. (2004). Post-transcriptional regulation of bacterial motility by aconitase proteins. *Molecular Microbiology, 51*(6), 1817-1826.

Terwilliger, T. C. (2000). Maximum-likelihood density modification. *Acta Crystallographica.Section D, Biological Crystallography, 56*(Pt 8), 965-972.

Terwilliger, T. C., and Berendzen, J. (1999). Automated MAD and MIR structure solution. *Acta Crystallographica.Section D, Biological Crystallography, 55*(Pt 4), 849-861.

Thanassi, D. G., and Hultgren, S. J. (2000). Multiple pathways allow protein secretion across the bacterial outer membrane. *Current Opinion in Cell Biology, 12*(4), 420-430.

Thirumalai, D., and Lorimer, G. H. (2001). Chaperonin-mediated protein folding. *Annual Review of Biophysics and Biomolecular Structure, 30*, 245-269.

Thomas, J., Stafford, G. P., and Hughes, C. (2004). Docking of cytosolic chaperone-substrate complexes at the membrane ATPase during flagellar type III protein export. *Proceedings of the National Academy of Sciences of the United States of America, 101*(11), 3945-3950.

Thompson, J. D., Higgins, D. G., and Gibson, T. J. (1994). CLUSTAL W: Improving the sensitivity of progressive multiple sequence alignment through sequence weighting, position-specific gap penalties and weight matrix choice. *Nucleic Acids Research, 22*(22), 4673-4680.

Tomb, J. F., White, O., Kerlavage, A. R., Clayton, R. A., Sutton, G. G., Fleischmann, R. D., Ketchum, K. A., Klenk, H. P., Gill, S., Dougherty, B. A., Nelson, K., Quackenbush, J., Zhou, L., Kirkness, E. F., Peterson, S., Loftus, B., Richardson, D., Dodson, R., Khalak, H. G., Glodek, A., McKenney, K., Fitzegerald, L. M., Lee, N., Adams, M. D., Hickey, E. K., Berg, D. E., Gocayne, J. D., Utterback, T. R., Peterson, J. D., Kelley, J. M., Cotton, M. D., Weidman, J. M., Fujii, C., Bowman, C., Watthey, L., Wallin, E., Hayes, W. S., Borodovsky, M., Karp, P. D., Smith, H. O., Fraser, C. M., and Venter, J. C. (1997). The complete genome sequence of the gastric pathogen *Helicobacter pylori*. *Nature, 388*(6642), 539-547.

Tsugane, S., Tei, Y., Takahashi, T., Watanabe, S., and Sugano, K. (1994). Salty food intake and risk of *Helicobacter pylori* infection. *Japanese Journal of Cancer Research : Gann, 85*(5), 474-478.

van der Wolk, J. P., de Wit, J. G., and Driessen, A. J. (1997). The catalytic cycle of the escherichia coli SecA ATPase comprises two distinct preprotein translocation events. *The EMBO Journal, 16*(24), 7297-7304.

Voland, P., Weeks, D. L., Marcus, E. A., Prinz, C., Sachs, G., and Scott, D. (2003). Interactions among the seven *Helicobacter pylori* proteins encoded by the urease gene cluster. *American Journal of Physiology.Gastrointestinal and Liver Physiology, 284*(1), G96-G106.

Wang, G., Alamuri, P., and Maier, R. J. (2006). The diverse antioxidant systems of *Helicobacter pylori*. *Molecular Microbiology, 61*(4), 847-860.

Wattiau, P., Woestyn, S., and Cornelis, G. R. (1996). Customized secretion chaperones in pathogenic bacteria. *Molecular Microbiology, 20*(2), 255-262.

Wen, Y., Marcus, E. A., Matrubutham, U., Gleeson, M. A., Scott, D. R., and Sachs, G. (2003). Acid-adaptive genes of *Helicobacter pylori*. *Infection and Immunity, 71*(10), 5921-5939.

Wilharm, G., Dittmann, S., Schmid, A., and Heesemann, J. (2007). On the role of specific chaperones, the specific ATPase, and the proton motive force in type III secretion. *International Journal of Medical Microbiology : IJMM, 297*(1), 27-36.

Williams, C. H., Stillman, T. J., Barynin, V. V., Sedelnikova, S. E., Tang, Y., Green, J., Guest, J. R., and Artymiuk, P. J. (2002). *E. coli* aconitase B structure reveals a HEAT-like domain with implications for protein-protein recognition. *Nature Structural Biology, 9*(6), 447-452.

Windle, H. J., Fox, A., Ni Eidhin, D., and Kelleher, D. (2000). The thioredoxin system of *Helicobacter pylori*. *The Journal of Biological Chemistry, 275*(7), 5081-5089.

Wong, B. C., Ching, C. K., and Lam, S. K. (1999). *Helicobacter pylori* infection and gastric cancer. *Hong Kong Medical Journal = Xianggang Yi Xue Za Zhi / Hong Kong Academy of Medicine, 5*(2), 175-179.

Wood, Z. A., Schroder, E., Robin Harris, J., and Poole, L. B. (2003). Structure, mechanism and regulation of peroxiredoxins. *Trends in Biochemical Sciences, 28*(1), 32-40.

Wootton, J. C., and Federhen, S. (1996). Analysis of compositionally biased regions in sequence databases. *Methods in Enzymology, 266*, 554-571.

World Health Organization. (2003). *Diet, nutrition, and the prevention of chronic diseases. WHO technical report series 916*. Geneva: World Health Organization.

Worst, D. J., Otto, B. R., and de Graaff, J. (1995). Iron-repressible outer membrane proteins of *Helicobacter pylori* involved in heme uptake. *Infection and Immunity, 63*(10), 4161-4165.

Wu, H., Nakano, T., Daikoku, E., Morita, C., Kohno, T., Lian, H. H., and Sano, K. (2005). Intrabacterial proton-dependent CagA transport system in *Helicobacter pylori*. *Journal of Medical Microbiology, 54*(Pt 12), 1117-1125.

Yamamoto, S., and Kutsukake, K. (2006). FliT acts as an anti-FlhD2C2 factor in the transcriptional control of the flagellar regulon in *Salmonella enterica serovar typhimurium*. *Journal of Bacteriology, 188*(18), 6703-6708.

Yamanaka, H., Kameyama, M., Baba, T., Fujii, Y., and Okamoto, K. (1994). Maturation pathway of escherichia coli heat-stable enterotoxin I: Requirement of DsbA for disulfide bond formation. *Journal of Bacteriology, 176*(10), 2906-2913.

Yan, J., Kumagai, T., Ohnishi, M., Ueno, I., and Ota, H. (2001). Immune response to a 26-kDa protein, alkyl hydroperoxide reductase, in *Helicobacter pylori*-infected mongolian gerbil model. *Helicobacter, 6*(4), 274-282.

Yokoseki, T., Iino, T., and Kutsukake, K. (1996). Negative regulation by fliD, fliS, and fliT of the export of the flagellum-specific anti-sigma factor, FlgM, in *Salmonella typhimurium*. *Journal of Bacteriology, 178*(3), 899-901.

Yokoseki, T., Kutsukake, K., Ohnishi, K., and Iino, T. (1995). Functional analysis of the flagellar genes in the fliD operon of *Salmonella typhimurium*. *Microbiology (Reading, England), 141 (Pt 7)*(Pt 7), 1715-1722.

Yonekura, K., Maki, S., Morgan, D. G., DeRosier, D. J., Vonderviszt, F., Imada, K., and Namba, K. (2000). The bacterial flagellar cap as the rotary promoter of flagellin self-assembly. *Science (New York, N.Y.), 290*(5499), 2148-2152.

Yoshida, N., Granger, D. N., Evans, D. J.,Jr, Evans, D. G., Graham, D. Y., Anderson, D. C., Wolf, R. E., and Kvietys, P. R. (1993). Mechanisms involved in

Helicobacter pylori-induced inflammation. *Gastroenterology, 105*(5), 1431-1440.

Yu, C. M., Chang, G. G., Chang, H. C., and Chiou, S. H. (2004). Cloning and characterization of a thermostable catfish alphaB-crystallin with chaperone-like activity at high temperatures. *Experimental Eye Research, 79*(2), 249-261.

Yu, J., and Kroll, J. S. (1999). DsbA: A protein-folding catalyst contributing to bacterial virulence. *Microbes and Infection / Institut Pasteur, 1*(14), 1221-1228.

Zhang, Z. W., Dorrell, N., Wren, B. W., and Farthingt, M. J. (2002). *Helicobacter pylori* adherence to gastric epithelial cells: A role for non-adhesin virulence genes. *Journal of Medical Microbiology, 51*(6), 495-502.

Zhong, Q., Shao, S. H., Cui, L. L., Mu, R. H., Ju, X. L., and Dong, S. R. (2007). Type IV secretion system in *Helicobacter pylori*: A new insight into pathogenicity. *Chinese Medical Journal, 120*(23), 2138-2142.